M.J.L. (Mitch) Frissen

# Determination of differential settlements of high-rise building foundations in soft soil conditions

*A framework for daily engineering practice*

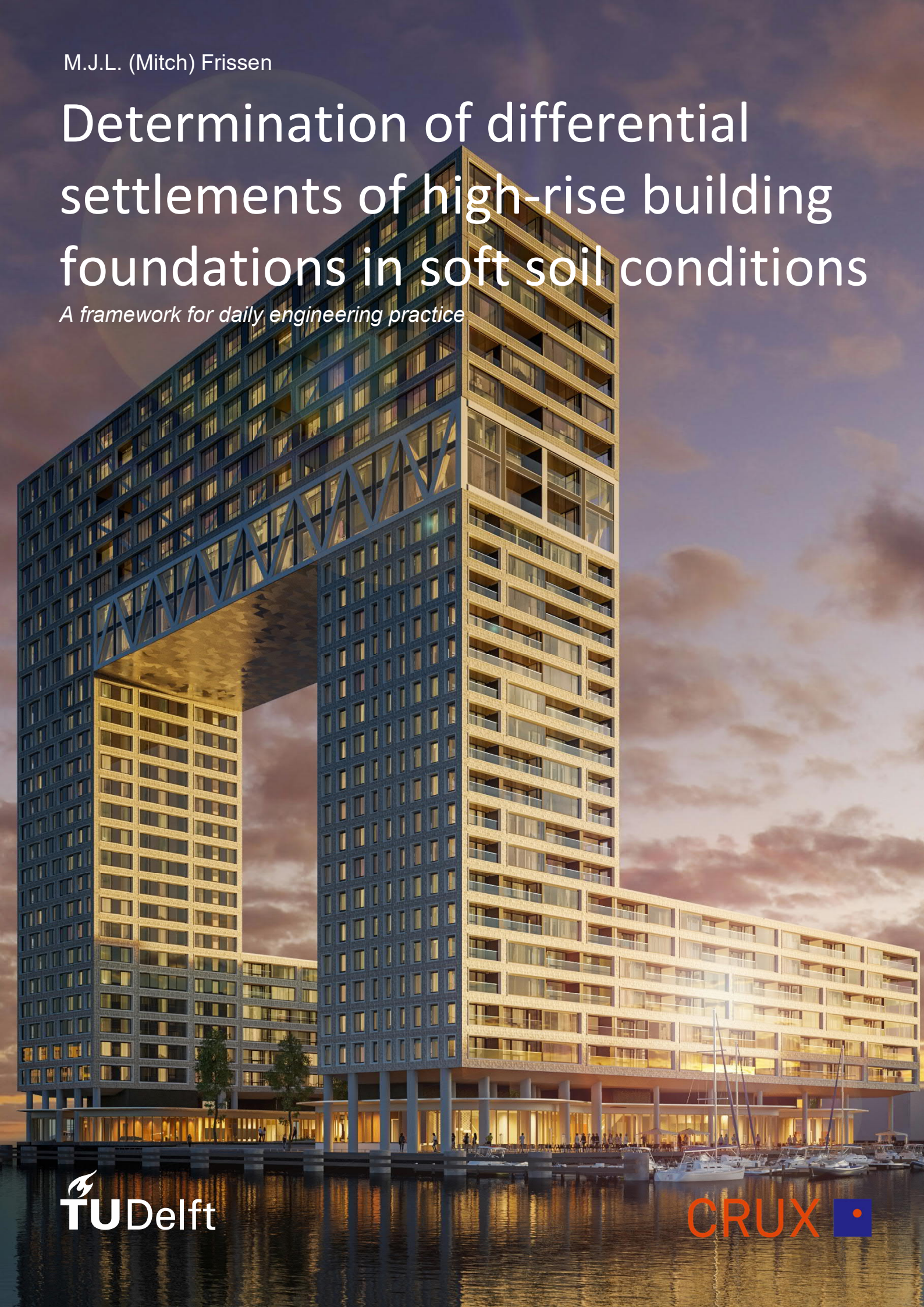

TU Delft

CRUX

[Cover picture: Pontsteiger, Amsterdam. Source: https://ikwilhuren.nu/amsterdam/pontsteiger/pontsteiger-209/34263366]

# Determination of differential settlements of high-rise building foundations in soft soil conditions

*A framework for daily engineering practice*

By

M.J.L. (Mitch) Frissen

in partial fulfilment of the requirements for the degree of

**Master of Science**
in Geotechnical Engineering

at the Delft University of Technology,
to be defended on Friday May 15, 2020 at 15:00 PM.

| | | |
|---|---|---|
| Supervisor: | Dr.ir. M. (Mandy) Korff | TU Delft |
| Thesis committee: | Dr.ir. R.B.J. (Ronald) Brinkgreve, | TU Delft |
| | ing. F.K. (Korneel) de Jong | CRUX Engineering BV |
| | R. (Roy) Crielaard MSc, | TU Delft & Heijmans Utiliteit |



TU Delft

CRUX

# Preface

This thesis is written to conclude my master's programme Geotechnical Engineering of the faculty of Civil Engineering at Delft University of Technology. The subject of this research is formulated in collaboration with CRUX Engineering BV and the Geo-Engineering Department of Delft University of Technology. This research contains an investigation related to settlement determination of high-rise buildings in soft soil deposits. Goal is to find an approach for modelling settlements of high-rise building foundations according to the applicable standards in the Netherlands including soil-structure interaction between the foundation and superstructure.

This report would not be possible with the help and support of many people. First of all, I would like to thank my graduation committee for their guidance and valuable input and discussions during the progress meetings. It helped me structuring the research in a professional and academic way. I believe this critical and academic analyzing of problems will support me in my entire professional and social life.

Moreover, I also would like to thank the employees of CRUX Engineering BV for their guidance during my research. Special thanks to Korneel de Jong and Christakis Iereidis for their valuable guidance during all the steps of my research and pushing me back on the track when I could not see a way out anymore. I have learned to stay positive in difficult and complex situation.

Last, I would like to thank my family and friends for their support during my bachelors and masters. Especially, my girlfriend Emma who had to deal during my entire student time with all my unfounded complaints about my study progress.

*M.J.L. (Mitch) Frissen*
*Delft, May 2020*

# Abstract

Currently, the settlements of high-rise buildings are calculated based on two methods. The single pile settlements ($s_1$), are generated due to mobilised shaft friction and pile tip resistance. These settlements are determined with analytical methods (i.e. NEN 9997-1, 2017). Settlements related to pile group behaviour in soil layers below pile tip level ($s_2$) are calculated with the equivalent raft approach i.e. Tomlinson (1977). However, an essential aspect for differential settlement calculations is the redistribution of loads by soil-structure interaction mechanisms, which are not currently incorporated in the calculation approach. A missing factor for a soil-structure interaction calculation is the lack of soil-displacement installation effects in the numerical methods for single pile behaviour. Therefore, this research is focussed on the implementation of a soil displacement single pile behaviour in PLAXIS 3D and thereby towards integration of the structural and geotechnical design in one calculation method for appropriate soil subgrade reactions and load redistribution.

In this research numerical methods are used in combination with the embedded beam approach applied in PLAXIS 3D. To approximate the NEN9997 load-displacement behaviour of soil displacement single piles, the behaviour of the embedded beam in combination with the multi-linear shaft friction is fitted in PLAXIS 3D. The fit is conducted by increasing the stiffness of a soil volume below pile tip level. Which does account for the residual stresses after pile installation. The solution of this fit consists of two parts: improvements on behalf of the new embedded beam formulation after Smulders (2018) and a soil stiffness fit below pile tip level. Regarding the new embedded beam formulation, improvements have been determined on mesh-dependency and a stiffer load-displacement response. The fit method performs well in combination with the embedded beams while approaching the load-displacement response of soil-displacement piles according to NEN9997. However, the ultimate bearing capacity of the embedded pile should still be calculated with D-Foundations (analytical method based on NEN9997).

In the pile group calculation, the behaviour of single piles is extrapolated to all piles in the PLAXIS 3D model. A plate element is modelled on top of the pile heads to achieve a redistribution of loads due to the overlying superstructure. In this way, the single pile behaviour and bending stiffness of the superstructure is implemented in the PLAXIS 3D model, and the soil-structure interaction calculation is possible. However, group effects due to the soil displacement installation method are only partly covered in this approach. The reduction or increase in skin resistance in pile groups is not covered since, the predefined maximum skin friction capacity is manually inserted as an input parameter and it is not an outcome of the PLAXIS 3D calculation.

Afterwards, the proposed framework is applied to a practical case study including measurement data of a high-rise project in Amsterdam. The proposed framework turned out to capture soil-structure interaction properly by taking into account a part of the superstructure bending stiffness and single pile behaviour. Compared to current calculation approaches, complex soil behaviour is captured in redistribution of the loads. However, the calculated settlements are still deviating from the measurement data. A probable explanation for the discrepancy is the shift in applied load over time in PLAXIS 3D relative to the real construction process.

In conclusion, an improvement in terms of modelling soil-structure interaction has been achieved by incorporating single pile behaviour and superstructure bending stiffness in PLAXIS 3D. Therefore, the possibilities of linking the structural design to the geotechnical design in an early stage of the design process will be feasible. Combining the designs in an early stage, the structural dimensions of columns and beams are calculated with appropriate soil subgrade reactions and load redistributions by the soil. However, it is recommended to apply more investigation on the behaviour of soil-displacement pile (groups) in combination with embedded beams because, group effects are still not completely incorporated.

# Table of contents

# List of Symbols

| Symbol | Description | Units |
|---|---|---|
| $A$ | Area of pile cross-section | [$m^2$] |
| $A_{4D}$ | Stressed area 4D below pile tip | [$m^2$] |
| $b$ | Width foundation plate element | [m] |
| $c_i$ | Cohesion interface elements | [$kN/m^2$] |
| $\mathbf{C}^{int}$ | Interface stiffness matrix | [$kN/m^2$] |
| $C_p$ | Empirical factor based on $E_s$ and $q_o$ | [-] |
| $C_s$ | Empirical factor based on $E_s$ and $q_o$ | [-] |
| $C_u$ | Undrained shear strength | [$kN/m^2$] |
| $C_v$ | Consolidation coefficient | [$m^2$/day] |
| $D$ | Pile diameter | [m] |
| $\mathbf{D}^{int}$ | Interface stiffness matrix | [$kN/m^2$] |
| $E$ | Young's modulus | [$kN/m^2$] |
| $E_{ea;gem}$ | Average elasticity module soil 4D below pile tip level | [$kN/m^2$] |
| $EI$ | Bending stiffness | [$kN/m^2$] |
| $f$ | Shear resistance | [$kN/m^2$] |
| $F_{foot}$ | Force at foot pile | [kN] |
| $\mathbf{F}^{int}$ | Nodal force at interface vector | [kN] |
| $F_{und}$ | Sum load on foundation | [kN] |
| $G_0$ | Small strain modulus | [$kN/m^2$] |
| $G_s$ | Shear modulus soil | [$kN/m^2$] |
| $h$ | Thickness of (foundation) plate element | [m] |
| $I_2, I_3$ | Moment of inertia of pile two cross-sections perpendicular to pile axis | [$m^4$] |
| $I_{avg}$ | Average moment of inertia for pile | [$m^4$] |
| $k$ | Permeability | [m/day] |
| $K_{foot}$ | Interface base stiffness | [$kN/m^3$] |
| $K_n$ | (Special) normal stiffness interface elements | [$kN/m^2$] |
| $K_s$ | (Special) interface stiffness | [$kN/m^2$] |
| $K_t$ | (Special) tangential stiffness interface elements | [$kN/m^2$] |
| $L_b$ | Embedded pile length | [m] |
| $L_p$ | Pile length | [m] |
| $m^*$ | Surface factor for $s_2$ settlements | [-] |
| $m_v$ | Compressibility coefficient | [$MPa^{-1}$] |
| $P_j$ | Load in pile j | [kN] |
| $P_t$ | Total applied pile load | [kN] |
| $q_o$ | Ultimate point resistance (Vesic, 1977) | [$kN/m^2$] |
| $q_c$ | Cone resistance | [$kN/m^2$] |
| $Q_p$ | Ultimate point load | [kN] |
| $Q_s$ | Ultimate shaft load | [kN] |
| $R$ | Pile radius | [m] |
| $r_0$ | Pile radius | [m] |
| $R_{b;cal;max;i}$ | Maximum base capacity pile CPT i | [kN] |
| $R_{c;cal;i}$ | Maximum bearing capacity pile CPT i | [kN] |
| $R_{eq}$ | Equivalent pile radius | [m] |
| $R_G$ | Group reduction factor | [-] |
| $R_{inter}$ | Interface reduction factor | [-] |
| $r_m$ | Magical radius (Randolph & Worth, 1978) | [m] |

| | | |
|---|---|---|
| $R_S$ | Settlement ratio | [-] |
| $R_{s;cal;max;i}$ | Maximum shaft capacity pile CPT i | [kN] |
| s | Pile cross-section influence | [-] |
| $S_g$ | Average settlement pile group | [mm] |
| $S_p$ | Settlement single pile | [mm] |
| **t** | Skin tractions | [kN/m] |
| $t_i$ | Virtual interface thickness | [m] |
| $t_{s,(max)}$ | (Ultimate) shear traction at interface | [kN/m] |
| $u_b$ | Displacement beam | [m] |
| $u_s$ | Displacement soil | [m] |
| $w_{pp}$ | Settlement of pile tip | [m] |
| $w_{ps}$ | Settlement of pile shaft | [m] |
| $w_t$ | Total pile settlement | [m] |
| $X^0_m$ | Location on beam axis | [m] |
| $X^0_r$ | Location on interaction surface | [m] |
| $\Gamma_{foot}$ | Multiplier for foot stiffness | [-] |
| $\Gamma_n$ | Multiplier for normal stiffness | [-] |
| $\Gamma_s$ | Multiplier for shear modulus of axial stiffness | [-] |
| $\varphi_i$ | Friction angle interface elements | [°] |
| $\eta$ | Depth factor (Randolph & Worth, 1978) | [-] |
| $\nu$ | Poisson ratio | [-] |
| $\rho$ | Inhomogeneity factor (Randolph & Worth, 1978) | [-] |
| $\beta$ | Pile foot influence factor | [-] |
| $\rho_1$ | Displacement of single pile under unit load | [m] |
| $\alpha_i$ | Interaction factor (Poulos, 1968) | [-] |
| $\alpha_{kj}$ | Interaction factor for spacing between piles k and j | [-] |
| $\alpha_s$ | Pile type factor | [-] |
| $\Delta \mathbf{u}^{int}$ | Relative displacement vector | [-] |
| $\Delta_n$ | Direct input values for $K_n/K_t$ | [kN/m$^2$] |
| $\Delta_s$ | Direct input values for $K_s$ | [kN/m$^2$] |

# List of Abbreviations

| Symbol | Description |
|---|---|
| avg | Average |
| EB | Embedded Beam |
| EC7 | Eurocode 7, NEN9991 (NEN 9997-1, 2017) |
| FEM | Finite element method |
| HSsmall | Hardening soil small strain (PLAXIS constitutive model) |
| max | Maximum |
| min | Minimum |
| NEN9997 | Eurocode 7, NEN9991 (NEN 9997-1, 2017) |
| SLS | Serviceability limit state |
| SSC | Soft soil creep model (PLAXIS constitutive model) |
| ULS | Ultimate limit state |

# 1 Introduction

## 1.1 Topic description

Over the last years, settlement based designs became more important in pile foundation engineering (Randolph & Worth, 1978). Especially, differential settlements could induce problems during serviceability load level conditions. Moreover, differential settlements between constructions with different foundation loads and structural connections causes additional forces and bending moments. This thesis tries to find a modelling method for differential settlements between piles with high foundation loads in soft soil environments. Soft soil environment is used as a term in this thesis for sand and clayey soils.

Currently, settlements from high rise buildings are calculated with two separated approaches[1]: single pile settlements ($s_1$), related to settlements in order to mobilise shaft friction and pile tip resistance, are obtained with an analytical approach (NEN 9997-1, 2017). Settlements related to pile group behaviour in soil layers below pile tip ($s_2$) are calculated with distributed loads according to the equivalent raft approach by Tomlinson (1977).

Ideally, the entire settlement calculation ($s_1$ and $s_2$) should be performed in one calculation model to make soil-structure interaction possible. However, there are limitations in modelling soil displacement piles which are in line with the load-displacement curves in NEN9997 (NEN 9997-1, 2017). This mismatch is caused by a difference in load-displacement stiffness of the current pile modelling method and the NEN9997 load-displacement curves for soil displacement piles. An example of current modelling methods is PLAXIS 3D in combination with the embedded pile/beam approach. The embedded piles are based and validated for bored piles, which has a soil-pile interaction not influenced by installation effects.

## 1.2 Relevance

Over the last decade, an increase amount of high-rise buildings is planned and developed in the Netherlands. Especially in cities like Amsterdam and Rotterdam this trend is going on to build higher structures in order to give accommodation for working and living. In the meanwhile, foundations of these high-rise buildings become more challenging due to modern architectural design, often resulting in higher foundation loads and challenging settlement requirements.

The subsurface in Amsterdam has a soil profile containing sand and clay layers. The soft soils are sensitive for settlements, especially differential settlements from deeper clay layers below pile tip level. These settlement causes problems (increased forces and bending moments) for high-rise buildings with a structural connection to low-rise buildings. If these settlements can be predicted with a higher accuracy, it will lead to a more optimal foundation and structural design, the projects can become more feasible due to the reduced foundation costs. In the meantime, PLAXIS 3D has implemented a new embedded pile formulation, which has improved capabilities for modelling piles and may perform better than the existing (current) embedded pile. Hypothetically, the new embedded pile formulation can be used to model soil displacement piles in an efficient way.

[1] During daily engineering practice at CRUX Engineering BV

## 1.3 Functionality

Foundations costs can be a significant amount of the total project costs for high-rise buildings. Moreover, reducing the amount of differential settlements is favourable for the structural design. For example, connections between the façade and the construction, floor levels and between high-rise and low-rise parts of the construction. An optimised foundation and superstructure design contribute to the feasibility of the entire project. In case settlements can be predicted more accurate, a more optimized pile foundation and superstructure design can be accomplished. There is an increasing trend in high rise building development in Amsterdam. Moreover, these structures increase in complexity. For example, structural connections between high-rise and low-rise buildings result in unequal foundation loads causing unequal settlement distributions. In case settlements of low rise and high-rise parts can be calculated more accurately with an integral modelling approach for the $s_1$ and $s_2$ settlements including soil-structure interaction, the foundation and structural design can be more cost effective.

## 1.4 Research objectives

This paragraph describes the research objectives addressed in this thesis. First, the main research question is presented. Second, the main question is subdivided into several sub-questions to answer the main question in a structured way.

### 1.4.1 Main question

The main research objective is formulated as:

> *"How to increase accuracy in determining differential settlements of high-rise buildings on soil displacement pile foundations in soft soil deposits?"*

**Hypothesis**

Foundation design in the Netherlands has to meet the standards stated in NEN9997 (2017). For pile design calculations it implies that pile behaviour has to be in line with the given load-displacement curves in NEN9997, in case no site-specific pile tests are available. The settlement according to NEN9997 is a superposition of two contributions, $s_1$ for single pile settlement and $s_2$ for group pile settlements.

Differential pile settlement calculations could be conducted with different methods; empirical, analytical and numerical methods. One of the numerical tools for settlement calculation of pile foundations is finite element software. Different commercial packages are available for daily engineering practice like ABAQUS, RS3 and PLAXIS 3D. Moreover, PLAXIS recently launched a new embedded pile formulation, which could be a promising feature for this research. Therefore, more focus will be on the possibilities of modelling pile foundations in PLAXIS 3D. The choice for PLAXIS is further explained in chapter 3.

Soil displacement piles have a stiffer load-displacement behaviour compared to the existing embedded pile formulation in PLAXIS 3D. The embedded pile is only validated for the less stiff bored piles (Engin & Brinkgreve, 2009). The new (improved) embedded pile implementation after Smulders (2018), was initially intended for improving the lateral behaviour of the pile. A secondary effect of this improvement was a stiffer pile (tip) behaviour of the embedded pile in PLAXIS 3D. This secondary effect has possibilities for modelling load-displacement curves of soil displacement piles However, the installation effects, which have a governing behaviour on the response of soil displacement piles, are still not taken into account in PLAXIS 3D.

Summarizing this hypothesis: Combining single pile behaviour, pile group behaviour and superstructure stiffness in one calculation model, should lead to a more accurate determination of the (differential) settlements due to more optimized soil-structure interaction mechanism.

### 1.4.2 Sub questions

This research is divided in five different parts; Introduction, Literature review, Parametric study, Model design and Application (case study). For each part, the research objective is divided into several sub questions:

**Literature review**

In the literature review a theoretical background is given about pile foundation settlement calculations in the past and present.

- Which mechanisms occur in reality during installation and loading of soil displacement single piles and pile groups?
- Which methods are available in the literature for differential settlement calculation of pile foundations?
- On which level are installation effects important and why is it still difficult in current engineering practice to predict differential settlements of high-rise building foundations on soil displacement piles in soft soil conditions (sands and clays)?
- What is the influence of the superstructure stiffness on differential settlements?

**Parameter study**

In the parameter study, different calculation methods are proposed for determination of single pile settlements.

- Which calculation method is the most optimal for describing settlements of single piles in soft soil deposits?
- What is the most optimal modelling approach in this calculation method to obtain $s_1$ settlements according to NEN9997 for a soil displacement pile with high foundation loads in soft soil deposits?

**Model design**

In the model design part, results of the Parametric study are used to propose a model for pile group settlements. Important topic in pile group behaviour is the influence of the superstructure stiffness on the differential settlements.

- What is the best calculation approach to obtain $s_2$ differential settlements for pile groups of high-rise building foundations in combination with the method for single pile behaviour obtained in the Parametric study?
- Which influence does the superstructure stiffness have on the differential settlement behaviour regarding pile groups of high-rise buildings?
- To what extent is the proposed calculation approach for differential settlements an improvement compared to the existing settlement calculation approach for high-rise building foundations?

**Application (case study)**

A case study is used to compare field measurement data with the proposed calculation approach.

- Is the calculation approach developed in this thesis suitable to be used in Dutch Engineering practice regarding workability and reliability?

## 1.5 Research approach - report outline

The goal of this research is to determine the differential settlements more accurate of high-rise building foundations on soil displacement piles. According to NEN9997, settlements are a superposition of two contributions, $s_1$ and $s_2$. Ideally, the $s_1$ and $s_2$ settlements should be calculated in one iteration step, to make soil-structure interaction possible.

**Literature review**

In chapter 2, 3 & 4 the results of the literature review are discussed. Chapter 2 starts off with an overview of mechanisms that occur in reality during single pile and a pile group loading. Second, a brief overview of pile calculation methods used in the past and present are discussed. Thereafter, current problems and challenges in pile design research are discussed. The third part of the literature review discusses the theoretically part of the hypothesis. It includes an analysis of the new (improved) embedded pile formulation in PLAXIS 3D (Smulders, 2018) as a possible tool for increasing reliability in differential settlement determination.

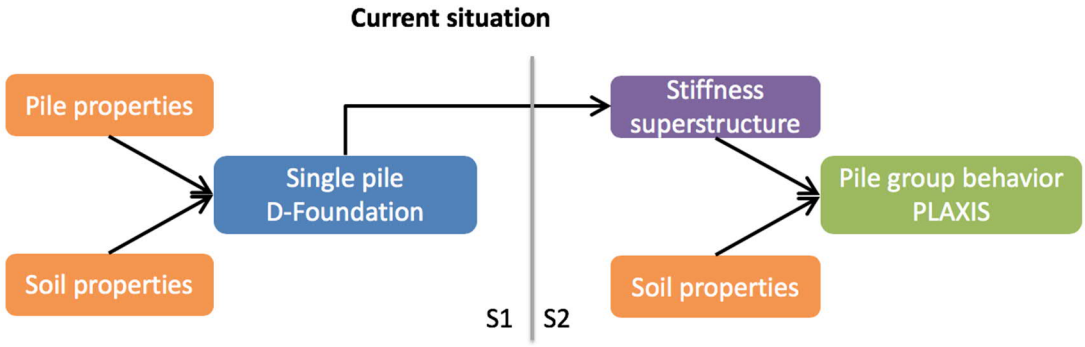


*Figure 1.1: One of the current modelling approaches for pile foundations in Dutch engineering practice*

**Parameter study**

This thesis is focusing on the settlement behaviour of soil displacement piles in sands and clays. In the Netherlands it is common to use soil displacement piles for settlement reduction and bearing capacity purposes for all kinds of constructions. For single pile design, several methods are available in the literature. In the Parametric study the old and new formulation of the embedded pile in PLAXIS 3D are compared with the NEN9997 load-displacement curve. Important in this part is to take into account the influence of the mesh sensitivity in both formulations. Second, a fit calculation is preformed to approximate the NEN9997 load-displacement curves.

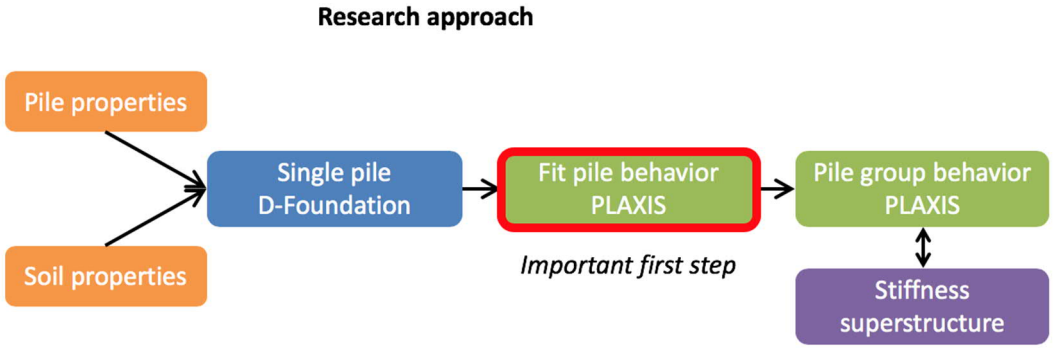


*Figure 1.2: Research approach single pile behaviour*

**Model design**
In the model design part different components of the settlement behaviour are coming together. Pile group behaviour is investigated by modelling a single pile with the proposed method in the Parametric study. The group behaviour is compared with the Tomlinson approach in combination with PLAXIS 3D. Besides pile behaviour, the influence of the pile cap stiffness on the (differential) settlements and soil-structure interaction is investigated.

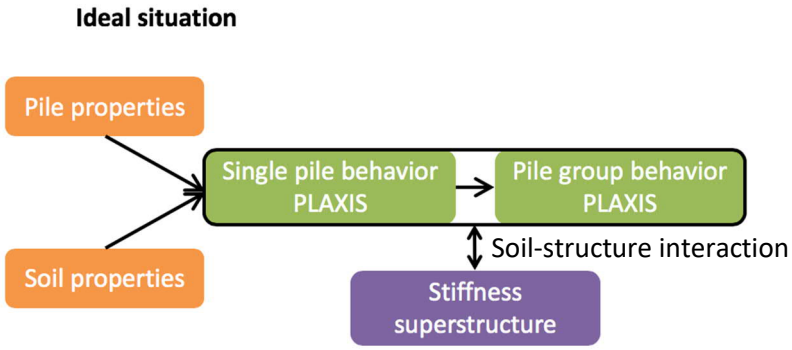


*Figure 1.3: Ideal situation modelling pile foundation settlements including soil-structure interaction with superstructure*

**Application**
In the last part the performance of the proposed method is tested by using field measurements of an existing construction. The foundation of a high-rise construction in the northern part of Amsterdam is modelled according to the proposed method and compared with available height measurement data. However, the measurement data has its limitations: no loadcells were installed during the construction so, the representative loads are not exactly known.

**Conclusion and recommendations**
The last part contains the conclusion about the possibilities and limitations for determining differential settlements with the proposed method. Remarks about the implementation in daily engineering practice and possibilities for future research are discussed in the Recommendations.

## 1.6 Research flow diagram

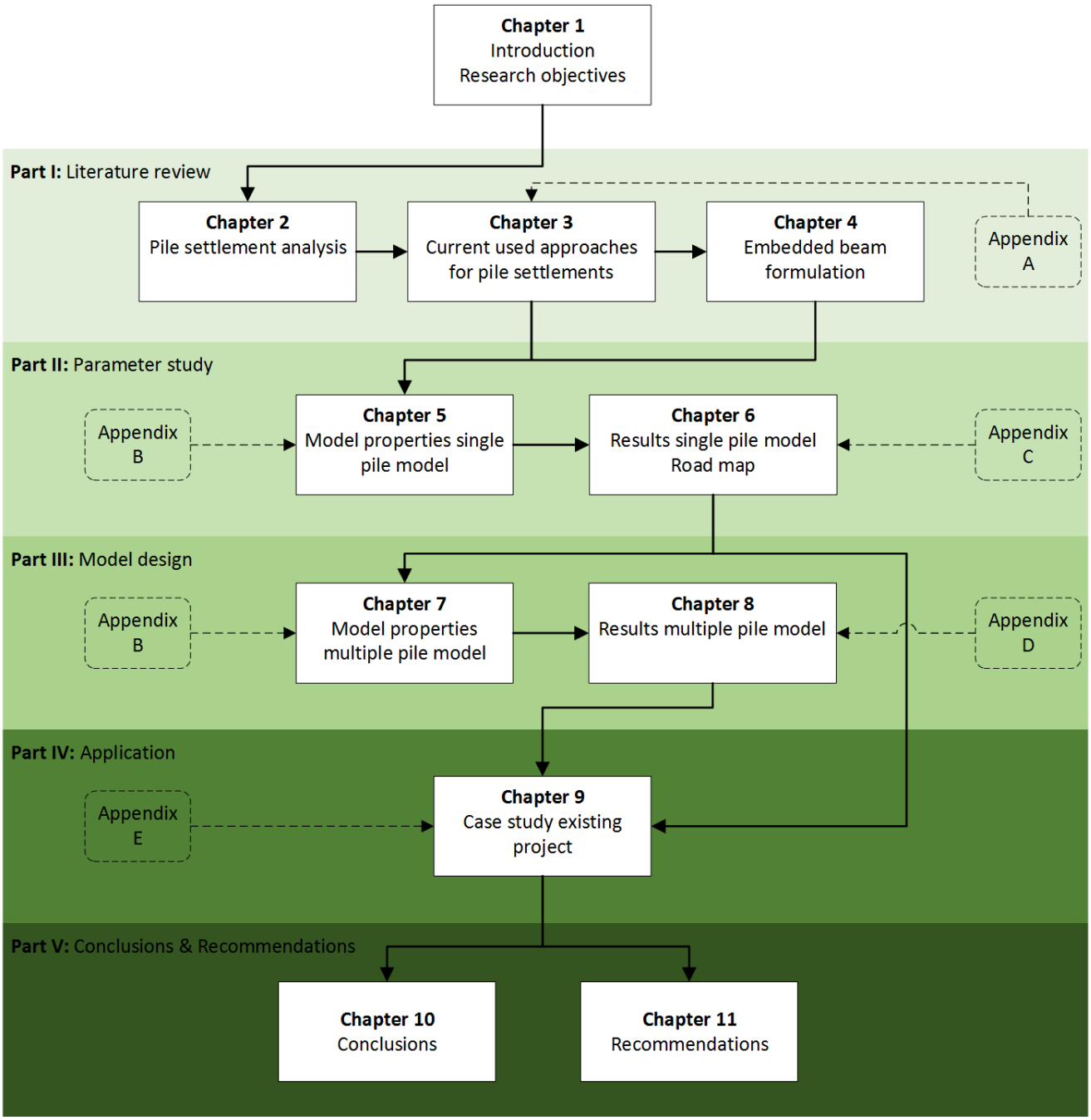

# I Literature review

# 2 Pile settlement analysis

Pile settlement behaviour has been investigated for a long period of time. Several authors have proposed different methods to analyse settlements and differential settlements of pile foundations. Poulos (1989) proposed a classification system for pile settlement analysis and design procedures, based on the accuracy of the underlying theory. Starting from theories based on empirical relationships towards theories with a sounder theoretical background. The classification of Poulos (1989) is presented in Table 2.1. Chen (2011) proposed a similar kind of classification system with different calculation methods. Chen divided the methods more explicitly in four different categories: analytical, numerical, semi-analytical/semi-numerical and semi-theoretical/semi-empirical methods. The classification by Chen (2011) is more explicit about which kind of background is used in the calculation.

| Category | Subdivision | Characteristics | Parameter determination |
|---|---|---|---|
| 1 | | Empirical | Simple in situ or laboratory, with correlations |
| 2 | 2a | Based on simplified theory or charts. Linear elastic deformation | Routine relevant in situ tests, may require some correlations |
| | 2b | As for 2a, but non-linear deformation | |
| 3 | 3a | Based on theory using site specific analysis, uses soil mechanics principles. Linear elastic deformations | Careful laboratory and/or in situ tests which follow appropriate stress paths |
| | 3b | As for 3a, but non-linearity is allowed for relatively simple manner | |
| | 3c | As for 3a but non-linearity is allowed for by way of proper constitutive models of soil behaviour | |

*Table 2.1: Different pile settlement analysis (after Poulos, 1989)*

Chapter 2 briefly describes the different methods for pile settlement analysis developed over the last years based on the classification system of Chen (2011). Moreover, possibilities and limitations of the presented methods are discussed. Behaviour of pile foundations is divided in two different mechanisms: single pile behaviour and pile group behaviour. Both mechanisms are important when the complete settlement behaviour of a pile foundation is obtained. Besides the pile behaviour itself, the cap stiffness has a major influence on the differential settlements (Dung et al., 2010; McCabe & Sheil, 2015). The literature review is focussing on these three aspects, single pile behaviour, pile group behaviour and pile cap stiffness.

## 2.1 Explanation pile problem

Pile installation behaviour and loading of piles is a complex process which is still not completely understood yet. A brief overview of the most important processes is visualized in a couple of drawings. These drawings are used to give the reader a brief overview of the mechanisms occurring during installation and loading of end bearing piles in a sand layer positioned underneath soft soil layers.

### 2.1.1 Single pile

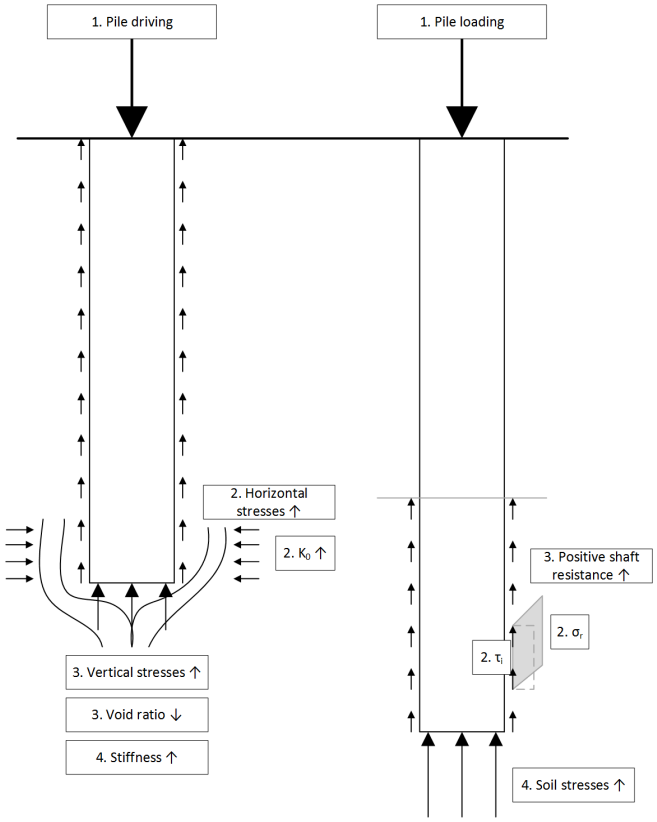


*Figure 2.1: Single pile during installation (left) and loading (right)*

During installation of soil displacement piles, the soil around the pile tip is stressed due to displaced soil volume in this area which cannot disappear. Consequently, deformations around the pile are predominately in shear mode (Randolph, 1985). After installation, these stresses remain in the soil and result in stiffer behaviour along the shaft and at the base due to preloading of the soil and stress dependent stiffness of the soil. During loading of the pile, shaft friction is mobilized first, since it requires less deformation compared to the base to fully develop friction. Subsequently, the base resistance is mobilized which requires more deformation to mobilize full resistance.

The positive and negative skin friction of the soft soil layers above the sand bearing layer have a limited influence on the bearing capacity. Therefore, in this thesis the contribution of the positive and negative skin friction from the soft soil layers is neglected.

### 2.1.2 Pile group

Pile installation by driving, drilling (in a soil displacement manner), hammering etc. introduces higher normal effective stresses in the soil compared to the in-situ situation due to the compacting effect (Fleming, 1992). On the contrary, installation of bored piles introduces hardly no additional soil stresses in the ground and can even lead to a decrease in soil stresses.

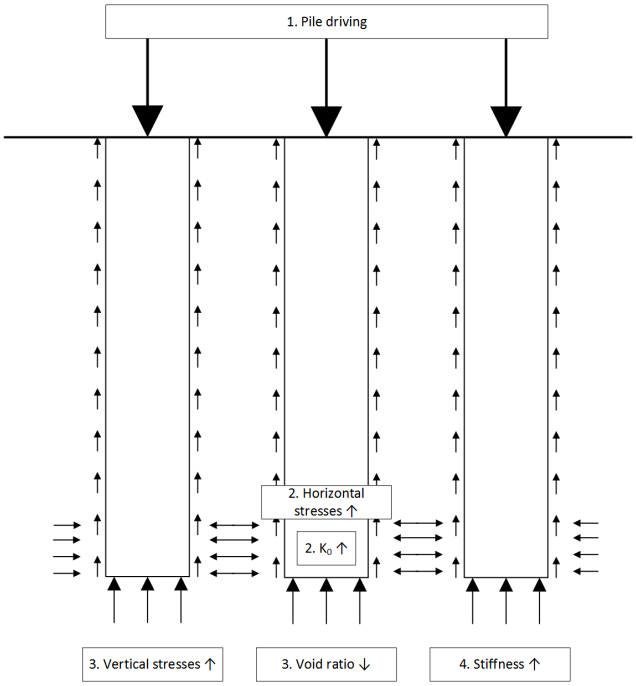


*Figure 2.2: Mechanisms occurring during installation of piles in a group pattern (spacing less then 10·D)*

After installation of the first pile, horizontal stresses are introduced in the soil body around the pile perimeter. Installation of the second pile experiences higher stresses due to the installation of the previous pile (compacting effect). This second pile increases the stress even more because of the increased friction along the shaft (eq. 4.12). In case more piles are added, the soil between the adjacent piles is getting reinforced and behaves like a soil plug with the corner piles as outer diameter.

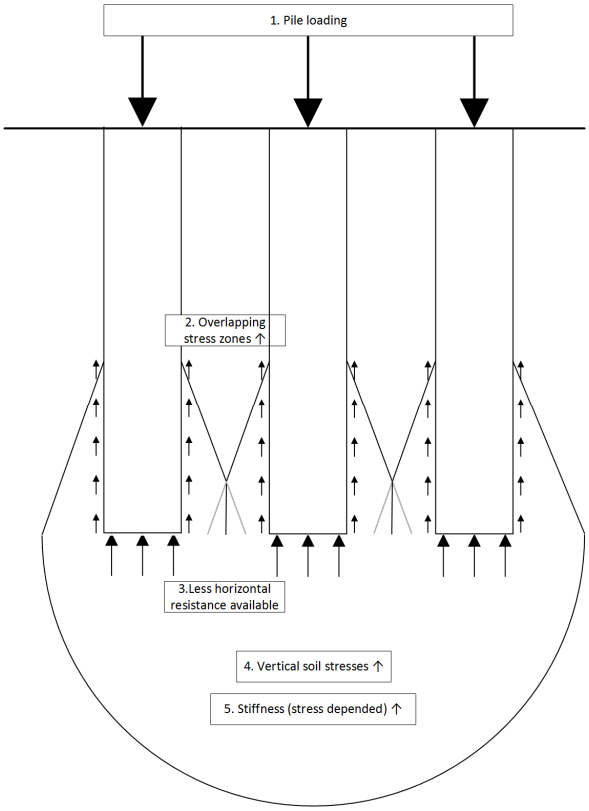


*Figure 2.3: Mechanisms occurring during loading of piles in a group pattern (spacing less then 10·D)*

Loading of a pile group is influenced by the overlapping stress zones introduced at the shafts. Mobilized soil resistance of one pile cannot contribute to the resistance of an adjacent pile. Therefore, the amount of possible friction that is available in case more piles are installed is less compared to single piles. Moreover, compared to single piles, more load is added on the same area which results in a deeper stress bulb (Figure 2.4). Stressing a larger soil volume results

theoretically in more settlement mobilization below pile tip level (Tomlinson & Woodward, 1977). However, other research proves that the settlement reduces in case more piles are installed. This is explained due to the higher horizontal stresses available after installation of soil displacement piles in a group (Sales et al., 2017).

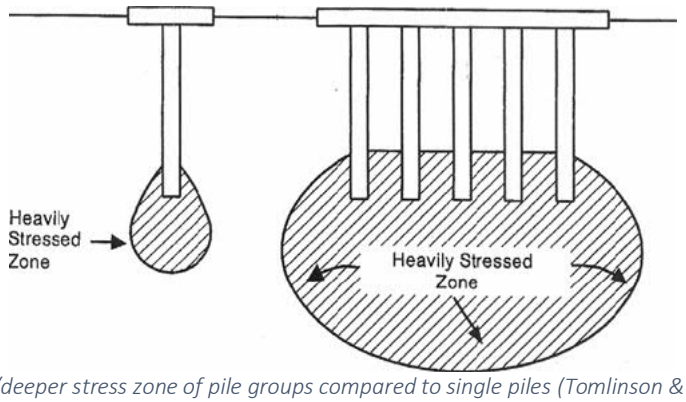


*Figure 2.4: Larger/deeper stress zone of pile groups compared to single piles (Tomlinson & Woodward, 1977)*

By varying the pile spacing and diameter of a pile group, the response is changing. Larger pile spacing results in less influence on adjacent piles (Appendix D.1.1). Moreover, larger pile diameters increase the influence on other piles.

## 2.2 General pile behaviour

**Stiffness**

Behaviour of piles is a superposition of two contributions, the shaft and base response. Both contributions have different stress analysis approaches. The shaft is subjected to shear stresses along the interface, the base experiences normal stresses at pile tip level. In average soft soil deposits the stiffness varies over depth (stress level dependency). Therefore, it is important to take into account the stiffness development over depth, in order to not overpredict the settlements (Poulos & Davis, 1980).

Besides stress level dependency, the stiffness of the soil will decrease with increasing strain level, called strain level dependency (Ju, 2015). Strain level dependency is something that occurs during pile driving and is discussed later on in this chapter in combination with the installation effects.

**Interface conditions**

Different theories about interface behaviour and pile-soil interaction are available in the literature. In a simple case, the interface condition remains elastic and no slip occurs between pile and soil. The relative movement between the pile and the soil remains zero (Poulos & Davis, 1980). However, real pile-soil interface behaviour has a finite adhesive strength, slip or a maximum local yield value when the shear stress reaches the maximum strength of the interface. In the latter case an elastic analysis is not possible anymore at the interface. In the literature are given different formulations when non-linear behaviour takes place and different opinions about the influence on the settlement contribution during working load conditions. For example, during serviceability limit state (SLS) load cases, the pile is loaded until 50% of its ultimate load capacity. Research (Ju, 2015) showed evidence for the effect of non-linear behaviour on the settlements of a single pile and pile groups in situations with load levels below the ultimate capacity. Which means, non-linear behaviour takes place in SLS load level ranges.

**Time effects**

The final settlements for piles situated in sand or unsaturated soils occur directly by applying the load. In this case, drained soil parameters should be used. For undrained soils like clays, the immediate settlements occur in undrained behaviour followed by time-dependent settlements. Therefore, undrained soil parameters are suggested. Here, the final settlement contains; immediate settlement, final consolidation settlement and creep settlement. For end bearing piles, almost the entire settlement contribution comes from the immediate settlements (Poulos & Davis, 1980). Consolidation has only a minor influence on the settlement behaviour of single piles. Effects due to creep at higher foundation loads are more important than consolidation behaviour, this is due to the relatively little changes in the mean stress (Poulos, 1989). However, in case a compressible layer does exist below pile tip level, a consolidation settlement analysis should be performed to take into account the long term settlement (Verruijt, 2012). Moreover, increasing the number of piles

situated in a group has an increasing influence on the consolidation settlements, due to the higher stresses on the undrained layers.

Besides consolidation and creep, negative skin friction (down drag) develops over time at the pile-soil interface. Due to time dependent settlement effects in the surrounding soil layers and the friction at the pile interface, a resulting force is acting downwards on the pile. This causes additional loads on the pile and results in additional settlements. Although, compared to the high foundations loads of high-rise buildings, negative skin friction can be negligible in this case.

**Installation effects**
In a large amount of pile settlement analysis the soil and the pile is assumed to be stress free, no residual stresses are present in the soil due to the installation (Poulos & Davis, 1980). However, in field situations this is not the case, a pile driven into a stiff soil layer causes residual stresses and remain in the subsoil and pile after installation. The stress distortion has large influences on the bearing capacity and settlement behaviour of soil displacement pile foundations (Phuong, 2014). The influence of installation effects due to residual stresses can be taken into account by choosing appropriate values for the stiffness of the soil (Poulos & Davis, 1980). The effect of stress distortion due to the installation is further discussed in § 3.4.1, including an exploration of possible solutions to take installation effects into account.

**Stress distribution**
For end bearing piles, the load transfer along piles depend on the stiffness of the bearing stratum. In case the stiffness of the bearing layer decreases, the load transfer increases. In case the stiffness of the pile decreases or the L/d ratio increases the load transfer also increases (Poulos & Davis, 1980).

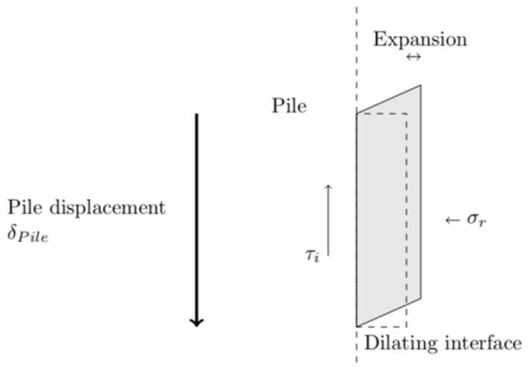


*Figure 2.5: Dilating behaviour during axial loading (Tschuchnigg, 2013)*

During axial loading of a pile, the volume associated with the shearing (dilatancy) increases the normal stresses at the pile shaft (Figure 2.5). As a consequence, the shaft resistance increases (Tschuchnigg, 2013).

## 2.3 Single pile

Single pile behaviour is affected by the soil profile, soil behaviour, pile characteristics, loading conditions and external soil movement (Poulos, 1989). More specific;

- Ratio between the Young's modulus of the soil and the Young's modulus of the pile
- Ratio between length and diameter of the pile
- In case of end bearing piles, ratio between Young's modulus of the bearing stratum at the pile tip and the Young's modulus of the soil.

Settlement of a single pile is a superposition of pile tip settlement and elastic deformation of the pile itself. The pile tip settlement can be obtained from the load-displacement curves in NEN9997 (2017) or from pile load tests. Moreover, this paragraph briefly describes different methods for single pile settlement calculations developed over the last years.

### 2.3.1 (Semi-) empirical method

Empirical methods are not based on soil mechanics principles, these methods are (mostly) based on a large amount of pile tests. The parameter determination is conducted by simple in-situ or laboratory tests in combination with

correlations (Poulos, 1989). There are several empirical methods available for determining pile settlements, most of them are normalised for pile diameter, cross section, pile length and the load applied on the pile. Two of them are discussed below.

**Vesic**

One of the semi-empirical methods is proposed by Vesic (1977). This method has divided the settlements in three different contributions:

- Settlements due to axial deformation of the pile shaft ($w_s$)
- Settlements due to load transfer at the pile tip ($w_{pp}$)
- Settlements due to load transmitted along the pile shaft ($w_{ps}$)

Vesic proposed the empirical relationships in equation 2.1 and 2.2 for respectively pile tip and shaft displacement. Both expressions contain the empirical factors $C_p$ and $C_s$ related to the soil Young's modulus (E), pile diameter (D), pile length ($L_p$) and the ultimate point resistance ($q_o$). The axial deformation of the pile shaft is the normal elastic shorting of the pile ($w_s$).

$$w_{pp} = \frac{C_p \cdot Q_p}{D \cdot q_o} \tag{2.1}$$

$$w_{ps} = \frac{C_s \cdot Q_s}{L_p \cdot q_o} \tag{2.2}$$

$$w_t = w_{pp} + w_{ps} + w_s \tag{2.3}$$

The empirical values $C_p$ and $C_s$ can be obtained from the tables given in Vesic (1977). However, empirical methods have no relation with soil mechanic principles and are therefore limited in use. Only situations which are similar to the situation of the empirical tests are meaningful for calculations with empirical methods.

**T-Z curves**

Another empirical method is the T-Z curve approach described in Stanton (2015). The t-z curve (side friction) and q-z curve (end bearing) approach allows the user to model non-linear stress strain behaviour in the soil. In this method, the pile is splits into multiple segments which are connected to non-linear springs. The response of the springs is modelled with mathematical descriptions of the load and movement behaviour from typical piles (Fellenius & Rahman, 2019). Different models exist in the literature with various mathematical descriptions for the load-settlement behaviour. A commonly used model is the hyperbolic description developed by Chin (1970). These mathematical described t-z curves are fitted to pile load tests, field measurements or analytical frameworks (Stanton et al., 2015). In case pile load tests are available on the building site, a good fit is obtained between the design and field situation. However, in the Netherlands it is not common or compulsory to conduct a pile load test before construction.

The empirical formulations give only a rough indication about the settlement behaviour (Gedeon, z.d.). Although, more elaborated empirical methods like T-Z curves give more accurate results if pile load test are available at the construction side. But these methods have a limited application area since, there is less sound theoretically soil mechanics background like stiffness and stress dependency incorporated.

### 2.3.2 Analytical methods

The analytical methods are based on theoretical soil mechanics principles and requires soil parameters as input. Both methods are elastic theory-based and divide the pile into uniformly loaded elements. The shaft and base are decoupled, where the base experiences uniform normal stresses and the shaft experiences uniform shear stresses along the entire shaft. The difference between both methods is the distribution of shear stresses along the shaft. Poulos & Davis (1968) assume shear stresses that are uniformly distributed around the circumference of the pile, were Randolph & Wroth (1978) assumes that the shear stress is acting as a single point load in the central axis of each element.

**Poulos & Davis**

The first method proposed by Poulos & Davis (1968) assumes a rigid cylindrical pile behaviour in an elastic homogenous soil. The method divides the pile into a number of elements which experience a uniform shear loading and radial stress, the base experiences a vertical normal stress. Since the pile is assumed to be incompressible, the displacements at each element should be equal. Poulos & Davis make use of vertical displacement factors, which are obtained by integration of Mindlin's equation for displacements in semi-finite mass resulting from vertical loading. The method is not capable in covering the adhesive strength when slip does occur. Moreover, the theory is based on elasticity, so is only applicable in perfect elastic, ideal, soil deposits, which is hardly never the case in practical foundation design.

**Randolph & Worth**

The second method to obtain settlements for rigid piles in homogeneous and non-homogeneous soils is proposed by Randolph & Wroth (1978). This method is better in non-homogeneous soil deposits since the method of Poulos & Davos makes large assumptions regarding the stiffness over depth.

The method is based on separation of loads carried by the base and shaft. The soil around the pile shaft is assumed to deform as concentric shearing cylinders. The soil layer below pile tip is acting as a rigid punch. The deformation in radial direction is decreasing inversely with the radial distance away from the pile. The decrease of the base deformation is more rapid in comparison with the deformation of the shaft. Therefore, a factor $\eta$ is introduced to account for the interaction of the upper and lower layer. The complete derivation can be found in the paper of Randolph and Wroth (1978), a brief description is presented here. The practical solution proposed by Randolph and Wroth (1978) to calculate settlement is a function of the pile radius presented in expression 2.4.

$$\frac{w_t}{r_o} = \frac{P_t}{2 \cdot \pi \cdot L_p \cdot r_o} \cdot \frac{L_p}{G_l \cdot \rho} \cdot \frac{\zeta \cdot \mu \cdot L_p}{\cdot \tanh(\mu \cdot L_p)} \tag{2.4}$$

Where:

$$(\mu \cdot l)^2 = [2 / (\mu \cdot \lambda)](l / r_0)^2 \tag{2.5}$$

$$\lambda = E_p / G_s \tag{2.6}$$

$$\zeta = G_\infty \int_{r_o}^{r_m} \frac{dr}{Gr} \tag{2.7}$$

*Parameters are explained in "List of symbols"*

It is discussable if this method is completely analytical, since the inhomogeneity factor is an empirical determined parameter but, the results of this method show good evidence with numerical calculations.

The goal of the proposed method by Randolph and Wroth (1978) was to make a reliable prediction of the settlements giving large savings in expenses and time. However, the overall stability regarding differential settlements remains an important part of the foundation analysis. Randolph and Worth (1979) preceded to study the effect of neighboring piles.

It is discussable whether these analytical methods are useful in practical engineering nowadays. The empirical factors are most of the time site specific and cannot be used in every arbitrary situation. Moreover, the linear character of these methods is often not realistic for practical cases since pile-soil interaction is most of the time non-linear.

### 2.3.3 Numerical methods

Over the last years, numerical methods are the most widely used approach to handle geotechnical engineering problems. With numerical codes it is possible to model non-linearity in pile-soil behaviour and time-dependent effects due to consolidation and creep. Different constitutive models are available to capture soil behaviour characteristics like non-linearity, stress path dependent stiffness and cap hardening/softening. Besides the soil model properties, it is

possible to model various soil layers and assign different soil properties. Moreover, special elements for pile-soil interface behaviour are available to capture the response of slip (relative displacement) between pile and soil which is lacking in the analytical models.

## 2.4 Pile group

In comparison with single pile settlements, pile group settlements are affected by interaction of neighbouring piles. The interaction results in overlapping stress distributions of adjacent piles in a group (Tejchman & Gwizdala, 2001). However, at higher load levels, which is the case with high-rise buildings, pile groups show a stiffer behaviour then single piles due to the change in stress state (Tschuchnigg, 2013). Moreover, the foundation slab (cap) stiffness is influencing the settlement distribution since, the foundation slab is redistributing the loads. Flexible slabs give large differential settlements, rigid slabs provide much more redistributions of the loads to the individual piles and results in less differential settlements.

Different opinions about group effects can be found in the literature. (Cairo et al., 2005; Poulos, 1968, 1989; Tejchman & Gwizdala, 2001; Tomlinson & Woodward, 1977) stated that pile groups show considerably more settlements in comparison with single piles due to the overlapping stress zones. Although, group effects could also have a reinforcement effect in the soil, resulting in less settlements compared to single piles (Sales et al., 2017). Therefore, it is important to carefully analyse the settlement behaviour of pile groups. Besides, the comparison with single piles, variations in pile group configuration like foundation size, soil conditions, installation method and number of piles have effect on the settlement behaviour.

### 2.4.1 Empirical method

Poulos (1968) stated that symmetrical pile groups (undergoing similar settlement at equal load), show an increase in settlement due to the interaction between two adjacent piles depending on the spacing. These additional settlements due to group effects are described with the interaction factor $\alpha_i$.

$$\alpha_i = \frac{\text{additional settlement due to adjacent pile}}{\text{settlement of pile under its own load}} \tag{2.8}$$

Starting from the interaction of two piles, an empirical method for pile group behaviour under static load is based on the assumption that settlement behaviour of pile groups is a function of single pile behaviour. For pile groups with more than two piles, Poulos & Davis (1980) obtained that each added pile in a group with equally loaded and spaced piles, displaces equally. That means additional displacements for each pile in the group caused by other piles, is the same as adding up the displacement increases caused by other piles in the group. The interaction factor between two piles can be superposed according to equation 2.9 for group settlements:

$$\rho_k = \rho_1 \cdot \sum_{\substack{j=1 \\ j \neq k}}^{n} (P_j \cdot \alpha_{kj}) + \rho_1 \cdot P_k \tag{2.9}$$

Equation 2.10 shows the relation between single pile behaviour and pile groups. $R_S$ is a coefficient that represents the ratio between settlements of piles in a group and the settlements caused by a single pile with the same average load as the pile in the group. This coefficient takes into account the pile length, pile spacing, Poisson's ratio of the soil and depth of the soil layer. $R_G$ gives a relative settlement for pile groups with different numbers of piles subjected to the same total load.

$$R_s = \frac{\text{Average group settlement}}{\text{Settlement of single pile at same average load as a pile in the group}} \tag{2.10}$$

$$R_g = \frac{\text{Average group settlement}}{\text{Settlement of single pile at same total load as the group}} \qquad 2.11$$

The $R_S$ value can be based on field or model tests where the behaviour of a single pile and a pile group is measured. Different $R_s$ values are available based on the number of piles used in the group and foundation size. Examples of these theoretical values are given in Poulos & Davis (1980). The $R_s$ value in most cases is higher than unity in relative low stress ranges. For example, the serviceability limit state load ranges (Pressley & Poulos, 1986).

The empirical interaction factor method is a reliable method to get a first impression about the behaviour of pile groups. However, since there is no theoretical soil mechanical background, the results should be handled with care when applying this method for pile design purposes. The method is capable in predicting the settlements in the right order of magnitude and with the right trends in reasonable accuracy. Therefore, the method is limited to pile groups with low amount of piles in rather homogenous soil profiles (Dung, 2010).

### 2.4.2 Equivalent foundation method

The method proposed by Tomlinson (1977) substituted the pile group by a simple form foundation at a certain depth. The depth is varying between $^2/_3$ $L_p$ to $L_p$, in case the soil profile consist completely out of cohesive soils, the equivalent raft is less deep, in case the pile tip is placed in the sand layer, the equivalent raft is deeper (Dung et al., 2010).

The simple foundation form (equivalent raft) can be an embedded shallow foundation, a large column treated as single pile or a block foundation depending on the used method. In order to calculate the settlements of the equivalent raft, the stress distribution has to be determined. This can be done by using the design charts given in Tomlinson (1977),

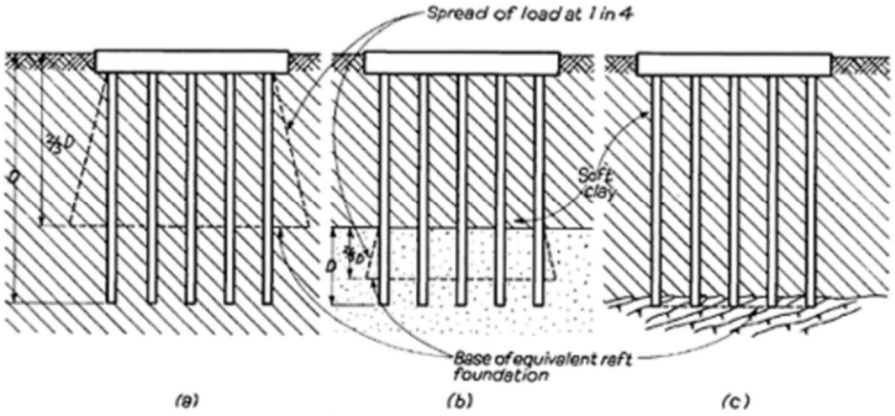


*Figure 2.6: Equivalent raft method, according to Tomlinson (1977)*

analytical software packages like D-Settlement or utilizing numerical codes. In the second step the depth is determined where the displacement has to be calculated. Tomlinson (1977) proposed a depth where only 20% of the net applied overburden pressure is still present (comparable with requirements in NEN9997). In case a very compressible soil layer is situated below the bearing stratum, a deeper level should be considered to obtain the amount of displacement.

Tomlinson (1977) stated that the equivalent raft method is sufficient to make reliable predictions for most day-to-day practice applications regarding settlements. Moreover, most practical problems have pile tips down to a layer of relative low compressibility. For most areas in the world, including large parts of the Netherlands, this assumption is correct. The low compressible layer affected to foundation loads has low total and differential displacements, an error minus or plus 50% results still in small absolute settlements. The equivalent raft is an efficient method in case a low compressible layer is present below the pile tip and settlements remain small. However, in case a medium/high compressible layer is present below pile tip level, the equivalent raft foundation could be not accurate enough. Since the relative error of the proposed method is large, absolute settlements can become quite significant. In addition, the stiffness of the equivalent raft foundation has a large influence on differential settlements. An advantage of this method is the ability to taken into account the stress dependency of the stiffness in case numerical codes are utilized together with appreciate constitutive models.

### 2.4.3 Numerical methods

Nowadays, numerical methods are widely used in settlement calculations for pile foundations. Different commercial packages are available with its own possibilities and limitations. Finite element methods offer a wide variety of functionalities that can be used for pile group settlement calculations. One of these functionalities is the utilization of constitutive models for soil and pile-soil behaviour. It is possible to model soil inhomogeneity, non-linearity, anisotropy, time dependency and subsequent loading in a consistent manner.

Ottaviani (1975) is one of the first researchers who compared a three dimensional finite element model with existing analytical models. One of the conclusions of this research is the total amount of settlements are governed for a large part by the compressible layers underneath the pile tips. This is due to the large area that is stressed by the pile groups in comparison with a small stressed area by single piles. More recently, Katzenbach (2015) described an optimized method where numerical methods play an important role in high level design for realistic modeling of soil-structure interaction, due to implementation of non-linear behaviour of the soil material.

Numerical methods, in this case finite element methods, contain different ways for modelling piles. Possible implementations are volume piles and embedded piles. In the volume pile approach the pile is modelled with explicit volume elements. The interface between the soil and the pile can be modelled with special interface elements to account for relative movement between pile and soil. For a reliable and accurate solution, this method requires small soil elements at the pile circumference, resulting in high computation costs.

Moreover, the embedded beam approach is original formulated by Sadek & Shahrour (2004) and the embedded pile is improved by Engin & Brinkgreve (2009), Tschuchnigg (2013), Turello et al. (2016) and Smulders (2018). The embedded pile is a beam element model where the connection to the soil is made by embedded skin and foot interfaces. The finite element mesh does not need to be adjusted for the location of the piles, which results in less computation costs. The embedded pile formulation, possibilities and limitations are discussed in chapter 4.

## 2.5 Conclusion

Chapter 2 summarizes general soil displacement pile settlement design problems over the last years. First, soil displacement pile behaviour related to; soil stiffness, soil-pile interface conditions, time dependency, installation effects and stress distributions are discussed. Secondly, various methods for settlement analysis of single pile and pile groups are discussed.

During single pile driving, the soil around the pile tip is stressed due to the soil volume which cannot disappear. The increase in stress result in higher stiffness of the soil around the pile tip and the pile shaft. In case a pile group is installed, the horizontal stresses between the adjunct piles increases even more. These higher stresses between the piles in a group ensure stiffer behaviour of the soil. Although, pile groups are stressing the soil also to a greater depth, which does increase the amount of settlements. Therefore, it is difficult to draw a conclusion whether group effects have a positive or negative influence on the amount of settlements.

The settlements are a superposition of three parts: immediate, consolidation and creep settlements. Most of the single pile settlement is caused by the immediate settlement (elastic compression of the soil and the pile). Only a small part is imposed by consolidation and creep along the shaft and directly at the base. In case of pile groups, the consolidation and creep become more important due to the higher stresses in the deeper consolidation layers compared to single piles.

Different calculation approaches are discussed for calculating settlements of either single piles or pile groups. Empirical, analytical and numerical methods have been developed and improved over the last years. Most of the methods do not incorporate residual stresses after pile installation in a soil displacement manner. Hence, the soil around the pile is assumed to be stress free. This assumption results in overprediction of the settlements, which leads to a conservative amount of settlements. The main conclusion that can be draw from the literature is stress/stiffness increase along the pile after soil displacement installation, results in stiffer load-displacement behaviour.

Moreover, numerical methods are currently the most used methods for settlement calculations of pile groups since they incorporate soil inhomogeneity, non-linearity, anisotropy, time dependent behaviour and subsequent loading in a consistent manner. Therefore, numerical methods are a good opportunity for modelling pile foundations of high-rise buildings.

# 3 State of practice

Design of large structure foundations is an interactive process between the structural and the geotechnical engineer. The superstructure transfers load through the foundation into the subsoil. Thereafter, the soil deforms depending on the soil stiffness. Subsequently, the subsoil transmits additional stresses, moments and displacements back to the superstructure. These additional stresses, moments and displacements in the soil are imposed at the superstructure, which gives again loads through the foundation back to the subsoil. This process is repeated until the stresses and displacements between the foundation and the subsoil are in equilibrium. There are two extreme situations for the iterative approach; a fully flexible or a fully rigid foundation (Figure 3.1). In most cases the response is somewhere in between.

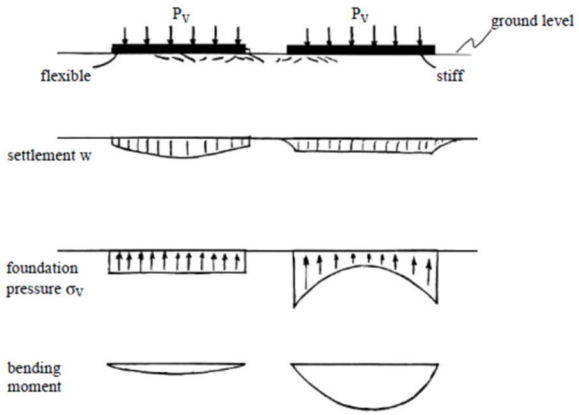


*Figure 3.1: Extreme cases foundation stiffness (Zoidi, 2015)*

In case the foundation plate is completely rigid, the differential settlements are small, and the stresses have a parabolic envelop. A completely flexible foundation plate has a parabolic settlement envelope (large differential settlements) and a constant stress distribution (see Figure 3.1). This chapter gives an overview of the different settlement contributions and the current used methods for pile foundation settlements in practice.

## 3.1 Engineering methods in practice

### 3.1.1 Different settlement contributions

Pile foundation settlement according to NEN9997 is a superposition of three contributions. All of them have their own mechanisms in developing settlements over time.

- Immediate settlements - elastic response: Due to shear deformations and volume reduction.
- Time dependent settlements – consolidation: Dissipation of pore water over time results in increase of effective stresses.
- Secondary compression – creep: No effective stress changes, but redistribution of soil particles results in volume changes and shear deformations.

The immediate settlements are often calculated with elastic approaches containing the initial tangent elastic modulus and Poisson ratio in undrained situations (Chen, 2011). Previous research (Chen, 2011; Poulos, 1989) stated that consolidation mechanisms has only a minor contribution to the total settlements of a pile foundation. The consolidation

effects are related to dissipation of excess pore water pressure. Therefore, in sand layers the consolidation effect has hardly no influence. However, in cases the fine-grained cohesive material is situated below pile tip, consolidation effects play an important role. Moreover, creep effects become also an important part in the amount of total settlements (Poulos & Davis, 1980). Creep settlements are not only important in clay layers but can also influence deep sand layers.

### 3.1.2 Soil-structure interaction

In engineering practice different strategies are available to model the soil-structure interaction. One of them is the iterative staggered coupling method (David & Forth, 2013; Zoidi, 2015).

- First, the structure is designed by the structural engineer with an accurate definition of the load distribution and overall stiffness of the construction. Most of the time, the structural engineer decides to model this stage on a rigid foundation (Zoidi, 2015). Since the internal forces significantly change during modification of the modulus of subgrade reaction, an initial volume for this factor is often obtained.
- The output of the previous phase is the input for the geotechnical engineer. The settlements are determined with a superstructure which is simplified to a slab containing the bending stiffness and the load distribution of the previous phase.
- The geotechnical engineer runs the analysis as described before and obtained the new modulus of subgrade reaction for the springs below the slab. The output of part of the analysis is the input for the first phase in order to repeat the process until convergences are achieved.

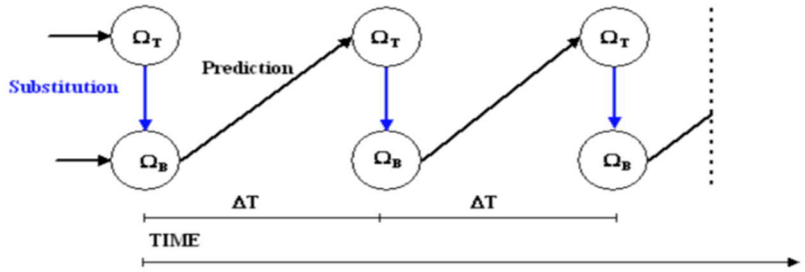


*Figure 3.2: Iterative staggered coupling for soil structure interaction modelling (David & Forth, 2011).*

In order to determine the right displacements, an iterative process is required to redistribute the load/settlements depending on the stiffness of the superstructure. Currently, the geotechnical model does not incorporate the entire building stiffness. In most cases, a slab with equivalent thickness and stiffness is modelled as a representation of the superstructure bending stiffness (Zoidi, 2015).

## 3.2 Geotechnical analysis

In § 3.1.2 is discussed the interaction between the structural and geotechnical design. This thesis is focussing on the geotechnical part of the soil-structure interaction including a straightforward approach to take into account the stiffness of the superstructure. The design for the geotechnical engineering is depending on a couple of factors, for example:

- Is a bearing capacity analysis required?
- Are the differential settlements critical in the design?
- Are the absolute vertical settlements critical?

Since this thesis is focussing on settlement determination, the bearing capacity is not further addressed here. The geotechnical design starts off with addressing single pile behaviour. For describing load-displacement behaviour of single piles, different methods exist as described in chapter 2. In Dutch engineering practice[2], single pile behaviour is analytical calculated according to NEN9997. For this purpose, D-Foundations can be used.

Currently, in the final design stage a numerical calculation is one of the most common approaches for settlement analysis for pile group effects. In case an accurate prediction of the settlement is required in the final design stage, numerical methods gives a good and reliable result (Gowthaman, 2017). Numerical methods are able to take into account complex

[2] Based on internal document of CRUX Engineering BV

soil mechanical principle and surrounding effects for example. However, noted is that input from soil properties remain one of the most important parts of a geotechnical analysis, and has a major influence on the results (Chen, 2011). Moreover, it is difficult to model pile installation effects in the current available numerical methods.

### 3.2.1 Analytical approaches for pile settlement modelling

On average, settlements are a superposition of three different contributions (van Grop, 2014):

- Elastic pile deformation ($s_{el}$)
- Settlement of the pile tip ($s_b$)
- Settlements caused by group effects ($s_2$)

In current engineering practice, above-mentioned analytical calculation for single pile settlements could be performed in different software packages. Two of them are discussed:

**Single pile with D-Foundations**

D-Foundations includes an analytical calculation approach for pile foundations in soft soil environments. The software is based on input from CPT data and calculates the bearing capacity according NEN9997. Here, pile tip settlement is determined based on standard load-displacement curves. The most influencing parameter for calculation of the pile tip settlement is the bearing capacity, which is directly related to the cone resistance. The built-in CPT interpretation tool automatically generates a soil stratigraphy based on corresponding cone resistance values. Based on these values the maximum shaft and bearing capacity is determined for different pile tip levels (Appendix A.1). Together with the dimensionless load-displacement curves in NEN9997 (Appendix A.2), the load-displacement curves for specific soil stratigraphy's and pile properties are generated.

**Limitations**

- The settlements obtained by D-Foundations are based on the predefined load-displacement curves in NEN9997. Hence, no soil mechanical properties are incorporated in these calculations.
- The software can only handle pile foundations in Geotechnical Category 2 which are loaded by static loads that cause compressive forces only (Deltares, 2016b).
- Pile group effects are only taken into account by calculation of the negative skin friction. Moreover, only a completely rigid or completely stiff pile cap can be selected for the pile group calculations, which is in most of the cases insufficient.

**Pile groups with D-Pile Group**

D-Pile Group is one of the analytical geotechnical software packages of Deltares specified for pile group calculations. The software enables 3 dimensional analysis of single piles and pile groups as a function of cap loading (Deltares, 2016a). The interaction between piles is incorporated by different interaction models which can be selected by the user. The interaction between pile and soil is described by horizontal and axial springs. The non-linear relationship between force and displacement is given by Dutch design rules or user defined load-displacement curves. Defining the load-displacement behaviour for the base by the Dutch design rules is one of the main advantages of this method compared to most numerical methods. Moreover, the shaft friction is calculated according to equation 3.1 and 3.2. The skin friction model is based on the Dutch design code (EC7-NL) and is similar to the D-Foundations outcome for single pile analysis.

$$Sand: f = \alpha_s \cdot q_c \quad 3.1$$

$$Clay: f = \alpha_s \cdot cu \quad 3.2$$

| | | |
|---|---|---|
| f: | shear resistance | [kN/m$^2$] |
| $q_c$: | cone resistance | [kN/m$^2$] |
| $c_u$: | undrained shear strength | [kN/m$^2$] |

Besides single pile behaviour, D-Pile Group incorporates group effects, which are taken into account by different interaction models. These models can be selected by the user which are standing out in accuracy, calculation effort and interaction possibilities. Ranging from the simple Poulos interaction model towards the more advanced Cap layered soil interaction model which can handle interaction between the pile and the soil in different layers (Figure 3.3). The latter model is the most suitable for pile group calculations in this thesis, since it incorporates interaction among multiple layers and takes into account cross direction interaction effects (3D effects). However, the interaction is only governed by the specified Young's modulus and the Poisson ratio for the specific layer. No installation effects for the shaft are taken into account.

**Limitations**

D-Pile Group is a tool for getting a quick impression about the magnitude of pile settlements. However, there are limitations to this method:

- Excess pore water pressures cannot be generated in the fine-grained materials. This has implications for determination of settlements over time. Because, consolidation and creep effects are not taken into account in case a D-Pile Group calculation is used.
- The 'Cap soil interaction model' uses homogeneous elastic soil properties for pile-soil-pile interaction which is a simplification for the non-linear plastic behaviour of the soil.
- The cap connected to the piles is assumed to be completely rigid. There is no possibility to specify the superstructure stiffness which underpredicts the differential settlement distribution.

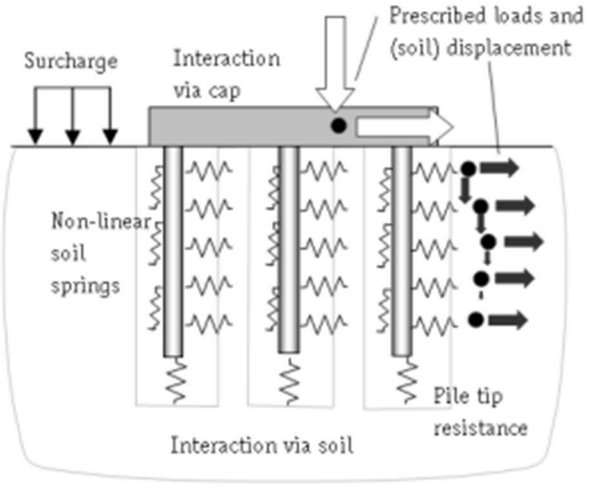


*Figure 3.3: Features in D-Pile Group pile-soil-pile interaction, Cap soil interaction model (Deltares, 2016a)*

### 3.2.2 Numerical approaches for pile settlement modelling

A finite element analysis is a powerful tool to perform settlement analysis on pile foundations (Tschuchnigg, 2013; Gowthaman et al., 2017). Different approaches are available to model a pile or pile group in commercially available software packages. This section gives a short overview about the opportunities and limitations of the different methods.

**Volume pile**

Pile foundations in finite element codes have been modelled with volume piles for a long time. The pile consists of discrete volume elements containing structural properties from the pile like Young's modulus and Poisson ratio. The soil-pile interaction is modelled with interface elements which count for the relative displacement (adhesion and friction between pile and soil). The volume pile gives reliable and accurate results in predicting pile settlements, but numerical stability decreases since large differences in stiffness between the pile and soil elements. This results in problems related to convergences as well as long calculations time due to complex and fine mesh elements. Moreover, since the volume pile is not considered in this thesis, there is no further elaboration and validation of this method included.

**Embedded beam**

The embedded pile formulation is a three dimensional embedded beam element for modelling reinforced geomaterials, first introduced by Sadek & Shahrour (2004). The embedded pile is a line element connected to the continuum with

special interface elements. Moreover, the bearing capacity of the embedded beam is a predefined value which have to be inserted prior to the calculation. So, the maximum bearing capacity is not a result of the soil-pile interaction calculation. The embedded beam have great advantages over other methods since no mesh adaption is necessary and only a few additional nodes are introduced (Septanika et al., 2007) (Engin & Brinkgreve, 2009). The embedded pile method is further discussed in chapter 4.

**Equivalent raft foundation**

For pile group calculations the equivalent raft foundation (Tomlinson, 1977) can be used to obtain foundation settlements (§ 2.4.2). The Tomlinson method is quite straightforward and user friendly, moreover it gives reliable results for soil layers with low compressibility. This method incorporates stress diffusion effects below pile tips in pile groups, i.e. the stresses are spread over an area downwards from the periphery with an angle of 30° in average cases.

The stress distribution underneath the piles can be obtained in different ways. Tomlinson (1977) proposed a method by using diagrams based on depth, surface load, pile dimensions and dimensions of the area where the surface load is acting. Another method to obtain stress and displacement distributions is the use of finite element software. The surface is modelled at $^2/_3$ of the embedded pile length into the stiff bearing stratum. The stress and displacement distribution are determined by the software itself. The settlements of the equivalent raft obtained with the FEM software has to be added to the single pile settlement ($s_1$) according to NEN9997 (2017). The calculation of $s_1$ settlements is currently done by analytical methods like D-foundations.

## 3.3 Eurocode 7 – Including Dutch annex

References to NEN9997 in this thesis, means referring to the Eurocode 7 standards including the Dutch Annex NEN 9997-1 published in 2017. Design of a pile foundations in the Netherlands has to follow the requirements stated in NEN9997 (2017). The goal of this thesis is to improve determination of differential settlements of high-rise building foundations. The prediction of settlements is a framework for the use in daily practical engineering. With this goal in mind, the behaviour of the pile has to fulfil the design requirements of NEN9997. Therefore, this thesis is using the load-displacement curves (Figure 3.4) in NEN9997 for fitting the single pile settlement $s_1$ and combines it to an integral model with $s_2$ settlements. Because, these curves are intended for design proposes, the safe design philosophy is used during determination of these curves. In all cases the curves have to return a safe design irrespective of the location and conditions.

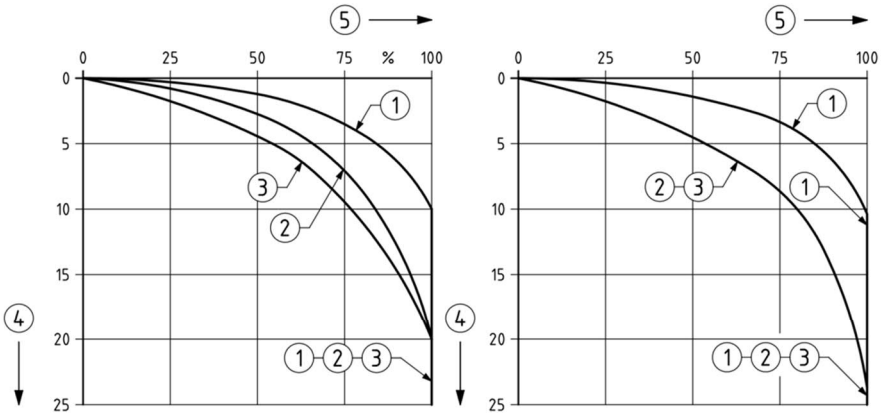


**Legenda**

1 last-zakkingslijn 1 volgens tabel 7.c
2 last-zakkingslijn 2 volgens tabel 7.c
3 last-zakkingslijn 3 volgens tabel 7.c
4 $\frac{s_b}{D_{eq}}$, in %
5 $\frac{R_{b;k}}{R_{b;k;max}}$, in %

**Legenda**

1 last-zakkingslijn 1 volgens tabel 7.c
2 last-zakkingslijn 2 volgens tabel 7.c
3 last-zakkingslijn 3 volgens tabel 7.c
4 $s_b$, in mm
5 $\frac{R_{s;k}}{R_{s;k;max}}$, in %

*Figure 3.4: Load displacement curves NEN9997 (NEN 9997-1, 2017, p. 186)*

## 3.4 Problems in practice

Determination of settlements have always been a difficult exercise in geotechnical engineering and foundation design. Outcomes of calculation methods as proposed in paragraph 2.3 & 2.4 are still not in line with field measurements (Chen,

2011). Design of pile foundations contains a board spectrum of variables and challenges. A distinction can be made between bearing capacity design and settlement-based design calculations. Both methods have their own points of attention and design approaches. Settlement-based design depends highly dependent on the stiffness of the soil along the shaft below the base. However, most of the structures are designed from a strength point of view leading to conservatism in determination of the loads. Which lead in turn to conservatism in settlement predictions. First of all, obtaining a reliable soil parameter set is challenging in every geotechnical project. Inappropriately chosen parameters result in calculation outcomes with either very large or very small settlements relative to field measurements (Chen, 2011). It is still difficult to obtain undisturbed sample parameters from laboratory and/or field measurement tests. Parameter studies for input of calculations is a self-standing research topic and is not addressed in this thesis.

For single pile calculations the settlements are hard to predict since the variety, complexity and regionality in the subgrade reaction of the soil (Chen, 2011). This has partly to do with the limited reliable information about the subsoil as discussed before. Another important problem is the interaction between high-rise buildings and low-rise buildings (different loads, different superstructure stiffness). The amount of differential settlements are of great importance for the construction, even though it is difficult and complex to obtain them. In the meanwhile, computers getting more powerful and numerical methods become more advanced. Large economical and technical benefits can be obtained by using optimization theory and techniques for settlement calculations of high rise constructions (Chen, 2011). During determination of soil displacement pile settlements, the calculation is facing different problems. Besides the soil variety and soil-pile interaction effects, three other aspects have a large influence on settlement behaviour. They are further discussed in this chapter; installation effects, shaft friction and stiffness of superstructure (soil-structure interaction).

### 3.4.1 Residual stresses after pile driving (installation effects)

Installation effects are important for the post-installation settlement response of driven piles in cohesionless soils. Nowadays, installation effects are still not completely understood yet and are not implemented in commercial finite element codes. Important aspects of the installation are; distribution of shaft friction due to cyclic loading, stress state changes around the pile, preloading of the soil and changes of the initial relative density (Beijer-Lundberg, 2014). During installation, the soil experiences large strain and stress changes along the shaft. The modelling of these installation effects is difficult since numerical methods used in practice are not suitable for handling large strains (Broere & van Tol, 2006). Advanced numerical models like MPM which can handle large displacements are currently not completely incorporated in commercially available software packages and are difficult to operate. Therefore, alternative methods have to be found to model installation effects for practical foundation design calculations. A possible method is proposed by Broere & van Tol (2006) and further analysed by Pham (2009). The authors utilized a modelling scheme where the installation effects are modelled without the pile penetration itself. This is possible by applying prescribed displacements in the soil volume before the pile is installed. But, the results show a large sensitivity for the amount of prescribed displacements and are validated for bearing capacity calculations instead of settlement calculations.

Current pile design stimulations in numerical models are using the “wished-in-place” assumption. The initial soil parameters assumed to remain unchanged after installation of the pile. Although, they have an influence on the load-displacement behaviour of the piles after installation.

The soil along the sides and below the base have influence on the behaviour of the pile tip. Literature describes that the pile tip behaves stiffer since the soil underneath and above the pile tip is compressed after installation (Beijer-Lundberg, 2014). The stiffer behaviour is explained by the compressed soil going towards a denser state which results in a higher stiffness and less settlements at equal stress level. The denser state of the soil can be compared with preloading behaviour of soil. During pile installation the soil is (pre-)loaded, after installation of the pile, the soil is loaded according to the stiffer unloading/reloading path.

This effect is used in the current design practice[3], by modelling an artificial layer with higher stiffness properties relative to the original layer. Additionally, this layer is fitted on the behaviour of the soil displacement pile in NEN9997. This method is further explained in chapter 6.

[3] According to design practice at CRUX Engineering BV, Amsterdam

To conclude, most of the pile installation research (Beijer-Lundberg, 2014; Broere & van Tol, 2006; Engin, 2013; Engin et al., 2015; Pham, 2009; Phuong et al., 2014) is performed by modelling the pile as a volume pile in commercial or scientific finite element codes. Modelling installation effects with the embedded pile (Engin & Brinkgreve, 2009) in PLAXIS 3D for example is not conducted yet. This thesis starts off with discovering possible methods to take into account pile installation effects in daily engineering practice. It implies that only common available FEM codes are used for the investigation of this practical framework. Since, it is still difficult to model installation effects, a practical solution is proposed instead of modelling the true installation effects.

### 3.4.2 Stiffness of superstructure (soil-structure interaction)

Zoidi (2015) has investigated the interaction between the geotechnical and structural design process related to the superstructure stiffness. Different model setups have been investigated, each containing a different overall bending stiffness. The calculations have been compared with the available measurement data and a fully structural design model. Zoidi concluded that a simple model with uniform stiffness represented by a basement or small building height above ground level for buildings without basement are accurate enough for the determination of settlements. Zoidi's research has mainly been focused on the influence of structural engineering on the settlements. Therefore, the soil-structure interaction in this thesis is investigated from a geotechnical point of view.

### 3.4.3 Shaft friction

Zoidi (2015) recommends to perform more research on the shaft friction modelling in large pile groups. When PLAXIS 3D is used to calculate settlements, different options are available for modelling shaft friction in combination with embedded piles: linear distribution, multi-linear distribution and layer dependent. These distribution options are part of research topics that has been performed in the past (Lebeau, 2008; Tschuchnigg & Schweiger, 2015). The linear and multi-linear option require input for the maximum shaft and base resistance. With the first two approaches it is possible to manually define envelops over depth in case a layered soil profile is used. However, this is difficult to give reliable results since predicting the capacity of the pile is hard. Because, mobilizing shaft friction depends largely on pile cap stiffness, spacing between piles and load levels (Tschuchnigg & Schweiger, 2015). A solution for this could be the layer dependent option, it uses the strength parameters from the adjacent soil elements around the shaft to calculate the capacity. The advantage of this method is the bearing capacity is a result of the PLAXIS analysis and not an input parameter. In the layer dependent option, the stress changes are automatically taken into account. However, due to the averaging of the stresses, in some cases this option could lead to unrealistic stress distributions and should therefore be used with care. For modelling soil displacement piles, the layer dependent option is not a perfect choice since it uses the initial in-situ stress distribution and does not take into account the residual stresses after installation.

### 3.4.4 Installation effects due to preloading

The stiffer response at soil displacement piles probably caused by installation effects and preloading of the soil. Preloading of the soil occurs during the installation of the pile in order to get the pile deeper in the soil. During the whole installation process the soil below pile tip is constantly preloaded in order to go deeper. After installation the pile is loaded again but, follows the stiffer unloading/reloading stress path. This preloading behaviour is also possible in PLAXIS by simulating the installation by preloading the pile, reset displacements and loading the pile again. Moreover, it is only possible in case a constitutive model is utilised which makes a difference between the primary and un/reloading stiffness. The "preloading" approach is basically equal to increasing the stiffness of a local soil volume below pile tip level. Because of time constrains the preloading/reloading is not further investigated in this thesis.

## 3.5 Conclusion

The settlements are split in three contributions; immediate, primary and secondary settlements. The immediate settlements are governed by single pile behaviour and in daily engineering practice often calculated with analytical methods. For single piles the pile tip and shaft settlements are determined based on the empirical load-displacement curves in NEN9997. The elastic pile compression is calculated over the pile length until the start of the positive skin friction. Moreover, the primary and secondary settlements are calculated with numerical methods. In current engineering practice the pile foundation is modelled like an equivalent raft. However, pile tip, pile shaft and elastic pile compression settlements are not addressed in this method.

The current approach for calculation of the total amount of settlements does not have the possibilities for modeling proper soil-structure interaction. Although, the soil-structure interaction is important for obtaining the correct load

distribution on the pile heads. Currently, this is not completely possible because, the single pile response is calculated in different (analytical) software. Since finite element methods have been proven to be a reliable and widely used method for modeling foundations of high-rise buildings around the world (Katzenbach & Leppla, 2015; Tschuchnigg, 2013), this could be a suitable method for proper soil-structure interaction in part III in this research.

Different ways of pile modeling are possible in numerical methods: e.g. the volume pile and embedded beam approach. The latter approach shows reliable results with efficient calculation costs compared to volume piles. Using the embedded beams make soil-structure interaction in numerical methods possible. However, this method is not utilized yet for soil displacement piles because, installation effects are not incorporated. The embedded beam method is designed and validated for the non-soil displacement bored pile.

In case soil-structure interaction is modelled properly, loads from the superstructure are redistributed in the foundation plate and transferred to the pile heads. The bending stiffness of the foundation plate has a significant influence on the redistribution of these loads. A fully flexible plate results in large differential settlements between the piles. On the other hand, a completely stiff plate does not show differential settlements due to maximum redistribution of loads in the plate.

To conclude, by taking into account single pile behaviour of soil displacement piles together with group effects and bending stiffness in one calculation approach, makes it possible to model proper soil-structure interaction. Important points of attentions are residual stresses in the soil after installation, the shaft friction model of the embedded beam and modelling of the superstructure bending stiffness.

# 4 Embedded pile formulation

Different approaches exist for settlement calculations of high-rise buildings founded on piles. A couple of these approaches have been discussed in chapter 2. One of them is the numerical method in combination with finite elements. Two different modelling approaches are possible for foundation piles: either with volume piles or embedded piles (beams). The volume pile is a well-known method developed over the last decades for simulating pile foundations in FEM calculations. The volume pile is modelled with explicitly continuum finite elements containing the properties of the pile, for example the stiffness and pile-soil interface conditions. Although, design problems related to high-rise buildings contain often large pile groups. In case this is modelled with volume piles, the calculations become complex and instable. This is where the embedded pile concept comes in. The embedded pile is an efficient method to reduce complexity and prevent numerical instability problems. Moreover, embedded beams are not explicitly modelled which saves al lot of computation costs (Tschuchnigg & Schweiger, 2015). Chapter 4 explains the embedded pile formulation in more detail and combines the different aspects of high-rise building pile foundations.

## 4.1 Development embedded pile formulation

### 4.1.1 Embedded beam by Sadek & Shahrour

The formulation of the embedded beam model is initially proposed by Sadek & Shahrour (2004). The authors originally developed the embedded beam formulation for reinforced geomaterial problems. The embedded beam formulation contains 3D solid elements, beam elements which can cross each other at an arbitrary location with an arbitrary inclination and non-linear springs at the pile base for describing the base resistance (visualised in Figure 4.1). The beam element remains a line structure, although in the soil elements around a pile element plasticity is disabled.

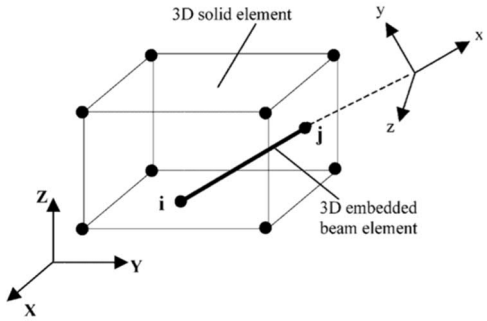


*Figure 4.1: Visualization embedded beam formulation (Sadek & Shahrour, 2004)*

Nodes from the beam elements are always generated when crossing the boundaries of solid elements. The nodes from the beam element can be considered as virtual nodes inside the solid element. Still, beam elements have to be formulated but their stiffness contribution is directly added to the soil elements, which saves computational costs in comparison with volume piles. There are two ways of connecting beam nodes to soil nodes. Without interfaces: The virtual pile nodes are directly expressed in element shape functions. With interfaces, the interface connects the real pile nodes to corresponding virtual nodes in the soil element. These interface elements allow relative displacements between the soil and the pile nodes. The displacements are linked with the stiffness of the interface by the bonding force vector (eq. 4.1).

$$\Delta u^{\text{int}} = u^b - u^s \tag{4.1}$$

$$F^{\text{int}} = C^{int} \cdot \Delta u^{\text{int}} \tag{4.2}$$

$$C^{\text{int}} = \begin{pmatrix} K_t & 0 & 0 \\ 0 & K_n & 0 \\ 0 & 0 & K_n \end{pmatrix} \tag{4.3}$$

$\Delta u^{int}$ relative displacement vector
$u^b$, $u^s$ Respectively beam and soil displacement
$F^{int}$ Nodal force at interface vector
$C^{int}$ interface stiffness matrix

In matrix 4.3 $K_n$ and $K_t$ are the stiffnesses of the interface elements in the normal and tangential direction respectively. With this method, no mesh alignment is needed between the soil domain and beam elements. Moreover, it is not necessary for the beam nodes to coincide with the solid nodes. This results in more efficient meshing and modelling of the pile elements. However, the method has its limitations. In case a very small mesh size is chosen, elements inside the pile radius can cause stress singularities. This implies the embedded beam formulation by Sadek & Shahrour (2004) behaves mesh sensitive (Smulders, 2018).

### 4.1.2 Implementation in PLAXIS 3D

The embedded beam formulation in PLAXIS 3D is based on Sadek & Shahrour (2004). However, there are some differences between both formulations, these are addressed in this paragraph. In the current formulation, beam elements are modelled as 3 noded line elements in combination with 3 dimensional 10 noded tetrahedral elements for the solid elements (Septanika et al., 2007). The interaction between the pile and the soil is modelled with interface elements similar to the formulation by Sadek & Shahrour (2004). The 3 noded skin interface elements containing pairs of nodes instead of single nodes. One side of the nodes belong to the beam, the other one is a virtual node used to interpolate the soil displacements.

**Interface elements**

The interface between the soil and the pile is described by the skin traction vector along the beam axis (**t**) and the stiffness matrix of the embedded interface elements as showen in equation 4.4.

$$\begin{bmatrix} t_s \\ t_n \\ t_t \end{bmatrix} = \begin{bmatrix} K_s & 0 & 0 \\ 0 & K_n & 0 \\ 0 & 0 & K_t \end{bmatrix} \begin{bmatrix} u_s^b - u_s^s \\ u_n^b - u_n^s \\ u_t^b - u_t^s \end{bmatrix} \tag{4.4}$$

The stiffness of the interface elements should not influence the total elastic pile-soil structure. This is needed to ensure the pile behaviour is only governed by the stiffness of the surrounding soil and the interface is only modelling plastic slip between pile and soil. To fulfil the requirements stated before, $K_s$ should be chosen high compared to $G_s$.

$$K_s = \frac{R_{\text{inter}}^{\ 2}}{t_i} \cdot G_S \quad \text{or} \quad K_s = 50 \cdot G_S \tag{4.5}$$

$$G_S = \frac{E}{2 \cdot (1+\nu)} \tag{4.6}$$

$$K_n = K_t = \frac{2 \cdot (1 - \nu_i)}{1 - 2 \cdot \nu_i} \cdot K_s \qquad 4.7$$

Figure 4.2 shows the orientation of all the different stiffnesses related to the embedded beam. The pile foot response (pile tip) is described by a linear elastic perfectly plastic interface element in expression 4.8. The stiffness of the foot is given in eq. 4.9, where $R_{eq}$ is the equivalent shaft radius according eq. 4.15. Moreover, the force applied at the foot is transmitted to one single node which inserts mesh dependency.

$$F_{foot} = K_{foot} \cdot (u^{b}_{foot} - u^{s}_{foot}) \leq F_{\max} \qquad 4.8$$

$$K_{foot} = 50 \cdot G_s \cdot R_{eq} \qquad 4.9$$

| | |
|---|---|
| $G_s$ | Shear modulus soil |
| $K_{foot}$ | Interface base stiffness |
| $K_s, K_n, K_t$ | Axial, normal and transversal interface stiffness along shaft of the pile |
| $u_b$ | Displacement beam |
| $u_s$ | Displacement solid |
| $F_{foot}$ | Force at foot pile |
| $R_{eq}$ | Equivalent pile radius |
| $t_i$ | Virtual thickness |

In case the shear stresses along the pile are below the maximum skin friction, elastic behaviour will occur.

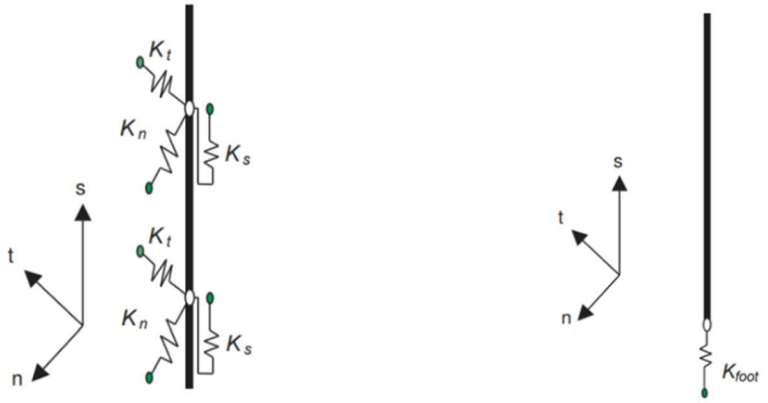


*Figure 4.2: Interface stiffness orientations (Smulders, 2018)*

The interface stiffness is revised and updated by Tschuchnigg (2013) by making the interface stiffness independently from the shear modulus of the soil. It allows to define axial stiffness apart from the normal/tangential stiffness.

**Definition skin resistance**

Currently, three methods are available for the definition of ultimate skin resistance along a pile: linear, multi-linear and layer dependent. For these methods the maximum skin friction has to be inserted manually. The different options are discussed below:

- The linear option requires input for skin resistance at the top and at the bottom, between the top and the bottom the values are interpolated linearly.
- In the multi-linear option, the user can insert at different locations around the shaft skin resistance values. Between the inserted values, the envelop is interpolated linearly.
- In the layer dependent option, the shear stress is obtained from the strength parameters and normal stresses of the adjacent soil layer. In this option, the elastic behaviour will continue along as eq. 4.10 holds on.

$$\left|t_s\right| < (c_i - \sigma_n^{avg} \cdot \tan(\varphi_i)) \cdot 2 \cdot \pi \cdot R_{eq} < t_{s,\max} \quad 4.10$$

Where:

$$\sigma_n^{avg} = \frac{\sigma_t' + \sigma_n'}{2} \quad 4.11$$

The strength reduction factor $R_{inter}$ is an input value and is used to reduce the strength parameters at the interface elements from the original layer properties as shown in eq. 4.13 & 4.14.

$$\tau_i = c_i + \sigma_n' \tan(\varphi_i) \quad 4.12$$

$$\tan(\varphi_i) = R_{inter} \cdot \tan(\varphi_{soil}) \quad 4.13$$

$$c_i = R_{inter} \cdot c_{soil} \quad 4.14$$

$t_{s,(max)}$ (Ultimate) shear traction at the interface
$R_{inter}$ Interface reduction factor
$\tau_i$ Shear stress in the interface

**Elastic zone approach**
In order to reduce mesh sensitivity in the formulation by Engin et.al (2007) the elastic zone approach is introduced. The mesh sensitivity introduces numerical instability problems for fine meshes and results in large displacements. In order to overcome the mesh sensitivity, a zone around the pile diameter is introduced and forced to behave elastic. This influence area is evaluated according to equation 4.15.

$$R_{eq} = \max\left\{\sqrt{\frac{A}{\pi}}, \sqrt{\frac{2 \cdot I_{avg}}{A}}\right\} \quad 4.15$$

$$I_{avg} = \frac{I_2 + I_3}{2} \quad 4.16$$

$R_{eq}$ Equivalent pile radius
A Pile cross section area
$\varphi_i$ Friction angle interface elements
$c_i$ Cohesion interface elements
$R_{eq}$ Equivalent pile radius
$I_{avg}$ Average moment of inertia for pile
$I_2$,$I_3$ Moment of inertia of pile two cross-sections perpendicular to pile axis

**Limitations**
The current embedded beam formulation has its limitations on different aspects (Smulders, 2018):

- Installation effects are not taken into account, which makes it not possible to capture real soil behaviour around the pile perimeter.
- Although, the elastic zone approach is introduced, the current formulation is still mesh sensitive.
- Stress singularities at pile tip level due to the single stress point at the pile foot.

## 4.2 Validation of embedded beam

The existing embedded pile method in PLAXIS 3D has been validated in several studies, e.g. Engin and Brinkgreve (2009) and Engin et al. (2008). These validation studies show an reasonable outcome for the behaviour of the embedded pile in comparison with other approaches; e.g. calculations or field measurements from pile tests (Tschuchnigg & Schweiger, 2015). However, these validation studies are based on bored piles which have a softer response because, no major installation effects occur. This thesis investigates the prediction of settlements from soil displacement piles which implies a large influence from installation effects.

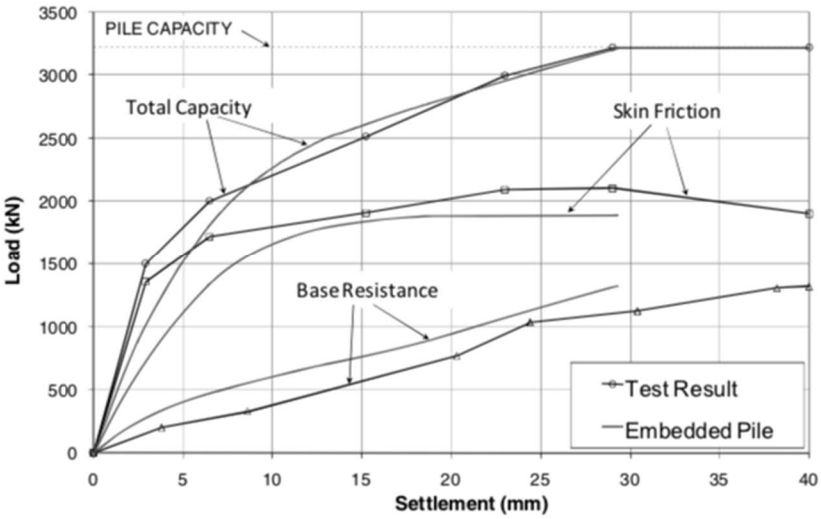


*Figure 4.3: Load-displacement curves for bored pile load tests and embedded piles (Engin & Brinkgreve, 2009)*

## 4.3 Pile group effects and embedded piles

Single pile cases are rare in high-rise building foundations, most of the time pile group effects have to be taken into account. Moreover, the response of a pile group is often an extrapolation of the single pile response by an interaction factor between two piles or pile group (Ju, 2015). Paragraph 2.4 describes the influence of piles on neighbouring piles during installation and loading. Engin & Brinkgreve (2009) stated that the response of a pile group is not equal to the multiplication of the response of one single pile in case a layer dependent shaft friction model is used. In the same paper, the authors show that the spacing between piles in a group has influence on the response of the pile group during numerical calculations with embedded beams. This paragraph gives a brief overview of the research on pile groups with embedded piles in finite element codes.

### 4.3.1 Capacity pile groups

For different spacings between piles: the piles modelled with a larger spacing, have a stiffer response. Subsequently, the response is less stiff with closely spaced piles. A reason could be the overlapping stress influence regions of the pile shaft. The shaft friction of the inner piles is limited due to overlapping stress zones from adjacent piles. Only the corner and edge piles are able to generate more shaft friction from the adjacent soil elements. Engin et al. (2008) modelled embedded beams with different spacings in combination with the layer dependent shaft friction model. By increasing the pile spacing, the load-settlement behaviour gets stiffer. This endorses the statement about the reduced capacity of a pile group compared to single piles.

### 4.3.2 Cap stiffness influence

Distribution of loads from the superstructure depends on the bending stiffness of the foundation and the superstructure. Subsequently, distribution of loads into the soil body depends on the stiffness of the cap (Poulos & Davis, 1980). Poulos & Davis divided two extreme situations:

- Equally divided loads with flexible cap
- Equally divided settlements with rigid cap

In practical engineering a fully rigid and fully flexible cap are not realistic and are therefore only be theoretical cases. A more practical response of the soil-structure interaction is somewhere in between flexible and rigid. Therefore, different stiffness cases are investigated in part III for the influence on individual pile settlements.

## 4.4 Improved embedded beam formulation

In order to overcome the limitations of the embedded pile stated in section 4.1.2, Smulders (2018) improved the current embedded beam formulation for PLAXIS 3D. The formulation, first developed by Turello (2016) and later used in Smulders (2018), includes explicit interaction surfaces to overcome mesh sensitivity and stress singularities of the current embedded beam formulation.

**Soil displacement**

The new formulation uses explicit interaction surfaces for modelling slip behaviour at the pile circumference. Therefore, interaction between the pile and the soil is evaluated at the pile circumference instead of along the centreline. The explicit interaction surface makes it possible to model beam and soil displacements at the outer pile diameter instead of at the line axis. For the evaluation of soil element displacement at the circumference of the pile (interaction surface), the interpolation is visualized in Figure 4.4.

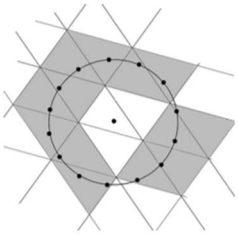

*Figure 4.4: Graphical representation of interaction surface (Smulders, 2018)*

**Shaft interface**

The soil-pile interaction in the new formulation is described at the pile circumference instead of along the pile axis. Therefore, a double integral is taken: one over the length (existing formulation) and one over the circumference of the pile (new formulation). The latter step makes the difference between the old and new formulation. The interface stiffness matrix ($D^{int}_{new}$) becomes:

$$D^{\text{int}}{}_{new} = \frac{D^{\text{int}}}{2 \cdot \pi \cdot R} \tag{4.17}$$

$D^{int}$ Interface stiffness matrix

In order to facilitate slip at the pile circumference, a maximum value for the allowable stress has been defined. Section 3.4.3 already described different shaft interface models: linear, multi-linear and layer dependent. The layer dependent option has a shaft friction capacity obtained from the finite element calculation itself instead of a manually inserted value. The maximum allowable shear traction at the interface in this shaft friction model is defined in eq. 4.18.

$$\sqrt{\sigma^2{}_s + \sigma^2{}_t} \leq c_i - \sigma_n \cdot \tan\varphi_i \tag{4.18}$$

$\sigma_s$, $\sigma_n$, $\sigma_t$ Stress components interaction surface in local coordinate system

**Foot interface**

The mobilization of the base resistance should primarily depend on the pile tip stiffness. Tschuchnigg (2013) showed that the stiffness of the pile tip has to increase in order to improve the load-settlement curve for reducing the amount of settlements needed to mobilize base resistance. Therefore, the foot interface of the embedded beam is described as a line (circle) with multiple points instead of one single stress point (visualized in Figure 4.5). Now, the base resistance contribution becomes a stress instead of a force by dividing the force over the area of the pile tip ($\pi R^2$).

$$\sigma_{foot} = \frac{K_{foot}}{\pi R^2} \cdot u_{rel,s} \leq \frac{F_{max}}{\pi R^2} \quad 4.19$$

$\sigma_{foot}$ stresses at foot interface

Where the foot stiffness is evaluated as:

$$K_{foot,new} = \frac{50 \cdot G_s \cdot R}{\pi R^2} = \frac{50 \cdot G_s}{\pi R} \quad 4.20$$

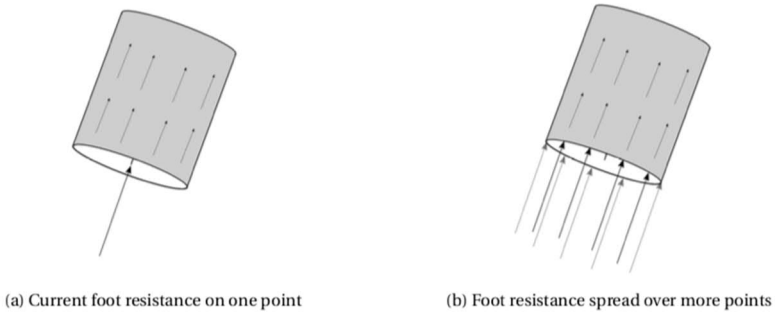


*Figure 4.5: Visualization of foot resistance (Smulders, 2018)*

Formulation of stiffness at the shaft and the base:

$$K_{foot} = 50 \cdot G_s \cdot R_{eq} \cdot \Gamma_{foot} \quad 4.21$$

$$K_s = 50 \cdot G_s \cdot \Gamma_s + \Delta_s \quad 4.22$$

$$K_n = K_t = 50 \cdot G_s \cdot \frac{2 \cdot (1 - \nu_i)}{1 - 2 \cdot \nu_i} \cdot \Gamma_n + \Delta_n \quad 4.23$$

$\Gamma_s$ Multiplier for shear modulus of axial stiffness
$\Gamma_n$ Multiplier for normal stiffness
$\Gamma_{foot}$ Multiplier for foot stiffness
$\Delta_s$ Direct input values added to $K_s$
$\Delta_n$ Direct input values added to $K_n/K_t$

## 4.5 Conclusion

Chapter 4 discussed the difference between the current and new embedded beam formulation in PLAXIS 3D. The new (improved) embedded beam formulation has several advantages over the existing formulation. For example, the mesh sensitivity is reduced and the behaviour at the base is less susceptible for stress singularities. This new formulation of the embedded beam reduces the need of the volume pile even more.

The volume pile approach is accurate in settlement predictions but requires a lot of computation costs and causes potentially numerical instabilities due to the sharp stiffness changes at the pile-soil interfaces. Where the embedded beam is a practical and powerful tool for calculation of large pile foundations since the piles are not explicitly modelled. Therefore, in the upcoming chapters the new embedded beam is used to investigate the suitability of modelling both $s_1$ and $s_2$ settlements according to NEN9997 in one calculation method.

For describing the shaft friction of the embedded beam in PLAXIS 3D, three different methods are available (linear, multi-linear and layer dependent). In the multi-linear distribution is a predefined maximum value required for the bearing

capacity. In the layer dependent option, the shaft friction is a result of the PLAXIS calculation itself. Suggested is that the multi-linear skin friction distribution is the most suitable for this application since more freedom is allowed by defining the capacity of the shaft (it is an input parameter). The maximum strength can be modified by a value for taking into account soil displacement effects on the shaft friction capacity. However, effects by increase of residual stresses between piles in a group are not taken into account with the multi-linear shaft distribution.

Finally, a secondary effect of the new embedded beam formulation is the increase in load-displacement stiffness at the base. This effect is favorable when soil displacement piles are modelled. Since these piles have a stiffer load-displacement response compared to bored piles for example.

# II Parametric study

# 5 Model setup single pile

Chapter 5 discusses the geometry, boundary conditions, constitutive model choice and soil parameter derivation of the single pile model in chapter 6. The current and new formulation of the embedded beam is investigated with PLAXIS 3D containing equal properties and geometry. In other words, all the input parameters are equal, only the embedded beam formulation has been changed.

## 5.1 Geometry & calculation settings

The used geometry, numerical control parameters and boundary conditions of the PLAXIS 3D calculations are presented in appendix B.3. The boundaries are far away enough in order to not influence the results. Moreover, a mesh refinement of 0.5 is applied around the pile perimeter, the location is indicated in Figure B.5.

**Calculation settings**

The calculation outline of the incremental loading in the staged construction part of PLAXIS 3D is presented in Table B.16, appendix B.3.7. In order to obtain smooth results between the different load steps, settlements are always calculated from the initial phase onwards. Moreover, each calculation stage is allowed to use one core, which makes it possible to run calculations parallel on the 8-core processor, resulting in less calculation time.

## 5.2 Soil stratigraphy

Soil profiles in engineering practice are often heterogenous, containing different kind of sand and clay layers. Heterogeneity of the subsoil is an isolated problem in describing differential settlements of pile foundations. This thesis is focussing primarily on the modelling of settlements. Therefore, an extensive research on heterogeneity in soil profiles is not included. In the first calculations, a 'simplified' soil stratigraphy is used to get a better understanding of the processes that occur during axial loading of a single pile in PLAXIS 3D (Figure 5.1). Second, a more advanced (heterogenic) soil stratigraphy is used, based on the average soil stratigraphy of Amsterdam. The latter is more adopted to daily engineering practice since it is more realistic to have various soil layers (Figure 5.2).

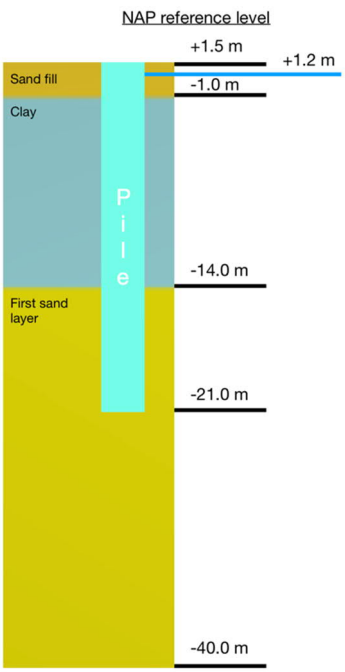


*Figure 5.1: Simplified soil stratigraphy layout*

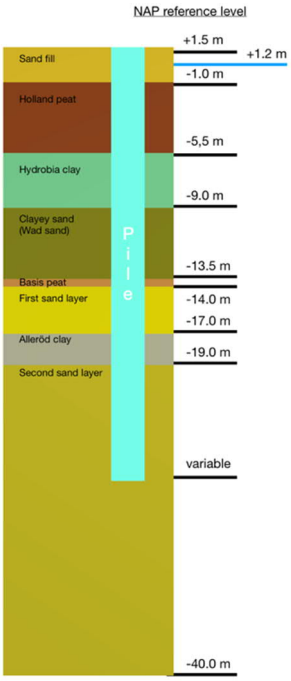


*Figure 5.2: Advanced soil stratigraphy*

Most of the high-rise building projects in Amsterdam have a pile tip level in the second sand layer, which is needed for meeting the requirements on bearing capacity and amount of settlements. Therefore, in the single pile model the pile tip level is set on -21 meter relative to NAP, which is a practical pile tip level in practice. The layering for the advanced soil stratigraphy is based on data from several high-rise building projects in Amsterdam.

### 5.2.1 Water levels

The water level in both soil stratigraphy's is set on +1.2 meter NAP, it implies a phreatic line of 0.3 meter below surface level. This kind of water levels are common in the western part of the Netherlands and are representative for this analysis. The water pressure distribution in the model is set hydrostatic to keep the stress distribution easy to analyse.

## 5.3 Soil model

Mechanical soil behaviour in PLAXIS 3D is governed by constitutive models with different levels of accuracy (Brinkgreve, 2018a). A large variety of constitutive models is available and requires understanding of which stress-strain relationship are most suitable for the related soil mechanical problem. More advanced models contain features like stress level dependent stiffness, strain softening/hardening, critical state behaviour, memory of pre-consolidation pressure and creep for example. For this thesis, three different constitutive models are investigated for their suitability. HSsmall and Hypoplasticity are presented in this chapter, the Soft Soil Creep model is discussed in chapter 7.

### 5.3.1 Hardening soil small strain model (HSsmall)

The HSsmall model accounts in addition to the normal Hardening soil model for increasing stiffness during small strain regimes. The advantage relative to the normal Hardening Soil model is the more accurate results under working load levels. Since settlement calculations are most of the time required under working load conditions, the HSsmall model fits this situation.

The Hardening Soil small strain model has a non-linear stress-strain behaviour defined by three different stiffness contributions. The triaxial loading stiffness ($E_{50}^{ref}$) is evaluated at 50% of the maximum load. Triaxial unloading and reloading stiffness is obtained during unloading/reloading stress paths ($E_{ur}^{ref}$). The Oedemeter stiffness ($E_{oed}^{ref}$) is obtained during Oedemeter tests at reference stress levels. The different stiffness contributions results in different stress path envelops during different types of unloading/reloading. Additionally, the power law (m) in the Hardening Soil small strain model gives a measure for the relation between stress and strain in axial loading (Brinkgreve, 2018b). Other features of the HSsmall model are listed below:

- Stress dependent stiffness with power law

- Hyperbolic stress strain relation in axial loading situations
- Elastic unloading/reloading behaviour
- Mohr-coulomb failure citerium
- Small strain stiffness behaviour
- Shear hardening
- Compaction hardening

**Limitations**
The Hardening Soil model reaches immediate residual strength, no peak strength and softening behaviour is incorporated. However, this is not of great importance since the displacements are calculated in serviceability limit state load levels. Peak strength values will not be reached during SLS load situations.

Moreover, no creep behaviour is incorporated in the HSsmall but, in the single pile model the layers above pile tip level are not suffering from secondary compression effects since these effects are relatively small in comparisons with immediate and primary compression (see § 2.2). Chapter 7 discusses time dependent effects of the soil layers below pile tip level which are prone to creep.

Void ratio changes have influence on the density of the soil during and after pile installation. Pile installation in a soil displacement manner densifies the soil around the pile. A constitutive model with void ratio as state parameter would be more sufficient for modelling pile installation effects. Since it can take into account different density states. A model containing this function is for example the Hypoplasticity model. However, even more advanced models like Hypoplasticity are used in research settings and are not common in (Dutch) engineering practice. Moreover, parameter determination is difficult because, since most of them have no direct relationship with common soil mechanic tests.

### 5.3.2 Hypoplasticity model
Another advanced model which is suitable for modelling pile foundations is the Hypoplasticity model. In addition to the HSsmall and SSC model, the Hypoplasticity model contains (Brinkgreve, 2018a):

- void ratio dependent stiffness
- strength and dilatancy behaviour
- intergranular strain concept and a Matsuoka-Nakai failure criterion

Due to the void ratio dependency, the model is useful for modelling pile installation effects. Since void ratio and density changes are occurring during installation of piles in a soil displacement manner (Broere & van Tol, 2006).

**Limitations**
The Hypoplasticity model contains a couple of soil parameters which are difficult to determine. They are not directly linked to common laboratory or field tests. In daily engineering practice this is one of the main disadvantages because, experienced users do not have any knowledge and experience with these kind of model parameters. Besides the model parameter determination, the parameter set is only suitable for particular stress ranges (Brinkgreve, 2018b). For high stress levels grain crushing and suppression of dilatancy will occur.

### 5.3.3 Constitutive model choice
Since this thesis tries to achieve a practical solution for modelling accurate pile deformations, the Hardening Soil small strain model is the most applicable option. Because, the soil parameters are relatively easy to obtain in practical situations and a lot of experience is already available by current users. Where the Hypoplasticity model is not commonly used yet and contains soil parameters which are difficult to obtain. Moreover, the HSsmall model is suitable for the used soil layers (peat, clay and sand). Important features for pile modelling are included: stress dependent stiffness, hyperbolic stress strain relationship and shear hardening. Especially, stress dependent stiffness is important because, the amount of settlement is highly influenced by the soil stiffness. So, large stress increment's due to high foundation loads results in a considerable increase of stiffness and therefore in less settlements. A single pile is loading a certain

area underneath the pile tip, where a pile group is loading the same area but with a higher stress due to the loads of the neighbouring piles (Figure 5.3).

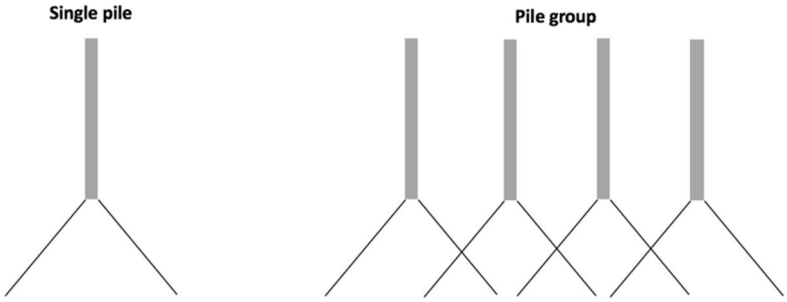


*Figure 5.3: Explanation stress-dependent stiffness single piles/pile groups*

The choice for the Hardening Soil small strain model implies that features like void ratio dependent stiffness and softening by dilatancy are missing in the analysis of this thesis (explained in chapter 2). The missing feature 'void ratio dependent stiffness' implies that during the change of the density the stiffness is not increasing and have to be updated manually. Moreover, softening is of importance in case dense sands are encounter in the soil stratigraphy. Loading of dense sands causes dilative behaviour which is not incorporated in the HSsmall model.

## 5.4 Soil properties

This thesis is not focussing on soil parameter determination or variations in soil parameters and therefore uses whenever possible a standard parameter set without taking into account soil variability.

Since both D-Foundations and PLAXIS 3D software is used, this section is divided in two subsections. Both software programs use different information as input for the calculation. PLAXIS 3D is based on constitutive model parameters were D-Foundations uses cone resistance values from CPT data as input.

For the sake of simplicity, negative skin friction is not taken into account during the calculations in this thesis. In the Holocene soft soil layers on top, negative skin friction is developed over time. However, high-rise buildings transfer often high foundation loads in the soil compared to the negative skin friction contribution. Therefore, it is realistic to disregard the negative skin friction as additional load on piles.

| | Start positive skin friction | Skin friction |
|---|---|---|
| Simplified | -14 [m] | 386 [kN/m] |
| Complex | -14 [m] | 365 [kN/m] |
| Complex long pile | -14 [m] | 373 [kN/m] |

*Table 5.1: Skin friction position and contribution PLAXIS 3D models*

Table 5.1 shows the absolute value of the skin friction is more or less increasing linear over time. It implies no additional soil mechanisms are taken into account in de D-Foundations calculation like soil dependent stiffness.

### 5.4.1 D-Foundations

In D-Foundations the cone resistance of the CPT test is used to calculate the bearing capacity of single piles according to the method described in appendix A.1. Moreover, the settlements related to a certain bearing capacity of the pile is predefined in load-displacement curves in NEN9997. These curves are also depending on the pile diameter.

In order to make a good comparison between the PLAXIS 3D and D-Foundations calculation an artificial CPT is constructed by the author with three clearly horizontally separated layers. In this artificial CPT the cone resistance is derived from an existing CPT and adopted to the desired soil stratigraphy. The CPT is still based on real soil data but fitted towards a predefined soil stratigraphy (sand-clay-sand). Moreover, since the positive skin friction in the clay layer is not taken into account and the cone resistance in the sand layer is limited to a maximum of 15 MPa, different CPT data does not have a lot of influence on the outcome of the bearing capacity calculation. The CPT is presented in appendix B.1.

The advanced soil stratigraphy corresponds to a 'real' soil stratigraphy with different soft soil layers. The CPT presented in Figure 5.2 is selected from a project in Amsterdam. The CPT is analysed based on the NEN-rule with the build-in CPT interpreter in D-Foundations.

### 5.4.2 PLAXIS 3D

The required soil parameters for the PLAXIS 3D calculation depend on the used type of constitutive model. Calculations with single piles are performed with the Hardening Soil small strain (HSsmall) model. Further elaboration about the choice for this model is given in § 5.3.

The soil model parameters for the HSsmall model are relatively easy to obtain from standard tests. In practice, most of the time standard parameters sets are used typical for the region where the project is situated. These data sets are validated in several projects and have proven to be reliable for the facing ground conditions in this area. The soil parameters used in the single pile calculation are taken from the North – South line parameter set. The used correlations between the model parameters and soil properties are shown in appendix B.3.

## 5.5 Pile characteristics

Due to the high foundation loads of high-rise buildings in combination with deep bearing layers in The Netherlands, screwed pile types with lost foot (Fundex) are often used. This pile type can relative easily be installed at large depths due to lubrication possibilities during installation at the pile shaft. The pile properties and pile class factors defined in NEN9997 for Fundex piles are summarized in Table 5.2.

| Pile type | Installation method | Diameter | NEN9997 factors |
|---|---|---|---|
| Screw pile with lost foot | Soil displacement | ⌀ 460/560 mm | $\alpha_p$ = 0.63 |
| | Grout injection (reduced friction) | | $\alpha_s$ = 0.009 |
| | In situ concrete | | s = 1,0 |
| | Withdrawn steel casing | | $\beta$ = 1,0 |
| | Lost foot | | |

*Table 5.2: Pile properties Fundex, single pile model*

In the simplified and advanced soil stratigraphy, the pile head is fixed at +1.5 m relative to NAP in order to make the results comparable with each other. In the advanced model, the pile tip is always situated in the second sand layer in order mobilize enough bearing capacity.

### 5.5.1 Pile loading

The geometric top node of the embedded beam is loaded through a connected point load. The load is increased in by several steps in order to construct a load-displacement curve with enough data points. Since displacements are most of the time calculated in the serviceability limit state, the focus will be on this stress range. A complete outline of the phasing and calculation types in each stage is summarized in Table B.16.

## 5.6 Different methods single pile behaviour

Chapter 3 describes different methods which are used in daily Dutch Engineering practice for calculations of pile settlements. Paragraph 5.6 is combining this information for single pile models in D-Foundations and PLAXIS 3D.

### 5.6.1 NEN9997 curves

The bearing capacity of piles can be obtained according to a couple of methods described in NEN9997: pile load test data on site, soil investigation based on CPT data, dynamic pile tests, wave equation analysis or pile driving correlation. In the Netherlands it is common to use CPT data in order to derive the bearing capacity of piles. Therefore, this section briefly discusses how to the derive bearing capacity from cone resistances data.

The capacity of the pile is divided in base and shaft resistance, both are derived separately from each other. The maximum capacity of both components in one CPT is superposed (eq. 5.1).

$$R_{c;cal;i} = R_{b;cal;\max;i} + R_{s;cal;\max;i} \qquad 5.1$$

Further derivation of the bearing capacity equations can be found in appendix A. The capacity below pile tip level is derived according to equation A.8. This equation includes factors related to the pile type ($\alpha_s$), foot surface ($\beta$), cross-section geometry(s) and interpolated values of the cone resistance over a specific length. The shaft resistance is calculated by integrating the cone resistance over the length of the pile times the circumference.

After the bearing capacity is calculated and no pile load tests are available for the specific site, the displacements can be calculated with empirical, normalised load displacement curves from NEN9997. These curves (Appendix A.2) require as input the maximum pile tip resistance, maximum shaft resistance and the equivalent pile diameter.

**Assumption**
NEN9997 load-displacements curves are empirical relationships based on field test data and therefore are not representing specific soil mechanical principles. However, all foundation designs in the Netherlands have to meet the standards written in the NEN9997. Therefore, it is a reasonable assumption that NEN9997 load-displacement curves are a conservative approach and, in terms of foundation design, can be considered as representing reality from a design perspective.

This assumption implies that comparisons with real measurement data could still deviate from the design model, because the reliability of load-displacement curves in EC7 are considered as conservative enough to apply to all foundations in the Netherlands. Therefore, the design values should always lead to larger deformations compared to the measurements

### 5.6.2 D-Foundation
In the Netherlands it is common to relate the bearing capacity on site-based CPT data. Therefore, the D-Foundations calculation is a useful tool to obtain the bearing capacity at different depths. Since PLAXIS 3D requires input data regarding bearing capacities of the pile, the D-Foundations calculation is still required as an input for PLAXIS 3D calculations with embedded beams.

The CPT interpreter in D-Foundations analyses the CPT data and returns the soil stratigraphy and correlation factors among different CPT's. It is discussable if all the safety factors should be set to 1.0 in case the D-Foundations calculation is used as input for PLAXIS. The finite element calculation in PLAXIS runs without taken into account safety or reduction factors for pile behaviour and variation in soil stratigraphy. The author's opinion is to set the safety factors to 1 in D-Foundations to make a fair comparison between both models since PLAXIS software is designed for SLS situations.

### 5.6.3 PLAXIS 3D
The embedded beam function in PLAXIS 3D requires input for the total bearing capacity. This input comes from the previous mentioned D-Foundations calculation because, PLAXIS is not able to calculate the ULS capacity. Moreover, the settlements are calculated in SLS and will not reach the ULS load levels.

**Current embedded beam**
First, the current embedded pile formulation in PLAXIS 3D described in section 4.1.2 is used. The simplified geometry is analysed to get a better understanding of the embedded pile behaviour in PLAXIS 3D. Moreover, a first fit of the parameters in combination with different skin friction distributions is conducted to analyse the differences. Second, the more advanced stratigraphy is used to fit the pile behaviour on the NEN9997 curve.

**New embedded beam**
In the hypothesis is proposed a better load-displacement behaviour for axially loaded piles in combination with the new embedded beam formulation. Therefore, exactly the same PLAXIS 3D models are used for testing both formulations to investigate the improvements between the current and new formulation.

# 6 Single pile results

Chapter 6 discusses the results of the single pile analysis, both the current and new embedded beam formulation are included. First, the load-displacement response of NEN9997 is discussed. D-Foundations is used to obtain the shaft and base resistance of the simplified and complex soil stratigraphy (§ 5.2). Subsequently, the shaft and base resistance is used to construct the dimensionless load-displacement curve according to NEN9997.

Second, a comparison with respect to the NEN9997 load-displacement curve is made between the current and new embedded beam formulation. An explanation is given why the response is different from the response according to NEN9997. Third, a parameter fit is conducted to get the single pile behaviour in line with the NEN9997 design standards for soil displacement piles. In the parameter fit is focused on increasing the stiffness parameters in a defined soil volume around pile tip depth. Finally, a roadmap is presented, and conclusions are drawn on the best possible fit that can be obtained with the proposed method.

**Explanation calculation name system**
The used variations in the soil profile and pile characteristics can be derived from the model names in the different graphs, Table 6.1 explains the structure of these names:

| | | | | | | | |
|---|---|---|---|---|---|---|---|
| 1 | C_25.5_m_373_2xE_1xOCR_K0=2xOCR=0.65 | | | | | | |
| 2 | 22.5_ld_2xE_2xOCR_K0=aut | | | | | | |
| 1 | C | 25.5 | m | 373 | 2xE | 1xOCR | $K_0$ |
| 2 | | 22.5 | ld | | 2xE | 2xOCR | $K_0$ = aut |
| | (C) Advanced (complex) soil stratigraphy (MP) Multiple pile model. | Pile length [m] | Multi-linear (m) or layer dependent (ld) | Tskin [kN/m] (only applicable with multi-linear) | Multiplication factor of stiffness parameters during fit calculations | Multiplication factor of OCR parameter during fit calculations | $K_0$ value \| aut means automatically calculated by PLAXIS |

*Table 6.1: Name system explanation PLAXIS 3D calculations single pile*

All the calculations preformed with the new embedded beam formulation are marked with “new_” in front of their (file)name. The other files are calculated with the current embedded beam formulation.

## 6.1 D-Foundations | NEN9997

In order to compare PLAXIS 3D results with NEN9997 load-displacement curves, D-Foundations calculations are conducted to obtain characteristic values for the base and shaft resistance (Table 6.2). The derived base and shaft resistance are combined with (dimensionless) NEN9997 curves.

| Pile length [m] | Simplified model L=22.5 | Complex model L=22.5 | Complex model L=25.5 |
|---|---|---|---|
| Pile tip level (NAP) | - 21 [m] | - 21 [m] | -24 [m] |
| $R_{cd}$ (Total pile capacity) | 3265 [kN] | 2880 [kN] | 3649 [kN] |
| $R_{bd}$ (Base capacity) | 1913 [kN] | 1601 [kN] | 1785 [kN] |
| $R_{sd}$ (Shaft capacity) | 1352 [kN] | 1279 [kN] | 1864 [kN] |
| Penetration in sand | 7 [m] | 2 [m] | 5 [m] |
| Base/shaft ratio | 1.41 | 1.25 | 0.96 |

*Table 6.2: D-Foundations pile capacities*

The required input parameters and CPT's for calculations of the bearing capacity in D-Foundations are given in appendix B.1. Moreover, the safety factors related to variations among the CPT's ($\xi_3$, $\xi_4$) are set to 1.0, because the variation in soil profile is not considered in the PLAXIS 3D calculation. The same holds for the material factors ($\gamma_b$, $\gamma_s$) at the base and the shaft. Since no safety factors are applied in the PLAXIS 3D calculation (SLS), they are set to 1.0 as well.

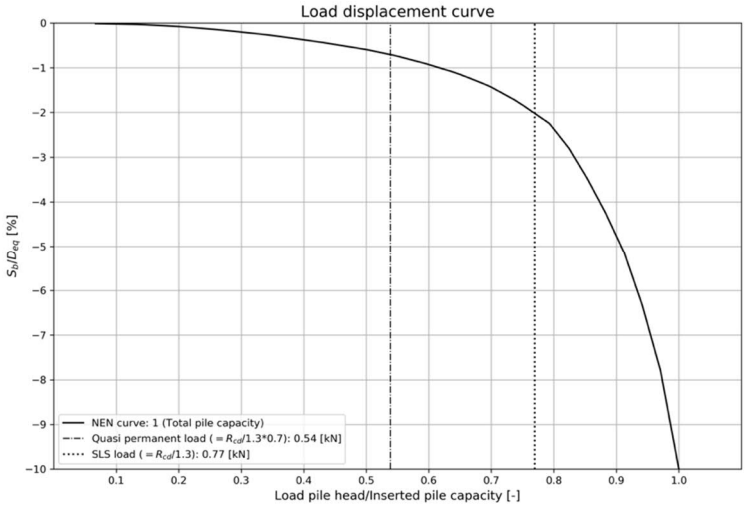


*Graph 6.1: NEN9997 dimensionless load-displacement curve (shaft + base)*

In order to make results comparable with different soil stratigraphy's, geometry's and pile characteristics, the outcome of D-Foundations and PLAXIS calculations are divided by their maximum capacity to construct dimensionless curves. Graph 6.1 shows the combined load-displacement curve containing base and shaft response, instead of two separated graphs (NEN9997 format, Appendix A.2). Since it is difficult to fit the base and the shaft response separately, a more useful approach is to approximate the combined base and shaft load-displacement curve like Graph 6.1 (further explanation in § 6.5.2).

## 6.2 Initial response

### 6.2.1 Current embedded beam

Graph 6.2 shows the behaviour of the current embedded beam under axial loading for a simplified, complex geometry and complex geometry with extended pile length. Additionally, the NEN9997 curve 1 response for soil displacement piles is plotted in the same graph. The difference between the PLAXIS 3D calculation and NEN9997 curve is explained with Graph 6.3. The model with the multi-linear skin friction distribution has a shaft response which is nearly similar to the NEN9997 curve 1. However, the base has a significant softer response due to the connection with the mesh by only one single stress point and the linear elastic perfectly plastic spring (explained in § 4.4).

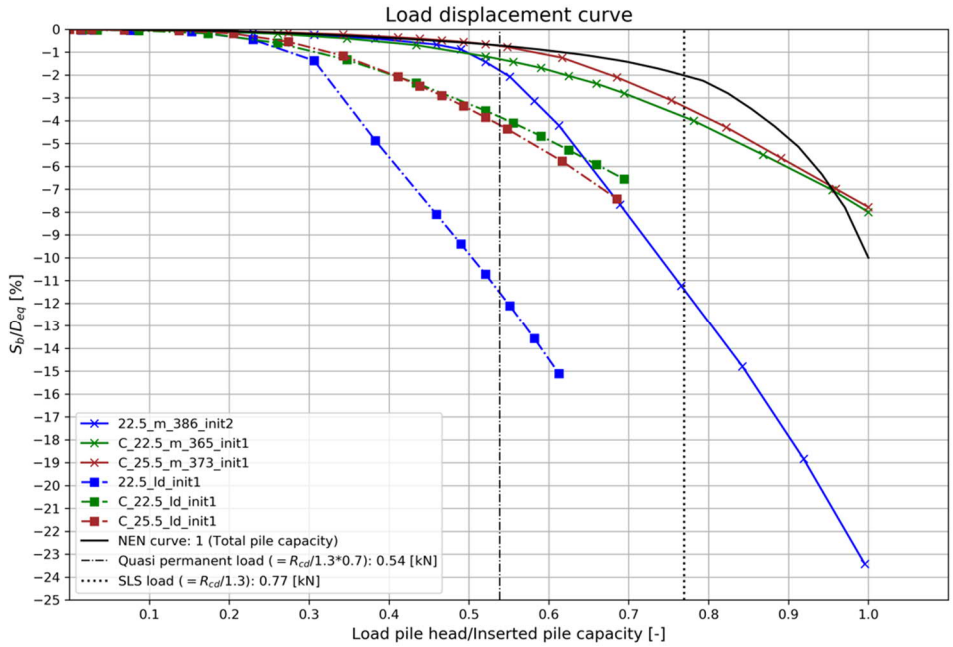


*Graph 6.2: Initial (virgin response) current embedded beam*

The layer dependent shaft friction distribution option deviates even more from the NEN9997 response. Moreover, Graph 6.3 shows clearly that the ultimate bearing capacity of the layer dependent skin friction distribution is less than the proposed pile capacity obtained by D-Foundations. The amount of possible skin friction mobilization is lower compared to the multi-linear model because, a limited amount of normal stress is available at the pile shaft (§ 4.1.2). The shaft resistance is calculated from the initial in-situ soil stress distribution. Because, no increase in horizontal stresses is incorporated from the pile installation.

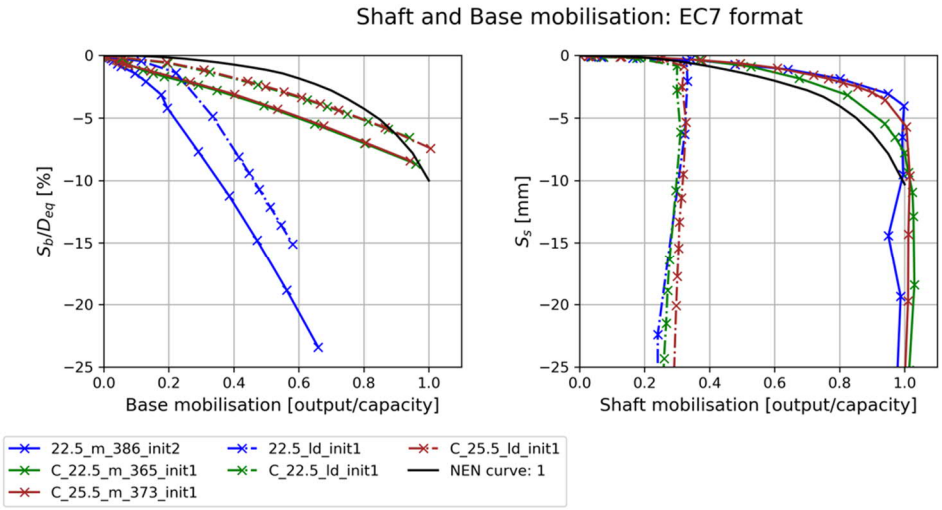


*Graph 6.3: Initial base and shaft response current embedded beam*

### 6.2.2 New embedded beam

The hypothesis in § 1.4.1 assumed a stiffer behaviour for the new embedded beam compared to the current formulation. The new formulation shows in all cases a stiffer behaviour compared to the current embedded beam. Explanation of this phenomena is given in § 4.4.

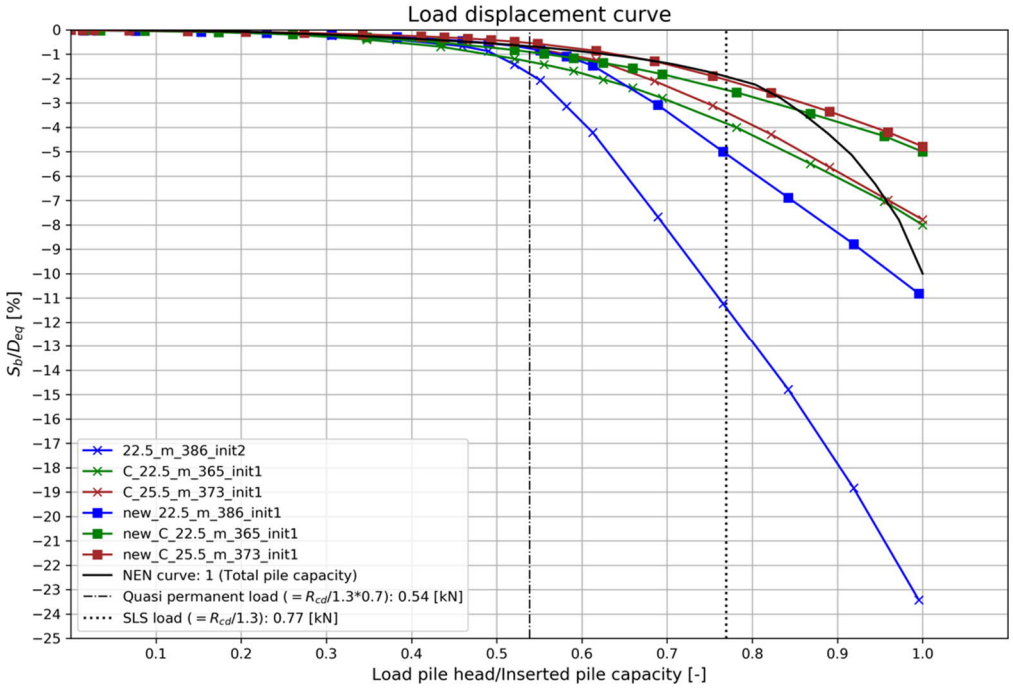


*Graph 6.4: Initial response current and new embedded beam*

The stiffer behaviour of the new embedded beam depends to a large extent on the response of the base. Graph 6.5 clearly shows the difference between both formulations in base displacement. Moreover, the shaft displacement at different load levels show no significant differences between the current and new formulation.

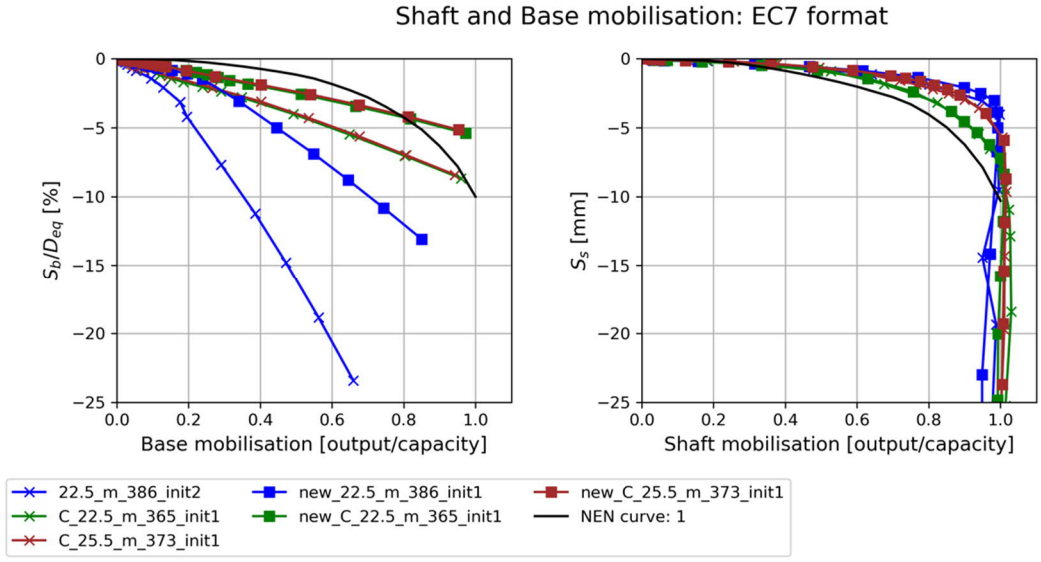


*Graph 6.5: Initial response current and new embedded beam (base and shaft separated)*

Side note, the last datapoint in the graph's above is the maximum capacity calculated by PLAXIS. After the final load step, the calculation brakes down because of too large displacements, which cannot be handled by small strain FEM codes. The brake down is governed by the linear elastic perfectly plastic spring at the base.

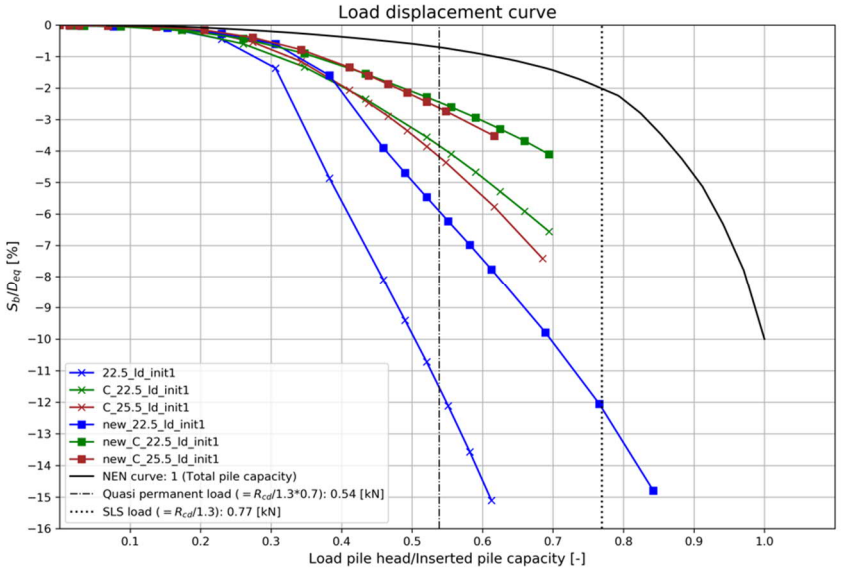


*Graph 6.6: Initial layer dependent response current and new embedded beam*

The layer dependent method in combination with the new embedded beam shows a stiffer load-displacement response when compared with the current formulation. Again, the base contributes for the largest part to the stiffer behaviour, which is in line with the expectations. Since it is difficult to increasing the stress regime around the pile shaft, because no installation effects are incorporated here, the layer dependent option is not suitable to use in this application. Ideally, the horizontal stresses around pile tip level and the shaft should be enhanced to incorporate the installation effect. But this is difficult since equilibrium of the stresses is required in the initial phase of the numerical calculation. By increasing the $K_0$ value around the pile shaft only, PLAXIS starts in the initial phase with restoring the distortions in stress equilibrium.

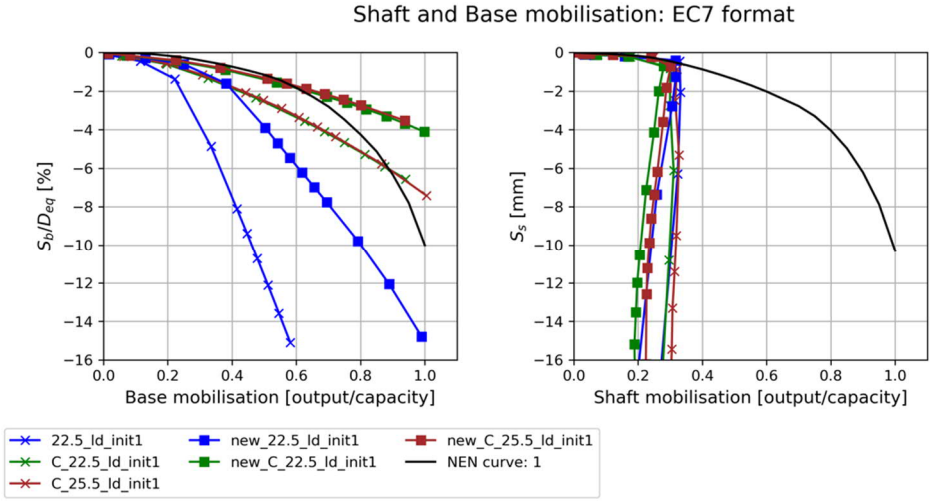


*Graph 6.7: Initial layer dependent response current and new embedded beam (base and shaft separated)*

## 6.3 Mesh sensitivity

Different mesh configurations are tested to obtain the influence of the mesh size on the displacement behaviour of the embedded beam. PLAXIS 3D provides different possibilities to influence the mesh density: the whole mesh can be refined and/or local areas/volumes can be refined. The 'standard' reference model in this thesis contains a mesh refinement of 0.5 around the pile (Figure B.5).

Mesh sensitivity investigation starts off with testing different levels of overall coarseness: coarse, medium, fine and very fine. Table B.12 shows the mesh generation results of the single pile model including the number of elements and nodes.

It turned out that the current embedded beam formulation shows a high degree of mesh sensitivity. Moreover, no convergences are reached by increasing the mesh density. In doing so, increasing the mesh density introduces strong

stress singularities at the base of the pile. The very high stresses are caused at the connection to the mesh by only one stress point (Figure C.1, Appendix B.3.6).

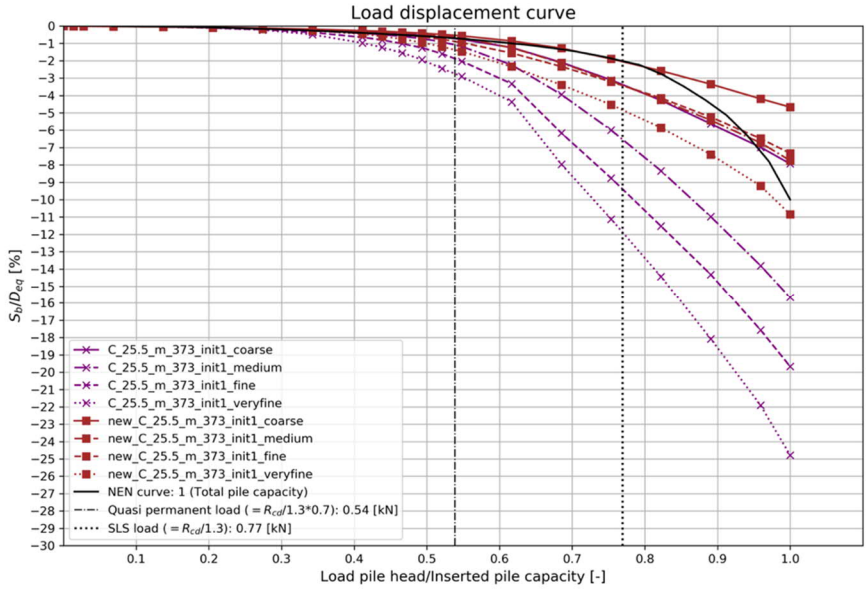


*Graph 6.8: Mesh dependency overall coarseness single pile current and new embedded pile*

The new embedded beam turned out to be less mesh dependent in combination with the used geometry. Graph 6.8 shows the difference in load-displacement behaviour between the current and new formulation. Moreover, convergences are achieved during mesh refinement from medium to fine It implies higher reliability for the embedded beams because, displacements become less dependent from the mesh generation.

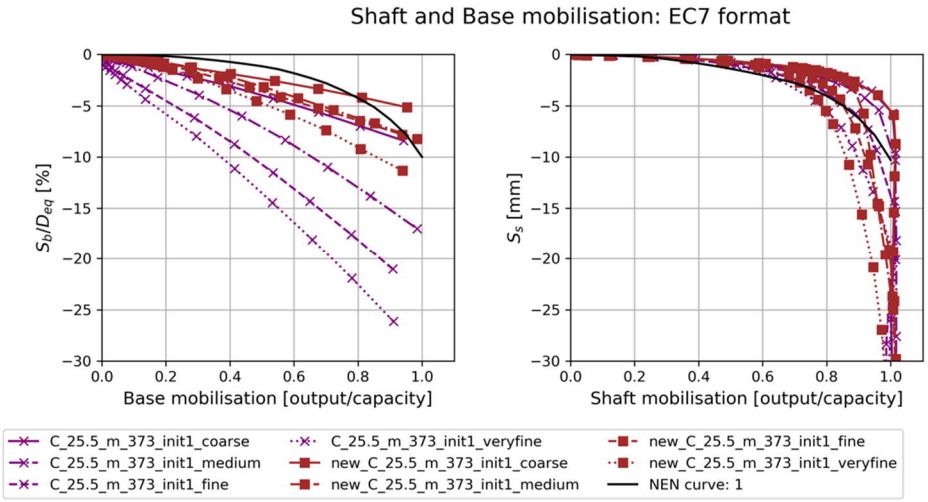


*Graph 6.9: Mesh dependency (base and shaft separated) current and new embedded pile*

**Base displacement**

The new embedded beam formulation shows an improved performance on the distribution of displacements over the base area of the real pile dimensions. The improvement in displacement distribution is due to the addition of stress points at the outer diameter of the real pile dimensions (§ 4.4). The new embedded beam is now connected to more points on the mesh resulting in equal distribution of stresses at the pile tip. The displacements are now more evenly distributed over the base (Figure 6.1).

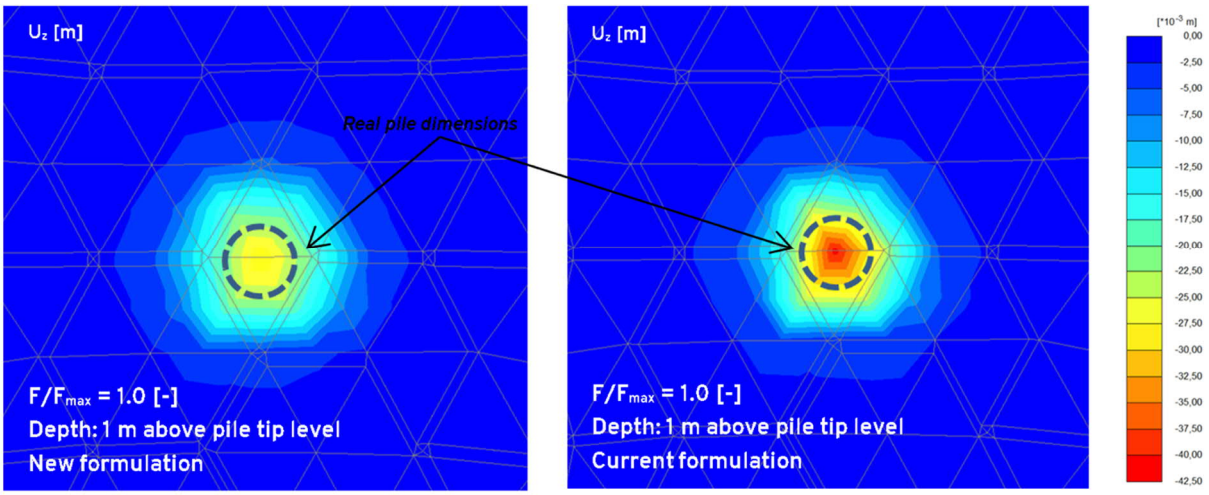


*Figure 6.1: Displacement distribution at base current (right) and new (left) embedded beam*

**Stress singularities**

High stress levels at pile tip are due to stress singularities in the FEM calculation. These singularities occur where the stress in the mesh does not converge towards a constant solution (Acín González, 2015). This occurs most of the time at mesh elements with re-entrant corners (external angels less than 180 degrees). Moreover, mesh refinements at this specific location does not solve the problem.

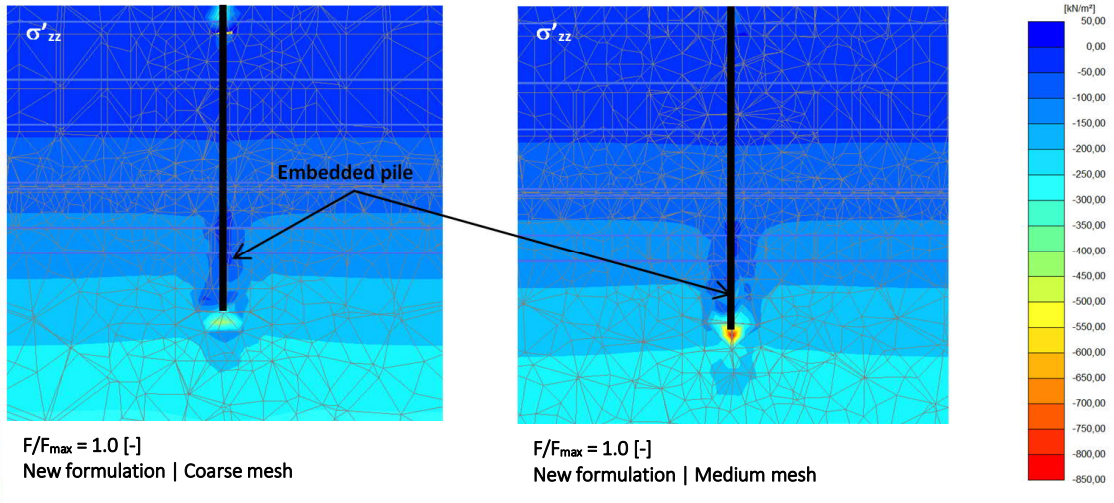


*Figure 6.2: Stress singularities at pile base: coarse (left) and medium (right) mesh*

In order to deal with stress singularities, two assumptions are made: The St. Venant's principle is assuming that singularities only disturb a small local area and do not have an influence on the overall stress distribution in the model (Acín González, 2015). The second assumption states that the displacement field is not affected by stress singularities. Therefore, a medium mesh size is an appropriate choice since displacement convergence have been achieved. Suggested is to use a relative coarser mesh in case stress singularities are occurring, because smaller element volumes cause large stress singularities at pile tip level in combination with the embedded beam.

## 6.4 Pile fit procedure

Based on the results in § 6.2, the pile response is softer compared to NEN9997 curve 1. In this paragraph the load-displacement response of the pile is improved by increasing the stiffness of the soil around pile tip level. A proposed starting point for the fit calculation in PLAXIS is improving the base response. The reason for this step is modelling the consequences of installation effects on pile behaviour. With installation effects is understood the stiffer response of the soil by soil displacement piles compared to non-soil displacement piles.

To achieve this stiffer response at the base without changing the internal code in PLAXIS 3D, a soil volume (box) with enhanced stiffness parameters is modelled around pile tip level. This box is simulating somehow the increased stiffness due to residual stresses in the soil after pile installation (Poulos & Davis, 1980).

The soil volume at pile tip level has fixed dimensions which are related to the pile diameter (Table 6.3). The volume (coloured black) is visualized by a PLAXIS 3D input screenshot in Figure 6.3. The dimensions of the box are based on the size of the influence region for pile loading in NEN9997 (2017). EC7 assumes 4D below pile tip level as influence region. For the single pile fit the 4D is extended to 8D below pile tip in order to reduce the fit factors. The influence of these dimensions is further analysed and discussed in § 8.3.

| | Value |
|---|---|
| Height (z) | 4D above pile tip<br>8D below pile tip |
| Width (x,y) | 8D towards all sides as square |

*Table 6.3: Increased soil properties box geometry (coordinate system according to default PLAXIS settings)*

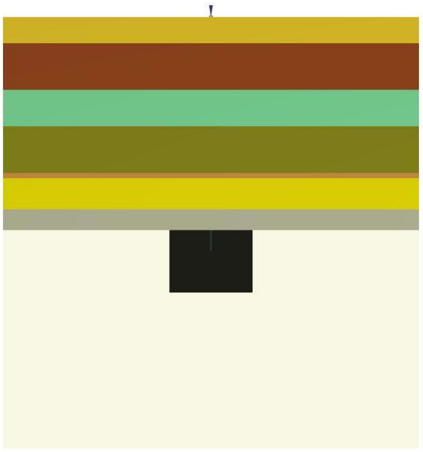

*Figure 6.3: Box (black) around pile tip with higher soil stiffness (cross section view)*

**Increasing stiffness**

Increasing the stiffness has influence on the amount of settlements at specified stress levels, the deviatoric stress – axial strain response is changing. Moreover, changing the OCR in this soil volume has an effect on the horizontal and vertical stress components (equation 6.1 - 6.4). In combination with the Hardening Soil small strain model, higher OCR values have initially more elastic strains compared to OCR values equals 1.

$$\sigma'_{xx,c} = K_0^{NC} \cdot OCR \cdot \sigma'_{yy} \quad 6.1$$

$$\sigma'_{yy,c} = OCR \cdot \sigma'_{yy} \quad 6.2$$

$$\sigma'_{zz,c} = K_0^{NC} \cdot OCR \cdot \sigma'_{yy} \quad 6.3$$

$$\sigma_{xy,c} = \sigma_{xy} \quad 6.4$$

### 6.4.2 Road map pile fit procedure

The fit procedure can be used as a practical tool in daily engineering applications for soil displacement pile problems. In order to give the geotechnical engineer a structured work plan, the fit method is captured in a graphical road map (Figure 6.4). Moreover, some clarification of the different steps in the road map is given below.

- Define soil stratigraphy (similar to the stratigraphy used in the full PLAXIS model)

- Model a soil volume below pile tip level with dimension 4D high and 8D wide (to ensure equal mesh generation in all PLAXIS models)
- Model one embedded beam with the multi-linear skin friction distribution in the final geometry (-> full model with all embedded beams)
- Insert the pile bearing capacity parameters from the D-Foundations calculation at the embedded beam
- Run the PLAXIS 3D analysis for the initial response by turning only one embedded beam active.
- Plot the pile response of NEN9997 and the PLAXIS 3D single pile response in one graph to make the comparison easier.
- In case the response is too soft:
    - Increase the soil stiffness in the soil volume below pile tip level
    - Increase the stiffness ($E_{oed}$) in this soil volume by a factor which is approaching the NEN9997 response (trial and error).
- When the response is in line with the NEN9997 curve (in SLS load levels), make all structural elements active and run the complete analysis with the updated fit parameters in the soil box.

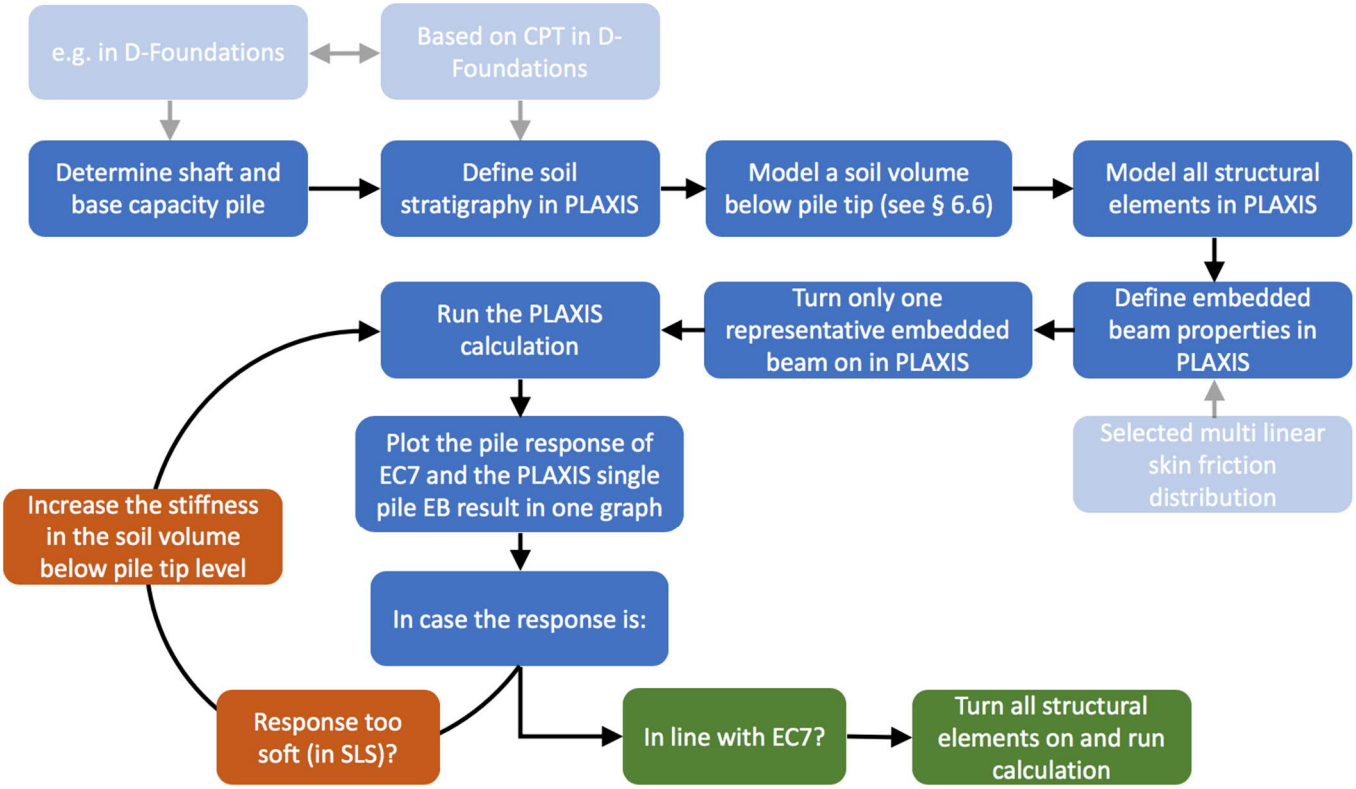


*Figure 6.4: Fit procedure road map*

## 6.5 Results

This paragraph discusses the results of the single pile models in combination with the current and new embedded beam. A couple of variations have been investigated like; a layer dependent or multi-linear skin friction distribution, different pile lengths, various model stratigraphy's and fit parameters.

### 6.5.1 Simplified soil stratigraphy

The simplified soil stratigraphy setup is described in § 5.2 and contains the comparison between the current and new embedded beam formulation. Important during this analysis is the load-displacement response compared to the NEN9997 load-displacement curve. The conclusions are presented below, an elaborated analysis is documented in Appendix C.2.

**Conclusion simplified soil stratigraphy model**

The simplified soil stratigraphy model is used to get a first impression about the possibilities of the embedded beam in combination with the fit procedure. Moreover, the performance of two different skin friction distributions is compared. It turned out that the multi-linear skin friction distribution outperforms the layer dependent distribution. Because, a limited amount of horizontal stresses is available (only initial stress distribution is present). During installation of soil displacement piles, the soil stress ratio $K_0$ and the skin friction distribution changes significantly (§ 2.1).

$$\tau_m = c' + \sigma_n' \cdot \tan(\varphi') \qquad 6.5$$

Equation 6.5 visualizes clearly the influence of the normal stresses ($\sigma_n'$) at the pile shaft, which are the $\sigma_3$ principal stresses related to the $K_0$ in the PLAXIS calculation.

The layer dependent option has a lower maximum amount of shear mobilization in comparison with the predefined shear resistance of the multi-linear skin friction option. Therefore, the shaft friction capacity is deviating a lot from the EC7 load-displacement curve for soil displacement piles. Based on the results of the single pile models, the multi-linear skin friction distribution seems to be the best solution for modelling soil displacement piles in PLAXIS 3D.

Besides the skin friction choice, the fit procedure has been tested on its performance. Based on the used PLAXIS model, the fit procedure work reasonably well in SLS load level ranges for fitting the pile tip settlement ($s_b$) in combination with the new embedded beam formulation.

Secondly, the difference between the new and current embedded beam is investigated. In all investigated models the new embedded beam behaves stiffer compared to the current embedded beam. Although, for soil displacement piles the stiffer behaviour is favorable, it requires attention for non-soil displacement piles in combination with embedded beams since this behaviour is in general softer.

### 6.5.2 Complex soil stratigraphy

The complex soil stratigraphy model setup is described in § 5.2. First, the response of the current embedded beam is discussed in combination with the pile fit procedure described in § 6.4.2. Secondly, the same procedure is applied on the new embedded beam formulation.

**Current embedded beam**

The complex model shows a similar result compared to the simplified model. Increasing the stiffness parameters in the soil box at pile tip level makes the load-displacement response stiffer. However, in this case the best response requires different fit factors compared to the simplified model. It implies a generally applicable factor is not possible for the pile fit.

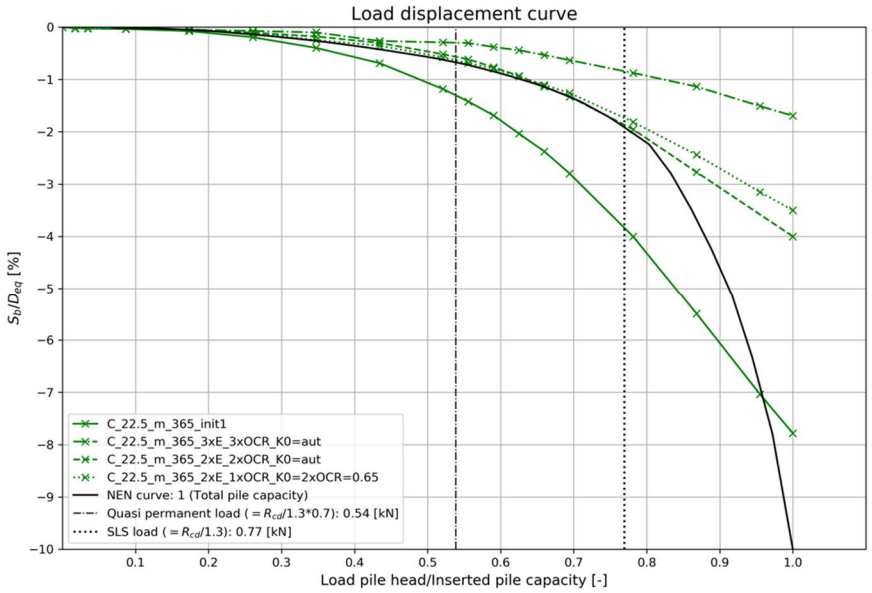


*Graph 6.10: Fit calculation multi-linear complex model l=22.5 | current embedded beam*

As predicted, the base gives a linear response due to the linear elastic perfectly plastic spring connected to the base node of the embedded beam. The shaft gives a somehow stiffer response compared to the NEN9997 curve. Since it is impossible to fit a linear spring on a non-linear envelop, the fit procedure has to be performed on the overall response (base + shaft). Therefore, it does not matter that the base is underpredicted and the shaft is overpredicted. Moreover, this method is a workaround to fit the behaviour on the Eurocode instead of modelling the true installation effects. So, this simplification will not influence the total amount of settlements.

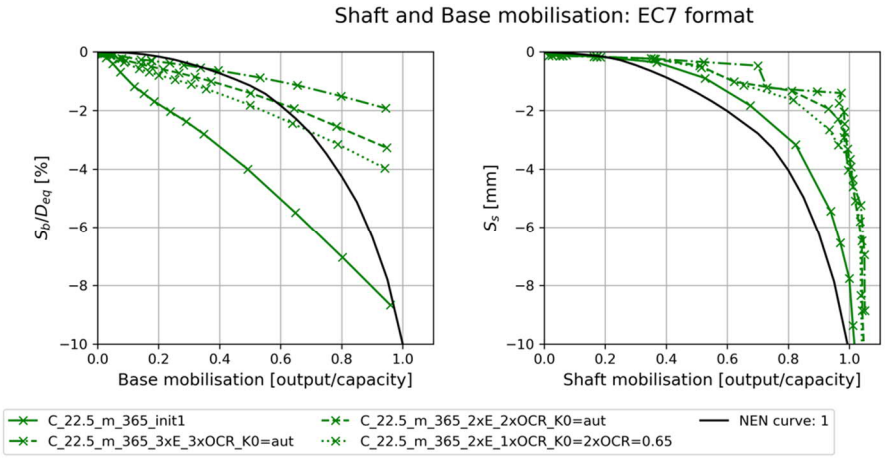


*Graph 6.11: Fit calculation multi-linear (shaft and base) complex l=22.5 | current embedded beam*

**New embedded beam**

Graph 6.12 and Graph 6.13 shows the initial current and new response and the new fit response were the fit requires lower factors to make the response stiffer compared to the simple soil stratigraphy. Based on § 6.5.1, the soil stiffness fit is depending on the soil stratigraphy of the model. Moreover, the new embedded beam requires lower fit factors for the same soil stratigraphy to get an equal response. It implies the new embedded beam has a stiffer load-displacement behaviour which is favourable for modelling soil displacement piles.

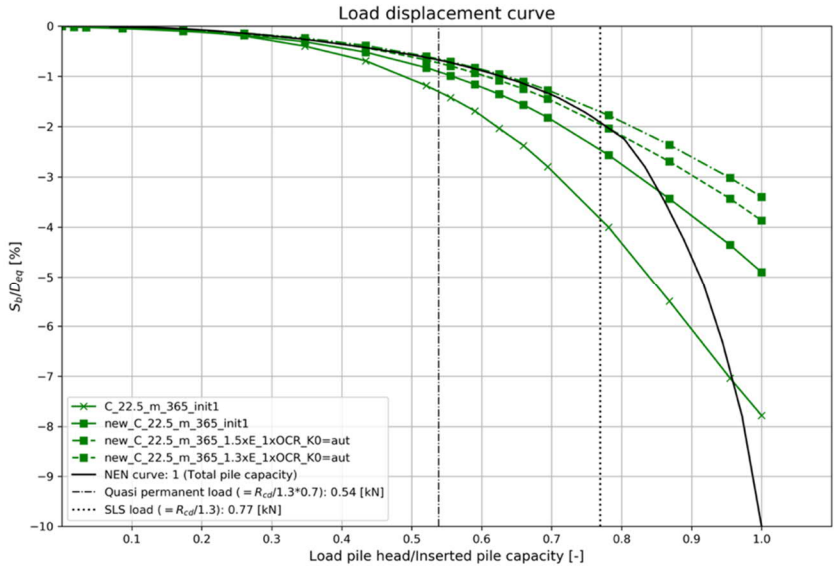


*Graph 6.12: Fit calculation multi-linear | new embedded beam*

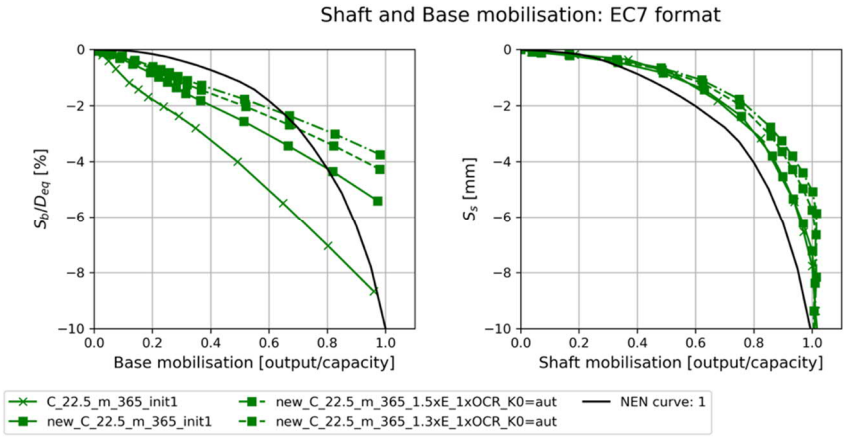


*Graph 6.13: Fit calculation multi-linear (shaft and base) | new embedded beam*

### 6.5.3 Complex soil stratigraphy with extended pile length

The model setup is equal to the model discussed in § 6.5.2 but the pile length is extended with 3 meters. As a consequence, the bearing capacity (base and shaft) has been increased in the D-Foundations calculation.

**Current embedded beam**

The extended piles have an increasing impact on the distribution of the shaft resistance and the maximum bearing capacity. The deeper pile tip level increases the bearing capacity in the D-Foundations calculation due to the higher cone resistance and increased shaft mobilisation. In PLAXIS the stiffness increases with depth due to the stress dependent stiffness in the Hardening Soil small strain model. It implies stiffer behaviour of the pile in PLAXIS and requires therefore less improvements on the soil stiffness parameters to approximate NEN9997.

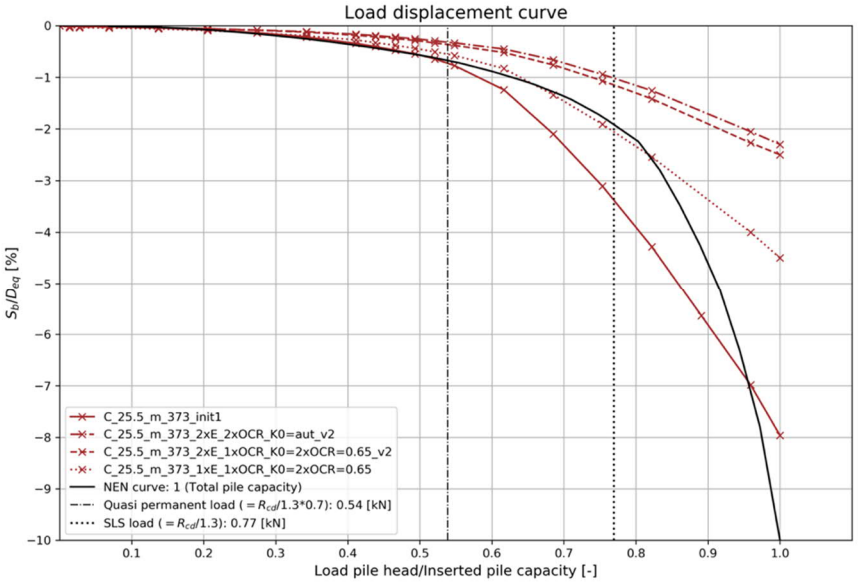


*Graph 6.14: Fit calculation multi-linear complex model l=25.5 | current embedded beam*

Moreover, since the maximum shaft capacity is an input parameter in the PLAXIS 3D calculation, installation effects are indirectly incorporated in the shaft friction. The maximum shaft resistance is calculated in D-Foundations which takes into account the installation effects by empirical correlations. Therefore, the amount of shaft capacity which can be allocated is higher compared to the original soil stress determined in PLAXIS 3D. In case Graph 6.11 right and Graph 6.15 right are compared, longer piles could mobilize relative more shaft friction which results in less settlements. Because, the relative displacement is smaller due to the higher available friction available.

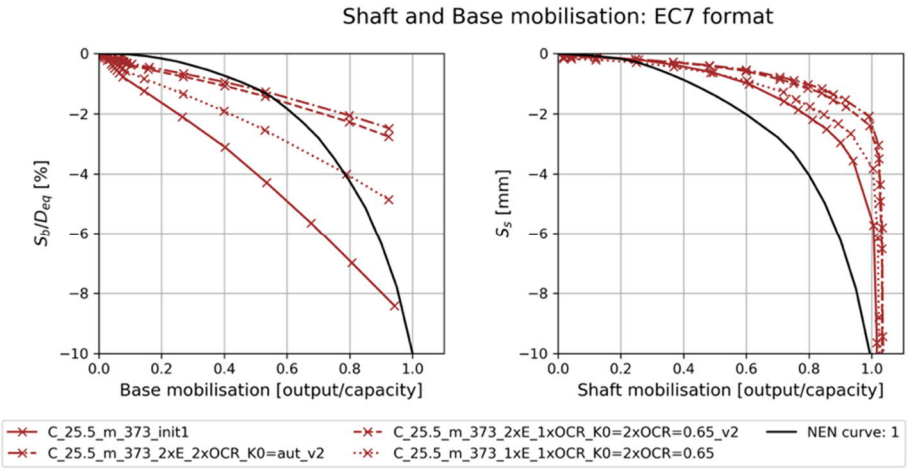


*Graph 6.15: Fit calculation multi-linear (shaft and base) complex l=25.5 | current embedded beam*

**New embedded beam**

The new embedded beam outperforms also in this setup the current embedded beam based on the response of EC7. The new formulation has a stiffer response and requires lower factors for the soil stiffness parameters.

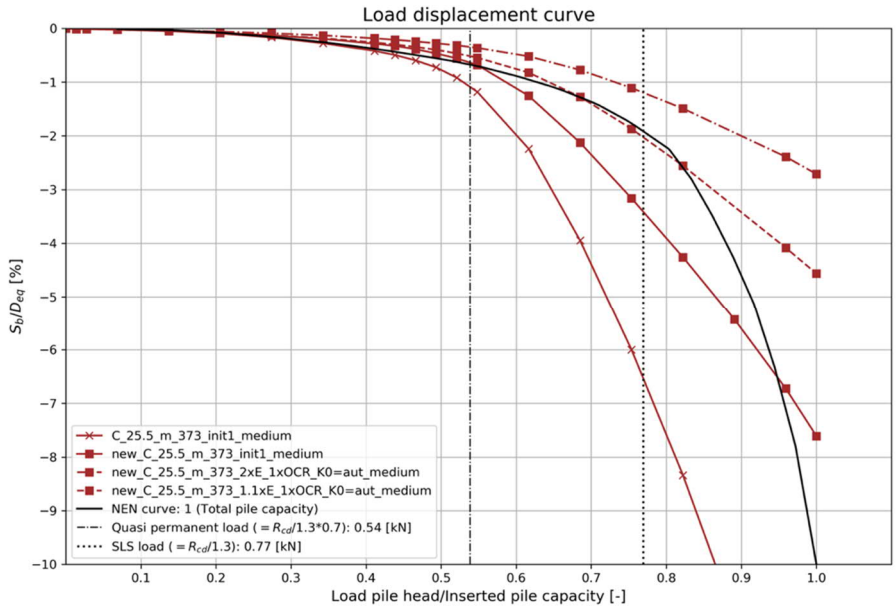


*Graph 6.16: Fit calculation multi-linear complex model l=25.5 | new embedded beam (medium mesh size)*

Due to the improvements at the base in the new formulation, the overall load-displacement response of the pile is stiffer, which is an improvement regarding soil displacement piles.

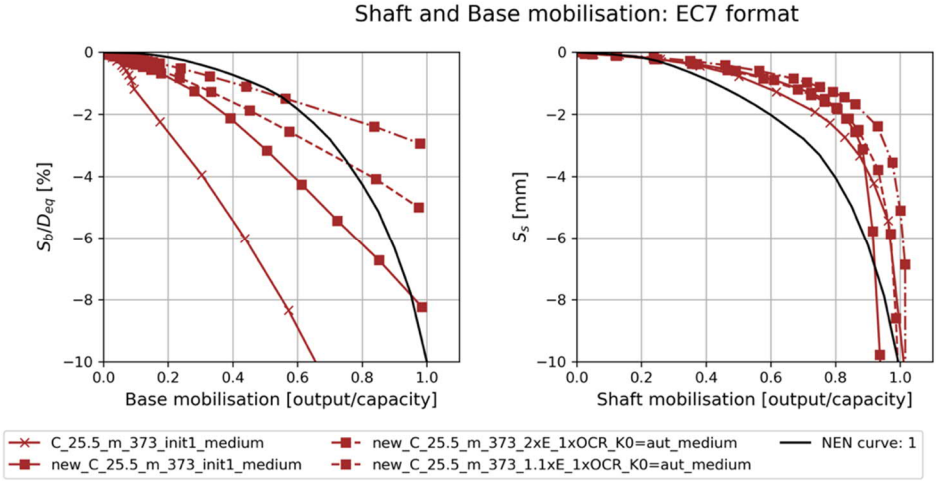


*Graph 6.17: Fit calculation multi-linear (shaft and base) complex l=25.5 | new embedded beam*

**p'-q spaces**

The p'-q spaces are visualizing the behaviour of the soil layers below pile tip level. Important is that the soil follows the initial stress path envelop in case the stiffness parameters are increased. Graph 6.18 shows p'-q graphs from the complex model with a pile length of 25.5 meters. The analyzed location is situated 1D below pile tip level. It implies that the soil follows its original stress envelop and is not influenced by the fit approach, which is positive in this case.

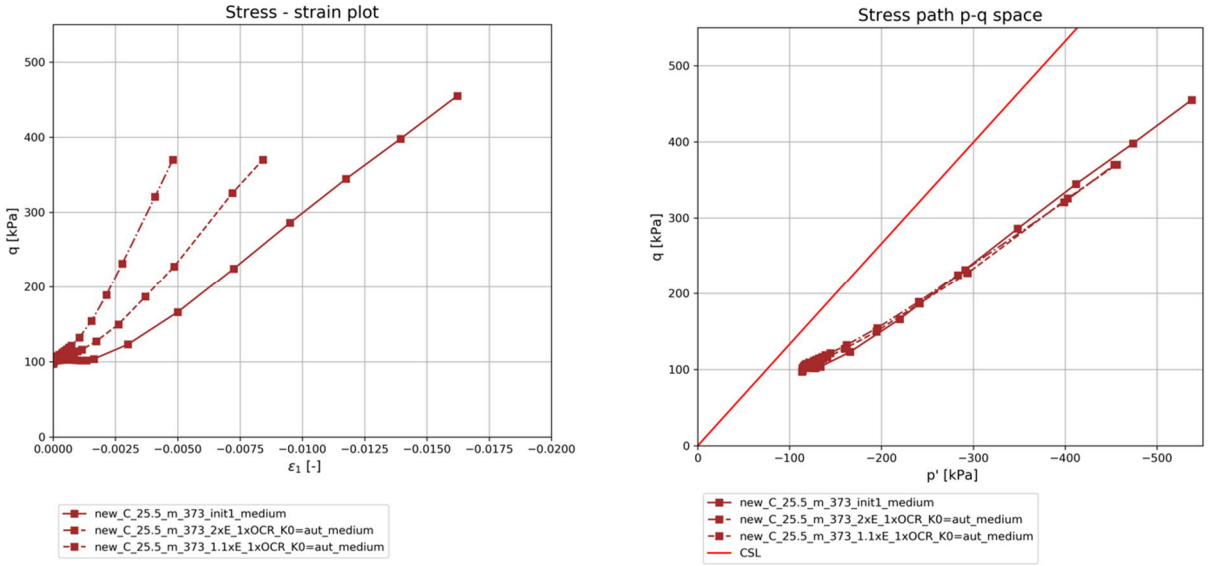


*Graph 6.18: q-$\varepsilon_1$ (left) and p-q (right) plot complex model long pile (1D below pile tip level)(coarse mesh) new formulation*

The q - ε plot clearly shows the influence of the different fit parameters, higher stiffness below pile tip level corresponds to a steeper line. The fact that the maximum deviatoric stress is more or less equal in all the calculations shows that the influence on stress levels are realistic and not influencing the stress state distribution after the fit factors are applied.

## 6.5.4 $s_1$ – elastic compression

The paragraphs above have been focussing on the contribution of pile tip settlements ($s_b$) only, the elastic compression of the pile itself has not been taken into account yet. Although, the elastic deformation of the pile is important and can be a large part of the total settlement ($s_1$). According to NEN9997, the contribution of elastic compression is integrated over a length from the neutral point to the pile head. Assumed is that the part of the pile where positive skin friction is active, does not have a significant displacement relative to the soil according to NEN9997. However, in PLAXIS 3D calculations there is no sharp transition between the positive and neutral skin friction level. Therefore, in the PLAXIS 3D calculation probably more elastic deformations are generated compared to the analytical calculation (Graph 6.20). Graph 6.19 shows a linear envelop of the elastic deformations over the pile length until the neutral point. Near the pile tip level, where positive skin friction is active, the elastic compression contribution starts to reduce.

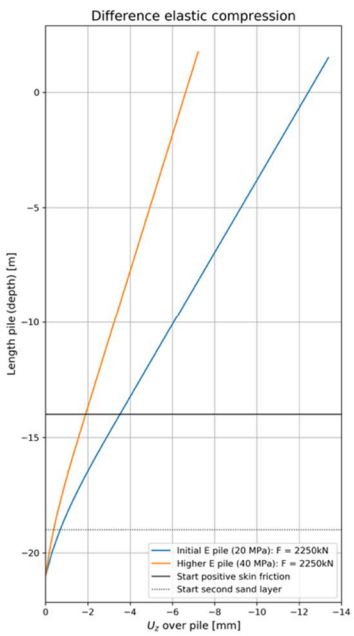


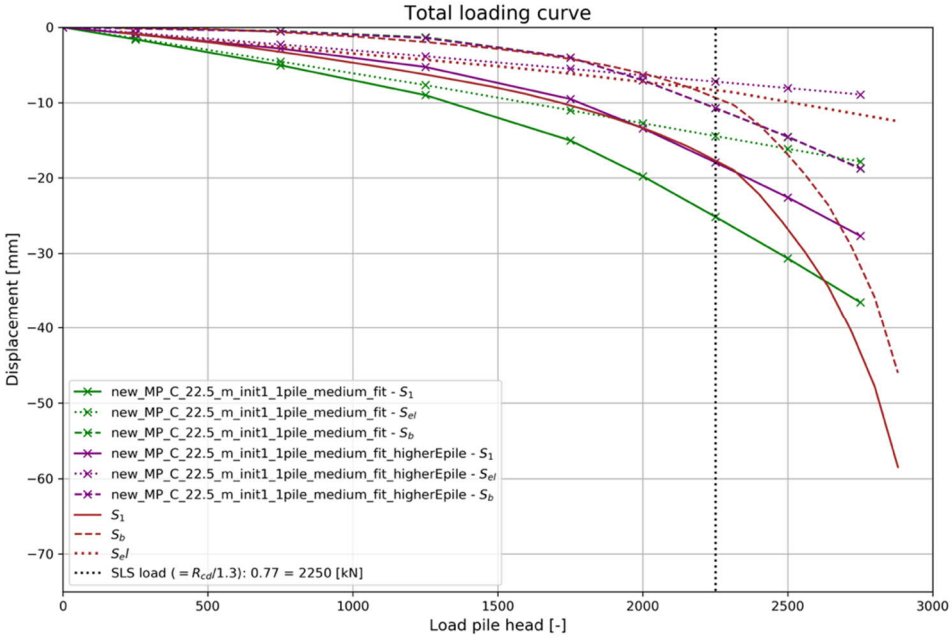


*Graph 6.19 (left): Elastic deformation envelop over pile, L=22.5 m, F = 2250 kN*
*Graph 6.20 (right): Total pile settlement in different contributions 1 pile, L=22.5 m, difference in elastic response*

In Graph 6.20 it becomes clear that the $s_b$ fit calculation is approximating the EC7 curve quite well due to the soil stiffness parameter fit from chapter 6. However, the calculation of the overall pile settlement ($s_1$) shows deviations compared to the EC7 curve. Therefore, the Young's modules of the embedded beam is increased until the response is approximating the EC7 curve. The updated fit parameters for the final single pile fit are presented in Table 6.4.

Updated fit parameters

| *Parameter:* | *Factor:* | *Value:* | *Unit:* |
|---|---|---|---|
| $E_{pile}$ | 2x | $40 \cdot 10^6$ | [kPa] |
| $E_{oed}^{ref}$, $E_{50}^{ref}$ | 1.5x | $75 \cdot 10^6$ | [kPa] |
| $E_{ur}^{ref}$, $G_0^{ref}$ | 1.5x | $225 \cdot 10^6$ | [kPa] |

*Table 6.4: Updated fit parameters in combination with elastic compression pile, L=22.5 m*

However, increasing the Young's modulus of the pile changes the entire elastic behaviour of the pile. Moreover, the elastic compression at positions without positive skin friction also reduces (entire line gets steeper in Graph 6.19). Theoretically, less relative displacement between soil and pile occurs in the upper part of the pile. The question is which behaviour is more realistic, the one described in NEN9997 or the PLAXIS 3D results. Again, assumed is the NEN9997 response is the truth from a design perspective, but it can be questioned if this assumption needs to remain as it is. In case large elastic compressions are expected, it is recommended to conduct additional analysis on this behaviour.

Some possibilities for fitting the elastic response of the pile are discussed in Appendix D.2. One of the tested approaches is modelling two embedded beam elements on top of each other with a different Young's modulus.

To conclude, for this specific example (model in Graph 6.19 and Graph 6.20) the elastic compression fit is adequate within in the given boundary conditions of the investigated model. Although, recommended is to perform further analysis on the influence of various cases and models.

## 6.6 Conclusion

The improvements for modelling soil displacement piles with embedded beams are divided in two parts: comparison between the current and new embedded beam formulation and a fit procedure for the stiffness of a predefined soil volume below pile tip level. First, the current and new embedded beam formulation was compared. Second, the soil fit procedure is tested on its applicability in single pile configurations for soil displacement piles.

The mesh generation in PLAXIS 3D has a large influence on the behaviour of the current embedded beam formulation. Moreover, mesh distributions with a comparable number of elements and element volumes, but a slightly different distribution, have a large impact on the load displacement response. Therefore, it makes the current embedded beam difficult and unpredictable in practical applications (based on the investigated models). On the other hand, the new embedded beam formulation shows improved performance on mesh dependency. Moreover, convergences are reached between medium and fine mesh size distributions. Besides the improvements on mesh reliability, the new embedded beam contains a stiffer load-displacement curve compared to the current formulation. The stiffer response is an improvement in case soil displacement piles are modelled. However, in combination with other pile types containing different installation effects the stiffer behaviour could be unfavourable due to underprediction of the amount of settlements. The embedded pile in combination with other pile (installation) types is out of the scope of this thesis.

From the options available for the shaft friction distribution (linear, multi-linear and layer dependent), the multi-linear option outperforms the other two. Because, the multi-linear option has the possibility to insert higher maximum shaft friction compared to the maximum shaft friction mobilised with the layer dependent option. During installation of soil displacement piles, the soil stress ratio $K_0$ and the skin friction distribution changes significantly. These changes are not incorporated in PLAXIS 3D, so only the initial stress distribution is used to calculate the shaft friction for the layer dependent option.

Secondly, a soil volume below pile tip level is fitted in order to get the pile tip load-displacement behaviour in line with the NEN9997 response. It turned out that increasing the soil stiffness parameters of the soil volume result in reasonable approximation of the NEN9997 load-displacement curve for SLS load levels. However, there are a number of limitations to this method: The fit procedure as proposed in this thesis applies reasonably well in the serviceability limit state load ranges. Moreover, failure behaviour of the pile is difficult to model since the embedded beam in PLAXIS 3D is connected to the mesh with a linear elastic perfectly plastic spring.

In the ideal situation, a generic fit procedure for pile behaviour is desirable for different soil stratigraphy's and pile lengths. However, in the current and new embedded beam formulation, it is not possible to define a generic procedure for fitting the shaft and base behaviour in a way that it is always applicable irrespective of the soil stratigraphy and pile length (Graph 6.21). The stiffness fit of the soil volume should be performed again in case the soil stratigraphy or pile properties are changed. There are several reasons: increase in mobilization of shaft friction in combination with longer piles relative to the increase in shaft friction in the analytical NEN9997 calculation. This is related to the stress dependent stiffness in the HSsmal model and the missing connection of the NEN9997 calculation with basic soil mechanic principles.

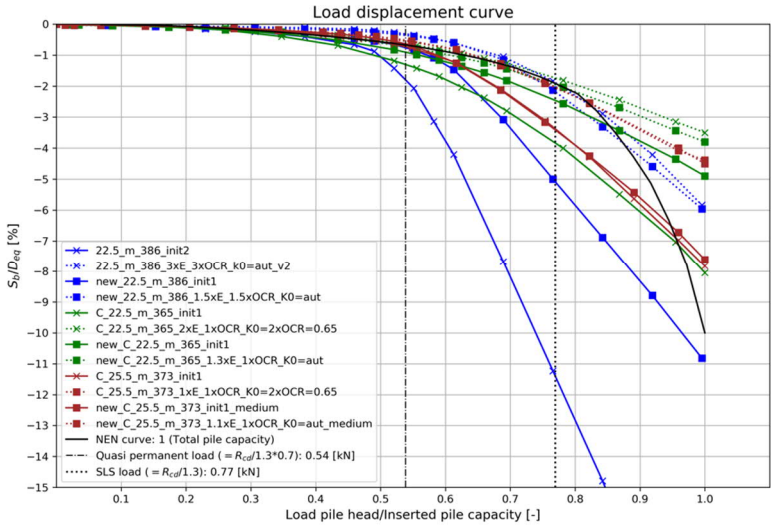


*Graph 6.21: Overall response current and new embedded beam (all coarse mesh, except new_C_25.5)*

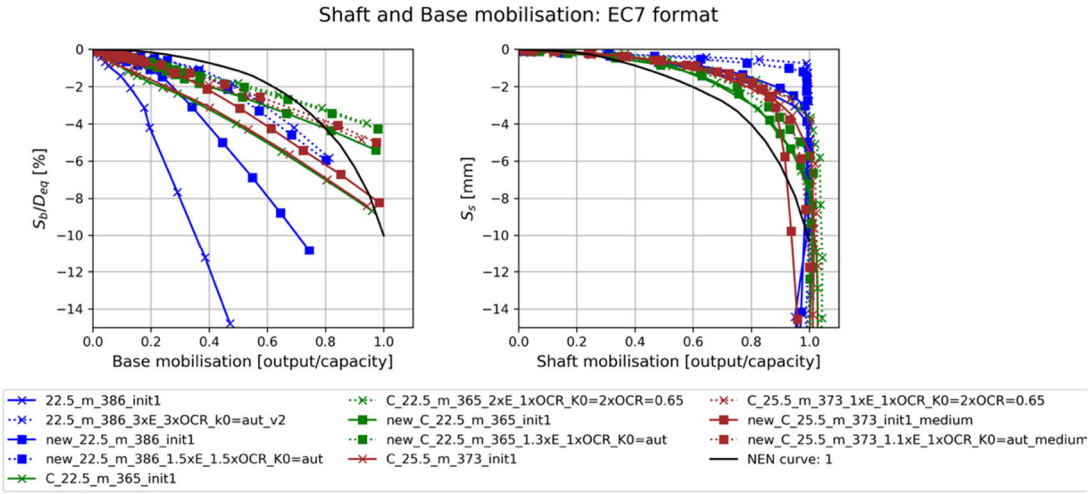


*Graph 6.22: Overall response (base and shaft) current and new embedded beam (all coarse mesh, except new_C_25.5)*

# III Model design

# 7 Model setup pile group

Single pile configurations (or large distances between adjacent piles) are rarely found in daily engineering practice for high rise buildings. Interaction between these neighbouring piles in a pile group is more likely. Influence on group settlement effects and foundation plate stiffness is therefore discussed in chapter 7 and 8. Moreover, the influence of a compressible clay layer below pile tip level is analysed. Because, a large part of the settlements in combination with high foundation loads is due to this compressible layer at great depths.

Another important parameter for the amount of settlements and the settlement distribution is the stiffness of the plate connected to the piles which is representing the superstructure stiffness. Higher bending stiffness is decreasing the displacement concentration due to the more evenly distributed load among the piles. In order to investigate the influence of the cap stiffness, a model containing 80 piles (5 x 16) is analysed in combination with various bending stiffnesses.

**Displacement definition in PLAXIS**

NEN9997 divides the displacements in different magnitudes: $s_{el}$, $s_b$, $s_1$ and $s_2$. In order to make a difference in the contribution of these displacements on the total amount of settlements, a decision is made on how to retrieve this data from the PLAXIS 3D results. Assuming, 4D underneath pile tip level settlements are occurring only due to group effects (NEN 9997-1, 2017). The points of interest are visualized in Figure 7.1 where a difference is made between data that is directly retrieved from the PLAXIS output and data which requires post processing.

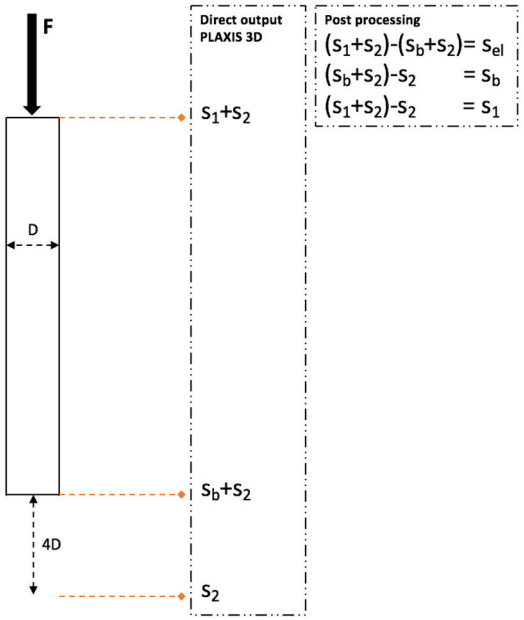


*Figure 7.1: Pile displacement reading points PLAXIS 3D pile groups*

Noted is that the separated settlement contribution in Figure 7.1 is not so clear during real pile loading. However, in order to make comparison possible this mathematical division has to be conducted. Moreover, the settlement contribution is now in line with NEN9997 which is assumed to be the truth in this research from a design perspective.

## 7.2 Soil

The soil properties and soil stratigraphy in the pile group model are similar to the single pile complex models (Chapter 5 & 6). Additionally, a compressible clay layer is added underneath the second sand layer (realistic for Amsterdam/Dutch soil profiles). Consequently, a consolidation calculation is required for taking into account dissipation of excess pore water pressure in compressible clay layers.

### 7.2.1 Soil stratigraphy

As already mentioned, the soil stratigraphy of the multiple pile model is similar to the single pile model. In order to calibrate the initial conditions of this multiple pile model, a validation calculation has been made with soil layers up to and including the second sand layer, so without taken into account consolidation and creep effects yet (results in paragraph 8.1).

Subsequently, a compressible clay layer is added underneath the second sand layer. This layer called Eem clay in Dutch requires a time-dependent calculation for taking into account consolidation and creep due to the low hydraulic conductivity and compressibility of this layer.

| Soil profiles in chapter 7 & 8 | |
|---|---|
| Bottom layer is sand | without consolidation |
| Bottom layer is Eem clay | with consolidation |

*Table 7.1: Soil profiles chapter 7 & 8*

### 7.2.2 Soil model

The soil layers up to and including the second sand layer are modelled according to the similar constitutive model (Hardening Soil Small Strain) as the single pile model. The clay layer underlaying the second sand layer is prone to consolidation and creep deformations. Therefore, the soft soil creep constitutive model is a good choice for modelling time-dependent effects of the clay layer because:

**Characteristics Soft Soil Creep model (Brinkgreve, 2018b):**

- Memory of preloading in the past
    - Eem clay layer is preloaded by ice during the ice ages (Keijer, 2015)
- Secondary compression (time dependent deformations)
    - Clay layers are prone to consolidation and creep
- Irreversible creep strain by viscous plasticity instead of plasticity
    - Clay layers are prone to creep (Verruijt, 2012)

**Limitations**

- The initial OCR values is also influencing the initial creep strain rate. Therefore, it is important to calibrate the autonomous surface settlements.
    - The OCR value for the clay layer used in this thesis is fitted on the equivalent age of the layer according to the article of Den Haan (2003).
- The $K_0^{NC}$ has a strong influence on the deformation behaviour of the model.
- The deformations due to creep are not always realistic in case a stress state is mainly governed by the initial self-weight.
    - Due to the high foundation loads of the high-rise buildings and therefore relatively low self-weight contribution, this should not lead to problems.

**Time dependent effects (consolidation & creep)**
Based on experience, it is expected that a deep clay layer underneath the second sand layer has a large contribution to the $s_2$ settlements at 4D below pile tip level. Therefore, a consolidation analysis is performed to take into account the dissipation of excess pore water pressure. The soil and hydraulic properties of the Eem clay layer are presented in appendix B.3.2.

Immediate settlements occur directly after the load is applied on the foundation, for example during the construction stage. These immediate settlements occur due to the elastic and plastic deformation of the soil. The secondary settlements have a long-term effect and are therefore calculated over 10, 20 and 50 years. Moreover, the consolidation calculation is divided in two parts; building phase (load increase) and operational phase (constant load). During the building phase a surface load is activated in 3 steps with a total duration of 147 days. After construction the load is kept constant for 10, 20 and 50 years were consolidation and creep are able to occur.

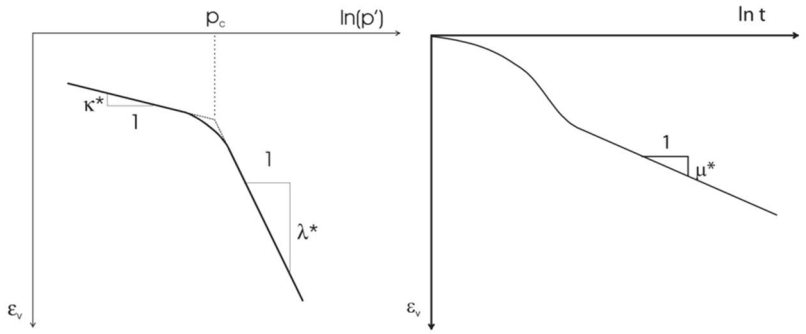

*Figure 7.2: Soft soil creep parameters (After Waterman & Broere (2004))*

## 7.3 Pile properties
A pile with equal properties is used in both the single pile and pile group calculations to make them comparable with each other. The pile properties can be found in § 5.5. Choices about shaft resistance, loading conditions and cap connection are addressed in this paragraph.

### 7.3.1 Shaft resistance
Part II discusses the single pile model in combination with the Eurocode $s_1$ settlement curve. This is an important first step in the calculation of pile groups, because the response of the single pile is now included in the overall behaviour of a pile group. Form part II has been concluded that the layer dependent option is difficult to fit on the desired NEN9997 curve. The multi-linear skin friction distribution shows more realistic fit possibilities and is therefore used in part III. Since the soil stratigraphy is equal to the analysis in part II, the inserted shaft capacity also remains equal.

### 7.3.2 Loading conditions
In calculations without a pile cap, the load is applied directly on the pile head by a point load. Which means there is no stress redistribution among the piles possible, i.e. the complete point load is directly transferred to the pile. This is the most unfavorable situation since differential settlements are large between the center and edge piles (chapter 3 introduction and Figure 3.1).

In the models where the plate (pile cap) is activated, a surface load with the equal amount of load is added. Here, the point loads are multiplied by the numbers of piles and divided over the surface. Redistribution of load is now possible among other piles which is favourable for the amount of differential settlements. Loading settings and further explanations are given in Appendix B.

## 7.4 Comparison multiple pile models

### 7.4.1 Initial response – mesh influence
To check the influence of the added geometrical objects in the mesh (additional embedded beams; Figure 8.1), a 9-pile model is analysed with equal stratigraphy compared to the single pile model without the 8 additional piles. Where the

current embedded beam shows large mesh dependency, expected is that the new formulation shows reduced mesh dependency.

### 7.4.2 $s_2$ – group settlements

According to the standards, the settlements are divided in two separate contributions; single pile ($s_1$) and pile group ($s_2$ at 4D below pile tip). In order to make a comparison with PLAXIS 3D results, different benchmark calculations are conducted; EC7 approach for group effects, Tomlinson in PLAXIS 3D and D-Pile Group. For purely $s_2$ settlements, the NEN9997 formula and Tomlinson approach in PLAXIS 3D are used.

**NEN9997 $s_2$ method**

The amount of settlements 4D below pile tip level can be calculated in two different ways according to NEN9997 (§7.6.4.2, p. 183). One method is equal to a foundation settlement calculation at surface level, the other one is a simple formula using the Young's modulus of the bearing layer. The latter one is used in this chapter to get an idea of the range that can be expected. The Young's modulus is calculated with a straightforward relationship between the cone resistance and a dimensionless factor. The ratio between the cone resistance and $E_{100}$ is a factor 3 according to the Eurocode 7, table 2b (NEN 9997-1, 2017). Moreover, the user manual of Deltares is also suggesting a factor 3 since the formula disappeared out of Eurocode 7 (Deltares, 2016b). Although, in previous versions of Eurocode 7 is explicitly written that a factor 5 is used as correlation between cone resistance and Young's modulus. Therefore, both factors are used to obtain a bandwidth of the expected settlements (Graph 8.3).

$$E_{ea;gem} = factor \cdot q_c \tag{7.1}$$

$$s_2 = \frac{m^* \cdot \sigma'_{v;4D} \cdot 0{,}9 \cdot \sqrt{A_{4D}}}{E_{ea;gem}} \tag{7.2}$$

With:

$$\sigma'_{v;4D} = \frac{F_{und}}{A_{4D}} \tag{7.3}$$

Noted is that formula 7.2 can only be used for settlement calculations in the elastic part of the sand layer. For the soil profiles visualized in Figure 5.2 this approach is applicable. However, in case a soil layer is subjected to time dependent effects, this approach is not realistic anymore due to consolidation and creep settlements.

**Tomlinson in PLAXIS 3D**

The Tomlinson method is explained in section 3.2.2 and is often used in Dutch engineering practice in combination with PLAXIS 3D. Therefore, the PLAXIS model geometry is equal to the model including the embedded beams. According to the Tomlinson method, a surface load is added at a given depth. Moreover, to make the method more realistic, the contribution of the shaft is added on $^2/_3$ of the embedded length of the pile in the sand layer. Subsequently, the base is added at the original pile tip level (see Figure 8.2).

**D-Pile Group**

The D-Pile Group calculations are only suitable for the models without time dependent effects, since D-Pile Group cannot handle excess pore pressure changes. More information is given in § 3.2.1. The 9-pile model is calculated in D-Pile Group with the Cap layered soil interaction model (FEM). The soil properties and calculation settings are given in appendix B.1.

### 7.4.3 $s_1$+$s_2$ – total settlements

In the complete settlement analysis two different models are analysed, 9 piles (3 x 3) and 80 piles (5 x 16). The 9-pile model is used to a make first indication on the performance and reliability in a pile group of the new embedded beam including the fit approach. The 80-pile model is utilized for variations in pile cap stiffness in combination with embedded beams. Moreover, the already discussed Eem clay layer is added underneath the bearing sand layer (second sand layer) for time dependent settlements.

## 7.5 Variations in cap stiffness

The pile cap (plate element) stiffness connected to the embedded beams has two parameters which are involved in the bending stiffness of the superstructure. Multiplication of the Young's modulus and moment of Inertia (height) results in the bending stiffness (EI) representing the superstructure (Formula 7.4). Variations in the bending moment should result in different settlement distributions (Zoidi, 2015). Table 7.2 shows the different bending stiffnesses values used in the 80-pile model.

$$EI = E \cdot \frac{1}{12} \cdot b \cdot h^3 \qquad 7.4$$

| Name model | Height [m] | Stiffness [GPa] | Factor | EI [$m^4$] * |
|---|---|---|---|---|
| No plate | - | - | - | - |
| Initial | 2 | 20 | 1x | $1.33 \cdot 10^4 \cdot b$ |
| 5xE | 3.4 | 20 | 5x | $6.55 \cdot 10^4 \cdot b$ |
| 10xE | 4.3 | 20 | 10x | $1.32 \cdot 10^5 \cdot b$ |

*Table 7.2: Plate properties 80 pile model*

* b is the in-plane width of the foundation plate

# 8 Pile group results

Practical application of piles comes often together with pile group effect problems. Therefore, chapter 8 discusses the performance of the new embedded beam formulation including the soil stiffness fit in combination with pile groups. The analysis starts off with a comparison between the single pile and 9-pile model. Subsequently, the $s_2$ response of the 9-pile model is compared with benchmark approaches. Finally, the response of an 80-pile model including different cap stiffnesses is analysed.

## 8.1 $s_1$ response - 1 pile / 9 pile model

### 8.1.1 Mesh influence

The initial (virgin) model is used for measuring the influence of small mesh changes at pile tip level and overall mesh sensitivity of the embedded beam. This is done by modelling 8 additional piles in the single pile model while keeping the mesh coarseness equal. It implicates minor mesh changes around the pile tip due to the additional geometrical points of the added embedded beams. The reason for this comparison has been explained in paragraph 6.3 were the mesh dependency of the current embedded beam formulation has been investigated. The current formulation shows large mesh dependency by changing the mesh very slightly around the pile tip level.

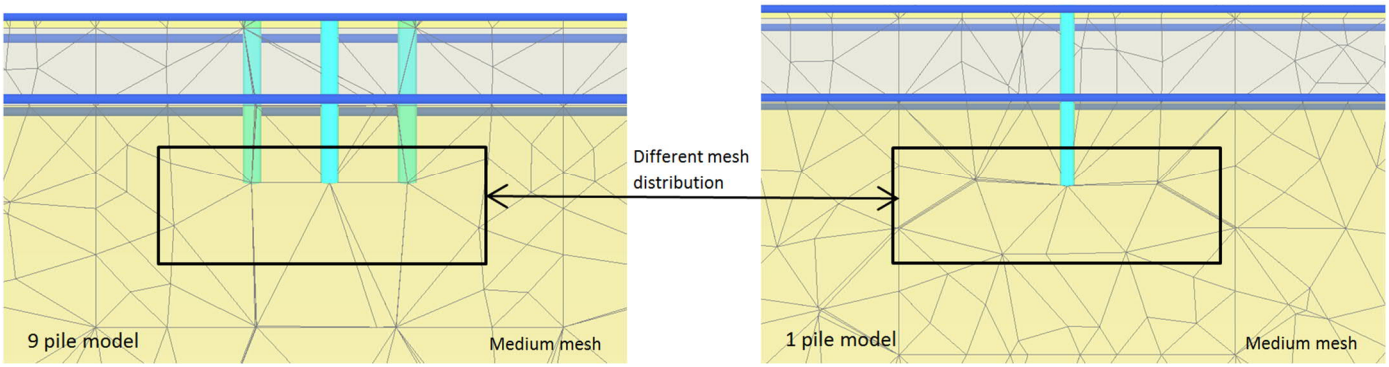


*Figure 8.1: Difference in mesh distribution underneath pile tip - medium mesh. Multiple pile (left) (one pile switch on), single pile (right))*

Changing the mesh very slightly is referred to as keeping the overall mesh density (medium) constant but, changing the position of the mesh elements and volumes a little bit (Figure 8.1). The new formulation of the embedded beam shows large improvements on this mesh sensitive behaviour (Graph 8.1).

Graph 8.1 shows the influence of changing the mesh by adding geometrical objects close to the pile tip (8 additional embedded beams, switched off, green). In case a coarse mesh is used, the response of both “single” pile models (brown and green) is still different. Decreasing the mesh coarseness results in behaviour that is similar between both “single” pile models. Compared to the behaviour of the current embedded beam model, large improvements are gained on mesh dependency with the new embedded beam formulation (paragraph 6.3).

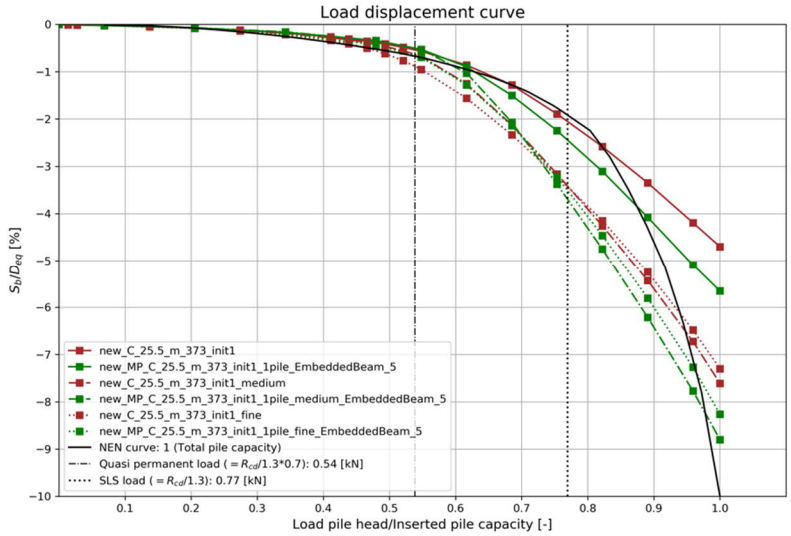


*Graph 8.1: Mesh sensitivity single pile (brown) multiple pile (green) (only one pile switch on)*

Moreover, convergences are obtained by using a medium mesh size distribution. A good balance is achieved between calculation costs and accuracy. Therefore, the medium mesh is the most optimal mesh for this application and is therefore used in this chapter.

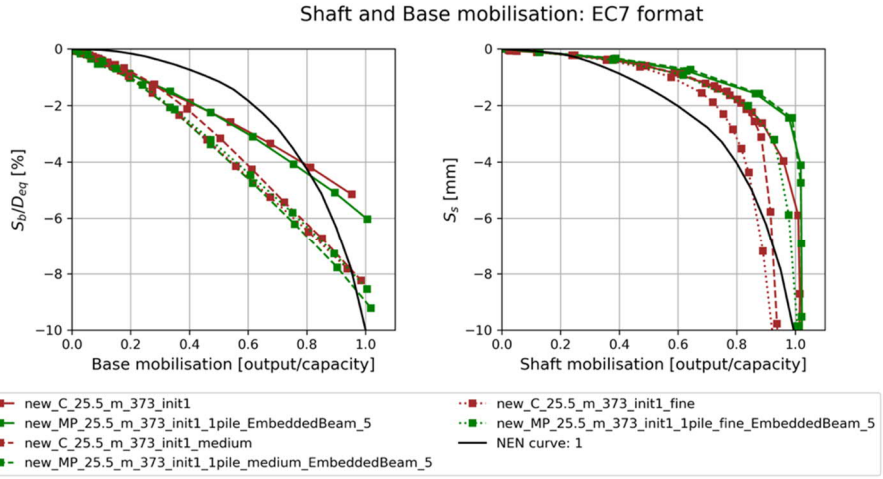


*Graph 8.2: Mesh sensitivity base and shaft separated. Single pile (brown) - multiple pile (green) (only one pile switch on)*

## 8.2 $s_2$ response - 9 pile model

The initial C_25.5_m_373 (§ 6.5.3, pile length 25.5 meter) model (without fit) approximates the NEN9997 curve in the overall response quite well probably due to the large penetration depth in the stiff second sand layer (explained in § 6.5 and § 9.2). Therefore, in the upcoming paragraphs the C_22.5_m_365 (§ 6.5.2, pile length 22.5 meter) model is used which deviates initially more form the EC7 response, in order to show the possibility of the improvements with the proposed fit method.

### 8.2.1 Tomlinson and EC7 method

The bearing capacity of a pile group differs from the bearing capacity of a single pile multiplied by the number of piles in the pile group (Engin et al., 2008). One reason for the difference is the overlapping stress zones between adjunct piles due to the mobilisation of shaft friction (Tomlinson & Woodward, 1977). Moreover, the area below the pile tip is stressed to a greater depth compared to a single pile, which results in more settlements (Figure 2.4).

One of the approaches to calculate the settlements underneath a pile group is proposed by Tomlinson & Woodward (1977). The design method is based on the assumption that the pile group behaves like a block foundation and basic soil mechanical principles can be applied. Additionally, results from the rather simple NEN9997 $s_2$ (§7.4.2) method are presented as bandwidth in this paragraph.

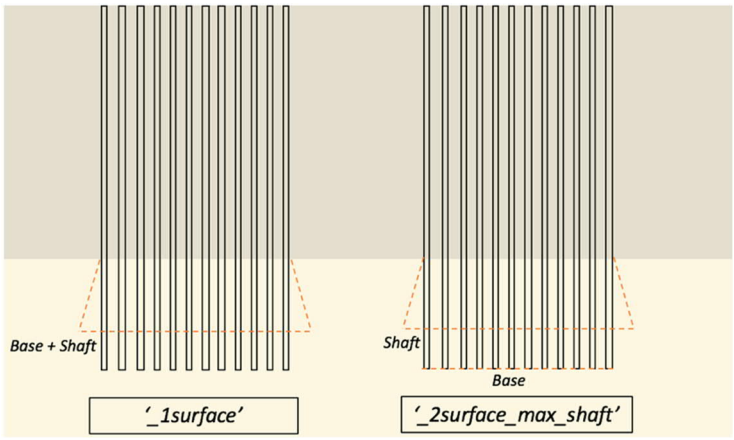


*Figure 8.2: Explanation different Tomlinson approaches*

The approach proposed by Tomlinson & Woodward (1977) assumes that the load from the base and the shaft is transferred to the soil at a certain depth. The first approach is indicated in Graph 8.3 by the name *'_1surface'*. However, a more realistic assumption is that the load is applied at two different depths by separating the base and the shaft in two separate contributions. The second method is indicated by the name *'_2surface_max_shaft'*. The shaft contribution is inserted at a depth of $^2/_3$ times the embedded length of the pile in the bearing sand layer starting from the positive skin friction level. The area is projected with an angle of ¼ from the start of the positive skin friction depth. The base contribution is added at the original pile tip level and divided over an area given by the outer pile circumferences (Figure 8.2). The latter method gives a more realistic distribution of the stresses into the soil. The spread of the load results in less stresses on the same area which reduces the amount of settlements.

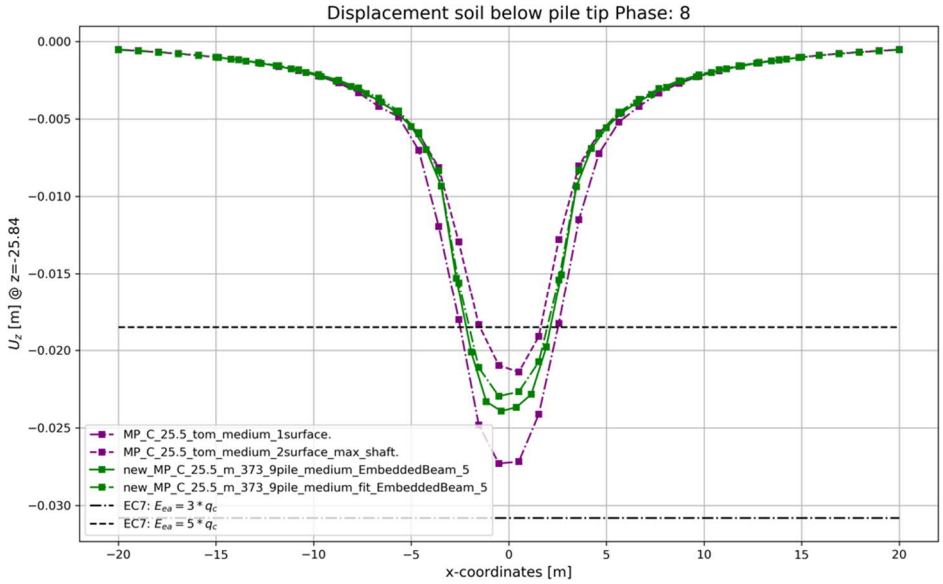


*Graph 8.3: $s_2$ settlement Tomlinson L=25.5, F=2750kN*

Graph 8.3 and Graph 8.4 show the difference between both Tomlinson approaches. The one with separated base and shaft surfaces shows less settlements compared to the method with only 1 surface. It implies the stresses are more evenly distributes over a larger area in the approach with two surfaces and results in less settlements. The EC7 lines are a simple approximation of elastic deformation of the sand layer below pile groups and is not addressed in the 80-pile model with the consolidation Eem clay layer. It gives an upper and lower bound for the expected amount of settlements.

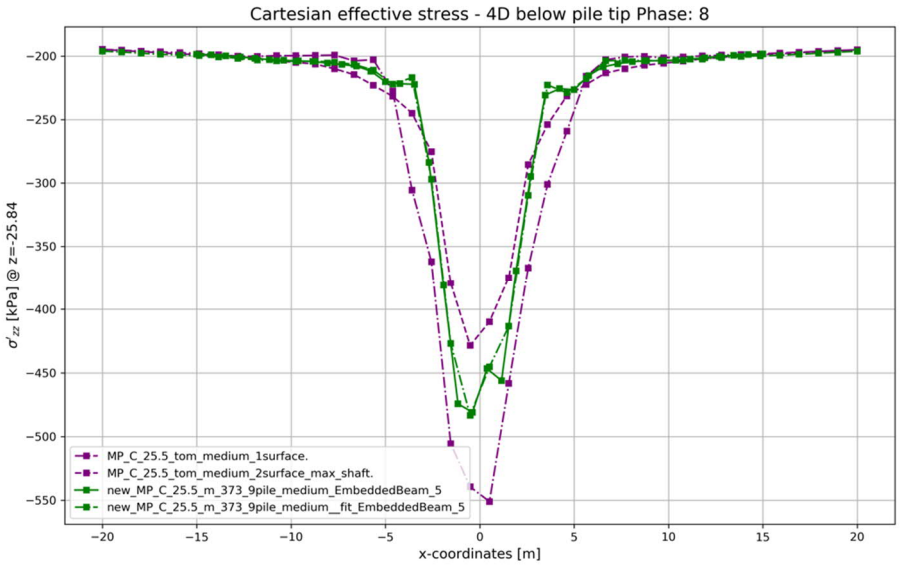


*Graph 8.4: $s_2$ settlement stress distribution 9 pile model, L=25.5 m, F=2750kN*

To give a better insight in the distribution of settlements between the Tomlinson approache and the PLAXIS 3D calculation, the stress distribution at 4D below pile tip level is given in Graph 8.4. The '2_surface' approach has stressed the soil over a wider area and results in a less deep settlement trough. On the other hand, the PLAXIS 3D calculation has a smaller stressed zone and results in a deeper settlement trough. The '2_surface' approach transfers the loads over a larger soil volume into the soil which ensures more spreading of the stresses.

### 8.2.2 Conclusion - 9 pile model

Since it is challenging to obtain the real settlement behaviour of a pile foundation, a comparison between benchmark solutions is made to get an idea about the differences between the proposed methods in § 7.4. Hence, different calculation approaches are investigated rather than different FEM software packages with the same modelling approach.

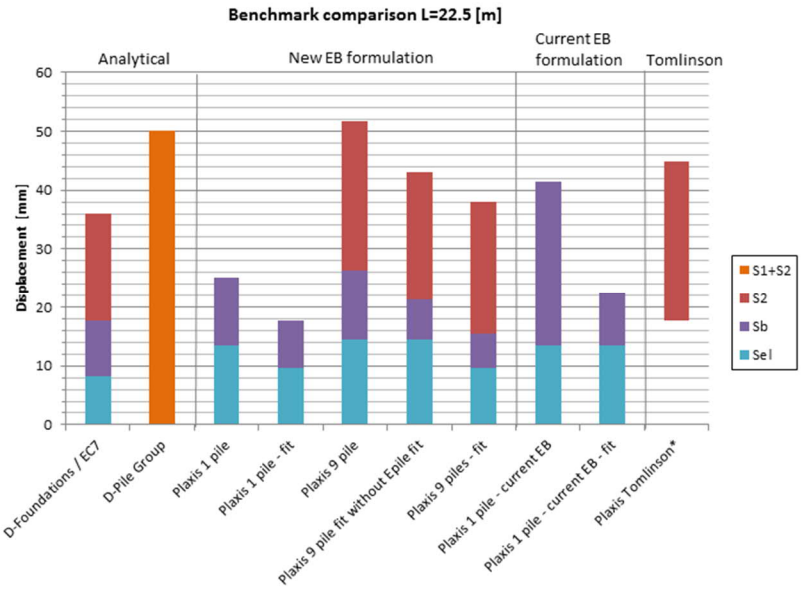


*Graph 8.5: Benchmark comparison calculation approaches L = 22.5 [m], F = 2250 kN*

| Approach | Explanation |
|---|---|
| D-Foundations/EC7 | EC7 approach single pile and elastic $s_2$ deformation bearing sand layer |
| D-Pile Group | EC7 approach single pile behaviour and between piles with cap interaction model |
| Plaxis 1 pile | New EB initial response |
| Plaxis 1 pile - fit | New EB with fitted soil layer parameters in sand bearing layer |
| Plaxis 9 pile | New EB including 9 piles initial response |
| Plaxis 9 pile - fit | New EB including 9 piles with fitted soil layer in sand bearing layer |
| Plaxis 1 pile – current EB | Current EB initial response |
| Plaxis 1 pile – current EB - fit | Current EB with fitted soil layer in sand bearing layer |
| Plaxis Tomlinson | Tomlinson approach in PLAXIS, *plotted on top of D-Foundations single pile result |

*Table 8.1: Explanation of the different benchmark approaches 1 pile / 9 pile models*

**Plaxis 1 pile**
The application of the new embedded beam formulation shows good results for modelling soil displacement piles in combination with embedded beam elements. The response in the single pile setup is stiffer compared to the current embedded beam formulation which is in favor of modelling soil displacement pile behaviour.

**Plaxis 9 pile**
Difficulties arise in case a pile group calculation is tested with the fit approach discussed in § 6.4. There is no clear difference anymore between the $s_1$ and $s_2$ settlements, which is basically a mathematical rule proposed by NEN9997 rather than real pile behaviour. Therefore, the separation of elastic ($s_{el}$), pile tip ($s_b$) and pile group ($s_2$) displacements in this thesis is according to a predefined model shown in Figure 7.1. The 9-pile model shows less pile ($s_1$) settlements compared to the single pile models, which is probably caused the by stress dependent stiffness of the soil (§ 5.3.3).

**D-Pile Group**
In case no soft soil layer (e.g. Eem clay layer) is situated underneath the sand bearing layer, a D-Pile Group can be used for a settlement calculation. The calculated settlements are on the upper boundary compared to the other approaches. Reason for this is the difference of the soil model used in D-Pile Group and the difference in the required soil parameter data. The PLAXIS calculation with the Hardening soil model has stress dependent stiffness and compaction hardening which results in stiffer behaviour of the soil at higher load levels. In D-Pile Group the skin friction distribution is described according to linear elastic perfectly plastic T-Z curves and the base resistance according to predefined pile tip curves (Deltares, 2016a), which causes softer behaviour.

**PLAXIS Tomlinson**
The difference in the Tomlinson approach and the embedded beam calculation is caused by the stress distribution below pile tip. Shaft friction of the embedded beam starts at the beginning of the positive skin friction zone, where the Tomlinson approach starts at a deeper level. Thus, in the embedded beam approach the stresses are distributed over a larger area. Moreover, only $s_2$ settlements are calculated in the PLAXIS Tomlinson approach where the embedded beam method in PLAXIS also incorporates $s_1$ settlements. This makes it difficult to compare both methods with each other. To conclude, the Tomlinson approach is basically the same as modelling embedded beams because: exactly the same PLAXIS geometry is used and exactly the same load is applied but in a different way. Thus, it is sound that the results are more or less equal to the PLAXIS calculation including embedded beams.

## 8.3 $s_1$+$s_2$ response - 80 pile model
Chapter 5 and 6 are focusing on pile tip ($s_b$) settlements in single pile models, chapter 7, 8 and 9 are trying to capture the entire pile behaviour. That includes $s_b$, $s_{el}$ ($s_b + s_{el} = s_1$) and $s_2$ settlement contributions in one PLAXIS 3D model as proposed in paragraph 1.5. As a benchmark, the approach with Tomlinson in PLAXIS 3D in combination with D-Foundations is used. This is one of the currently used methods in daily engineering practice.

### 8.3.1 Group effect PLAXIS 3D embedded beams

**Centre pile**
In pile group calculations it is not straightforward anymore to separate and plot the contributions of the single pile and group behaviour. In order to give information about group effects that occur in large PLAXIS 3D models, the single pile

model is compared with the response of the centre pile in the 80-pile model. Pressley & Poulos (1986), Fleming (1992) and Tschuchnigg (2013) (§ 2.4) mentioned that in case of high foundation loads, the load-displacement behaviour gets stiffer in pile groups compared to single pile setups. This can be explained by the stress dependent stiffness characteristics of the soil, which is described in § 5.3.3. Graph 8.6 visualizes this effect for the single pile and the 80-pile model, where the 80-pile model shows less displacements compared to the single pile model.

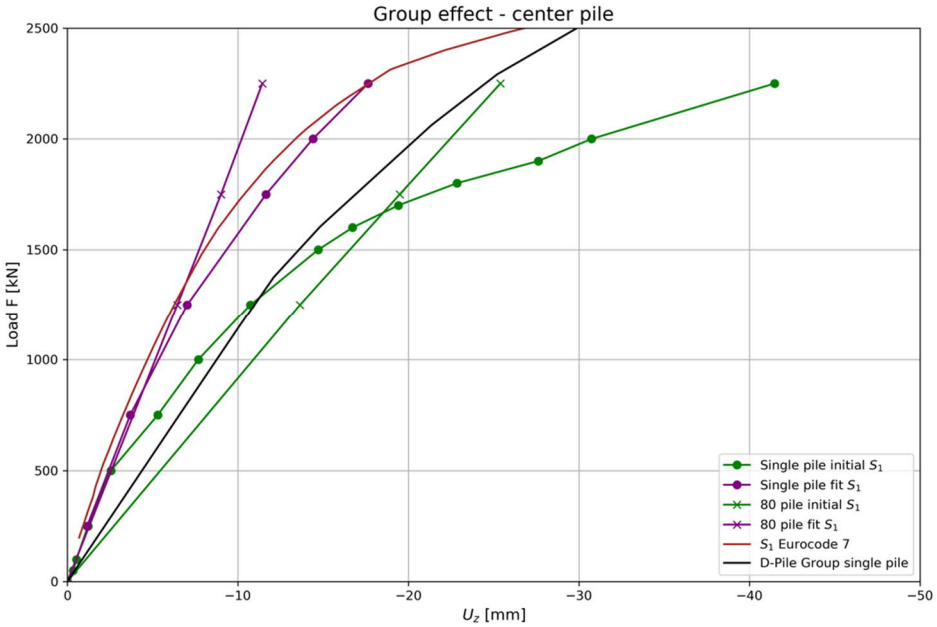


*Graph 8.6: Load settlement curve, comparison single pile and 80 pile model (center pile)*

Bearing capacity mechanism of pile groups are different compared to settlement mechanisms. In case a bearing capacity calculation is performed, the maximum shaft friction mobilization reduces among the inner piles. For the bearing capacity, the piles are behaving like a block foundation with an efficiency factor smaller than one (Pressley & Poulos, 1986). This is also partly true for the settlement behaviour, although the base stiffness is increased due to the stress dependent stiffness and increased horizontal stresses after installation. Taking into account the pile spacings, the settlement behaviour of a pile group is stiffer compared to single piles (Poulos, 1968), resulting in an efficiency factor higher than one for the amount of settlements.

**Pile group**

In the calculation with the 80-pile model, it turned out at 4D below pile tip the fit parameters have an influence on the $s_2$ settlements (see Graph 8.7). Because, the single pile behaviour should not influence the group behaviour, the fit volume below the pile tip is reduced to a depth of 4D below pile tip, this is in line with NEN9997 (see also § 6.4, Graph 8.7 and Graph 8.8 right). The fit calculations with the single pile are preformed again and result in higher fit parameters (Table 8.2) due to the smaller fit volume. In Graph 8.8 is visualized that the $s_2$ response is now similar to the initial model before fitting the parameters.

Updated fit parameters after 9 pile model

| *Parameter:* | *Factor:* | *Value:* | *Unit:* |
|---|---|---|---|
| $E_{pile}$ | 1.5x | $30 \cdot 10^6$ | [kPa] |
| $E_{oed}^{ref}$, $E_{50}^{ref}$ | 3x | $150 \cdot 10^6$ | [kPa] |
| $E_{ur}^{ref}$, $G_0^{ref}$ | 3x | $450 \cdot 10^6$ | [kPa] |

*Table 8.2: Updated fit parameters after Table 6.4 - 80 pile model*

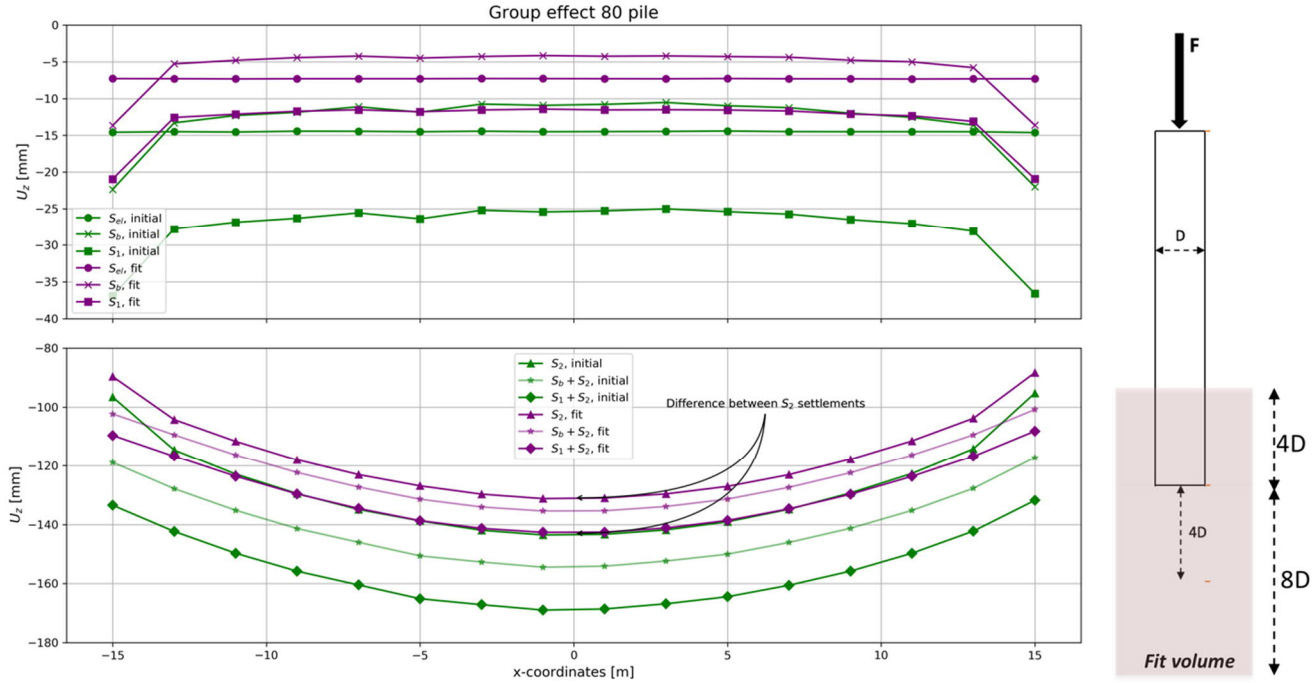


*Graph 8.7: Splits contributions 80 pile model, cross section middle row, no plate stiffness, F = 2250 [kN] {left} , initial fit volume {right}*

In Graph 8.8 the $s_2$ settlements are not influenced by the single pile response anymore. The overall settlements are still reduced due to the fit on single pile response. Moreover, except from the edge piles, the $s_1$ and $s_b$ settlements are constant along the entire foundation in x direction. This implies the single pile behaviour is equal in all the piles. This behaviour is correct according to NEN9997 because, the $s_1$ settlements are not influenced by group effects and only count for the single pile settlement by equal loading. The $s_2$ settlements varies over the x-direction because of the stress concentration in the middle of the pile group.

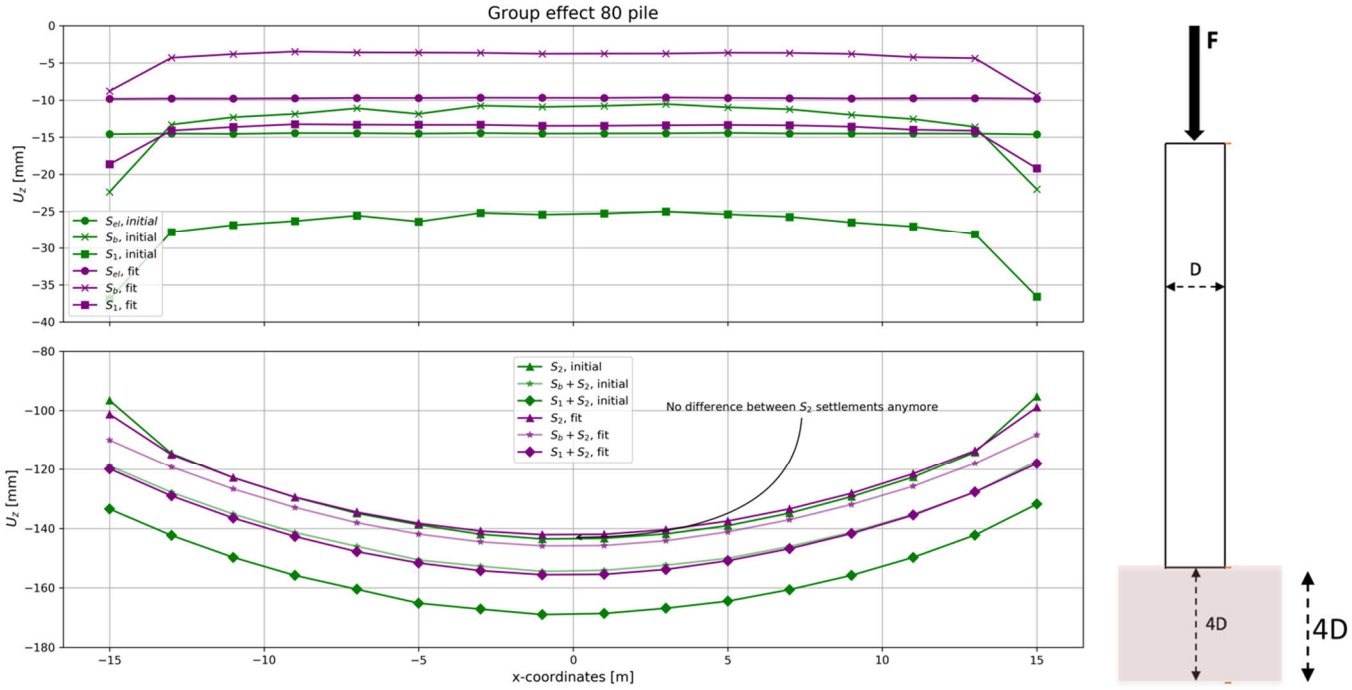


*Graph 8.8: Splits contributions 80 pile model, cross section middle row, no plate stiffness, F = 2250 [kN] {left} , reduced fit volume {right}*

Fit calculations are intended to improve the single pile response only, rather than influencing the settlements at the deeper layers. Graph 8.9 and Table 8.3 are indicating that the contribution and distribution of the settlements in the Eem clay layer at -30 meters below reference level are not changing. Which is important because, the Eem clay layer contributes to a large extent on the total amount of settlements and should therefore not be influenced by the single pile fit.

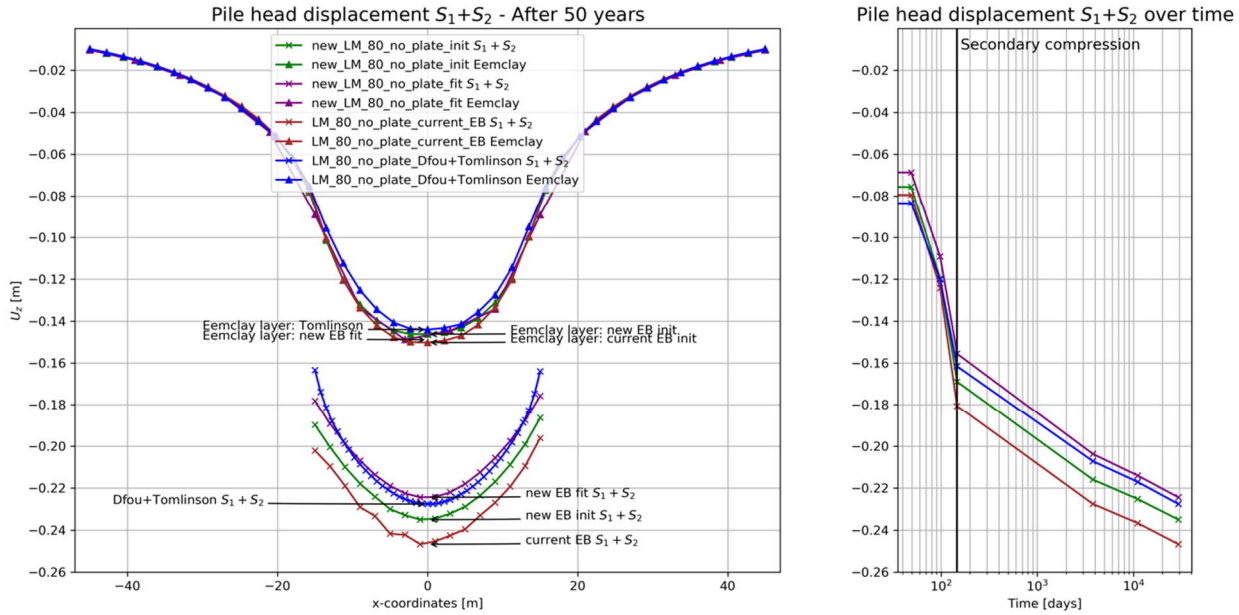


*Graph 8.9: Overview different calculation approaches pile head settlement, no cap stiffness*

In Table 8.3 the improvements are visible due to the fit factors. The single pile settlement shows the largest reduction compared to the other contributions. Moreover, the settlement in the sand layer and Eem clay layer are more or less equal to the initial calculation. It implies only the single pile behaviour is changed and the overall settlement remains equal after applying the updated soil stiffness parameters.

Separated contribution 80 pile model

| *Measure location:* | *Name:* | *Initial:* | *Fit:* | *Difference (initial fit):* | *Unit:* |
|---|---|---|---|---|---|
| Pile head | $s_1$+$s_2$ | 0.235 | 0.224 | 0.011 | [m] |
| Single pile (calculated) | **$s_1$** | **0.028** | **0.013** | **0.015** | **[m]** |
| 4D below pile tip | $s_2$ | 0.207 | 0.211 | -0.004 | [m] |
| Top Eem clay layer | Eem clay layer | 0.146 | 0.146 | 0 | [m] |
| Elastic sand | Elastic sand | 0.061 | 0.065 | -0.004 | [m] |

*Table 8.3: Settlement comparison 80 pile model, center foundation*

### 8.3.2 Influence cap stiffness – 80 pile model

The cap stiffness plays an important role in the (differential) settlements of (pile) foundations. Using the right building stiffness, a large advantage can be gained regarding the amount of calculated settlements, especially differential settlements. Since the single pile behaviour is included in the same calculation, it is easier to incorporate the stiffness of the building and preform several scenarios. The redistribution of stresses is governed by soil mechanical principles rather than equivalent springs in the structural design (§ 9.3).

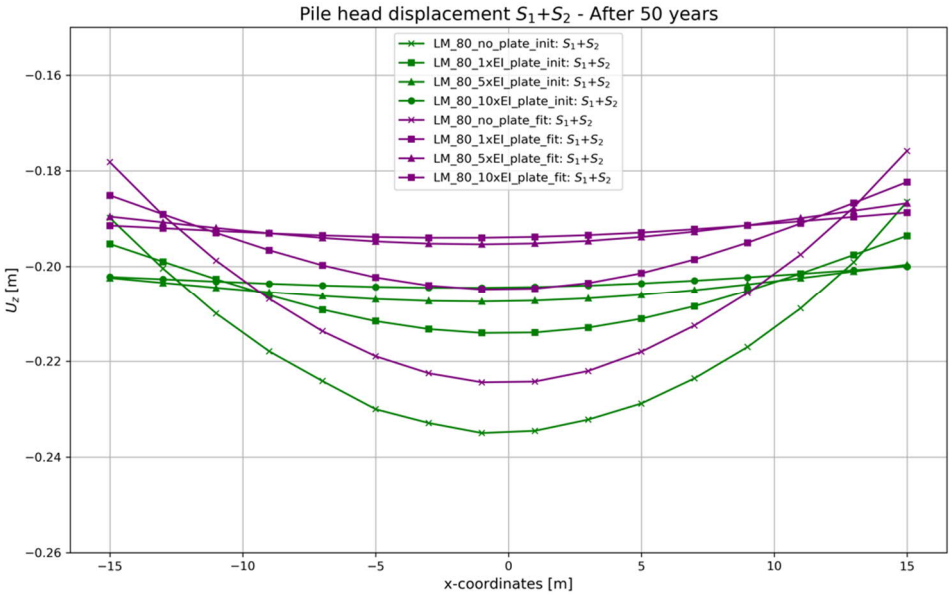


*Graph 8.10: Influence pile cap stiffness on total settlements*

In combination with a pile cap, it is even more difficult to separate information regarding single pile and pile group behaviour. The cap with a certain stiffness distributes the loads the piles, which makes it difficult to relate the different load contributions to the different pile settlements. Graph 8.10 visualize the reduction of differential settlements by applying a stiff pile cap. In practice, the superstructure turned out to be a relative stiff structure because, the foundation plate is often a thick concrete slab. Therefore, it is beneficially to take into account the stiffness of this concrete slab in the geotechnical analysis to reduce the amount of settlements. However, care must be taken by choosing too optimistic values for the plate stiffness in order to not underpredict the settlements. More explanation and discussion about soil-structure interaction is given in chapter 9.

### 8.3.3 Result different approaches – 80 pile model

**D-Pile Group**

Paragraph 3.2.1 already discussed the features and limitations of the D-Pile Group software. Due to the limitation of not being able to handle pore water pressures, D-Pile Group is not suitable for settlement calculations containing a compressible layer underneath the bearing layer. Therefore, D-Pile Group is only suitable for settlement comparison up to and including the second sand layer, so in this case only the 9-pile model.

**Current 80 pile (LM) PLAXIS 3D model initial**

This thesis is designing a framework for modelling soil displacement piles in a practical and workable way. On the one hand the improvement in the embedded beam formulation plays an important role in achieving this. On the other hand, the fit procedure below pile tip level is part of the solution. In order to assess the improvement with the new EB formulation, the 80-pile model has been calculated by changing only changing the formulation of the embedded beam.

Graph 8.9 visualizes that the current formulation experiences the most settlements, due to the soft base response (§ 4.4). Since the current formulation has a high degree of mesh dependency, no further elaboration with the current formulation is included in this chapter. The combination of large mesh dependency and softer base response makes the formulation not suitable for the desired application.

**New 80 pile (LM) PLAXIS 3D model initial**

The initial 80-pile model does not have the updated fit parameters in the sand bearing layer yet but, runs with the new formulation of the embedded beam. Improvements regarding settlement behaviour are visible between the current and new embedded beam formulation. The stiffer behaviour of the new embedded beam has a positive influence on the application of modelling soil displacement piles, which is the overall goal of this thesis.

**New 80 pile (LM) PLAXIS 3D model fit**

Initially, the fit parameters are similar to the single pile calculations in § 6.5.2. Graph 8.9 visualizes that changing the stiffness of the fit volume in the sand layer does not have an influence on the consolidation settlements in the Eem clay layer. Moreover, the fit parameters should not influence the $s_2$ behaviour. This is the case with the fit volume and parameters from paragraph 6.5.2. Therefore, the depth of the fit volume below pile tip level of the 80-pile model is reduced (right figure Graph 8.8). Consequently, the stiffness parameters of the soil have to be increased to approximate the behavior of soil displacements piles in NEN9997 (see Table 8.2).

Conclusion, the single pile behaviour is implemented correctly based on EC7, because the piles along the x-direction showing the same single pile settlements by equal load. Due to the stress dependent stiffness, the single pile response is stiffer compared to the single pile model because of the higher load from the adjacent piles in the same area.

**Tomlinson ($s_2$) + D-Foundation single pile ($s_1$)**

One of the currently used calculation schemes for determining settlements of pile foundations is a D-Foundations calculation in combination with the Tomlinson approach in PLAXIS 3D. D-Foundations is used for single pile behaviour and the Tomlinson calculation for the group settlement response[4]. Graph 8.9 shows the settlement of the Tomlinson-PLAXIS 3D model including the D-Foundations contribution for a single pile. The response of the fitted new embedded beam model approximates the behaviour of the Tomlinson calculation in combination with the D-Foundations calculation. It implicates the "new" approach is approximating the current methodology. Due to the lack of real measurement data for this case, no conclusion can be draw if this method determines the differential settlements more accurate. Although, the modeling technique including embedded beams approximates the real soil structure interaction more realistic. Which can be seen as an improvement compared to the current modelling technique.

## 8.4 Conclusion

To determine the behaviour of soil displacement piles in pile groups, two improvements are investigated. The new embedded beam formulation and a soil stiffness fit below pile tip level should approximate the enhanced soil stiffness after the installation of soil displacement piles. By combining the single pile behaviour, group behaviour and superstructure bending stiffness, soil-structure interaction becomes possible.

The new embedded beam formulation is an overall improvement regardless of the installation method for pile calculations with embedded beams in PLAXIS 3D. Convergences are achieved at reasonable mesh sizes which result in acceptable calculation costs. Moreover, improvements on the load-displacement response of soil displacement piles are obtained. Although, the embedded beam is not designed for this type of pile, the load-displacement response of the new formulation is stiffer compared to the current formulation.

Second, the proposed fit method is partly effective for the desired application. It is difficult to separate the different settlement contributions in case more piles are modelled. During the first attempt of modelling large pile groups, it turned out that the fit volume is influencing the group settlements at 4D below pile tip level ($s_2$). For this reason, the height of the soil fit volume is reduced to 4D below pile tip level. In doing so, the fit parameters have to be increased due to the smaller fit volume. By decreasing this fit volume, the single pile settlements are still reduced, and the group settlements are not influenced anymore. A limitation for the outcome of this research is that no real experimental data was available to test the validity of the proposed method.

Moreover, group effects are only partly covered in the approach presented in chapter 8. The reduction or increase in skin resistance is not incorporated because, the predefined maximum skin friction capacity is manually inserted and is not a result of the PLAXIS calculation. To conclude, it is possible to approximate soil displacement pile behaviour with embedded beams however, not all group effects are taken into account yet, due to the choice for the utilised shaft friction model.

Regarding soil-structure interaction, different pile cap stiffnesses are tested in combination with the proposed improvements. The soil-structure interaction makes it possible to redistribute the loads in the pile group, resulting in less overall and differential settlements. More information on soil-structure interaction is given in chapter 9.

[4] At CRUX Engineering B.V. Amsterdam

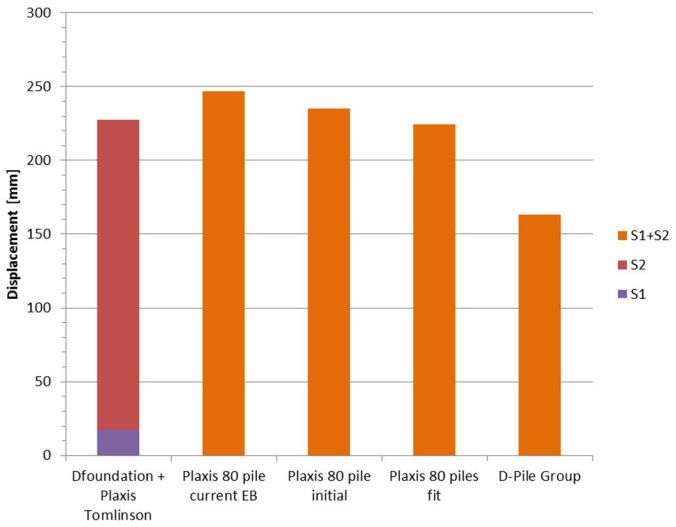


*Graph 8.11: Total overview of settlements from different calculation approaches (D-Pile Group contains no Eem clay layer) (Tomlinson approach in PLAXIS 3D)*

# IV Application

# 9 Case study comparison

In this case study a high-rise project in Amsterdam is analysed based on available measurement data of this building. A large part of the building is intended for living space. The construction consists of multiple buildings, each with different foundation loads. Two of these buildings are 18 and 14 storey high constructions, the other buildings have a maximum height of 8 floor levels. The two tallest buildings are founded on a thick concrete slab including Vibro-piles in the second sand layer. Unfortunately, the case study is anonymized because of contractual agreements, therefore no pictures and detailed information are published.

The case study is in particular relevant since an increasing trend is going on in high-rise project developments in densely populated areas in the Netherlands. The lack of space and the increasing demand for living space in these areas results in feasible high-rise projects. Most of these densely populated areas in the Netherlands is facing difficult ground conditions containing sands and clays. To reduce investments costs, accurate determination of differential settlements results in cost effective foundation and structural designs.

In the design of this case study, relatively large displacements were expected. During construction period, the expected amount of settlements turned out the be lower than calculated. It makes the case study in particular suitable for investigations on the calculation approach for differential settlements.

Chapter 9 combines the research in the previous chapters on single pile, pile group and superstructure stiffness. Therefore, all the calculations in this chapter (9) are conducted with the new embedded beam formulation. First, the model setup of the case study is discussed. Secondly, the analysis including the fit method described in § 6.4 is applied and the influence of the superstructure stiffness on the load distribution is investigated. Finally, conclusions are drawn after comparison with the available measurement data of the construction.

## 9.1 The model

In this paragraph the model, soil and pile properties of the case study are explained. Most of the geometrical and geotechnical data are retrieved from the design documents available at CRUX Engineering BV. Additional drawings and background information is given in appendix E.

### 9.1.1 Soil stratigraphy and soil properties

**Soil stratigraphy**

The goal of this case study is to compare modelling methods rather than the variations in soil parameters. Therefore, the same soil stratigraphy is used relative to the original design calculations. The soil stratigraphy of these calculations is based on CPT DKM32 which is attached in appendix E.1.2.

Specially attention is paid to the modelling of the Eem clay layer underneath the second sand layer. This layer is prone to consolidation and creep which requires an excess pore water dissipation calculation. In order to make it possible for the Eem clay layer to drain on both sides, the third sand layer is modelled as well.

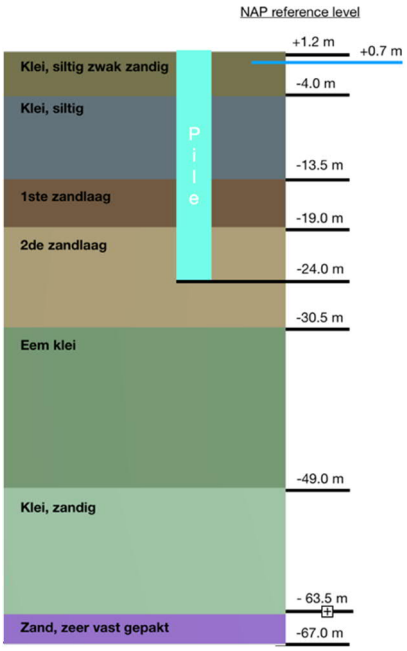


*Figure 9.1: Soil stratigraphy case study*

**Soil properties**

Equal to the soil stratigraphy, the soil properties are adopted from the original design calculations. The soil parameters in the design calculations were based on CPT's, laboratory data from a project nearby and the North South metro line parameter set. The soil model parameters of PLAXIS are correlated with soil investigation data according to correlations described in Appendix B.3.3. The soil properties of the case study are given in appendix E.1.3.

Moreover, attention is paid to the OCR value of the Eem clay layer. In the soft soil creep model, the OCR value is influencing the initial creep strain rate. Therefore, the OCR is calibrated on the equivalent age according to den Haan (2003). The calibration of this OCR value is done during the design calculations and review sessions at CRUX Engineering (OCR = 1.9) and is not further elaborated here.

### 9.1.2 Pile properties

The Vibro pile system is applied since high foundation loads and a deep bearing layer are expected. In comparison to the pile used in the previous chapters, the pile class factors are slightly higher due to the driven installation method instead of screwing (Table 9.1). Moreover, the design calculations are performed before 31 December 2016, which means the old pile class factors have been used.

| Pile type | Installation method | Diameter | NEN9997 factors* |
|---|---|---|---|
| Driven cast-in-place pile, tube back by driving | Soil displacement | ⌀ 606/680 mm | $\alpha_p$ = 1.0 |
| | Lost foot | | $\alpha_s$ = 0.014 |
| | In situ concrete | | $\beta$ = 1,0 |
| | Withdrawn steel casing | | s = 1,0 |

*Table 9.1: Pile properties Vibro-pile – case study*
** design is calculated before 31 December 2016*

**D-Foundations results**

The pile bearing capacity is calculated in the same way as in the previous chapters for the single pile model (chapter 5 & 6). This includes a D-Foundations calculation based on an CPT given in appendix E.1.2.

| | CPT DKM 32<br>L=23.6 |
|---|---|
| Pile tip level (NAP) | - 24 [m] |
| $R_{c;cal;max}$ (Total pile capacity) | 7264 [kN] |
| $R_{b;cal;max}$ (Base capacity) | 4633[kN] |
| $R_{s;cal;max}$ (Shaft capacity) | 2631 [kN] |
| Base/shaft ratio | 1.76 |

*Table 9.2: D-Foundations pile capacities*

PLAXIS is designed for SLS load level ranges and does not incorporate safety factors on materials or spatial variability. Therefore, the characteristic values obtained from the D-Foundations calculation are used for the maximum pile capacity, which implies less conservative results.

### 9.1.3 Geometry

For the single pile analysis as well for the full calculation model, exactly the same geometry is used. This ensures equal mesh distribution and boundary conditions in both models. The boundary conditions and other numerical model parameters are summarized in appendix E.1.

**Structural overview**

The geometrical elements and pile positions of the case study are presented in appendix E.1.1.

**Prevent plate touching the soil**

In case the foundation plate would rest on the soil, it could contribute on the load transfer from the surface level to the soil (like a raft foundation). In order to prevent this, an excavation is modelled with gentle slopes from surface level towards 20 centimeters below the foundation plate (Figure E.4, Appendix E). It ensures that the plate can move freely without touching the soil.

**Mesh**

The different mesh coarseness's have a different number of elements, they are summarized in Table E.5. The mesh influence is discussed in § 9.2.1.

### 9.1.4 Loading of foundation in time

Figure E.5 and Figure E.6 visualizes the load transfer from the superstructure towards the foundation plate. The self-weight of the building the largest part of the total load on the foundation. In order to determine the load transfer to the piles, the self-weight is obtained from the structural design documents. First, the floor levels are divided in different areas which transfer the load through the structural walls and columns towards the foundation slab. Secondly, the load contribution on a certain area is determined by the self-weight of the walls and concrete floors acting on this specific area. Finally, the contribution of all the areas at each floor level are modelled as a line load representing the structural walls on the foundation plate and point loads representing the columns (see Figure E.5 and Figure E.6).

Since the measurements were conducted during construction time, the loads are not applied in one go. Hence, the load increase is governed by the amount of floor levels constructed. In each phase, the total amount of load on the construction is multiplied by the ratio between finished floor levels and total amount of floor levels (eq. 9.1 and Table 9.3).

$$\text{load}_{phase\ x} = \frac{\text{amount of constructed floor levels}}{\text{total amount of floor levels}} \cdot \text{total load} \qquad 9.1$$

| | Construction | | | | | | | | Consolidation |
|---|---|---|---|---|---|---|---|---|---|
| **Phase** | **1** | **2** | **3** | **4** | **5** | **6** | **7** | **8** | **9** |
| Duration in days | 147 | 98 | 14 | 21 | 42 | 21 | 49 | 42 | 9564 |
| Duration days cumulative | 147 | 245 | 259 | 280 | 322 | 343 | 392 | 434 | 10000 |
| Tower 2 | 2/14 | 12/14 | 13/14 | 14/14 | Finished | Finished | Finished | Finished | |
| Tower 1 | 2/18 | 2/18 | 3/18 | 5/18 | 11/18 | 13/18 | 18/18 | Finished | |

*Table 9.3: Phasing of loads during construction and operational phase - case study*

The ratio's in Table 9.3 are the amount of constructed floor levels at a certain time divided by the total number of floor levels.

## 9.2 Single pile

### 9.2.1 Mesh sensitivity

Mesh sensitivity analysis is an important step before running PLAXIS calculations, especially in combination with embedded beams (§ 6.3). For the complete model including all piles, only minor influence is noted between the different mesh distributions. Therefore, the coarse mesh size distribution is used.

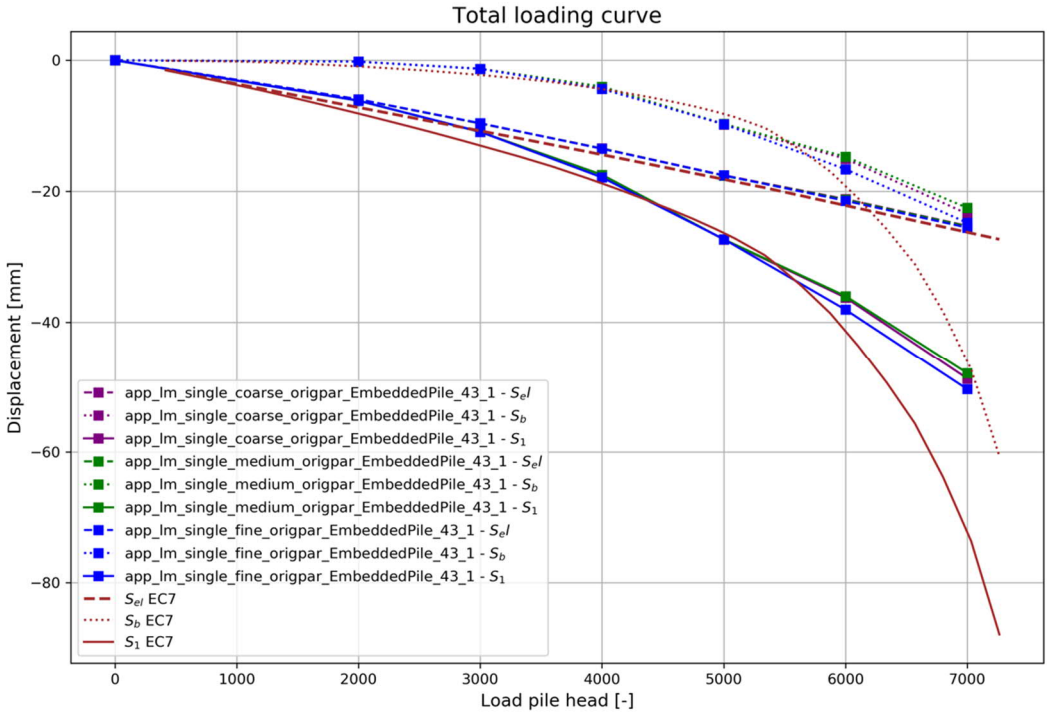


*Graph 9.1: Mesh sensitivity case study single pile*

**Pile position**

The mesh is randomly distributed around the pile tips which results in different mesh element sizes around each pile in the same model. Because, the mesh sensitivity is negligible, the position of the piles is not influencing the response. This is important when the response of a single pile fit is extrapolated to other piles in the same model. Based on Graph 9.2, assumed is independent from their position in the mesh all the piles follow the same load-displacement curves initially.

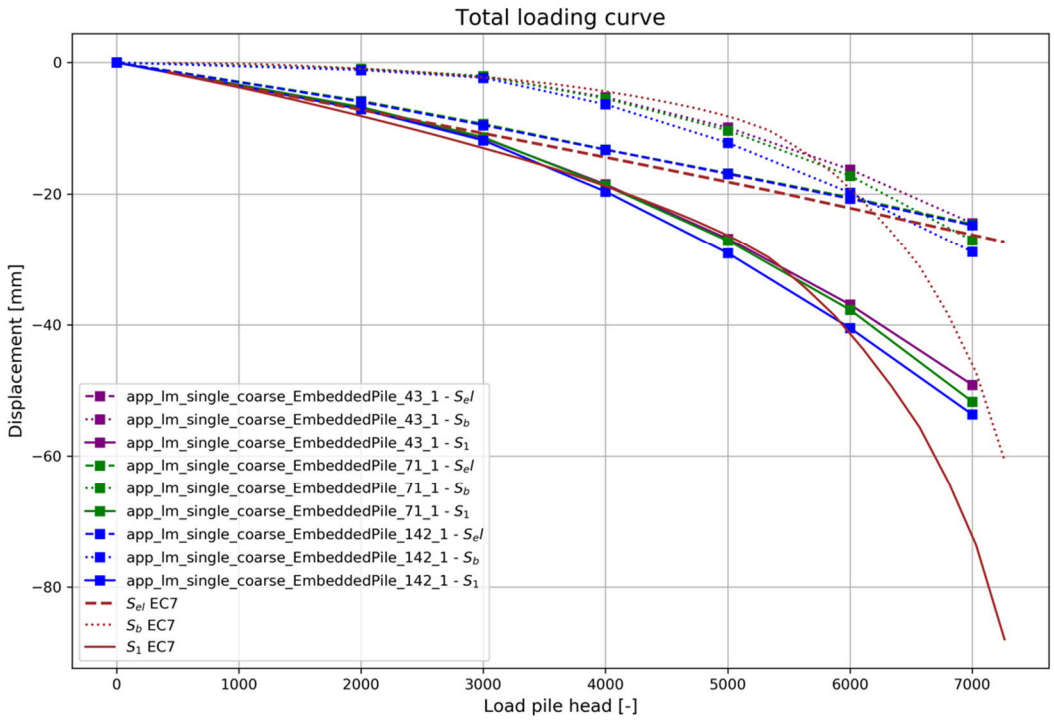


*Graph 9.2: Mesh influence different pile positions in same model and mesh*

## 9.2.2 Fit single pile

**Soil stiffness fit**

Graph 9.1 and Graph 9.2 are indicating that the initial response of the embedded beam is already in line with NEN9997. Which means no fit in PLAXIS 3D is required for the base as well for the elastic compression of the pile. The difference with the previous chapters were a pile fit is required can be caused by:

- The problem addressed here is soil stratigraphy and model dependent.
- The new embedded beam behaves too stiff for a pile which was intended to be a pile without installation effects. The spring at the bottom of the new embedded beam could be too stiff compared to the current formulation. Although, this is favourable for a soil displacement pile which is investigated in this thesis.
- The deeper penetration in the sand bearing layer ensures that more shaft friction and base resistance is mobilised with less displacements compared to the shorter pile models. Because of the higher stresses and stiffness of the soil at larger depths. This mechanism is further explained below.

**Explanation why fit is not required**

In order to proof the statement about the stiffer behaviour in combination with a deeper pile penetration, an additional single pile test is conducted. Similar to the PLAXIS geometry in § 6.5.2, three different pile lengths are compared with the NEN9997 curve. The soil stratigraphy of the PLAXIS model is described in § 5.2 including the bearing sand layer properties at -19 meter. In this model, 3 different pile lengths with pile tip levels of 20, 21 and 22 meters are tested.

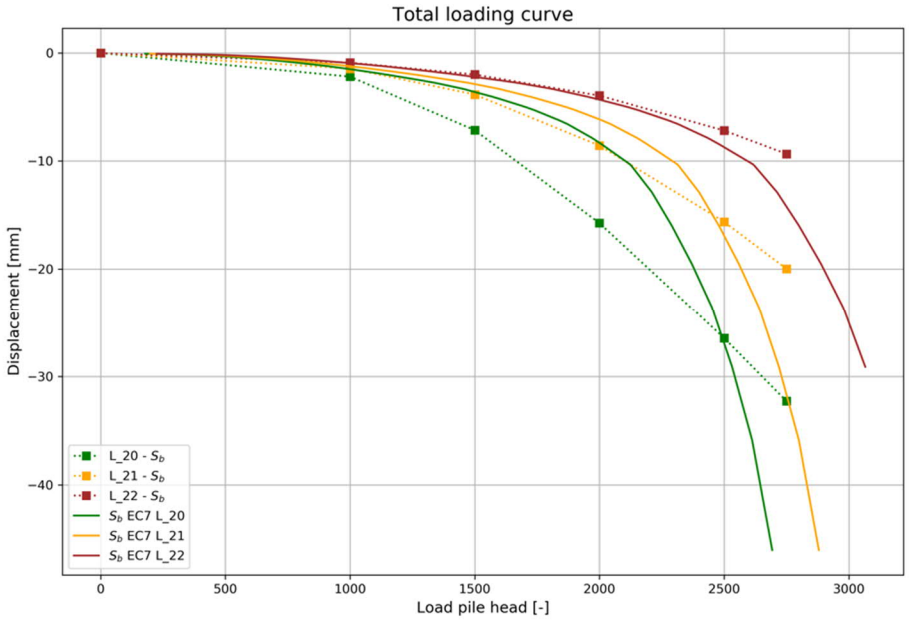


*Graph 9.3: Single pile calculation compared with EC7 load-displacement result*

Graph 9.3 visualizes that increasing the penetration length in the bearing layer, the response of PLAXIS approximates the NEN9997 curves better and better. The load-displacement response of NEN9997 is based on the bearing capacity and the curves given in Graph A.1. They assume a constant stiffness of the soil over depth. The settlements in NEN9997 are therefore only influenced by the length of the pile in combination with the cone resistance. However, in the PLAXIS calculation also the stress dependent stiffness features for example reduce the amount of settlements by an increasing penetration length.

Moreover, the NEN9997 curves show a strong deflection in the higher load ranges. This deflection is not visible in the PLAXIS response. In PLAXIS the pile tip of the embedded beam is connected to a linear elastic perfectly plastic spring which cannot return the deflection obtained in the NEN9997 curve.

## 9.3 Soil - structure interaction methodology

Soil-structure interaction is an integral topic in geotechnical and structural design of constructions. The structural components in the superstructure are interdependent from the soil medium underneath (David & Forth, 2011). The soil parameters/reaction is important for representing the behaviour of the structural elements in the superstructure. The superstructure imposes forces and stresses into the soil medium due to loading conditions determined by the structural engineer, which in turn imposes deformations in the soil. As a consequence, the soil transmits additional deformations and forces back to the superstructure. This interaction process continues until equilibrium has been achieved in the soil and the superstructure.

The interaction between the soil and the superstructure is subdivided in two different parts. On the one hand, the stiffness of the superstructure divided in the stiffness of the individual structural components and the interaction between these components. On the other hand, the stiffness of the soil, which is depending on several components like: stress state, loading rate and stress path. A measure for the relative stiffness of the superstructure of the foundation is k, which is a ratio of the two separate contributions (Breeveld, 2013). In case the building reacts fully flexible $k < 0.01$, if the building reacts infinite stiff $k > 0.1$. Between those two values an interaction calculation is required.

Settlements in the foundation due to soil displacements could modify the stress distribution in the superstructure. In the superstructure, stiff elements show almost no settlements and attract loads from elements which settle more. This process is increasing or decreasing the total amount of settlements. The process of interaction is repeating until an equilibrium is achieved between the settlements in the soil and in the superstructure.

### 9.3.1 Current interaction approach case study (used in original design)

During the original design of the case study, an 'iterative staggered coupling for soil structure interaction modelling' approach is used (§ 3.1.2 and Figure 3.2). This approach is commonly used in practice but is lacking a fully coupled soil-structure interaction calculation.

First, the structural design of the superstructure is determined by the structural engineer. This includes determination of dimensions from the structural elements, so they perform sufficient under the applied load combinations. However, the dimensions of the structural elements based on the initial value of the modulus of subgrade reaction ($s_1$) are highly influenced by this modulus of subgrade reaction. Therefore, an appropriate soil-structure interaction calculation is required to determine the amount of loads.

Second, the output of from the structural engineer in the first calculation phase is input for the geotechnical engineer. The structural engineer has two possibilities for obtaining the loads for the superstructure. Either the loads on the foundation plate from the superstructure without the soil interaction or the loads on the pile heads including redistribution due to the influence of the modulus of soil subgrade reaction on the superstructure. In this case study the structural engineer reported the loads on the pile heads after redistribution of the stresses in the superstructure and foundation plate. The geotechnical engineer inserted these loads as surface load on $^2/_3$ of the embedded pile depth in the bearing sand layer to obtain the $s_2$ response.

Third, the deformation ($s_2$) imposed by the surface load should be reported back to the structural engineer for a new interaction calculation with the structural design. This iterative process is important in order to define the equilibrium load and moment distribution in the foundation. This is required for increasing accuracy in differential settlement determination of high-rise buildings on soil displacement pile foundations in soft soil deposits.

### 9.3.2 Proposed interaction approach case study (used in this research)

The interaction between the structural and geotechnical design is a challenging part in the design of high-rise buildings. One of the missing parts is the implementation of single pile behaviour of soil displacement piles in the geotechnical models. This thesis tries to contribute on the implementation of soil displacement single pile behaviour in PLAXIS 3D and thereby towards integration of the structural and geotechnical design in one calculation method. Although, a complete interaction calculation which includes the complete structural design and thereby a full soil-structure interaction calculation is not solved here. However, the method in this thesis narrows the gap to a full interaction calculation by modelling the stiffness of the superstructure by a representing plate element including the single pile behaviour as support reaction.

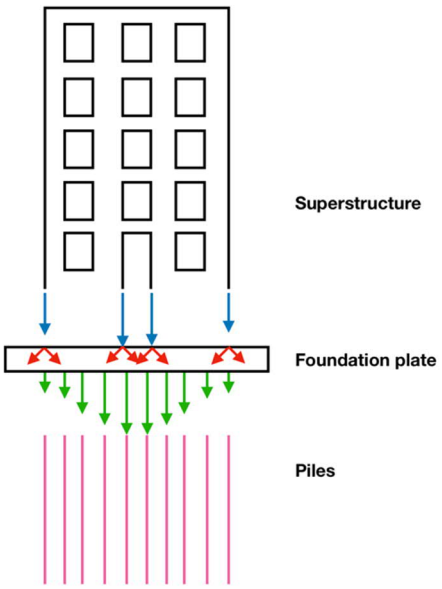


*Figure 9.2: Definition stiffness high-rise buildings*

Moreover, Zoidi (2015) concluded that modelling small heights of the total construction, for example the foundation plate or the plinth, already considered most of the core stiffness from the total superstructure. Therefore, in this case study, the foundation plate (1.8 meter) is modelled to count for the whole superstructure stiffness.

The loads from the superstructure are transferred to the foundation plate by walls and columns supporting the entire structure. Hence, walls are represented by line loads and columns are represented by point loads. The foundation plate is redistributing the loads over the different pile's underneath. In normal situations the superstructure contributes to the stiffness of the foundation plate. Hence, the redistribution of loads is relatively high in case the superstructure is very stiff (in most of the cases with high-rise buildings).

## 9.4 Analysis outline

First, the expected parameter set is used from the original design calculations. Here, the stiffness of the superstructure and foundation slab (tower 1 and 2) is represented by a 1.8 meter thick plate and a Young's modulus of 40 MPa. The plate element is used for redistribution of the loads by the superstructure towards the embedded piles. These piles are modelled according to the approach discussed in § 6.4 including the new embedded beam formulation. The main advantage over the original design is the modelling of the support reactions by the embedded beams including proper single pile ($s_1$) and pile group ($s_2$) behaviour. Where the support reactions in the original design model are only governed by springs underneath the foundation plate without connection to soil mechanics principles.

Expectation values original design

| Name | $k_v$ [m/day] | $\kappa^*$ [-] | E [MPa] | h [m] |
|---|---|---|---|---|
| Original design | $0.04 \cdot 10^{-3}$ | 0.01340 | 40 | 1.8 |

*Table 9.4: Expectation values original design – case study*

Moreover, the low-rise buildings are constructed between both towers (Figure E.1). Although, there is no structural connection between the low- and high-rise parts, these foundations are influencing each other by increasing the stress at pile tip level. The loads of the low-rise buildings are inserted as surface loads according to the Tomlinson approach as discussed in § 2.4.2. This simplification is done to reduce the amount of modelled embedded beams and therefore calculation time. However, the increase in stress due to the load from the low-rise buildings is small relative to the load from both towers.

### 9.4.1 Superstructure stiffness

The self-weight of the superstructure is transferred to the foundation plate by walls and columns. The soil interaction calculation in PLAXIS 3D is redistributing the imposed loads on the plate element towards the pile heads. As described in § 3.4.2 the bending stiffness of the superstructure in combination with the foundation slab has influence on the load and settlement distribution. Ideally, the entire structure should be modelled in PLAXIS for the most accurate stiffness values. However, in daily engineering practice this is one of the largest challenges. Therefore, a plate element is representing the bending stiffness of the entire structure. The bending stiffness can be changed by the Young's modulus and the thickness of the plate. In order to model the influence of the bending stiffness, 3 different variations have been analysed. A relative flexible, intermediate and a relative stiff plate which ensures maximum redistribution of loads.

Bending stiffness plate element variation

| *Name* | *EI [MPa]* | *E [MPa]* | *h [m]* |
|---|---|---|---|
| Cracked | 4.86 · b | 10 | 1,8 |
| Design value (initial) | 19.44 · b | 40 | 1,8 |
| Stiff | 1666 · b (≈ ∞) | 20 | 10 |

*Table 9.5: Bending stiffness representing superstructure – case study*

$$I = \frac{1}{12} \cdot b \cdot h^3 \qquad 9.2$$

The real constructed foundation slab is 1.8 meters thick. However, the superstructure is also contributing to the bending stiffness of the construction. Therefore, the height of the plate has been varied to count for the high bending stiffness in combination with the concrete core of the construction.

### 9.4.2 Eem clay layer

The Eem clay layer underneath pile tip level is contributing to a large extent on the total amount of settlements. Single pile behaviour is of importance by the redistribution of loads to the foundation plate. In case the loads are perfectly redistributed over the piles, the peak stress below the pile tips and on top of the Eem clay layer is decreasing. Hence, the soil structure interaction is important, on the other hand the soil properties of the Eem clay layer are also influencing the settlements to a large extent.

In order to obtain the influence on the velocity of the settlements in the consolidation phase, the consolidation coefficient ($C_v$) is changed with respect to the design value. Reduction of the $C_v$ increases the consolidation time and reduces only the speed of the settlement process. The total amount of settlements is independent from the $C_v$ value. In Table 9.6 three different values for the hydraulic permeability are given. Low k values result in long consolidation times which influences the shape of the settlement curve according to eq. 9.3. High k values result in faster consolidation times.

Consolidation coefficient variation

| *Name* | $k_v$ *[m/day]* |
|---|---|
| Lower bound | $0.02 \cdot 10^{-3}$ |
| Design value (initial) | $0.04 \cdot 10^{-3}$ |
| Upper bound | $0.08 \cdot 10^{-3}$ |

*Table 9.6: Variation consolidation coefficient used models – case study*

$$C_v = \frac{k}{\gamma_w \cdot m_v} \tag{9.3}$$

Based on the first calculations in § 9.5, the OCR value in the Eem clay layer is not changing significantly relative to the initial OCR value. That means the loading in the Eem clay layer is according to the unloading/reloading stress path governed by $\kappa^*$. To obtain the influence of the stiffness from the Eem clay layer, variations are calculated with a lower $\kappa^*$ value. The virgin compression $\lambda^*$ has not been changed, because the load applied on the foundation is below the pre-consolidation pressure of the Eem clay layer.

Unloading/reloading stiffness variation

| *Name* | $\kappa^*$ *[-]* | *OCR* |
|---|---|---|
| Lower bound | 0.0067 | 1.9 |
| Design value (initial) | 0.01320 | 1.9 |

*Table 9.7: Variation unloading/reloading stiffness Eem clay used models – case study*

## 9.5 Result discussion

The results of the analysis described in § 9.4 are presented in this paragraph including an explanation of the field measurement data. Moreover, a couple of suggestions are given why the calculated settlements could be different from the measurement data. First, the model with the original best estimate values is discussed. Second, variations in the bending stiffness of the foundation plate, consolidation coefficient and unloading/reloading stiffness are discussed. Finally, the load increase over time in the PLAXIS model and measurement data is discussed.

### 9.5.1 Measurement data

The foundation of the superstructure has been measured over a time span of 1 year. Unfortunately, the measurements started after tower 2 had reached its final height and the foundation plate of tower 1 was finished. Hence, the PLAXIS 3D data has been corrected for the missing measurement data at the beginning of the construction period. This has been done by shifting the settlements in PLAXIS at 280 days to zero, the number of days between the construction (and start of PLAXIS calculation) and the first measurements.

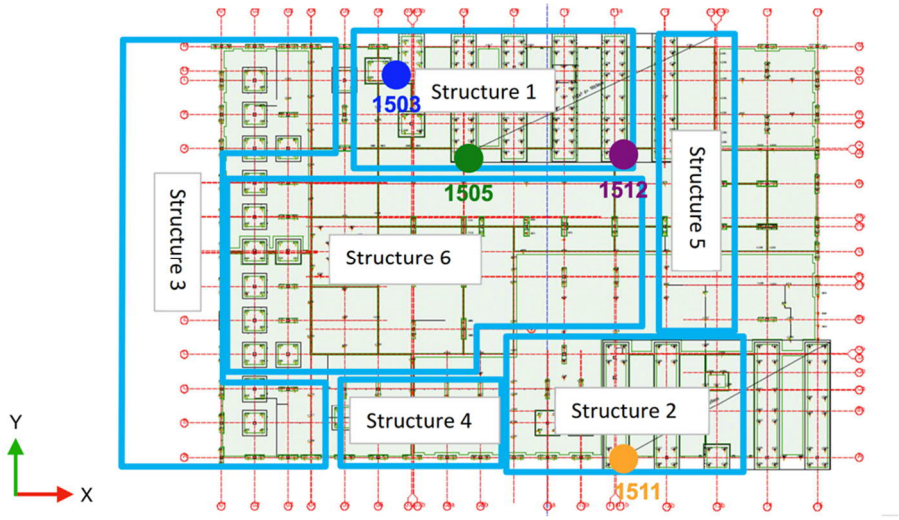


*Figure 9.3: Measurement points on tower 1 and 2*

In the PLAXIS 3D model the positions of the field measurement points are inserted in the mesh before the calculation has started. This makes it possible to directly compare the PLAXIS displacements and the field measurements with each other when the calculation is finished.

### 9.5.2 Best estimate

In this paragraph the PLAXIS 3D results of the case study are compared with the field measurement data. Graph 9.4 visualizes the PLAXIS 3D results (continues lines) and field measurements (round dots) together in one graph. The black vertical lines mark the start of phase 4 (p4) and phase 7 (p7). During these phases the largest load increase takes place due to the construction of tower 1. Moreover, the construction of tower 2 has already been finished before the measurements started. Therefore, less settlements are visible in the 'corrected measurement data' graph for tower 2 compared to tower 1. The immediate settlements have already occurred before the measurements started and is therefore outside this graph (left side of the origin).

In the upcoming graphs the colours belong always to the same measurement points on the construction (Figure 9.3). Moreover, the markers are indicating the variations in the calculation at each measurement point.

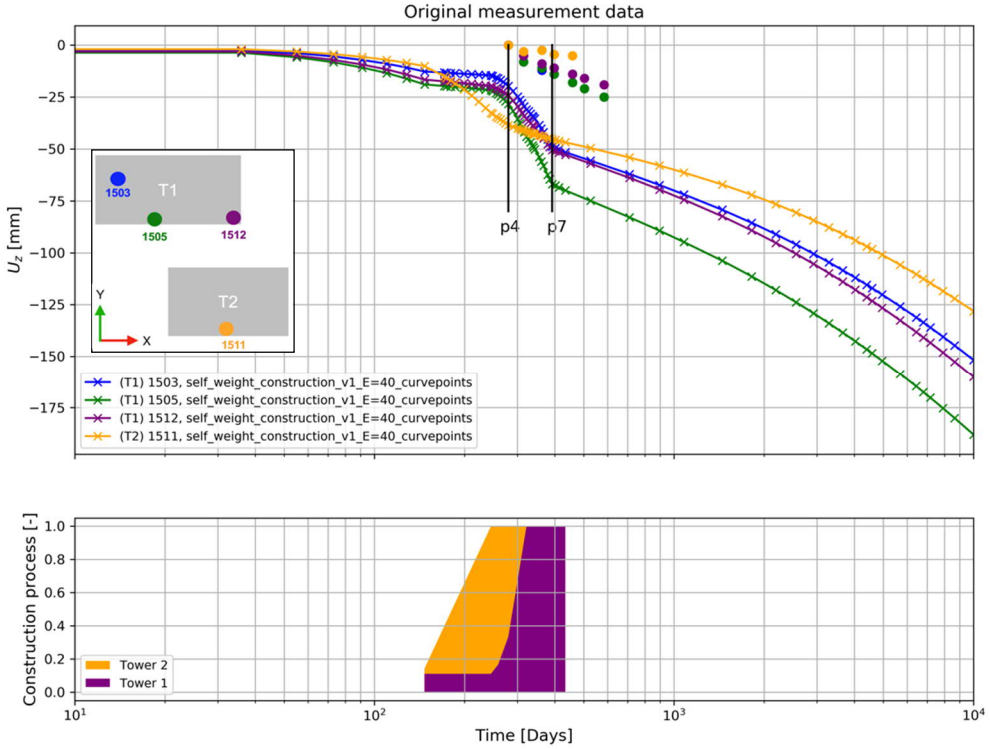


*Graph 9.4: Original measurement & PLAXIS 3D data, best estimate values – case study*

The first calculation contains soil parameters equal to the original best estimate design calculation (Graph 9.5). However, after shifting the PLAXIS 3D data, the displacements are still deviating from the field measurement data. The reason for the discrepancy could be due to the influence of the stress distribution below pile tip, the consolidation coefficient, unloading/reloading stiffness of the Eem clay layer and the load increase over time or a combination of these.

Moreover, a general note on the discrepancy between measurements and PLAXIS 3D (design) calculations: design standards are intended to make a safe and reliable construction. Therefore, settlement determination based on the standards is on the conservative side, even though best estimate values are used for the soil parameters. The used load-displacement curves in NEN9997 are design curves rather than describing accurate real pile behaviour.

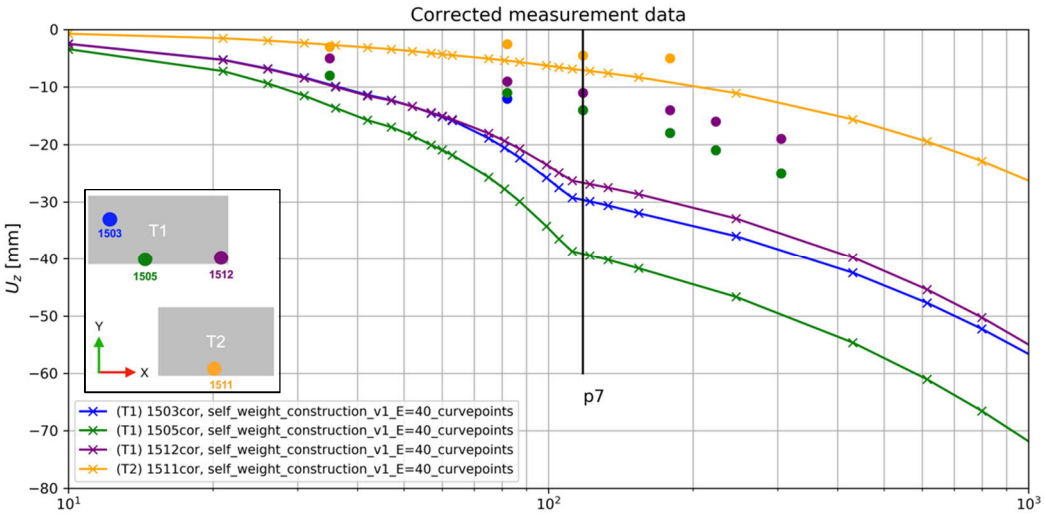


*Graph 9.5: Corrected measurement & PLAXIS 3D data, expectation values – case study*

To gain insight why the settlements are deviating from the measurement data, the sensitivity of different parameters has been calculated:

- Superstructure bending stiffness
- Consolidation coefficient Eem clay
- Unloading/reloading stiffness Eem clay
- Load increase over time

The values for these parameters have been discussed in paragraph 9.4,

### 9.5.3 Superstructure stiffness

As a measure for the differential settlements in the foundation plate, the maximum relative deflection ratio is calculated. In the models with high bending stiffnesses, the maximum relative deflection ratio is decreasing and approaching zero in case the plate is infinitely stiff. The yellow dots in Graph 9.6 representing the settlements of a very stiff foundation plate/construction. Here, maximum redistribution of load has taken place and the relative deflection is almost zero.

In order to clearly visualize all the settlement data, only the settlements on the central axis of tower 1 in x and y direction has been plotted (see drawing in Graph 9.6 and Graph E.4). Table 9.8 summarizes the values for the bending stiffness variation calculations in x-direction. It can be concluded from these graphs that redistribution of load is influencing the differential and absolute amount of settlements.

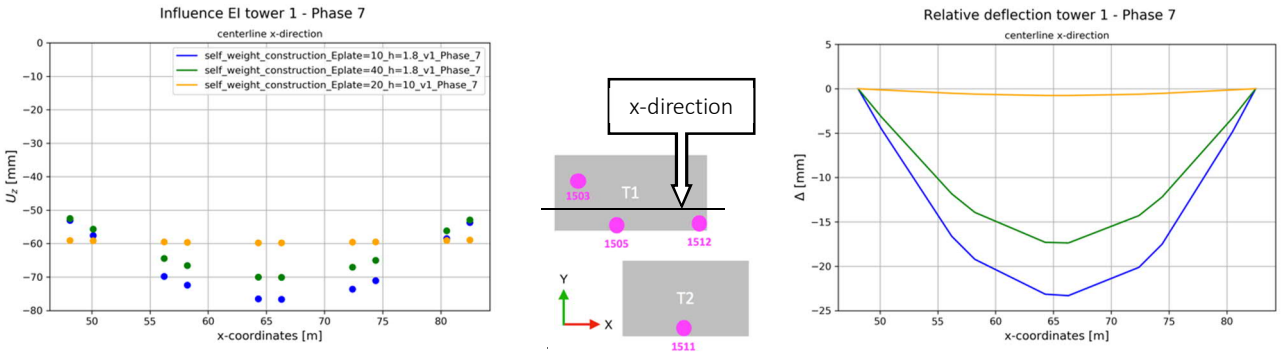


*Graph 9.6: Influence plate stiffness phase 7 (almost all load applied) tower 1, $s_1 + s_2$, x-direction*

**Influence bending stiffness**

| | | *Models with different stiffness* | | |
|---|---|---|---|---|
| *EI* | *[MPa]* | *4.86 · b* | *19.42 · b* | *1666 · b (≈ ∞)* |
| E | [MPa] Young's modulus | 10 | 40 | 20 |
| h | [m] Foundation plate height | 1.8 | 1.8 | 10 |
| Δ/L | [-] Max relative deflection ratio | 1:1476 | 1:1980 | 1:44627 |
| $\beta_{max}$ | [°] Max angular distortion | 0.14 | 0.09 | 0.004 |

*Table 9.8: Influence stiffness on differential settlements, x-direction*

For daily engineering practice is suggested to take into account appropriate stiffness values when modelling high-rise buildings. This can be done in two ways with different levels of accuracy:

- An accurate option is importing the complete structural design including the stiffness of all elements and the stiffness of all connections between these elements. Disadvantages: the structural model have to be provided by the structural engineer (sometimes not possible because of contractual agreements) and the calculation costs increases because of the more complicated numerical model.
- An easier and faster option is modelling a part of the superstructure only (e.g. foundation plate, first floor levels) and determining the upper and lower bound of the stiffness (flexible/stiff) which gives a good indication of the expected settlements. Disadvantages: the stiffness is an approximation of the real stiffness and is missing the interaction between several construction elements.

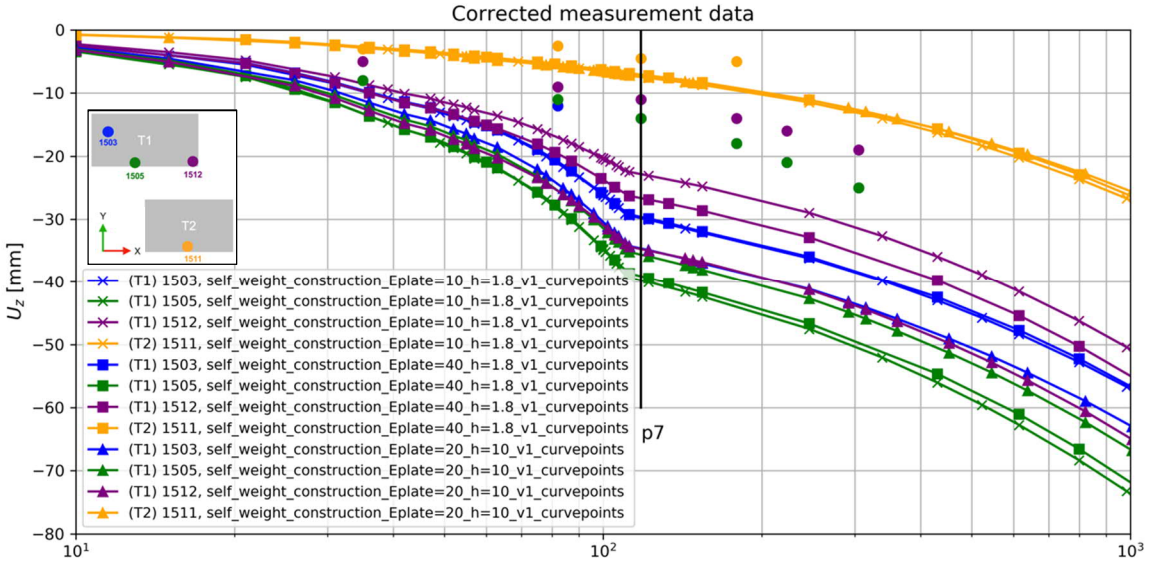


*Graph 9.7: Corrected measurement & PLAXIS 3D data, variation stiffness – case study*

Graph 9.7 visualizes the variation in bending stiffness for the different measurement points on the construction. The markers represent the different bending stiffnesses applied on the construction. Each colour is representing a measurement point on the construction. The result shows that the soil-structure interaction in this case has only a small

influence on the settlements. In this case other variations have probably a larger impact since the measurements still deviate from the PLAXIS results.

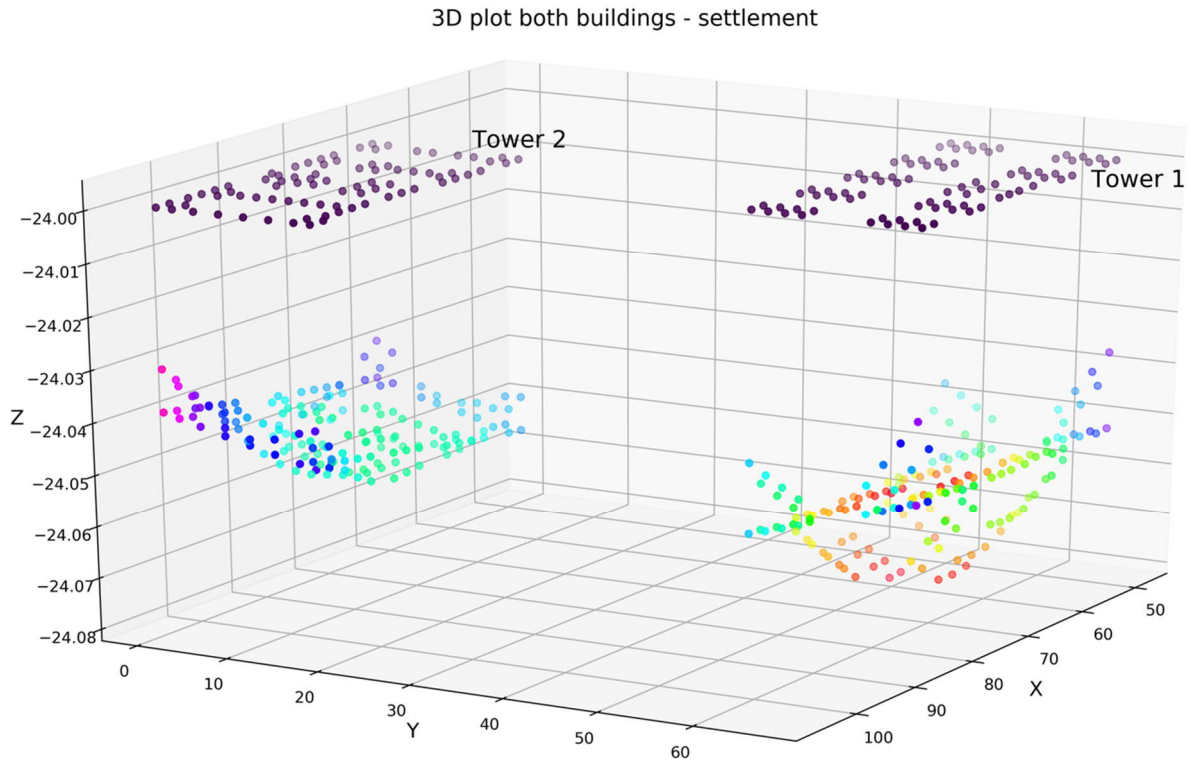


*Graph 9.8: 3D plot pile settlements of both towers - upper and lower bound bending stiffness – end of construction (without shifting)*

Graph 9.8 gives an overview of the difference between a flexible and stiff foundation plate for tower 1 and 2. The 3D visualizations of the pile settlements (dots are representing the piles) show that an appropriate load transfer to the plate is still of importance for the distribution of the settlements.

### 9.5.4 Variations Eem clay layer

**Consolidation coefficient**

The measurement data does not capture the entire consolidation and creep period of the construction. Therefore, it is difficult to determine the final settlements. Besides the final settlements, the rate of consolidation is important for the comparison between the measurement and PLAXIS data. The rate of consolidation is governed by the consolidation coefficient of the Eem clay layer.

In Graph 9.9 three different values for the consolidation coefficients are represented by the different markers. They are determined by multiplication and dividing the best estimate value of the hydraulic permeability by two. Graph 9.9 shows that the rate of consolidation has a little bit more influence in comparison with Graph 9.7. However, large differences are still visible between measurement and PLAXIS data.

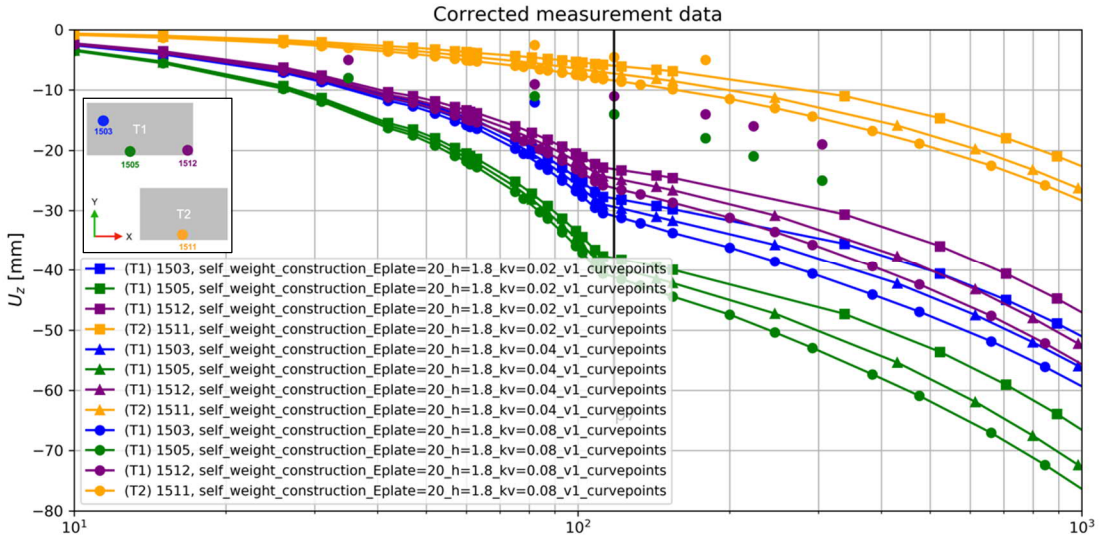


*Graph 9.9: Corrected measurement & PLAXIS 3D data, variation consolidation coefficient – case study*

Especially in the construction period (before phase 7) large deviations are visible. This could be due to the immediate (elastic) stiffness of the soil layers underneath. Since the rate of consolidation has less influence in this part of the settlement curve.

**Unloading/reloading stiffness**

The immediate settlements in PLAXIS during the construction phases (until phase 7) are large with respect to the measurement data. Moreover, it turned out that the load increase in the Eem clay layer in PLAXIS remains below the pre-consolidation pressure. It implies the stress path is following the unloading/reloading envelop during the construction. Reducing the $\kappa^*$ *value* decreases the total amount of settlements in the construction and user phase.

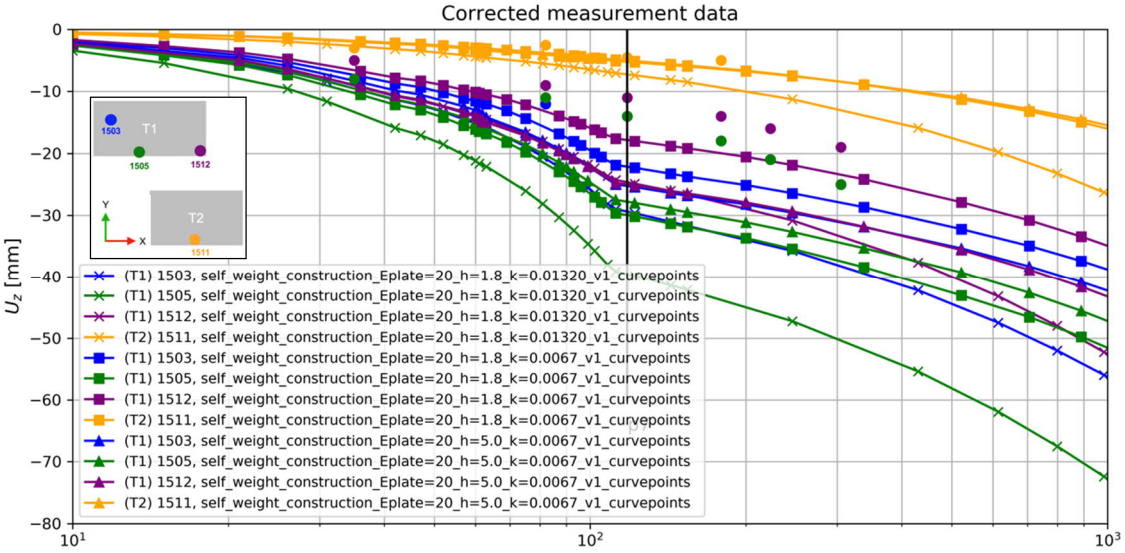


*Graph 9.10: Corrected measurement & PLAXIS 3D data, variation κ* – case study*

Graph 9.10 shows the influence of the unloading/reloading stiffness $\kappa^*$ by the different markers. The different measurement points are again represented by the colours. A large effect has been achieved by increase the immediate stiffness, the settlements are more in line with the measurement data. However, based on the North-South line parameter set, the new (reduced) $\kappa^*$ is probably too optimistic for the Eem clay layer which is unrealistic. To conclude, the unloading/reloading stiffness has large influence on the calculated settlements but is probably not solving the main discrepancy between the measurement and calculation data. The immediate settlements have probably a large influence on the settlements in PLAXIS.

### 9.5.5 Variations in load over time

The load increase over time is determined by construction documents set up prior to the construction and simplified on the assumption of a uniform load increase coupled with the increase in tower height. Moreover, the correct load at each measurement point is not known (load cells have not been installed). In § 9.1.4 the loading sequence is related to the number of constructed floor levels in the construction timeline. However, the real construction sequence can be shifted from the planned construction timeline. Moreover, the calculated load on the pile head in each phase can be different from the real situation.

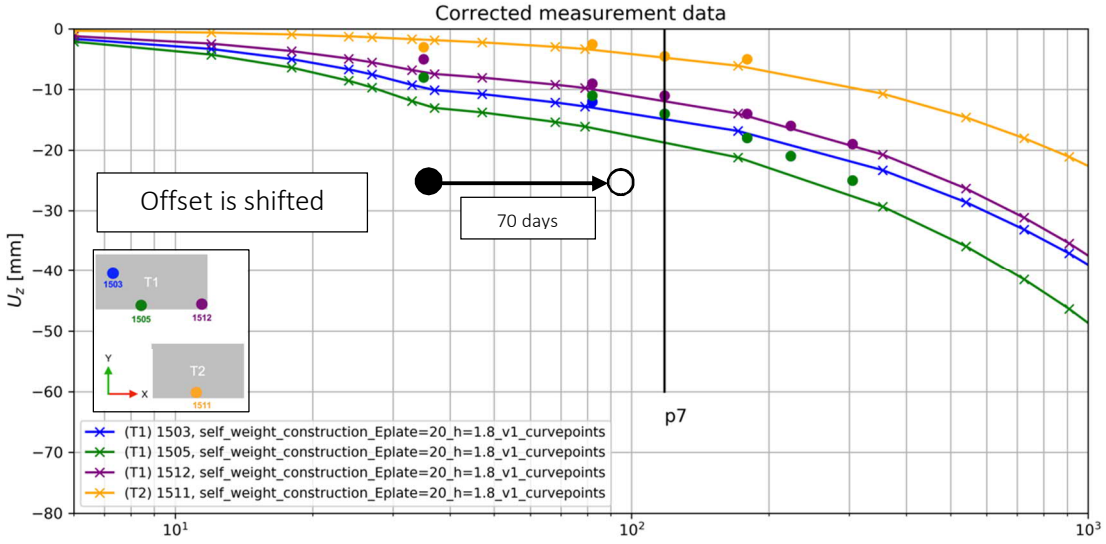


*Graph 9.11: Shifting the offset to count for variations in load increase over time*

In § 9.1.4 is assumed that all floor levels have equal self-weight. However, the foundation plate and the first floor level are heavier compared to higher floor levels. This effect is not taken into account in the PLAXIS calculation. Moreover, the measurements have been started after construction of floor level 1 and 2 (thus including the foundation plate). So, a large part of the load increase is not captured by the measurements but is still included in the PLAXIS settlements presented in the 'corrected measurement data' graphs. Therefore, shifting the offset or increasing the accuracy in the load increase over time approaches the measurement data better. For example, in Graph 9.11 the PLAXIS data is shifted with 70 days to show what could happen if the construction sequence is shifted compared to the design calculations.

The recorded measurement settlements could be imposed by less load compared to the settlements at exactly the same time in the PLAXIS calculation. Recommended is to increase the accuracy in implementing the load increase over time in PLAXIS prior to the design calculations. Connection with the structural and contractor design is important during foundation design and comparison with measurement data.

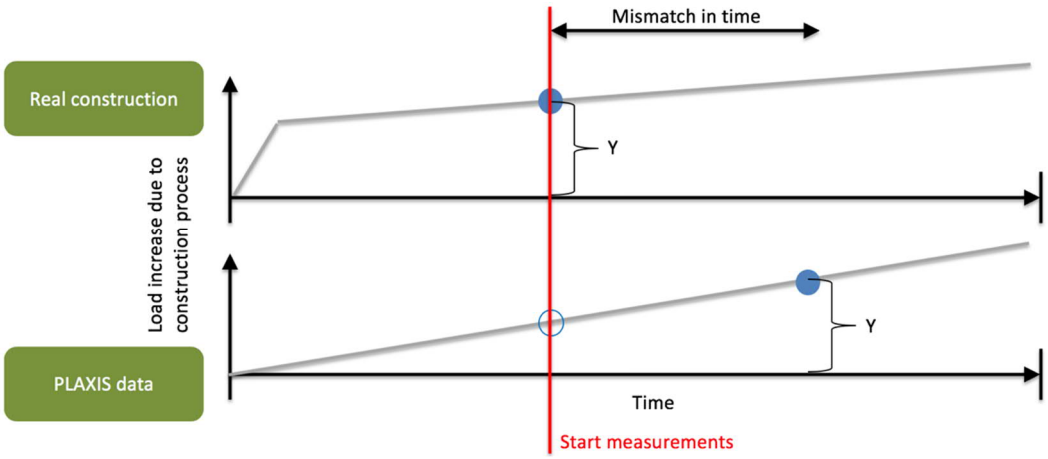


*Figure 9.4: Explanation mismatch in load over time*

## 9.6 Conclusion

The case study discussed in chapter 9 proves that soil-structure interaction plays a role in determining differential settlements of high-rise buildings. A complete interaction calculation including single pile, pile group and the structural stiffness is required for accurate load distribution to the pile heads. In the ideal situation, the entire structural model should be implemented in PLAXIS 3D to count for the stiffness of individual structural components and the interaction between these components. Although, in most cases a complete structural model is not available. Therefore, a method is presented to take into account load transfer from the superstructure to the piles and redistribution of these loads in the foundation plate. Using a plate element with appropriate stiffness properties and a simplified load transfer approach turned out to be a fast method to take into account the superstructure stiffness.

However, the calculated settlements in PLAXIS 3D based on best estimate values from the original design are still deviating from the measurement data. The difference is subdivided in three contributions for the geotechnical design: structural uncertainty, soil behaviour uncertainty and applied load over time uncertainty.

- Structural uncertainty: the bending stiffness is influencing the redistribution of load to the piles. Choosing appreciate stiffness and load transfer mechanism has only a small influence on the amount of settlements for this specific case study.
- Soil behaviour uncertainty: soil parameters like stiffness and consolidation coefficient are influencing the amount and rate of settlements. An elaborated parameter study could reduce the uncertainty. Although, it is very hard to derive for every point in space and time the most realistic soil parameters. Moreover, the measurements were not going on long enough to check the consolidation and creep parameters for this specific case study.
- Applied load over time uncertainty: the most sensitive input and uncertainty in this measurement comparison is the load increase over time. In the PLAXIS 3D calculation is the construction sequence simulated with the amount of constructed floor levels over time. Assumed is that all floor levels have an equal self-weight. However, the foundation plate and the first floor levels are heavier compared to the higher floor levels. Therefore, the load increase over time in the PLAXIS 3D calculation could be shifted relative to the load increase in the real construction sequence. To account for the shift in load increase, the PLAXIS data in this case study is shifted with 70 days which results in almost perfect approximation of the settlements relative to the measurement data.

All these solutions contribute towards a more accurate settlement determination. Moreover, in this specific case study the author believed that the load increase over time in PLAXIS 3D with respect to the load increase during the measurements is shifted due to insufficient information of the real construction sequence and inaccurate load formulation. Improving the implementation of the loading sequence shows the largest improvements in this specific case study.

# V Conclusions and recommendations

# 10 Conclusions

The aim of this research is to develop a framework for modelling soil displacement pile foundations in soft soil conditions (sands and clays) which is directly applicable in engineer practice. To achieve this, the research objective is divided in several sub-questions which lead to the final answer.

**Literature review**

- *Which mechanisms occur in reality during installation and loading of soil displacement single piles and pile groups?*
  Pile installation and pile loading mechanisms are complex processes which are not completely understood yet. During the installation of soil displacement piles, soil around the pile tip is stressed due to the displaced soil volume in this area. After installation these stresses remain in the soil and result in stiffer behaviour along the shaft and at the base of the pile. In case piles are installed in a group, the horizontal stresses increase even further due to the installation of neighbouring piles, which result in more friction along the pile shafts. This higher friction result in less settlements compared to equally loaded single pile configurations.
- *Which methods are available in the literature for differential settlement calculation of pile foundations?*
  Over the years, different approaches have been developed based on empirical, analytical or numerical methods. Poulos & Davis (1968) and Randolph & Worth (1978) applied a lot of research on analytical methods. Nowadays, numerical approaches are mainly used in the design calculations due to increased complexity of the projects. The numerical approach contains various options for modelling pile settlements; the equivalent raft, volume pile or embedded beam are dominantly used. The embedded beam approach combines pile behaviour and pile settlement determination although, the calculation costs are reduced compared to volume piles.
- *On which level are installation effects important and why is it still difficult in current engineering practice to predict differential settlements of high-rise building foundations on soil displacement piles in soft soil conditions (sands and clays)?*
  Commercially available numerical methods presume wished-in-place installation of piles, regardless of the installation method. Although, soil displacement installation effects have a positive influence on settlement reduction of pile foundations. These effects are not incorporated yet because, commercial FEM codes are not able to handle large strains which occur during installation of piles. Moreover, current research projects are focussing on modelling numerical volume pile configurations which result in high calculation costs compared to embedded beams.
- *What is the influence of the superstructure stiffness on differential settlements?*
  In addition to pile behaviour, the superstructure stiffness influences the differential settlement distribution of the pile foundation. A fully flexible superstructure results in large differential settlements because, no load redistribution takes place. On the other hand, a completely stiff superstructure results in no differential settlements due to maximum redistribution of loads in the foundation plate.

**Parameter study (single pile)**

- *Which calculation method is the most optimal for describing settlements of single piles in soft soil deposits?*
  Currently, the analytical model is the most used in daily engineering practice for describing single pile behaviour. The method is based on theoretical soil mechanical principles, is versatile to use and requires soil parameters as

input. However, soil-structure interaction and non-linear soil features are difficult to incorporate in analytical methods.

On the other side, numerical methods contain; robust implementation of constitutive models for describing realistic/advanced soil behaviour, the possibility to take into account existing neighbouring constructions and a user-friendly interface for the geotechnical engineer. However, calculations increase in complexity, pile-soil interaction modelling becomes rather difficult and requires a certain amount of experience from the user.

In this research PLAXIS 3D is utilized because, the software is commonly used in engineering practice and a lot of scientific information is available. During the parameter study different options are tested in the single pile model: new versus current embedded beam, layer dependent versus multi-linear shaft friction distribution and different soil fit approaches.

- The new embedded beam formulation outperforms the current formulation on mesh dependency and stiffer load-displacement response. The base of the new formulation is less sensitive for variations in mesh element distributions because, the mesh connection is divided over more than one stress point. Moreover, the load-displacement response of the new embedded beam is stiffer which is favourable for approximating the load-displacement curve of NEN9997 for soil displacement piles.
- For the shaft friction of the embedded beam, it is recommended to use the multi-linear option. Because, at the shaft of soil displacement piles higher stresses are allowed compared to the initial wished-in-place stress distribution calculated by PLAXIS 3D. Therefore, the layer dependent distribution is less suitable since it makes use of the initial in-situ stress distribution of PLAXIS 3D.
- The soil stiffness parameter fit below pile tip level enables to approximate the response of the NEN9997 soil displacement pile tip curve. However, the fit procedure well captured only in SLS load ranges because, failure behaviour is not implemented correctly in PLAXIS 3D due to the linear elastic perfectly plastic spring at the base of the embedded beam. Moreover, unloading/reloading behaviour in combination with the stiffness fit is not part of the investigation for this thesis.

- *What is the most optimal modelling approach in this calculation method to obtain $s_1$ settlements according to NEN9997 for a soil displacement pile with high foundation loads in soft soil deposits?*
  The optimal model in PLAXIS 3D is divided in three parts: input for the bearing capacity, improvement of the base response by a soil stiffness fit ($s_b$) and the elastic compression fit of the pile itself ($s_{el}$).
  - The embedded beam in PLAXIS still requires input from a (analytical) bearing capacity calculation for the base and shaft capacity (NEN9997, used in D-Foundations). This process remains equal to the current design practice because, ULS calculations in combination with embedded beams cannot be conducted in PLAXIS 3D.
  - For the soil stiffness fit ($E_{oed}$) below the pile tip, no generic factor or relationship is found based on the investigated models. The fit is depending on the pile length, pile type, soil stratigraphy and soil properties. In case the soil fit procedure is conducted in engineering practice, a fit is required for every single soil stratigraphy.
  - The elastic response and the fit of the pile is dependent from the soil stratigraphy and soil properties as well. More research has to be conducted on the influence of the elastic compression of piles in PLAXIS 3D and what is expected from the field.

  Approaching the $s_1$ response based on NEN9997 requires in all cases a fit of the soil and pile properties. Every configuration requires different fit factors to approach the NEN9997 response for soil displacement piles. Moreover, increased pile penetration in the bearing layer requires lower fit factors. Because, PLAXIS 3D in combination with the HSsmall model has stress dependent stiffness mechanisms where the NEN9997 curve lacks a connection with basic soil mechanics principles like strength and stiffness parameters.

**Model design (pile group)**

- *What is the most optimal calculation approach to obtain $s_2$ differential settlements for pile groups of high-rise building foundations in combination with the method for single pile behaviour obtained in the Parametric study?*
  Currently, the equivalent raft approach is often utilized for settlement analysis of pile foundations. The main disadvantages are; single pile behaviour ($s_1$) is not incorporated, installation effects are not possible to model and pile group effects are occuring. However, a disadvantage of the embedded pile is that the bearing capacity is an input parameter. Three mechanisms related to pile group behaviour are discussed:
  - Single pile behaviour of the pile group is represented by the embedded beams. Moreover, immediate settlements due to shear deformation, volume change and elastic pile compression are covered. The values for the multi-linear shaft friction and base resistance are obtained from a D-Foundations calculation based on NEN9997.
  - The installation effects are incorporated in a same way as the single pile models by fitting a soil volume below pile tip level. The fit factors are based on the single pile fit values. Although, in the pile group model it becomes difficult to separate the settlement contributions based on NEN9997 for comparison with analytical methods. For the investigated models, the stiffness fit procedure applies reasonably well for simulating installation effects in the SLS load level range.
  - Pile group behaviour is influenced by installation of neighbouring piles. This effect is only partly covered in the proposed method. An equally loaded single pile in a pile group reacts stiffer in PLAXIS 3D due to stress dependent stiffness of the soil below the pile tip. However, group effects are not entirely covered because, there is no increase in shaft friction by inserting a larger amount of piles.
- *Which influence does the superstructure stiffness have on the differential settlement behaviour regarding pile groups of high-rise buildings?*
  The bending stiffness of the superstructure, which is modelled as a plate element in this research, influence the distribution of the loads in the plate and thereby the settlements at the individual piles. This effect can easily be simulated in PLAXIS 3D by variations in bending moment of the plate element. Suggested to the geotechnical engineer is to have a close interaction with the structural engineer about the most appropriate stiffness for the superstructure. Because, the settlement distribution is depending on the load distribution which is related to the structural stiffness.
- *To what extent is the proposed calculation approach for differential settlements an improvement compared to the existing settlement calculation approach for high-rise building foundations?*
  The correct single pile behaviour for soil displacement piles in a pile group calculation is a large improvement for the redistribution of loads imposed by the superstructure. The load distribution from the superstructure is not only influenced by the single pile response anymore but also incorporates the soil response underneath the pile tip in one iteration. The soil-structure interaction between the soil around the pile and the superstructure increase the accuracy in determination of differential settlements of high-rise buildings. It narrows the gap towards a full soil-structure interaction model.

**Application (case study)**

- *Is the calculation approach developed in this thesis suitable to be used in Dutch Engineering practice regarding workability and reliability?*
  The soil-structure interaction in combination with the new embedded beam formulation, the fit method and the plate element is a fast approach for determining the load distribution on the pile heads. Subsequently, the accuracy for determination of settlements is increased due to the improved soil-structure interaction. Compared to current approaches where linear springs are used for single pile behaviour in the structural model, complex soil behaviour is now captured in the load redistribution calculation in PLAXIS 3D. However, in the investigated case study the PLAXIS 3D settlements are still deviating from the measurement data. In this PLAXIS 3D calculation the construction sequence is simulated with the amount of constructed floor levels over time. Assumed is that all floor levels have an equal self-weight. However, the foundation plate and the first floor levels are heavier compared to the higher floor levels. This causes difference in load increase and settlements over time between the PLAXIS calculation and reality.

**Main research question**
The main objective of this research is formulated as:

> *"How to increase accuracy in describing differential settlements of high-rise buildings on soil displacement pile foundations in soft soil deposits?"*

Summarizing, from the main research question can be concluded that:

- The proposed method consists out of two parts:
    - New embedded beam formulation in PLAXIS 3D
    - Soil stiffness fit method

- The new embedded beam outperforms the current formulation in terms of:
    - Mesh sensitivity in axial loading
    - Load-displacement stiffness in axial loading
- The embedded beam in combination with the multi-linear shaft friction distribution applies reasonably well. Although, group effects are not completely covered.

- The soil stiffness fit for approximating the NEN9997 curve is adequate, although:
    - The fit is depending on soil stratigraphy, soil properties, pile type and pile length.

- Due to the incorporated single pile, pile group and soil-structure interaction, the accuracy in determination of differential settlements of high-rise buildings is increased. It narrows the gap towards a full soil-structure interaction model for soil-displacement pile foundations.

# 11 Recommendations

This chapter give recommendations for the use of the proposed method and recommendations for future research on this topic.

**Recommendations for use of proposed model:**

- *Embedded beam*
  The response of the embedded beam should always be validated before extrapolating the behaviour to the complete model including all embedded beams. In a couple of investigated cases in this thesis, it turned out that the fit method was not needed to approximate the load-displacement curve of soil displacement piles. That means also the load-displacement response could be too stiff in case no soil displacement piles are modelled.
- *Fit procedure*
  In case a foundation is founded on soil displacement piles it becomes challenging to model installation effects by numerical methods. By applying a soil stiffness fit based on the NEN9997 curve, an approximation is obtained for the soil displacement single pile behaviour in PLAXIS 3D. However, the geotechnical engineer should be critical by defining the fit volume and fit factors. The fit should not influence other basic soil mechanical principles in the calculation.
- *Superstructure stiffness*
  The load distribution from the superstructure should be obtained from the structural design without taking into account the redistribution of the loads by the structural engineer. Most of the time the self-weight of the construction gives an accurate representation of the total load. The stiffness of the superstructure can be represented by a plate element with a bending stiffness approximating the superstructure stiffness. Recommended is to define the upper and lower bound of the load redistribution by using a flexible and stiff plate for the superstructure stiffness.

**Recommendations for future research:**

- *Testing on more cases with measurement data*
  One case study is not representative enough for generalizing and testing the behaviour of a new method. The proposed method should be compared with several other case studies to give a better idea about the general applicability. Moreover, the measurements used in this case study are not reliable enough. In the beginning of the construction, measurements are lacking and no loads are available relative to the measurements. Ideally, situation, the load over time should be known to properly model the load increase during the construction phases.
- *Group effects*
  This thesis has mainly focussed on incorporating and improving the single pile behaviour in PLAXIS 3D. However, research on group effects of soil displacement piles is necessary because, the proposed model with the multi-linear shaft friction is not completely incorporating reinforcement mechanism in a group due to installation of adjacent piles.

- *Ratio immediate/secondary settlements*
  It is useful to investigate case studies where the immediate settlements and individual pile behaviour play a dominant role relative to the total amount of settlements, instead of large time dependent settlements in the Eem clay layer. It is expected that the fit method has more influence on the total amount of settlements if the time dependent settlement contribution is reduced.

- *Soil - structure interaction*
  In this research the bending stiffness of the superstructure is represented by a plate element connected to pile heads. Some variations have been performed on the superstructure stiffness in combination with the plate element. Ideally, the whole superstructure should be modelled for obtaining the most realistic load redistribution in the foundation plate. Therefore, it is suggested to link the complete structural model with the geotechnical design in PLAXIS 3D. A promising feature could be using the Building Information Modelling approach. Here, an interdisciplinary information model is generated which incorporates for example the structural and geotechnical design. All changes in the design are automatically implemented in the design of all the other disciplines. Which results in a up to date stiffness description of the construction in the geotechnical calculation.

# Bibliography


Acín González, M. (2015). Stress singularities and concentrations—Mesh convergence in FEA [Linkedin].

Beijer-Lundberg, A. (2014). Displacement pile installation effects in sand: An experimental study. Delft University of Technology.

Breeveld, B. J. S. (2013). *Modelling the Interaction between Structure and Soil for Shallow Foundations* [Master Thesis]. Delft University of Technology.

Brinkgreve, R. B. J. (2018a). PLAXIS Manual. Plaxis BV Netherlands.

Brinkgreve, R. B. J. (2018b). Lecture notes MSc course Behaviour of Soils & Rocks [Lecture]. TU Delft, Delft.

Broere, W., & van Tol, A. F. (2006). Modelling the bearing capacity of displacement piles in sand. Proceedings of the Institution of Civil Engineers - Geotechnical Engineering, 159(3), 195–206.

Cairo, R., Conte, E., & Dente, G. (2005). Interaction Factors for the Analysis of Pile Groups in Layered Soils. *Journal of Geotechnical and Geoenvironmental Engineering*, *131*(4), 525–528.

Chen, X. (2011). *Settlement Calculation on High-Rise Buildings*. Springer Berlin Heidelberg.

Chin, F. K. (1970). *Estimation of the Ultimate Load of Piles Not Carried to Failure*. 81–90.

David, T. K., & Forth, J. P. (2011). Modelling of Soil Structure Interaction of Integral Abutment Bridges. 78, 769–774.

Deltares. (2016a). *D-PILE GROUP user manual version 16.1*. Deltares.

Deltares. (2016b). *D-FOUNDATIONS user manual version 16.1*. Deltares.

Dung, N. T., Chung, S. G., & Kim, S. R. (2010). Settlement of piled foundations using equivalent raft approach. *Proceedings of the Institution of Civil Engineers - Geotechnical Engineering*, *163*(2), 65–81.

Engin, H. K. (2013). *Modelling Installation Effects—A Numerical Approach* [PhD]. Delft University of Technology.

Engin, H. K., & Brinkgreve, R. B. J. (2009). Investigation of Pile Behaviour Using Embedded Piles. *Proceedings of the 17th International Conference on Soil Mechanics and Geotechnical Engineering*, 1189–1192.

Engin, H. K., Brinkgreve, R. B. J., & van Tol, A. F. (2015). Simplified numerical modelling of pile penetration - the press-replace technique: SIMPLIFIED NUMERICAL MODELLING OF PILE PENETRATION - PR TECHNIQUE. *International Journal for Numerical and Analytical Methods in Geomechanics*, *39*(15), 1713–1734.

Engin, H. K., Septanika, E. G., & Brinkgreve, R. B. J. (2007). Improved embedded beam elements for the modelling of piles. *Numerical Models in Geomechanics*.

Engin, H. K., Septanika, E. G., & Brinkgreve, R. B. J. (2008). Estimation of Pile Group Behavior using Embedded Piles. *The 12th International Conference of International Association for Computer Methods and Advances in Geomechanics (IACMAG)*, 1–8.

Fellenius, B. H., & Rahman, M. M. (2019). Load-movement Response by t-z and q-z Functions. *Geotechnical Engineering Journal of the SEAGS & AGSSEA*, *50*(3), 11–19.

Fleming, W. G. K. (1992). A new method for single pile settlement prediction and analysis. *Géotechnique*, *42*(3), 411–425.

Gedeon, G. P. E. (z.d.). *Design of Pile Foundations*. CED Engineering.

Gowthaman, S., Nasvi, M. C. M., & Krishnya, S. (2017). Numerical Study and Comparison of the Settlement Behaviours of Axially Loaded Piles using Different Material Models. *Engineer: Journal of the Institution of Engineers, Sri Lanka*, *50*(2), 1.

den Haan, E. J. (2003). Het a,b,c-isotachenmodel: Hoeksteen van een nieuwe aanpak van zettingsberekeningen. *Geotechniek*, 27–35.

Ju, J. (2015). Prediction of the Settlement for the Vertically Loaded Pile Group Using 3D Finite Element Analyses. *Marine Georesources & Geotechnology*, *33*(3), 264–271. Katzenbach, R., & Leppla, S. (2015). Realistic Modelling of Soil-structure Interaction for High-rise Buildings. *Procedia Engineering*, *117*, 162–171.

Keijer, H. (2015). *1-2-3 Geologie voor Ingenieurs*. KIVI, afdeling Geotechniek.

Lebeau, J.-S. (2008). *FE-Analysis of piled and piled raft foundations* [Master Thesis]. Graz University of Technology.

Lunne, T., & Christoffersen, H. P. (1983). Interpretation of Cone Penetrometer Data for Offshore Sands. *Offshore Technology Conference*. Offshore Technology Conference, Houston, Texas.

McCabe, B. A., & Sheil, B. B. (2015). Pile Group Settlement Estimation: Suitability of Nonlinear Interaction Factors. *International Journal of Geomechanics*, *15*(3), 1–11.

NEN 9997-1. (2017). *Eurocode 7: Geotechnical Design, including Dutch national annex and NCCI. Nederlandse Norm.* NEN.

Ottaviani, M. (1975). Three-dimensional finite element analysis of vertically loaded pile groups. *Géotechnique*, *25*(2), 159–174.

Pham, D. H. (2009). *Modelling of Installation Effect of Driven Piles by Hypoplasticity* [Master Thesis]. Delft University of Technology.

Phuong, N., van Tol, A., Elkadi, A., & Rohe, A. (2014). Modelling of pile installation using the material point method (MPM). In M. Hicks, R. Brinkgreve, & A. Rohe (Red.), *Numerical Methods in Geotechnical Engineering* (pp. 271–276). CRC Press.

Poulos, H. G. (1968). Analysis of the Settlement of Pile Groups. *Géotechnique*, *18*(4), 449–471.

Poulos, H. G. (1989). Pile behaviour—Theory and application. *Géotechnique*, *39*(3), 365–415.

Poulos, H. G., & Davis, E. H. (1968). The Settlement Behaviour of Single Axially Loaded Incompressible Piles and Piers. *Géotechnique*, *18*(3), 351–371.

Poulos, H. G., & Davis, E. H. (1980). *Pile foundation analysis and design*. John Wiley and Sons.

Pressley, J. S., & Poulos, H. G. (1986). Numerical analysis of pile group behaviour. *International Journal for Numerical and Analytical Methods in Geomechanics*, *10*, 213–221.

Randolph, M. F. (1985). *Settlement of pile groups*. 1–19.

Randolph, M. F., & Worth, C. P. (1978). Analysis of deformation of vertically loaded piles. *Journal of Geotechnical and Geoenvironmental Engineering*, *104*(12), 1465–1488.

Randolph, M. F., & Wroth, C. P. (1979). An analysis of the vertical deformation of pile groups. *Géotechnique*, *29*(4), 423–439.

Sadek, M., & Shahrour, I. (2004). A three dimensional embedded beam element for reinforced geomaterials. *International Journal for Numerical and Analytical Methods in Geomechanics*, *28*(9), 931–946.

Sales, M. M., Prezzi, M., Salgado, R., Choi, Y. S., & Lee, J. (2017). LOAD-SETTLEMENT BEHAVIOUR OF MODEL PILE GROUPS IN SAND UNDER VERTICAL LOAD. *Journal of Civil Engineering and Management*, *23*(8), 1148–1163.

Sanglerat, G. (1972). *The penetrometer and soil exploration*. Elsevier.

Septanika, E. G., Bonnier, P. G., Brinkgreve, R. B. J., & Bakker, K. J. (2007). An efficient 3D modeling of (multi) pile-soil interaction. *Proceedings of the International Geomechanics Conference, Nessebar, Bulgaria*, 67–76.

Smulders, C. M. (2018). *An improved 3D embedded beam element with explicit interaction surface* [Master Thesis]. Delft University of Technology.

Stanton, K. V., Motamed, R., Elfass, S., Ellison, K., Francisco, S., & Ellison, K. (2015). An Evaluation of T-Z Analysis Methods. *Proceedings of the 40th Annual Conference on Deep Foundations*. Proceedings of the 40th Annual Conference on Deep Foundations, Oakland, CA.

Tejchman, A., & Gwizdala, K. (2001). Analysis of settlements of piled foundations. *Proc. XV Int. Conf. Soil Mech. Found. Eng.*, 1025–1030.

Tomlinson, M., & Woodward, J. (1977). *Pile Design and Construction Practice, Fifth edition* (Vol. 5). Taylor & Francis.

Tschuchnigg, F. (2013). *3D Finite Element Modelling of Deep Foundations Employing an Embedded Pile Formulation* [PhD]. Graz University of Technology.

Tschuchnigg, F., & Schweiger, H. F. (2015). The embedded pile concept – Verification of an efficient tool for modelling complex deep foundations. *Computers and Geotechnics*, *63*, 244–254.

Turello, D. F., Pinto, F., & Sánchez, P. J. (2016). Embedded beam element with interaction surface for lateral loading of piles. *International Journal for Numerical and Analytical Methods in Geomechanics*, *40*, 568–582.

van Grop, G. J. C. (2014). *Optimization of modelling pile foundations* [Master Thesis]. Delft University of Technology.

Verruijt, A. (2012). *Soil Mechanics*. Delft University of Technology.

Vesić, A. S. (1977). *Design of pile foundations*. Transportation Research Board, National Research Council.

Waterman, D., & Broere, W. (2004). *PRACTICAL APPLICATION OF THE SOFT SOIL CREEP MODEL – PART III*. Plaxis BV Netherlands.

Zoidi, E. [FGSBV]. (2015). *Prediction of settlements for high-rise buildings on deformable subsoil* [Master Thesis]. Delft University of Technology.

# Appendix

# A NEN9997

## A.1 Bearing capacity calculation

During design calculations in the Netherlands, the bearing capacity of a single pile has to be calculated according to the standards given in NEN9997. The calculation method for bearing capacity in EC7 is based on cone resistance data from CPT tests. Besides the cone resistance several factors are included in the calculations to count for different effects like pile tip shape, installation method, in-situ or prefab pile and material properties. Moreover, safety factors are used to account for uncertainties in ground profile and pile characteristics. These factors are all incorporated in the bearing capacity calculation of NEN9997.

$$q_{s;\max;z} = \alpha_s \cdot q_{c;z;a} \tag{A.1}$$

$$q_{b;\max} = \frac{1}{2} \cdot \alpha_p \cdot \beta \cdot s \cdot \left( \frac{q_{c;\mathrm{I};gem} + q_{c;\mathrm{II};gen}}{2} + q_{c;\mathrm{III};gem} \right) \tag{A.2}$$

$$R_{s;cal;\max;i} = \mathrm{O}_{s;\Delta L;gem} \cdot \int_{\Delta l} q_{s;\max;z;i} \cdot dz \tag{A.3}$$

$$R_{b;cal;\max;i} = A_b \cdot q_{b;\max;i} \tag{A.4}$$

$$R_{c;cal;i} = R_{b;cal;\max;i} + R_{s;cal;\max;i} \tag{A.5}$$

$$(R_{c;cal})_{\min} = (R_{b;cal} + R_{s;cal})_{\min} \tag{A.6}$$

$$(R_{c;cal})_{gem} = (R_{b;cal} + R_{s;cal})_{gem} \tag{A.7}$$

$$R_{c;k} = R_{b;k} + R_{s;k} = \frac{R_{c;cal}}{\xi} = \min\left( \frac{(R_{c;cal})_{gem}}{\xi_3}; \frac{(R_{c;cal})_{\min}}{\xi_4} \right) \tag{A.8}$$

$$R_{b;d} = R_{b;k} / \gamma_b \tag{A.9}$$

$$R_{s;d} = R_{s;k} / \gamma_s \tag{A.10}$$

Equation A.8 contains the characteristic values for the bearing capacity, where $q_b$ and $q_s$ are cone resistances values at different levels around the pile tip. $\alpha_p$ $\alpha_s$ $\beta$ and s are pile factor values related to the pile characteristics, which are specified in NEN9997, Table 7c.

## A.2 Derivation of NEN9997 load-displacement curves

Load displacement curves NEN9997 (NEN 9997-1, 2017).

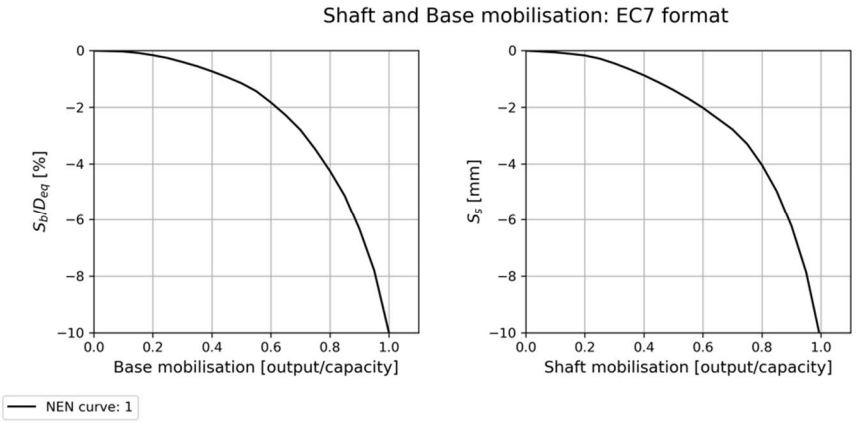


*Graph A.1: Load displacement curve soil displacement piles NEN9997*

# B Input calculation software

## B.1 D-Foundations

D-Foundations calculations require CPT data in order to calculate bearing capacity. Additionally, water levels and the positive/negative skin friction zones have to be defined (Table B.1).

| Name | Value | Unit |
|---|---|---|
| Phreatic level | 1.2 | [m] |
| Pile tip level | -21.00 | [m] |
| OCR bearing layer | 1 | [-] |
| Top of positive skin friction zone | -14.00 | [m] |
| Bottom of negative skin friction zone | 0.00 | [m] |
| Expected ground level settlements | 0.11 | [m] |

*Table B.1: Input additional data CPT D-Foundations (simplified and complex model)*

### B.1.1 Soil stratigraphy

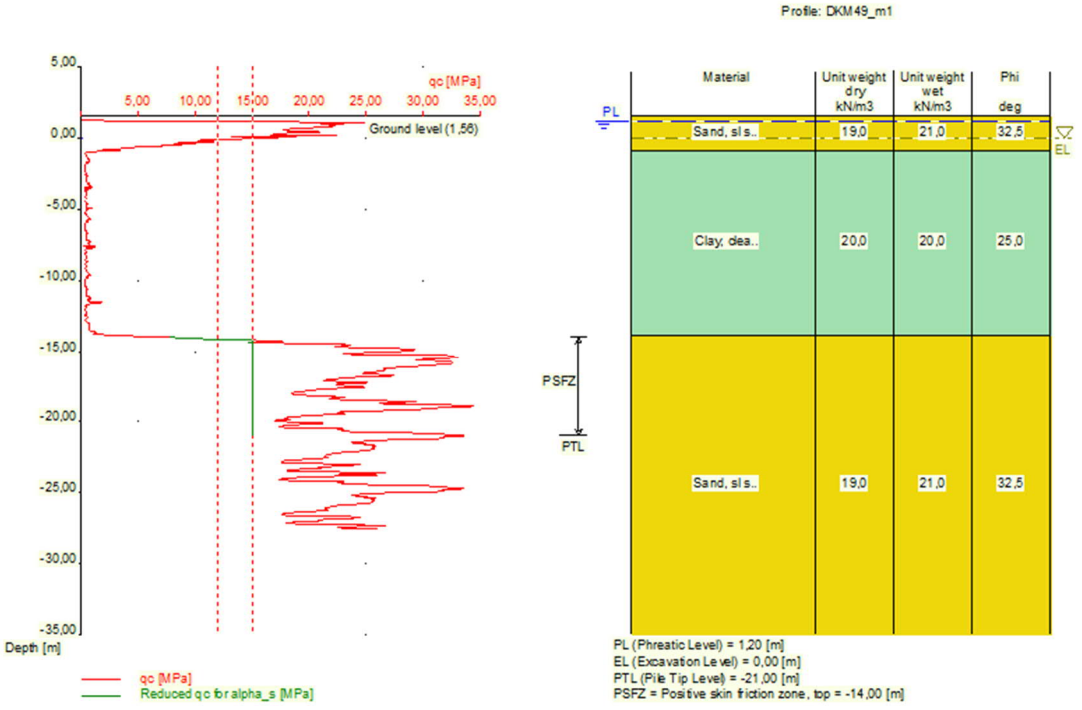


*Figure B.1: Soil stratigraphy input D-Foundation - simple model*

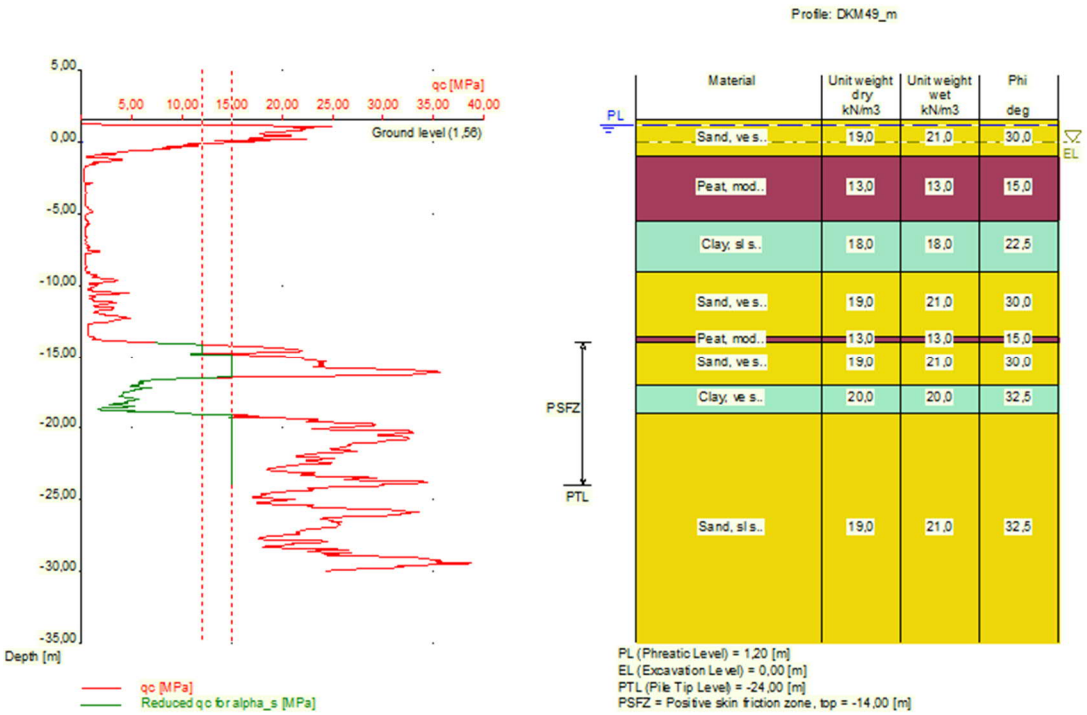


*Figure B.2: Soil stratigraphy input D-Foundation - complex model*

### B.1.2 CPT

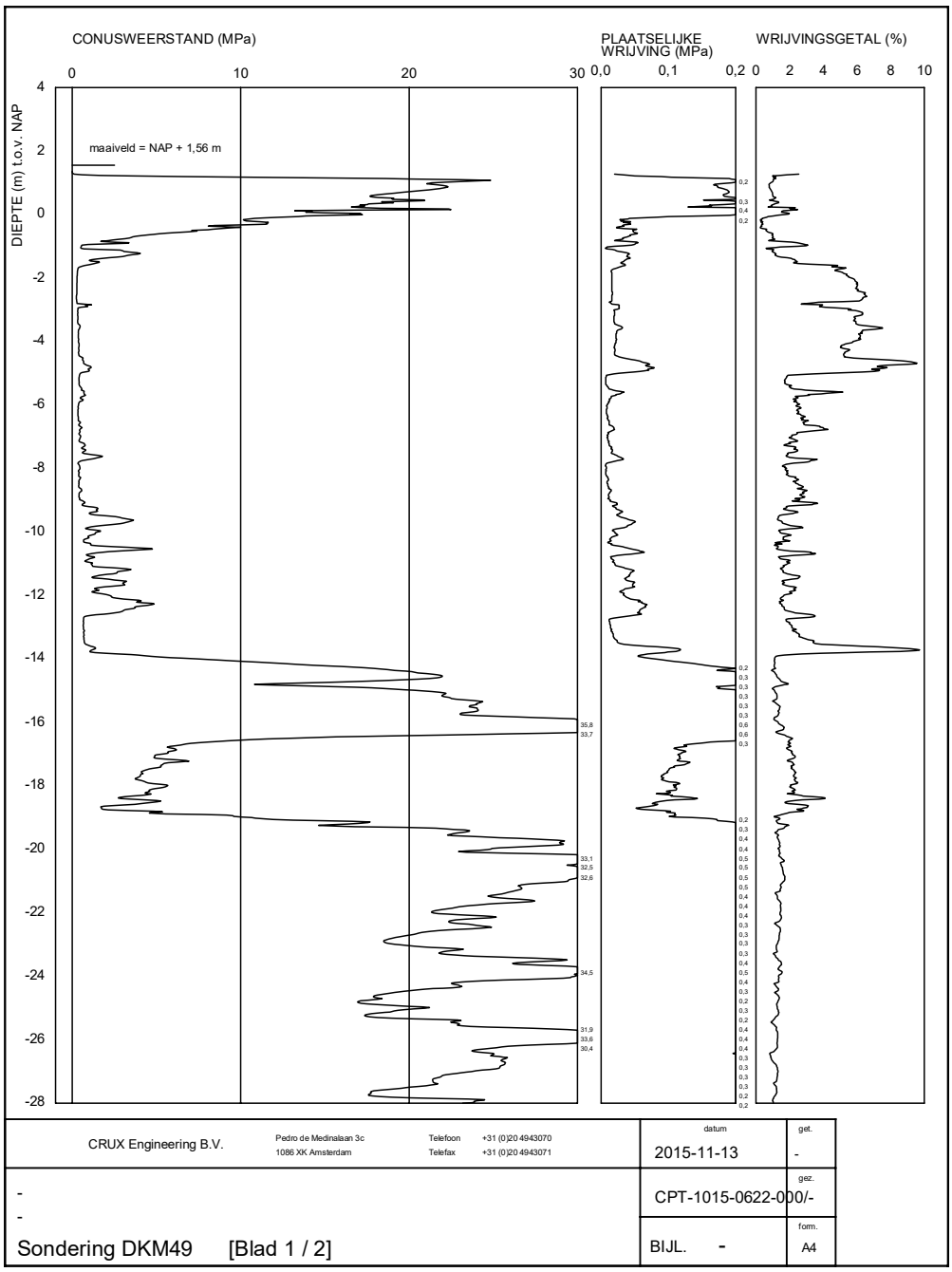


*Figure B.3: CPT DKM49 project in North Amsterdam*

## B.2 D-Pile Group

### B.2.1 Geometry

The 80 piles are modelled with the same grid spacing as the PLAXIS 3D calculation (2 meters). Obviously, the pile head and tip level are exactly the same as the PLAXIS 3D model.

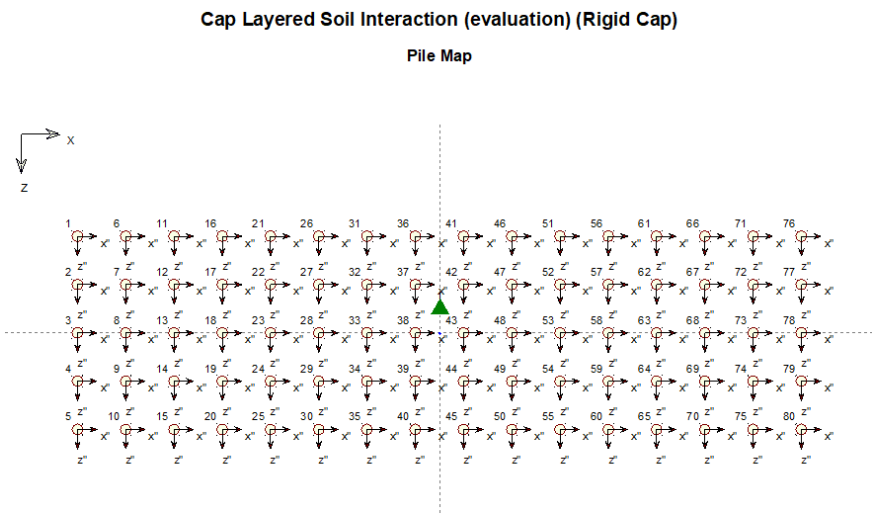


*Figure B.4: Top view D-Pile Group geometry*

## B.2.2 Model properties

Cap Layered soil interaction model (FEM) in D-Pile Group is used.

## B.2.3 Soil layer properties and soil interaction properties

D-Pile Group soil parameters

| | *Holocene* | | *First sand* | | *Allröd clay* | | *Second sand* | | *Eem clay* | | Unit |
|---|---|---|---|---|---|---|---|---|---|---|---|
| | Top | Bottom | Top | Bottom | Top | Bottom | Top | Bottom | Top | Bottom | |
| Dry weight | 14.8 | 14.8 | 19.8 | 19.8 | 18.5 | 18.5 | 19 | 19 | 18.5 | 18.5 | [kN/m$^3$] |
| Wet weight | 14.8 | 14.8 | 19.8 | 19.8 | 18.5 | 18.5 | 19 | 19 | 18.5 | 18.5 | [kN/m$^3$] |
| φ | | | 33 | 33 | | | 33 | 33 | | | [°] |
| $q_c$ | | | 20000 | 20000 | | | 23000 | 23000 | | | [kN/m$^2$] |
| $K_0$ | | | 0.46 | | | | 0.46 | | | | [-] |
| $C_u$ | 20 | 20 | | | 20 | 20 | | | 100 | 100 | [kN/m$^2$] |
| J | 0.25 | | | | 0.25 | | | | 0.25 | | [-] |
| 50% failure | 0.02 | | | | 0.02 | | | | 0.01 | | [-] |
| Friction rule | Ratio | | Cone | | Ratio | | Cone | | Ratio | | |
| dz 100% | 40 | | 0.0025 | | 0.0046 | | 0.0025 | | 0.0046 | | [m] |
| $\alpha_s$ | 0.0001 | | 0.009 | | 0.03 | | 0.009 | | 0.03 | | [-] |
| | *Soil interaction: Cap layered soil interaction model (FEM)* | | | | | | | | | | |
| Young's modulus | 4274 | | 18000 | | 8100 | | 45000*10 [5] | | 6000 | | [kN/m$^2$] |
| Poisson ratio | 0.2 | | 0.2 | | 0.2 | | 0.2 | | 0.2 | | [-] |

*Table B.2: Soil layer properties D-Pile Group*

$$E_{oed}^{ref} = \frac{(1-\nu)\cdot E}{(1-2\cdot\nu)(1+\nu)} \qquad \text{B.1}$$

[5] Increased by factor 10 according to calculations in Van Grop's (2014) Master Thesis, elastic medium around pile causes additional settlements.

## B.3 PLAXIS 3D

Soil properties constitutive models for all PLAXIS 3D models used in this thesis.

### B.3.1 Geometry

Single pile model

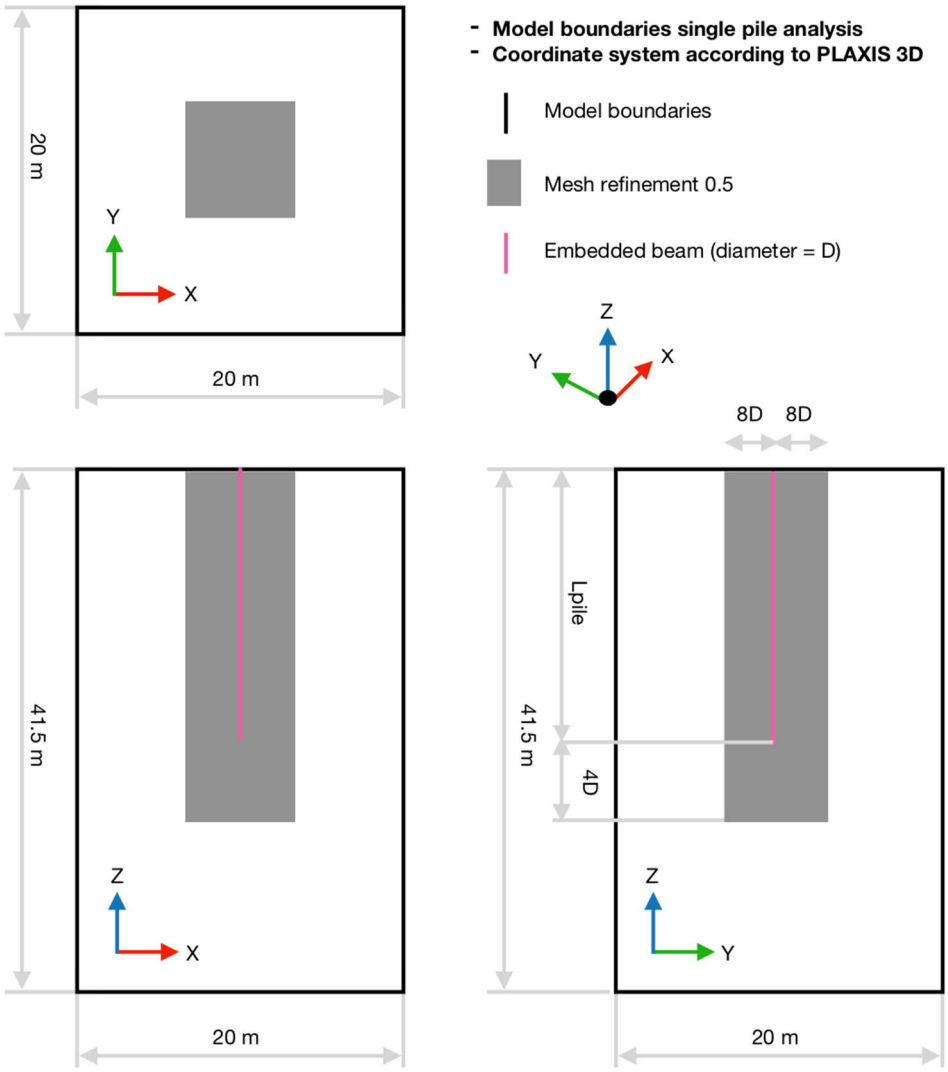


*Figure B.5: Model geometry single pile model*

80 pile model

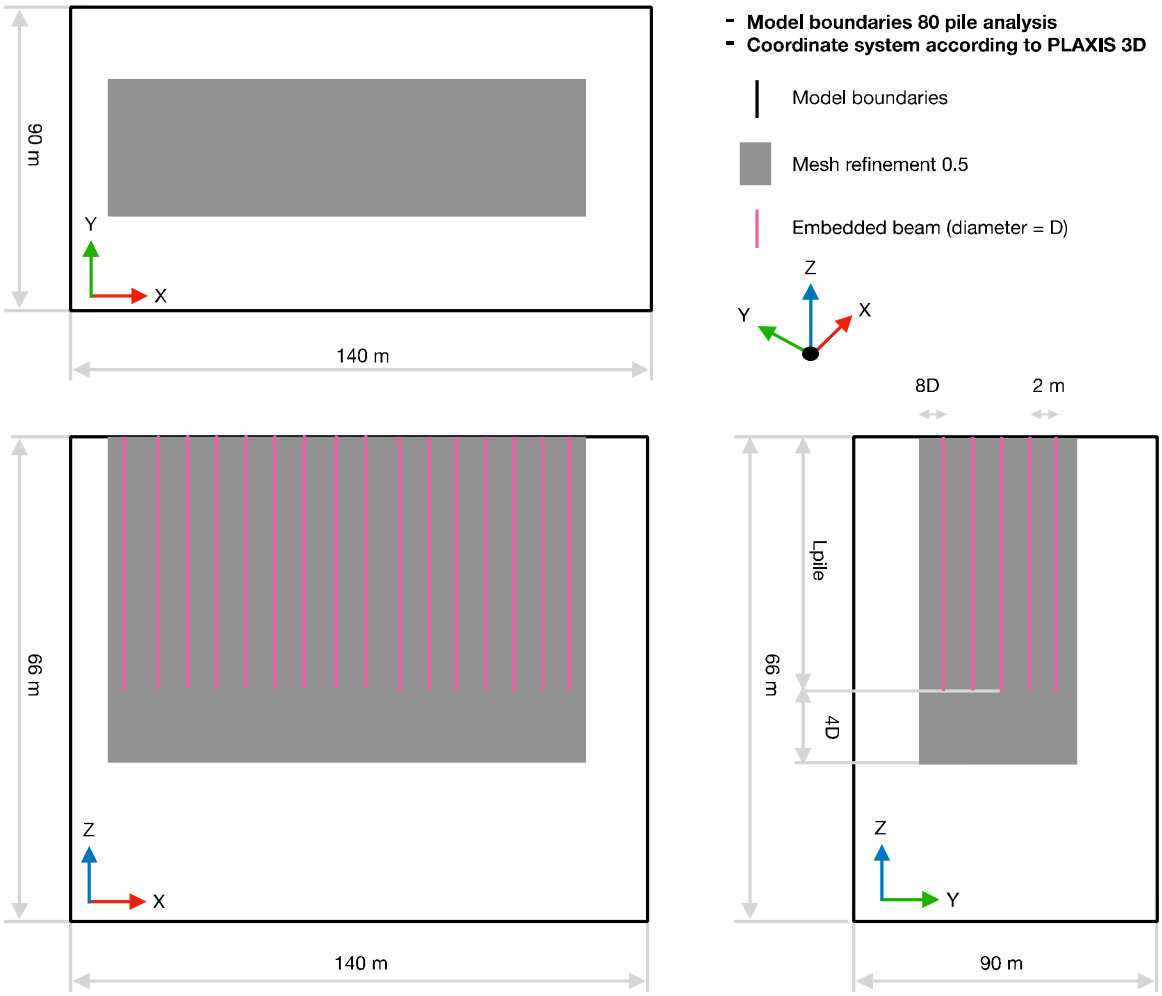


*Figure B.6: Model geometry 80 pile model*

**Boundary conditions PLAXIS 3D models**

| | Deformations | Groundwater flow |
|---|---|---|
| $X_{min}$ | *Normally fixed* | *Open* |
| $X_{max}$ | *Normally fixed* | *Open* |
| $Y_{min}$ | *Normally fixed* | *Open* |
| $Y_{max}$ | *Normally fixed* | *Open* |
| $Z_{min}$ | *Fully fixed* | *Closed* |
| $Z_{max}$ | *Free* | *Open* |

*Table B.3: Boundary conditions single pile and 80 pile model*

## B.3.2 Soil properties

Advanced model – Soil properties (initial)

| | *Sand fill* | *Peat* | *Clay* | *Clayey sand* | *Peat* | *First sand* | *Clay* | *Second sand* | Unit |
|---|---|---|---|---|---|---|---|---|---|
| | Ophoog zand | Holland veen | Hydrobia klei | Wadzand | Basisveen | Eerste zandlaag | Allröd | Tweede zandlaag | |
| Thickness | 2.5 | 4.5 | 3.5 | 4.5 | 0.5 | 3 | 2 | 21 | [m] |
| Soil model | HSS | HSS | HSS | HSS | HSS | HSS | HSS | HSS | |
| $\gamma_{sat}$ | 17 | 10.5 | 15.2 | 18 | 11.7 | 19.80 | 18.50 | 19.00 | kN/m$^3$ |
| $\gamma_{unsat}$ | 19 | 10.5 | 15.2 | 18 | 11.7 | 19.80 | 18.50 | 19.00 | kN/m$^3$ |
| $e_0$ | 0.5 | 0.5 | 0.5 | 0.5 | 0.5 | 0.5 | 0.5 | 0.5 | [-] |
| Dilatancy cut-off | False | False | False | False | False | False | False | False | |
| $E_{50}^{ref}$ | 15000 | 2000 | 7500 | 10000 | 2000 | 35000 | 15000 | 50000 | [kN/m$^2$] |
| $E_{oed}^{ref}$ | 15000 | 1000 | 3500 | 6000 | 1000 | 20000 | 9000 | 50000 | [kN/m$^2$] |
| $E_{ur}^{ref}$ | 50000 | 9000 | 20000 | 25000 | 9000 | 100000 | 30000 | 150000 | [kN/m$^2$] |
| m | 0.5 | 0.9 | 0.8 | 0.5 | 0.9 | 0.5 | 0.8 | 0.5 | [-] |
| $c'_{ref}$ | 0.1 | 5 | 5 | 2 | 5 | 0 | 3 | 0 | [kN/m$^2$] |
| $\varphi'$ | 27 | 18 | 26 | 27 | 18 | 33 | 28 | 33 | [°] |
| $\psi$ | 0 | 0 | 0 | 0 | 0 | 0 | 0 | 3 | [°] |
| $\Upsilon_{0.7}$ | 1.670E-4 | 9.3E-4 | 3.3E-4 | 1.9E-4 | 9.3E-4 | 1.210E-4 | 2.4E-4 | 9.8E-5 | [-] |
| $G_0^{ref}$ | 83470 | 18000 | 48000 | 55000 | 18000 | 122100 | 60000 | 150000 | [kN/m$^2$] |
| $K_0^{NC}$ | 0.5460 | 0.6910 | 0.5616 | 0.5460 | 0.6910 | 0.4554 | 0.5305 | 0.4554 | [-] |
| $R_{inter}$ | 0.01 | 0.01 | 0.01 | 0.01 | 0.01 | 1.0 | 1.0? | 1.0 | [-] |
| OCR | 1 | 1 | 1 | 1 | 1 | 1 | 1 | 1 | [-] |
| $K_0$ | 0.5460 | 0.6910 | 0.5616 | 0.5460 | 0.6910 | 0.4554 | 0.5305 | 0.4554 | [-] |
| POP | 0 | 0 | 0 | 0 | 0 | 0 | 0 | 0 | [-] |
| Drainage type | Drained | Drained | Drained | Drained | Drained | Drained | Drained | Drained | |
| $K_x = k_y = k_z$ | 7,128 | 0,0475 | 0,0475 | 0,3145 | 0,05 | 7,128 | 0,0475 | 0,0475 | [m/day] |

*Table B.4: Soil properties advanced model initial: [Values based on project in Amsterdam]*

Compressible layer

| | *Clay* | |
|---|---|---|
| | Eem klei | Unit |
| Thickness | 33 | [m] |
| Soil model | SSC | |
| $\gamma_{sat}$ | 18.5 | kN/m$^3$ |
| $\gamma_{unsat}$ | 18.5 | kN/m$^3$ |
| $e_0$ | 0.5 | [-] |
| Dilatancy cut-off | False | |
| $\lambda^*$ | 0.09110 | [-] |
| $\kappa^*$ | 0.02360 | [-] |
| $\mu^*$ | 0.00213 | [-] |
| $c'_{ref}$ | 10 | [kN/m$^2$] |
| $\varphi'$ | 30 | [°] |
| $\psi$ | 0 | [°] |
| $\nu'_{ur}$ | 0.15 | [-] |
| $K_0^{NC}$ | 0.5 | [-] |
| OCR | 1.75 | [-] |
| $K_0$ | 0.7426 | [-] |
| POP | 0 | [-] |
| Drainage type | | |
| $K_x = k_y = k_z$ | 0.04E-3 | [m/day] |

*Table B.5: Soil properties Eem clay layer*

### B.3.3 Soil parameter correlations

The soil stratigraphy is based on a project in the Northem part of Amsterdam. This location is selected because of the available CPT and soil parameter data that was available. The stratigraphy is one of the typical soil profiles which can be encountered in the Netherlands. The soil parameters for the PLAXIS calculations are derived partly on correlations discussed in this section and engineering judgement within CRUX Engineering.

PLAXIS parameter sets are often based on experience in engineering firms developed over the years. These parameter sets based on experience incorporated responses of the soil which are back calculated after projects are finished. Therefore, these parameters are close to realistic soil behaviour which can be encountered at these locations.

Starting off with an CPT, a soil classification is made based on the NEN-rules (NEN 9997-1, 2017). Subsequently, the basic soil properties are derived according to table 2b from the NEN. Basic soil parameters incorporate; unit soil weight, friction angle and cohesion including correction for the reference pressure. Based on experience with CRUX, these parameters are slightly changed to be more in line with back calculation data of projects in the past.

The hardening soil parameters are calculated with correlation found in the literature. Reference stiffnesses are obtained with empirical relationships. The Eoed parameters are based on correlations with the cone resistance according to Sanglerat (1972), plaxis and Lunne & Christophersen (1983).

$$E_{oed} = E_{oed;ref}\left(\frac{\sigma'_1}{p_{ref}}\right)^m \qquad \text{B.2}$$

For clays and sand:

$$G_{0;ref} = \frac{E_{0;ref}}{2\cdot(1+\nu_{ur})} \qquad \text{B.3}$$

For peat:

$$G_{0;ref} = 2\cdot E_{ur;ref} \qquad \text{B.4}$$

Small strain parameter Hardening soil small strain:

$$\gamma_{0.7} = \frac{1}{9\cdot G_0}\cdot 2\cdot c'^{(1+\cos(2\varphi))} - \sigma'_1\cdot(1+K_0)\cdot\sin(2\varphi) \qquad \text{B.5}$$

| | |
|---|---|
| $M_0 = 4.q_c$ | for $q_c < 10$ MPa |
| $M_0 = 2.q_c + 20$ (MPa) | for 10 MPa $< q_c <$ 50 MPa |
| $M_0 = 120$ MPa | for $q_c > 50$ MPa |

*Table B.6: $M_0$ is Eoed for sands: after Lunne & Christoffersen (1983)*

| | | |
|---|---|---|
| $q_c < 0.7$ MPa<br>$0.7 < q_c < 2.0$ MPa<br>$q_c > 2.0$ MPa | $3 < \alpha < 8$<br>$2 < \alpha < 5$<br>$1 < \alpha < 2.5$ | Clay of low plasticity |
| $q_c > 2.0$ MPa<br>$q_c < 2.0$ MPa | $3 < \alpha < 6$<br>$1 < \alpha < 3$ | Silts or low plasticity clays |
| $q_c < 2.0$ MPa | $2 < \alpha < 6$ | Highly plastic silts and clays |
| $q_c < 1.2$ MPa | $2 < \alpha < 8$ | Organic silts |
| $q_c < 1.2$ MPa<br>$50 < w < 100$<br>$100 < w < 200$<br>$w > 200$<br>w = water content | <br>$1.5 < \alpha < 4$<br>$1 < \alpha < 1.5$<br>$0.4 < \alpha < 1$ | Peat and organic clays |

*Table B.7: $E_{oed}$ for clay and silts: after Sanglerat (1972)*

| type | $E_{50;ref}$ | $E_{ur;ref}$ |
|---|---|---|
| zand | 1 x $E_{oed;ref}$ | 4 x $E_{50;ref}$ |
| leem | 1.2 x $E_{oed;ref}$ | 5 x $E_{50;ref}$ |
| klei, st zandig | 1.3 x $E_{oed;ref}$ | 5 x $E_{50;ref}$ |
| klei | 2 x $E_{oed;ref}$ | 5 x $E_{50;ref}$ |
| klei, organisch | 2 x $E_{oed;ref}$ | 6 x $E_{50;ref}$ |
| veen | 2 x $E_{oed;ref}$ | 6 x $E_{50;ref}$ |

*Table B.8: $E_{50;ref}$ and $E_{ur;ref}$*

| Soil | $E_{oed;ref}$ | m |
|---|---|---|
| clay | 0.6 - 5 | 0.9 - 1 |
| silt | 3 - 11 | 0.6 – 0.9 |
| sand | 20 - 60 | 0.5 – 0.7 |
| gravel | 40 -110 | 0.4 – 0.7 |

*Table B.9: m values hardening soil small strain model after Soos (1995)*

### B.3.4 Fit parameters first sand layer

Simplified model - Sand box variations properties

| | Initial Sand layer | Variation box | Variation box | Variation box | Unit |
|---|---|---|---|---|---|
| | | 3xE 3xOCR | 2x 2xOCR | 1xE K0=2xOCR | |
| Thickness | 26 | 10* | 10* | 10* | [m] |
| Soil model | HSS | HSS | HSS | HSS | |
| $\gamma_{sat}$ | 19.80 | 19.80 | 19.80 | 19.80 | [kN/m$^3$] |
| $\gamma_{unsat}$ | 19.80 | 19.80 | 19.80 | 19.80 | [kN/m$^3$] |
| $e_0$ | 0.5 | 0.5 | 0.5 | 0.5 | [-] |
| Dilatancy cut-off | False | False | False | False | |
| $E_{50}^{ref}$ | 35000 | **70000** | **105000** | 35000 | [kN/m$^2$] |
| $E_{oed}^{ref}$ | 20000 | **40000** | **60000** | 20000 | [kN/m$^2$] |
| $E_{ur}^{ref}$ | 100000 | **200000** | **300000** | 100000 | [kN/m$^2$] |
| m | 0.5 | 0.5 | 0.5 | 0.5 | [-] |
| $c'_{ref}$ | 0 | 0 | 0 | 0 | [kN/m$^2$] |
| $\varphi'$ | 33 | 33 | 33 | 33 | [°] |
| $\psi$ | 0 | 0 | 0 | 0 | [°] |
| $\gamma_{0.7}$ | 0.1210E-3 | 0.1210E-3 | 0.1210E-3 | 0.1210E-3 | [-] |
| $G_0^{ref}$ | 122100 | **244200** | **366300** | 122100 | [kN/m$^2$] |
| $K_0^{NC}$ | 0.4554 | 0.4554 | 0.4554 | 0.4554 | [-] |
| $R_{inter}$ | 1.0 | 1.0 | 1.0 | 1.0 | [-] |
| OCR | 1 | **3** | **2** | 1 | [-] |
| $K_0$ | 0.4554 | 0.4554 | 0.4554 | **0.75** | [-] |
| POP | 0 | 0 | 0 | 0 | [-] |

*Table B.10: Soil properties - sand box variations*

### B.3.5 Numerical control parameters

| Numerical control parameters | |
|---|---|
| Solver type | Picos (multicore iterative) |
| Max cores to use | 1 |
| Max number of steps stored | 1 |
| Use Compression for result files | Check box off |
| Use default iter parameters | Check box off |
| Max steps | 1000 |
| Tolerated error | 0.02000 |
| Max unloading steps | 5 |
| Max load fraction step | 0.5 |
| Over-relaxation factor | 1.2 |
| Max number of iterations | 80 |
| Desired min number of iterations | 20 |
| Desired max number of iterations | 60 |
| Arc-length control type | On |
| Use line search | Check box off |
| Use gradual error reduction | Check box off |

*Table B.11: Numerical control parameters PLAXIS 3D calculations*

### B.3.6 Meshing information

Single pile

| | Nodes | Elements | Avg. mesh element size [m] | Max. element size [m] | Min. element size [m] |
|---|---|---|---|---|---|
| Mesh 1 (coarse) | 45538 | 32107 | 2.180 | 9.121 | 0.5 |
| Mesh 2 (medium) | 61578 | 43302 | 2.156 | 7.770 | 0.5 |
| Mesh 3 (fine) | 102580 | 72371 | 1.952 | 5.258 | 0.4931 |
| Mesh 4 (very fine) | 212253 | 151559 | 1.545 | 3.857 | 0.3641 |

*Table B.12: Meshing results single pile model current/new embedded beam*

| Mesh type information | |
|---|---|
| Model | Full |
| Elements | 10 - noded |

*Table B.13: Mesh type information single pile model*

80 pile

| | Nodes | Elements | Avg. mesh element size [m] | Max. element size [m] | Min. element size [m] |
|---|---|---|---|---|---|
| Mesh 2 (medium) | 185940 | 128139 | 2.870 | 18.07 | 0.2528 |

*Table B.14: Meshing results 80 pile model current/new embedded beam*

| Mesh type information | |
|---|---|
| Model | Full |
| Elements | 10 - noded |

*Table B.15: Mesh type information 80 pile model*

### B.3.7 Pile loading

Single pile model

| Identification | Phase | Load [-] | Start calculation | Calculation type | Loading type | Pore pressure |
|---|---|---|---|---|---|---|
| *Unit* | | *Load/Pile capacity* | | | | |
| Initial phase | 0 | - | - | K0 procedure | - | Phreatic |
| Phase 1 | 1 | 0.017 | Initial phase | Plastic | Staged construction | Phreatic |
| Phase 2 | 2 | 0.034 | Initial phase | Plastic | Staged construction | Phreatic |
| Phase 3 | 3 | 0.086 | Initial phase | Plastic | Staged construction | Phreatic |
| Phase 4 | 4 | 0.174 | Initial phase | Plastic | Staged construction | Phreatic |
| Phase 5 | 5 | 0.260 | Initial phase | Plastic | Staged construction | Phreatic |
| Phase 6 | 6 | 0.288 | Initial phase | Plastic | Staged construction | Phreatic |
| Phase 7 | 7 | 0.434 | Initial phase | Plastic | Staged construction | Phreatic |
| Phase 8 | 8 | 0.521 | Initial phase | Plastic | Staged construction | Phreatic |
| Phase 9 | 9 | 0.555 | Initial phase | Plastic | Staged construction | Phreatic |
| Phase 10 | 10 | 0.590 | Initial phase | Plastic | Staged construction | Phreatic |
| Phase 11 | 11 | 0.625 | Initial phase | Plastic | Staged construction | Phreatic |
| Phase 12 | 12 | 0.660 | Initial phase | Plastic | Staged construction | Phreatic |
| Phase 13 | 13 | 0.694 | Initial phase | Plastic | Staged construction | Phreatic |
| Phase 14 | 14 | 0.781 | Initial phase | Plastic | Staged construction | Phreatic |
| Phase 15 | 15 | 0.868 | Initial phase | Plastic | Staged construction | Phreatic |
| Phase 16 | 16 | 0.955 | Initial phase | Plastic | Staged construction | Phreatic |
| Phase 17 | 17 | 1.000 | Initial phase | Plastic | Staged construction | Phreatic |

*Table B.16: Phasing single pile PLAXIS model*

80 pile model

Phasing of calculation

| Name | Load [kN] | Type of calculation | Duration [days] |
|---|---|---|---|
| Initial phase 0 | 0 | $K_0$ procedure | 0 |
| Loading phase 1 | 1250 | Consolidation | 49 |
| Loading phase 2 | 1750 | Consolidation | 49 |
| Loading phase 3 | 2250 | Consolidation | 49 |
| Consolidation after 10 years | 2250 | Consolidation | 3650 |
| Consolidation after 20 years | 2250 | Consolidation | 7300 |
| Consolidation after 50 years | 2250 | Consolidation | 18250 |

*Table B.17: Phasing of consolidation calculations 80 pile model*

# C Single pile model

## C.1 Single pile

### C.1.1 Mesh dependency current embedded beam formulation

High stress singularities occur at the pile base in combination with dense mesh sizes. These high stress concentrations are caused by the connection of the embedded beam by only one stress point to the mesh. By refining the mesh in combination with the current embedded beam, the stress below the pile tip keeps increasing. This phenome is described by Acín González (2015) and is called stress singularities. The red marked location in Figure C.1 shows very high stresses (45000 kPa) which is unrealistic for situations in the field. Therefore, it is concluded that the fine mesh is not suitable for practical application due to the unrealistic stresses and the problems become mesh dependent.

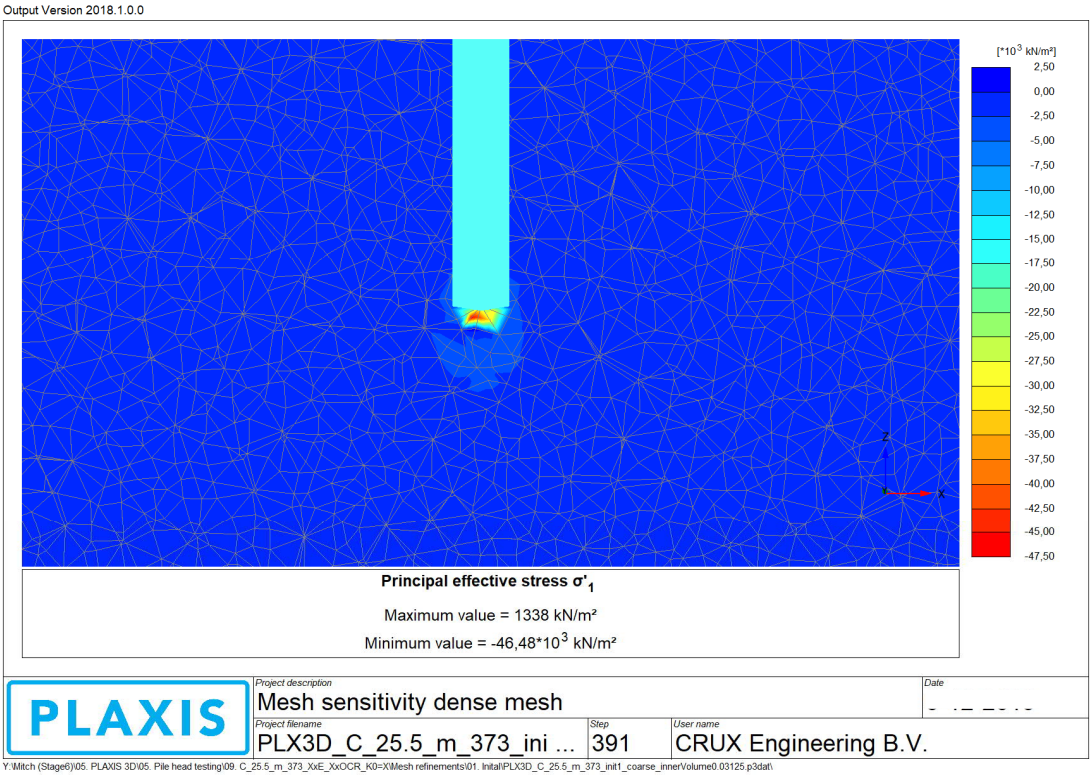


*Figure C.1: Stress singularities dense meshes single pile*

## C.2 Simplified soil stratigraphy

### C.2.1 Current embedded beam

Graph C.1 visualize the response of the multi-linear skin friction distribution including 3 different parameter sets for the soil box around pile tip level. By increasing the stiffness and OCR parameter(s) with a factor 3, the overall response (base and shaft) gives an outcome closer to NEN9997 curve 1.

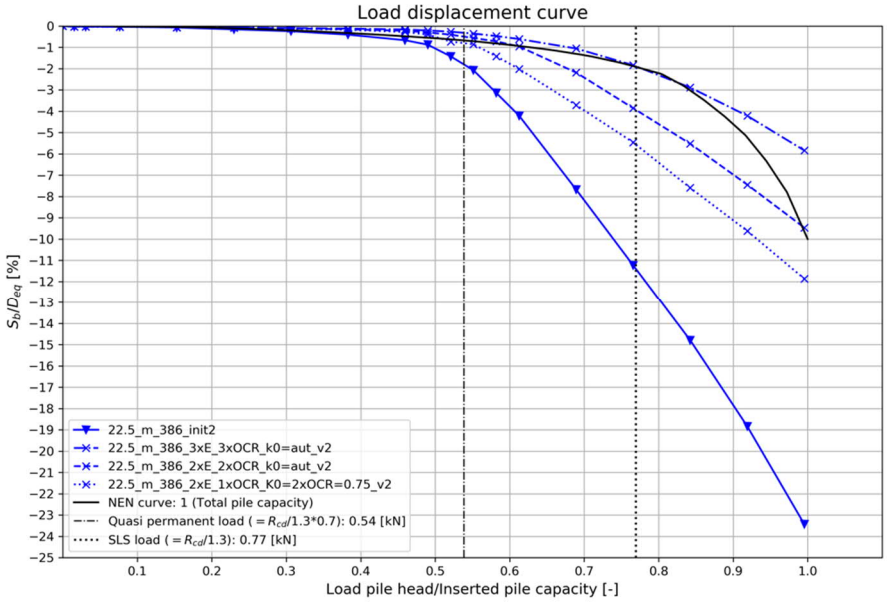


*Graph C.1: Fit calculation multi-linear | current embedded beam*

By separating the base and the shaft in two separate plots, the model with stiffness and OCR parameter(s) multiplied by 3 has a base response closer to NEN9997. The linear behaviour of the base is due to the linear elastic perfectly plastic spring attached at the bottom of the embedded pile and there is no possibility to change the stiffness in the user interface of PLAXIS.

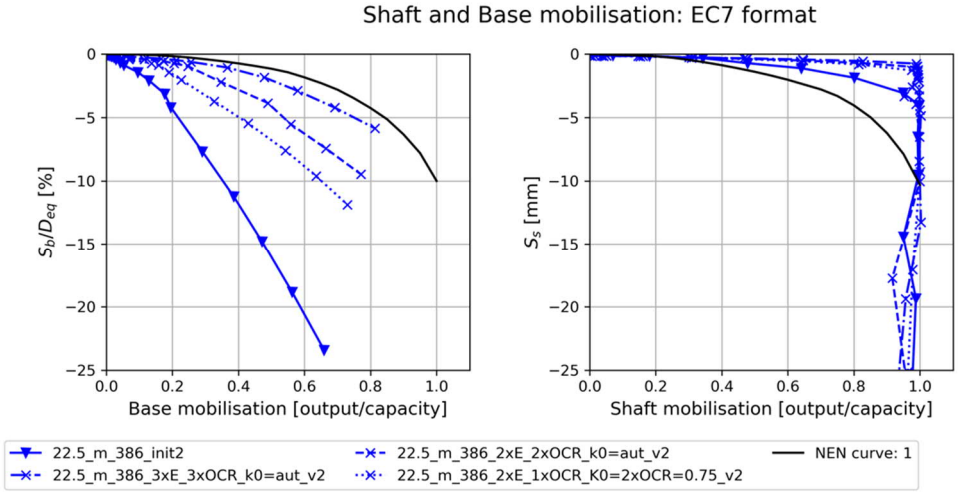


*Graph C.2: Fit calculation multi-linear (shaft and base) | current embedded beam*

None of the proposed approaches for fitting the behaviour is a perfect match with the NEN9997 curve 1. However, it is possible to get a good approximation of the Eurocode curve by increasing 3 times the stiffness and OCR, at least in the serviceability state stress range. An explanation of the influence on the soil body by increasing the stiffness, OCR and $K_0$ is given in section 6.5.3 .

## C.2.2 New embedded beam

The comparison between the current and new embedded beam in paragraph 6.2 concluded that the new formulation has a significant stiffer behaviour. Subsequently, during the fit calculation less improvements are necessary to approximate the NEN9997 curve.

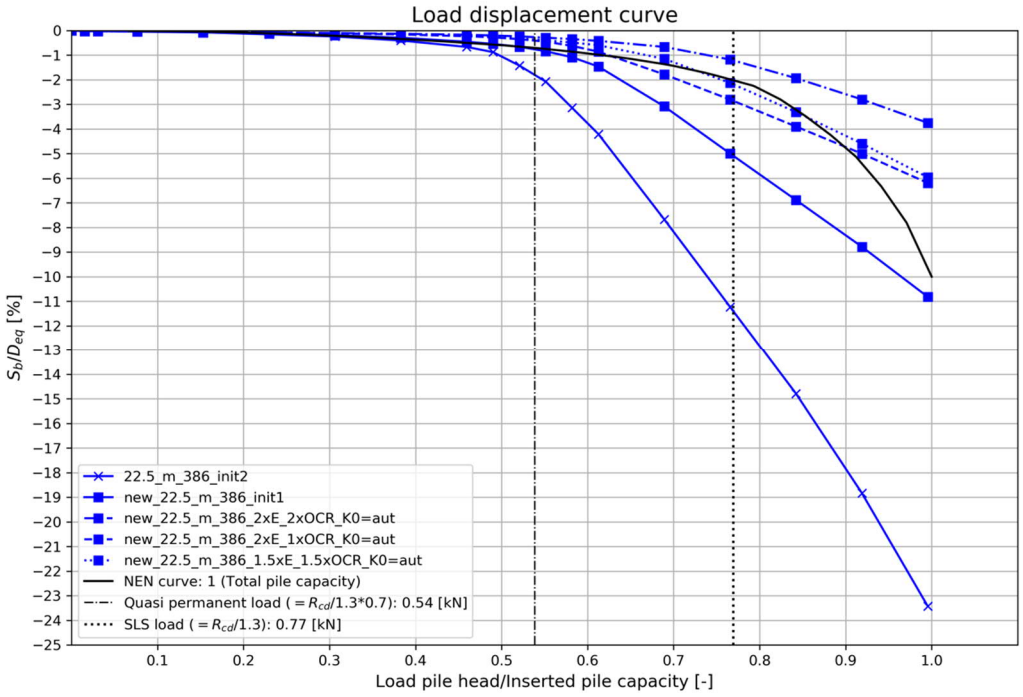


*Graph C.3: Fit calculation multi-linear | new embedded beam*

In case the current formulation is used, the best fit is achieved by increasing the stiffness parameters and the OCR by a factor of 3. In case the new formulation is used, the best fit is obtained by increasing the stiffness parameters and the OCR by a factor 1.5. In Graph C.4 can be seen that the main improvement is contributed by the base response.

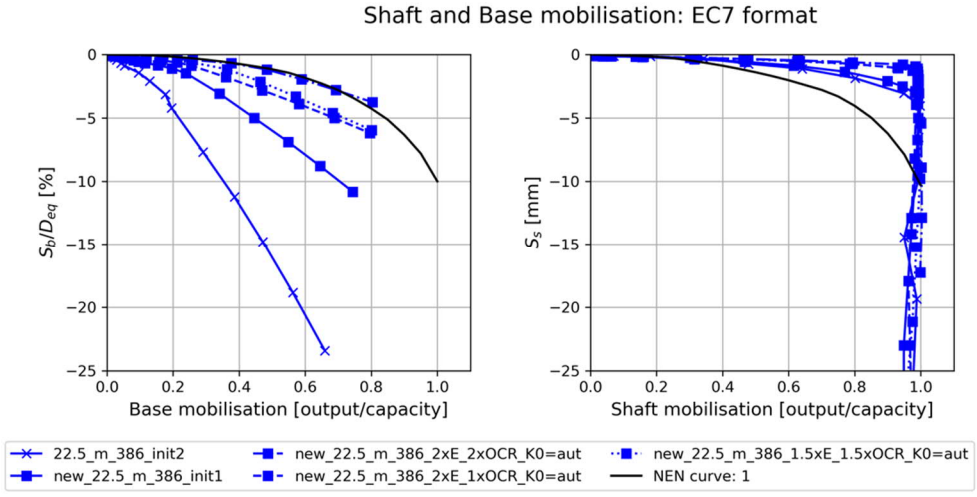


*Graph C.4: Fit calculation multi-linear (shaft and base) | new embedded beam*

## C.3 Layer dependent skin friction simplified model

### C.3.1 Current embedded beam

The same procedure for the multi-linear skin friction distribution is used for the layer dependent skin friction distribution. Graph C.5 shows the response of the pile with the layer dependent distribution and 3 different box variation parameters sets. Compared to the multi-linear skin friction model, the obtained fit is far away from the desired Eurocode response. The reason can be derived from the base and shaft response plots: the skin friction remains constant even with higher stiffness and higher $K_0$ values around the pile tip. The response of the model with layer dependent skin friction distribution has an even softer response compared to the multi-linear model. The softer response is due to the lower amount of shaft friction that can be mobilized. The shaft mobilization in the layer dependent model is a function

of the normal stresses acting on the pile shaft (eq. C.1). These normal stresses are assumed to be higher due to installation effects obtained from field test. However, the installation effects are not perfectly taken into account in the layer dependent model and therefore the skin friction mobilization is based on the in-situ soil stresses which are not including the installation effects.

$$\tau_m = c' + \sigma_n' \cdot \tan(\varphi') \qquad \text{C.1}$$

Equation C.1 visualizes clear the influence of the normal stress at the pile shaft, which is the $\sigma_3$ principal stress related to the $K_0$.

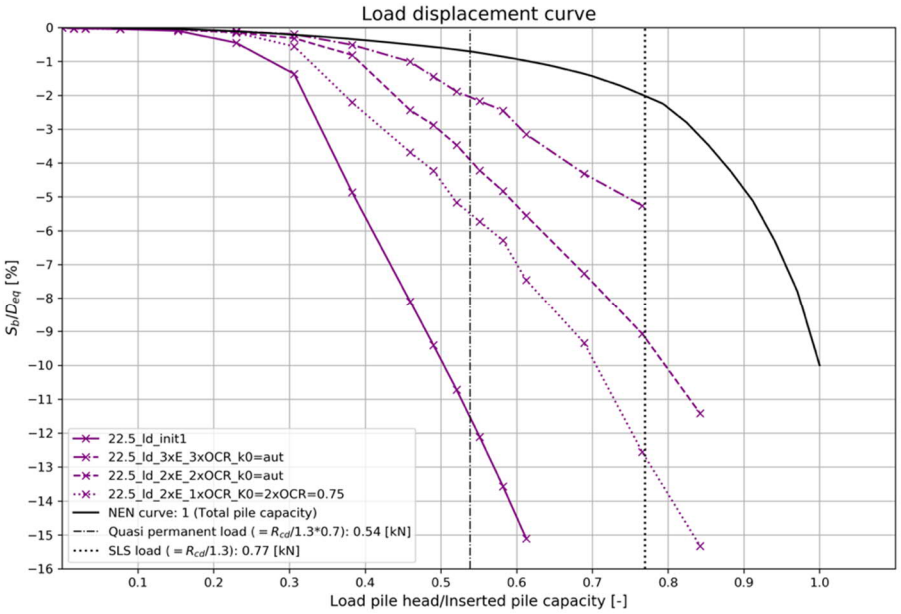


*Graph C.5: Fit calculation layer dependent | current embedded beam*

Tschuchnigg (2013) mentioned that the mobilization of skin friction is mainly related to the stiffness of the interface definition instead of the stiffness of the soil around the pile. Since, the interface stiffness is determined by springs connected to the mesh, it is not possible to change them in the PLAXIS user interface and requires more research on the influences and consequences by varying these parameters.

Graph C.6 shows the improvements in the base resistance by increasing the stiffness parameters at pile tip level. On the contrary, the skin friction does not mobilize the proposed skin resistance.

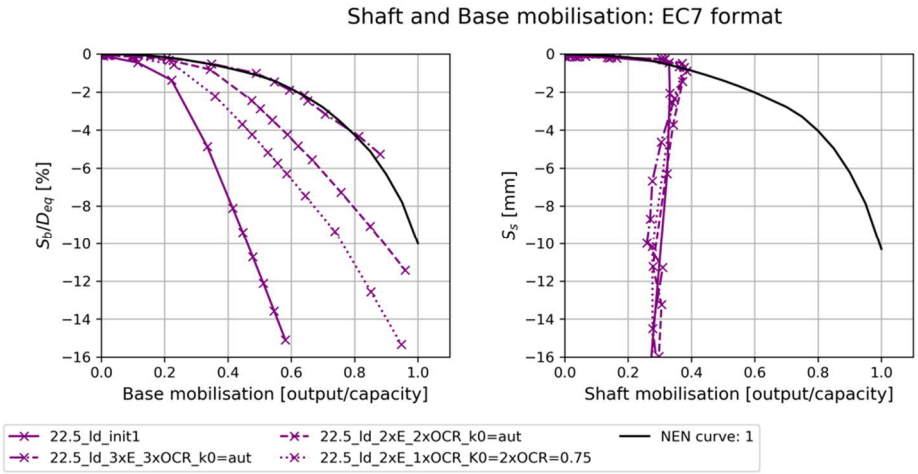


*Graph C.6: Fit calculation layer dependent (shaft and base) | current embedded beam*

## C.3.2 New embedded beam

The layer dependent skin friction distribution shows some improvement regarding the load-displacement behaviour. This improvement is mainly achieved by the stiffer base response. However, the pile capacity calculated in the D-

Foundations calculation is never reached in the PLAXIS 3D calculations. The reason for this is still the limited amount of skin friction which can be mobilized along the shaft since the installation effects are not taken into account.

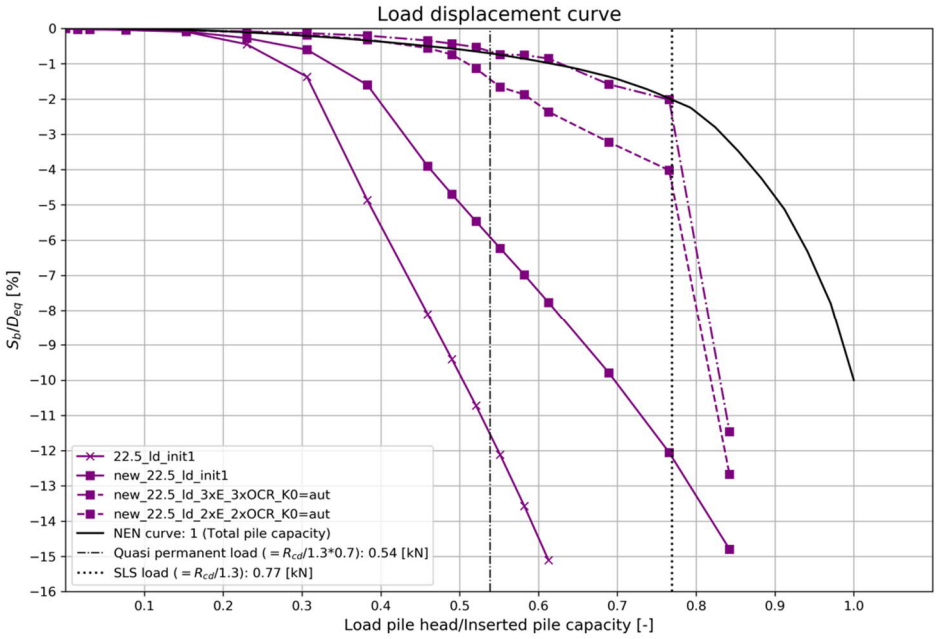


*Graph C.7: Fit calculation layer dependent | new embedded beam*

The PLAXIS 3D calculation with a layer dependent skin friction distribution is less stable compared to the multi-linear distribution based on the load displacement curves given. Especially the shaft mobilisation during loading is not a smooth line as expected when maximum skin friction is mobilized (Graph C.8, right graph).

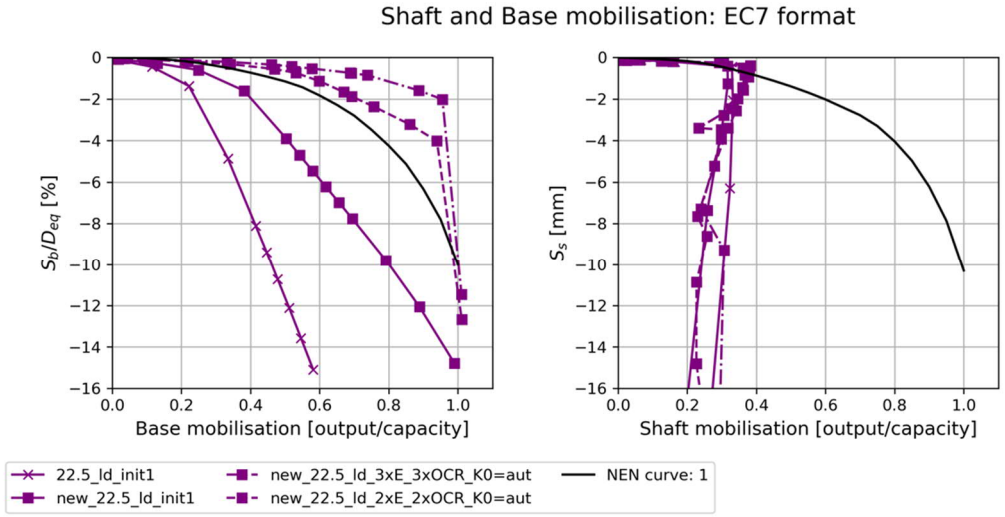


*Graph C.8: Fit calculation layer dependent (shaft and base) | new embedded beam*

The base resistance in the new formulation is stiffer compared to NEN9997, but compensates the lower shaft resistance in the overall behaviour. The drop in Graph C.7 at the last data point is due to the linear elastic perfectly plastic spring connected at the base of the embedded beam. In Graph C.8 (left) can be seen that the inserted maximum capacity of the base is reached. Therefore, the base resistance drops down.

# D Model variations

## D.1 Multiple pile

### D.1.1 Pile spacing

In order to show the influence of the pile spacing on the stress and settlement distribution, 3 different spacings have been tested: 2, 3 and 4 meter centre-to-centre distance. As expected, the larger spacings results in a wider stress distribution and less deep settlement trog.

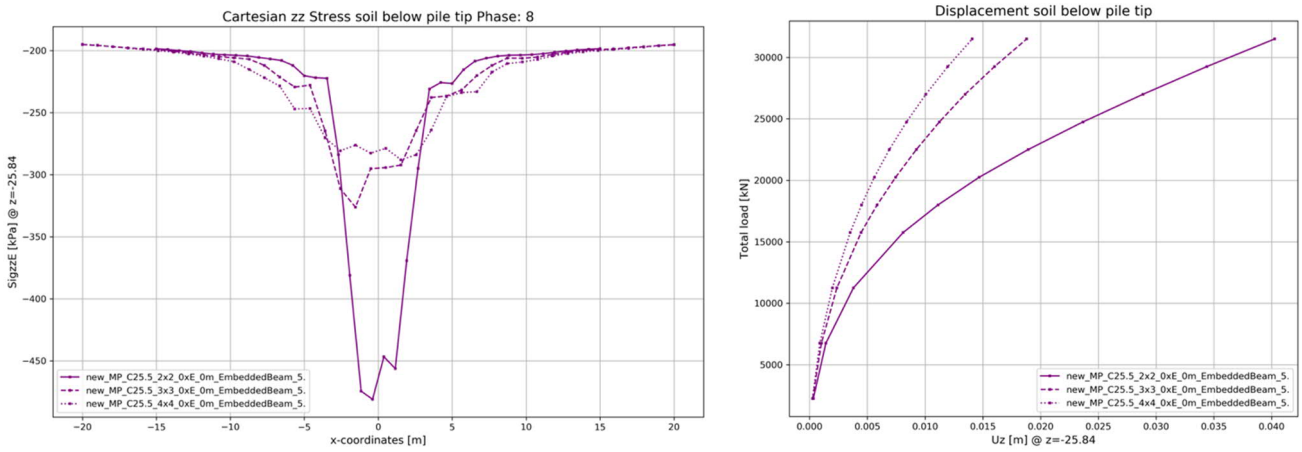


*Graph D.1: Pile spacing influence 9 pile model*

The initial pile spacing configuration is based on the idealized problem in the paper of Engin (2008). The 2 by 2 meter pattern, a realistic spacing for engineering practice. The distance between the piles is equal to 4 times the pile diameter.

| Name model | Pile spacing [m] | Relative to pile diameter s/D [-] |
|---|---|---|
| Initial | 2 x 2 | 4 |
| | 3 x 3 | 6 |
| | 4 x 4 | 8 |

*Table D.1: Pile spacings in different models*

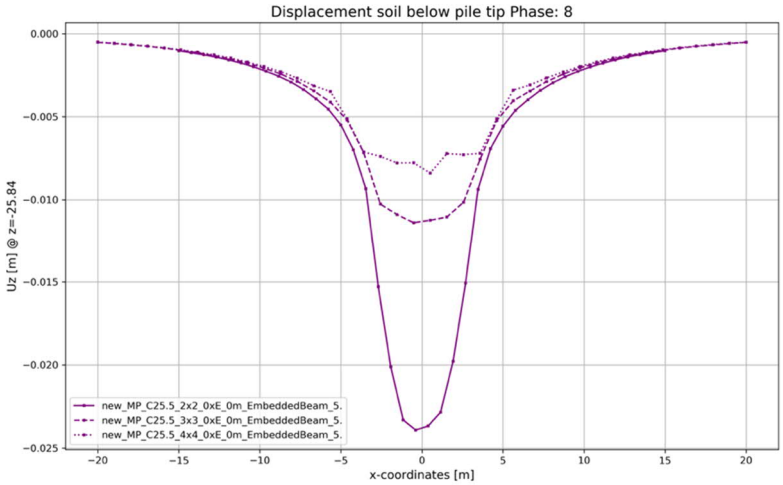


*Graph D.2: Pile spacing influence 4D below pile tip*

The graphs above visualizing the settlements and stresses at 2750 kN load on each pile head. This is 0.75 times the ultimate bearing capacity of the pile.

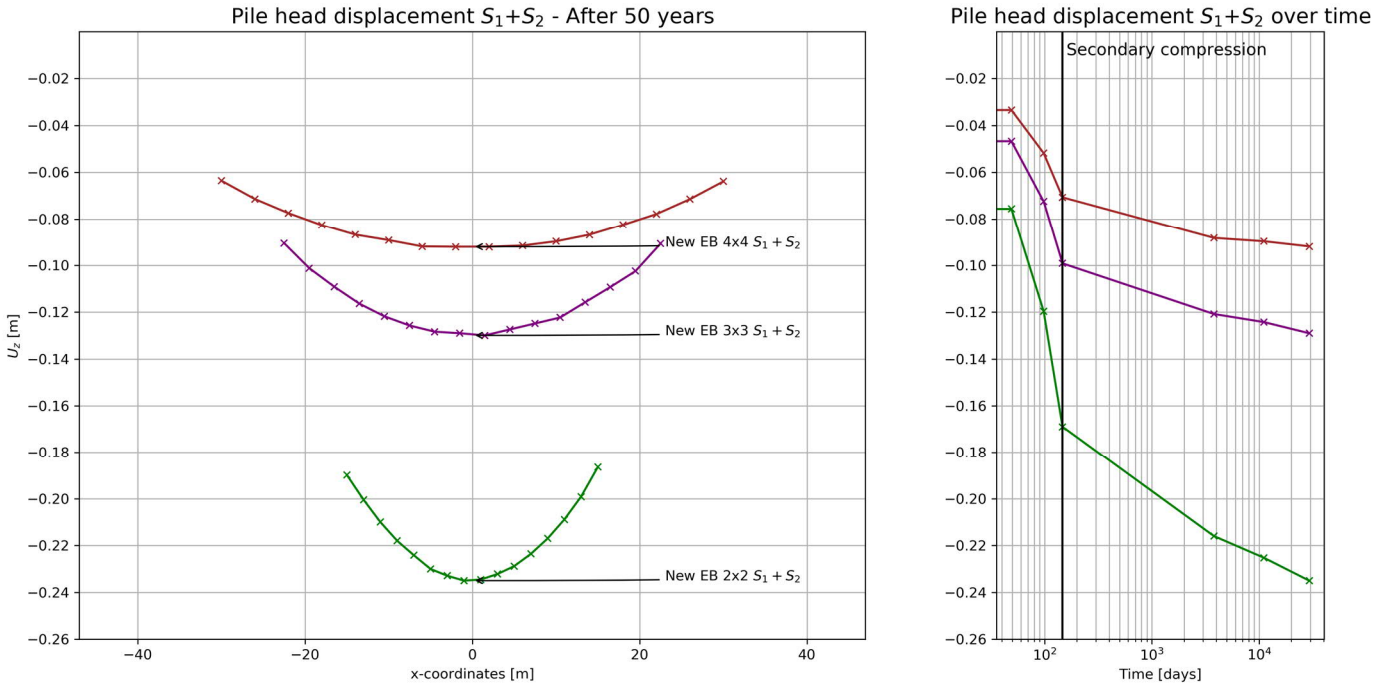


*Graph D.3: Variations in pile spacing on settlement envelop*

## D.2 **Elastic compression**

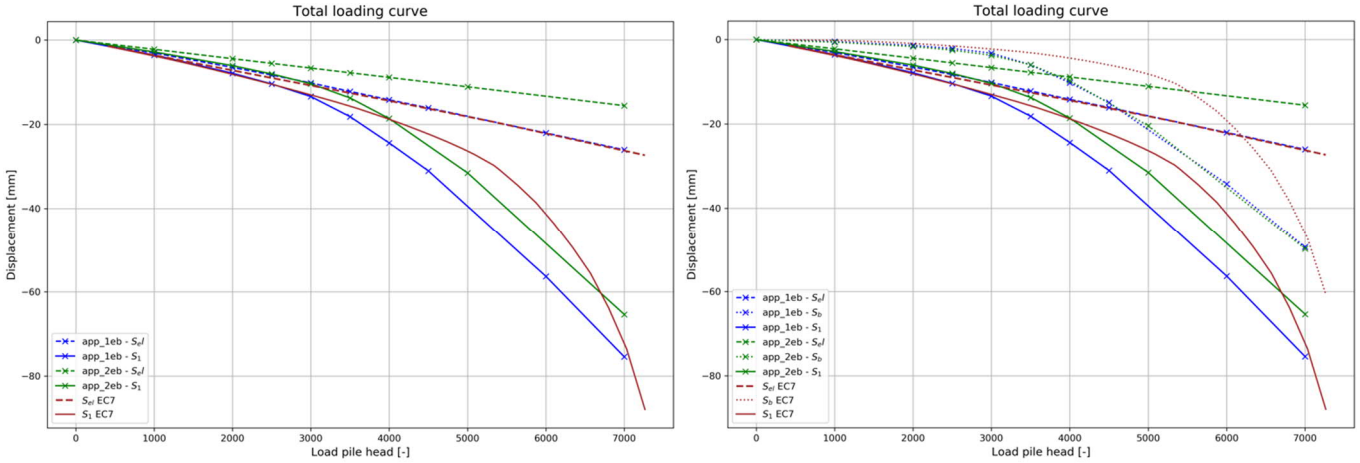


*Graph D.4: Single pile response with elastic compression fit*

In chapter 8 are the results of the elastic pile compression discussed. Initially the elastic response was to soft, therefore the entire elasticity is increased in the pile. However, according to the Eurocode elastic compression in the positive zone is assumed to be zero. Therefore, an experiential single pile model was tested with two embedded beams on top of each other. The lower one, entirely in the positive skin friction zone, has an infinite axial stiffness, the upper one has a realistic stiffness for concrete.

The axial elastic compression is as excepted, no elastic compression in the positive skin friction zone (Graph D.5). But in combination with the application data, the response of the two embedded beams on top of each other were too stiff. Moreover, the single embedded beam seems to be the correct method for modelling the elastic compression (Graph D.4). Because of time constrains no further elaboration or investigation is performed on the two-embedded beam configuration. Moreover, limitations that were noticed during this thesis was reading out the results from the embedded beams. Because, the pile is splits in two elements.

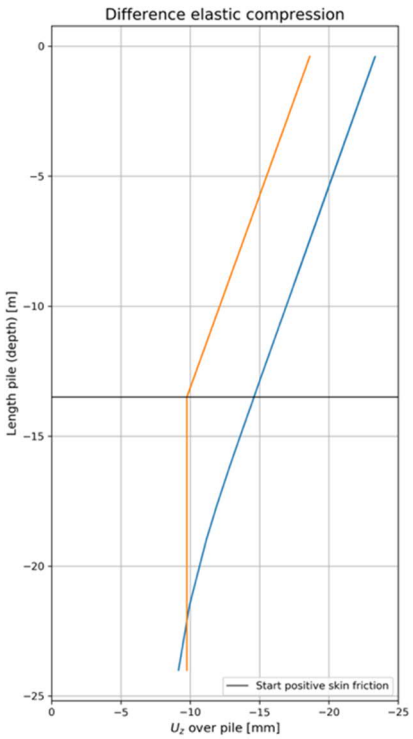


*Graph D.5: Elastic compression; two beams on top of each other (orange) and one embedded beam (blue)*

Two embedded beams on top of each other. Influence on behaviour have to be investigated further.

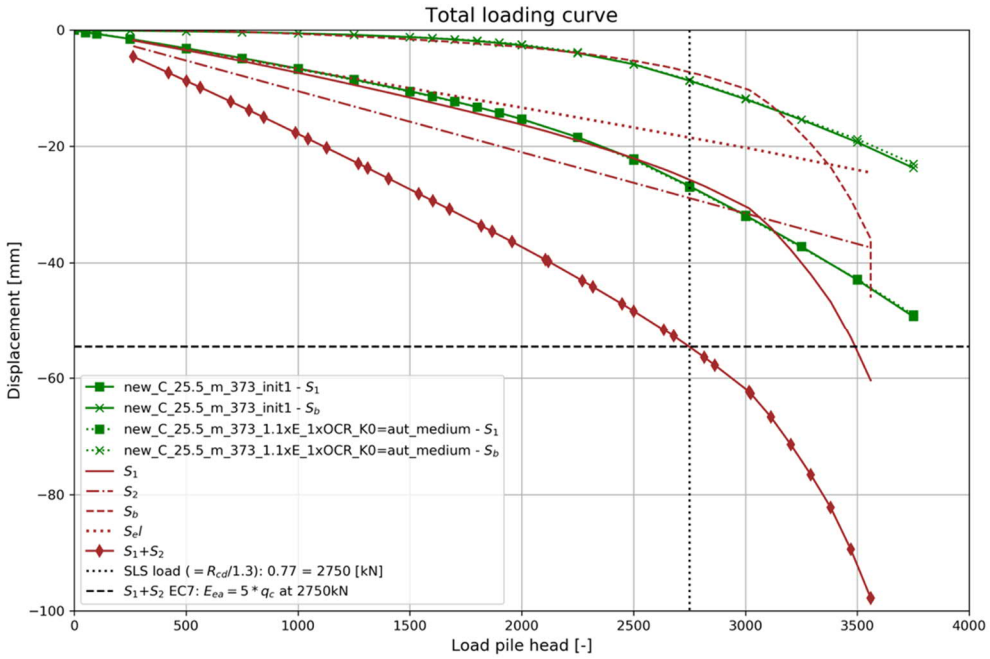


*Graph D.6: Total pile settlement in different contributions, L=25.5 m*

## D.3 Benchmark comparison 9 pile model

For the 25.5 m long pile model the elastic compression seems to be in line with the EC7 outcome and does not need updated fit parameters for the elastic compression. This could be due to the stiffer behaviour of the shaft caused by the deeper penetration in the sand bearing layer, the relative displacement is therefore decreased over this part of the pile. Although, the pile tip does require updated soil stiffness parameters in order to be in line with the NEN9997 result.

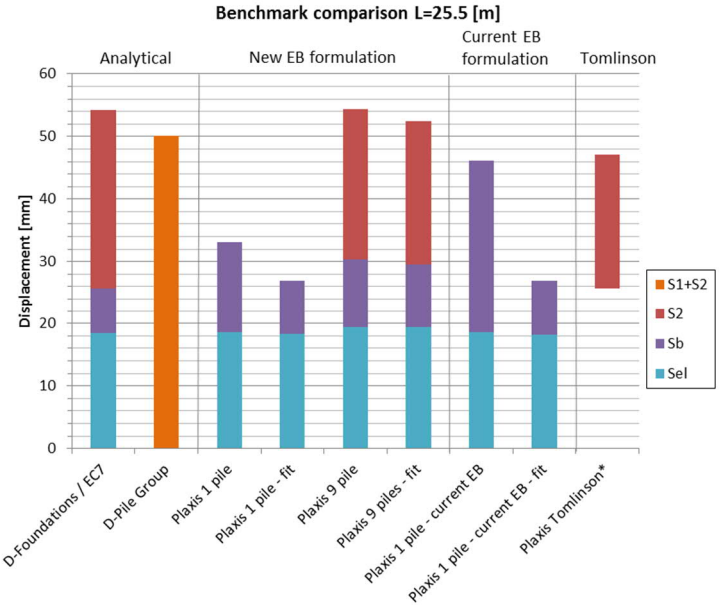


*Graph D.7: Benchmark comparison calculation approaches L = 25.5 [m], F = 2750 kN*

# E Case study

## E.1 PLAXIS 3D input

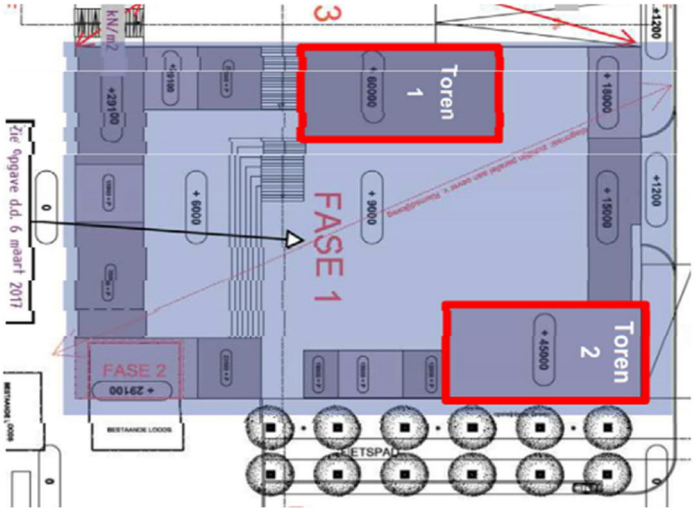


*Figure E.1: Overview map high-rise and low-rise buildings case study*

### E.1.1 Geometry

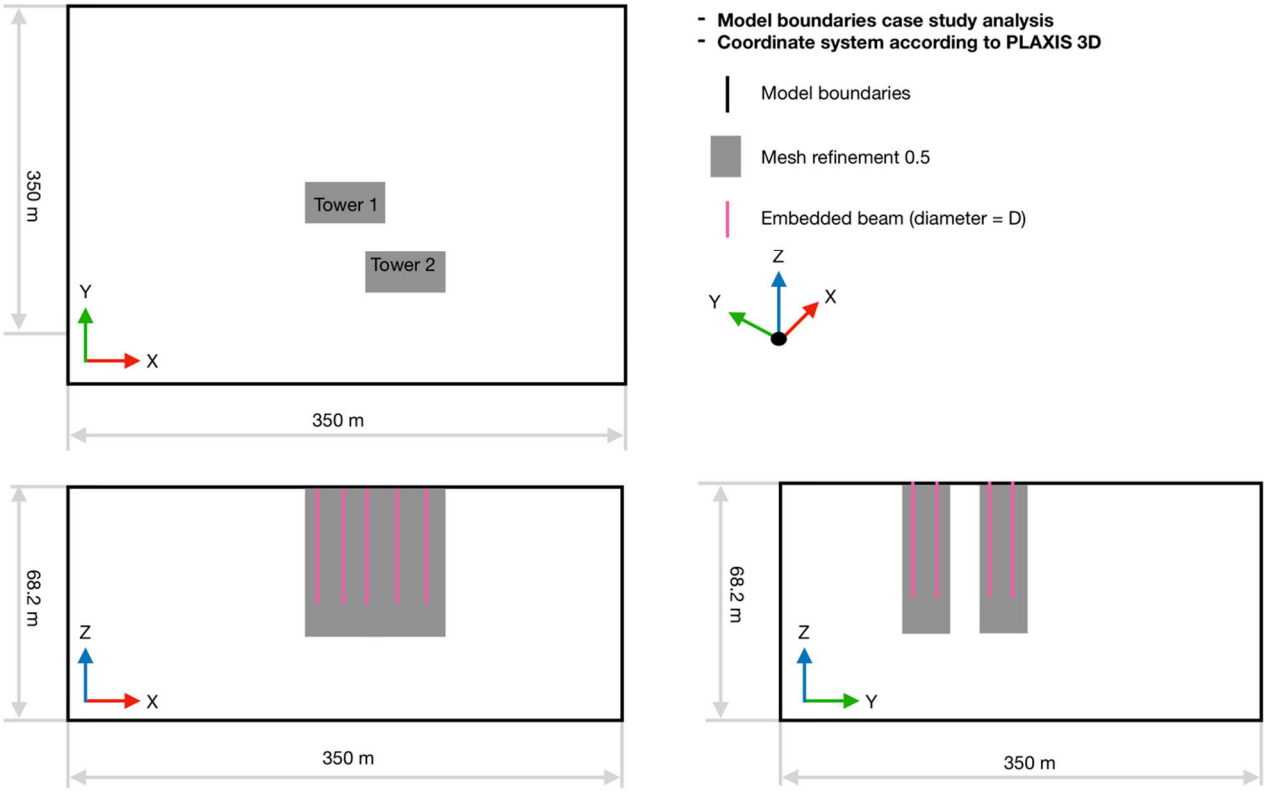


*Figure E.2: Model geometry case study*

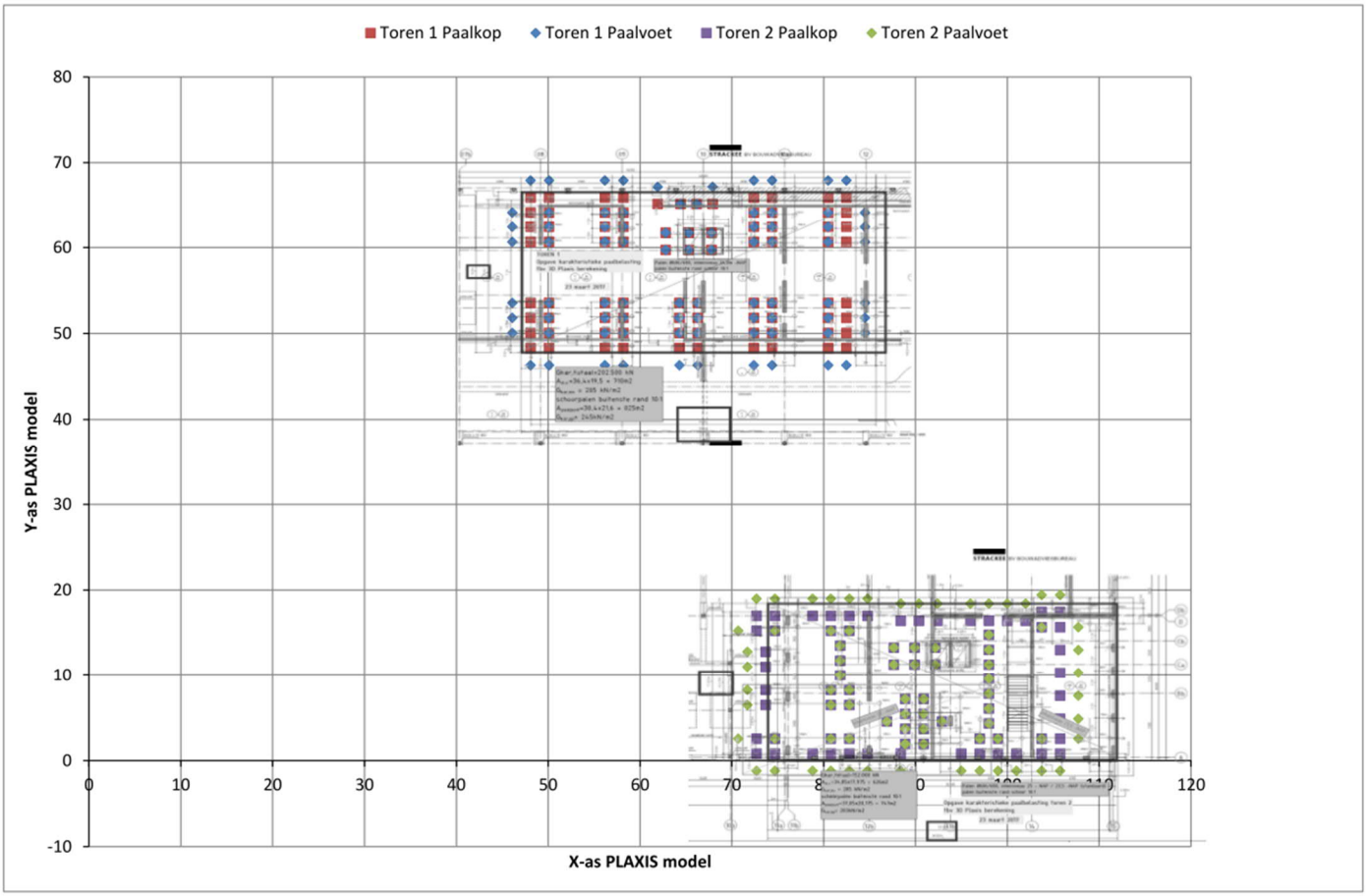


*Figure E.3: Pile plan case study tower 1 and 2*

**Boundary conditions PLAXIS 3D models**

| | Deformations | Groundwater flow |
|---|---|---|
| $X_{min}$ | *Normally fixed* | *Open* |
| $X_{max}$ | *Normally fixed* | *Open* |
| $Y_{min}$ | *Normally fixed* | *Open* |
| $Y_{max}$ | *Normally fixed* | *Open* |
| $Z_{min}$ | *Fully fixed* | *Closed* |
| $Z_{max}$ | *Free* | *Open* |

*Table E.1: Boundary conditions case study model*

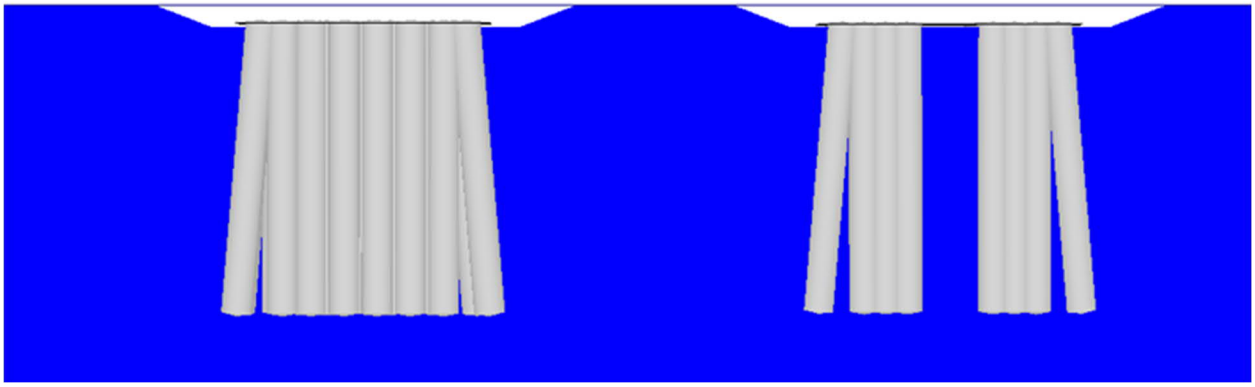

*Figure E.4: Slopes to prevent plate touching the soil (PLAXIS 3D cross section screenshot)*

## E.1.2 CPT - DKM32

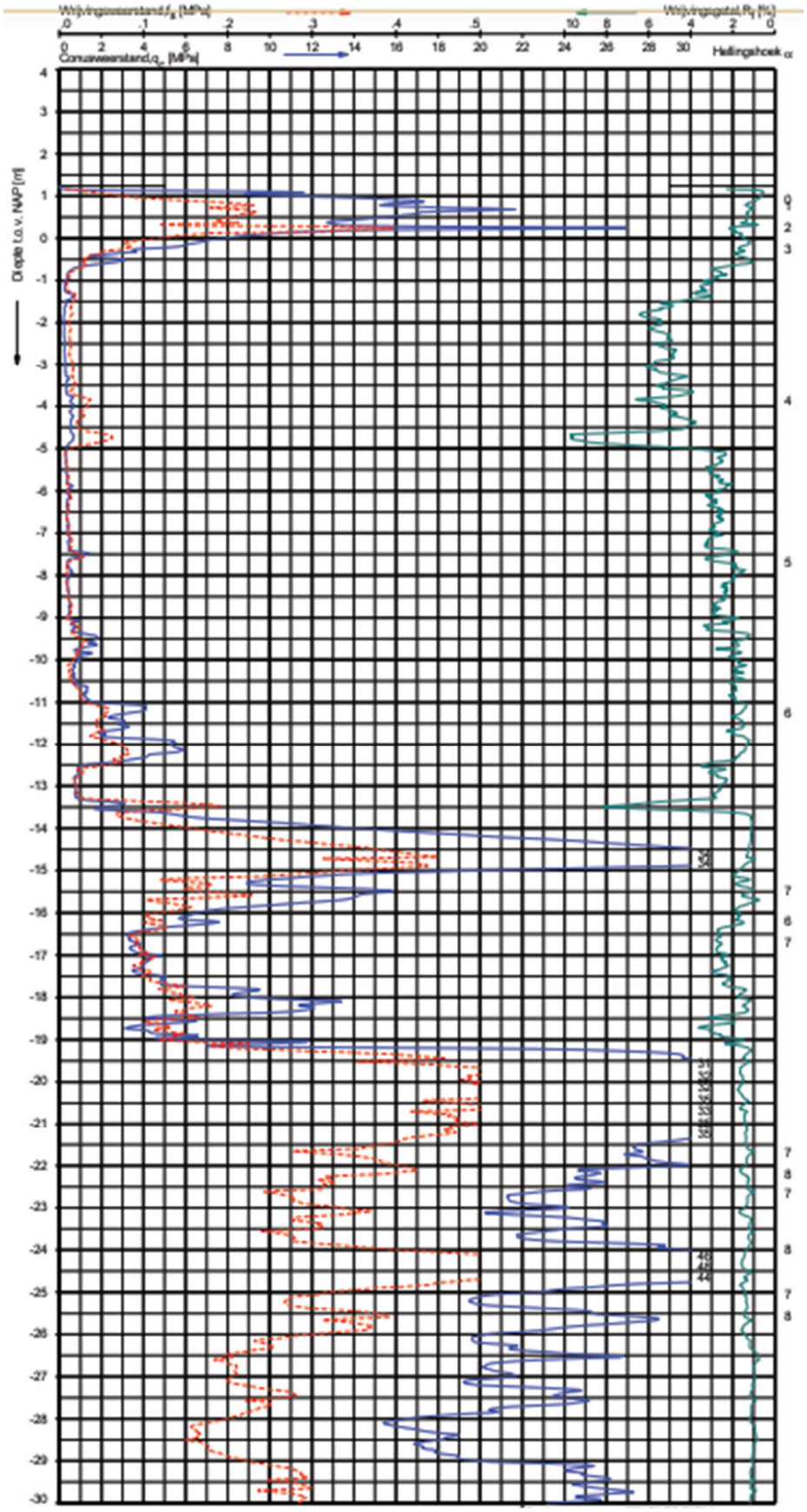


*Graph E.1: CPT case study: soil stratigraphy and bearing capacity piles*

## E.1.3 Parameter set case study PLAXIS 3D

From design data project

| | *Klei* | *Klei* | *Zand* | *Zand* | *Zand* | |
|---|---|---|---|---|---|---|
| | *Siltig zwak zandig* | Siltig | 1e zandlaag | 2e zandlaag, vast gepakt | Zeer vast gepakt | **Unit** |
| Thickness | 5.2 | 9.5 | 5.5 | 11.5 | 3.5 | [m] |
| Soil model | HSS | HSS | HSS | HSS | HSS | |
| $\gamma_{sat}$ | 16 | 17 | 18 | 19 | 19 | kN/m$^3$ |
| $\gamma_{unsat}$ | 16 | 17 | 20 | 21 | 21 | kN/m$^3$ |
| $e_0$ | 0.5 | 0.5 | 0.5 | 0.5 | 0.5 | [-] |
| Dilatancy cut-off | False | False | False | False | False | |
| $E_{50}^{ref}$ | 3000 | 3000 | 35000 | 50000 | 50000 | [kN/m$^2$] |
| $E_{oed}^{ref}$ | 15000 | 1566 | 20000 | 50000 | 50000 | [kN/m$^2$] |
| $E_{ur}^{ref}$ | 12000 | 12000 | 100000 | 150000 | 150000 | [kN/m$^2$] |
| m | 0.7 | 0.5 | 0.5 | 0.5 | 0.5 | [-] |
| $c'_{ref}$ | 2 | 5 | 0 | 0 | 0 | [kN/m$^2$] |
| $\varphi'$ | 25 | 22.5 | 30 | 35 | 35 | [°] |
| $\psi$ | 0 | 0 | 0 | 5 | 5 | [°] |
| $\Upsilon_{0.7}$ | 0.4130E-3 | 1.0E-3 | 0.165E-3 | 0.0982E-3 | 0.0982E-3 | [-] |
| $G_0^{ref}$ | 32.50E3 | 15000 | 100E3 | 150000 | 150000 | [kN/m$^2$] |
| $K_0^{NC}$ | 0.5774 | 0.6173 | 0.5 | 0.4264 | 0.4264 | [-] |
| $R_{inter}$ | 1.0 | 1.0 | 1.0 | 1.0 | 1.0 | [-] |
| OCR | 1 | 1 | 1 | 1 | 1 | [-] |
| $K_0$ | 0.5 | 0.5 | | 0.4264 | 0.4264 | [-] |
| POP | 10 | 10 | 0 | 0 | 100 | [-] |
| Drainage type | Drained | Drained | Drained | Drained | Drained | |
| $K_x = k_y = k_z$ | 0.6 | 0.6 | 0.6 | 0.6 | 0.6 | [m/day] |

*Table E.2: Soil properties case study model initial: [project Amsterdam]*

| | *Klei* | *Klei* | |
|---|---|---|---|
| | Eem klei | Zandig | Unit |
| Thickness | 18.5 | 14.5 | [m] |
| Soil model | SSC | SSC | |
| $\gamma_{sat}$ | 18.5 | 18.5 | kN/m$^3$ |
| $\gamma_{unsat}$ | 18.5 | 18.5 | kN/m$^3$ |
| $e_0$ | 0.5 | 0.5 | [-] |
| Dilatancy cut-off | False | False | |
| $\lambda^*$ | 0.06700 | 0.034 | [-] |
| $\kappa^*$ | 0.01340 | 0.0067 | [-] |
| $\mu^*$ | 0.0033 | 0.00165 | [-] |
| $c'_{ref}$ | 0 | 0 | [kN/m$^2$] |
| $\varphi'$ | 30 | 32.5 | [°] |
| $\psi$ | 0 | 0 | [°] |
| $\nu'_{ur}$ | 0.15 | 0.15 | [-] |
| $K_0^{NC}$ | 0.5 | 0.4627 | [-] |
| OCR | 1.9 | 1.9 | [-] |
| $K_0$ | 0.7912 | 0.7203 | [-] |
| POP | 0 | 0 | [-] |
| Drainage type | Undrained | Undrained | |
| $K_x = k_y = k_z$ | 0.04E-3 | 0.06E-3 | [m/day] |

*Table E.3: Soil properties Soft soil creep model*

### E.1.4 Numerical control parameters

| Numerical control parameters | |
|---|---|
| Pore pressure calculation type | Phreatic |
| Force fully drained behaviour newly | Check box on |
| Solver type | Picos (multicore iterative) |
| Max cores to use | 256 |
| Max number of steps stored | 1000 |
| Use Compression for result files | Check box off |
| Use default iter parameters | Check box on |
| Max steps | 1000 |
| Tolerated error | 0.01000 |
| Max load fraction step | 0.5 |
| Over-relaxation factor | 1.2 |
| Max number of iterations | 60 |
| Desired min number of iterations | 6 |
| Desired max number of iterations | 15 |

*Table E.4: Numerical control parameters PLAXIS 3D calculations – case study*

### E.1.5 Meshing information

| | Nodes | Elements | Avg. mesh element size [m] | Max. element size [m] | Min. element size [m] |
|---|---|---|---|---|---|
| Mesh 1 (coarse) | 88898 | 57508 | 9,016 | 33.62 | 3.333E-3 |
| Mesh 2 (medium) | 90201 | 58428 | 9.070 | 30.16 | 3.333E-3 |
| Mesh 3 (fine) | 100816 | 65944 | 9.193 | 25.83 | 3.333E-3 |

*Table E.5: Meshing results case study model*

Noted is that the difference between the mesh size distributions is not so large compared to the single pile models. This is probably due to the large dimensions of the model. The elements far away from the area of interest become larger and the elements in the area of interest becomes smaller.

| Mesh type information | |
|---|---|
| Model | Full |
| Elements | 10 - noded |

*Table E.6: Mesh type information cases study model*

## E.1.6 Loading

| | Construction | | | | | | | | Consolidation |
|---|---|---|---|---|---|---|---|---|---|
| **Phase** | **1** | **2** | **3** | **4** | **5** | **6** | **7** | **8** | **9** |
| Duration in days | 147 | 98 | 14 | 21 | 42 | 21 | 49 | 42 | 9564 |
| Duration days cumulative | 147 | 245 | 259 | 280 | 322 | 343 | 392 | 434 | 10000 |
| Tower 2 | 2/14 | 12/14 | 13/14 | 14/14 | Finished | Finished | Finished | Finished | |
| Tower 1 | 2/18 | 2/18 | 3/18 | 5/18 | 11/18 | 13/18 | 18/18 | Finished | |
| Low rise 1 | 2/9 | 2/9 | 2/9 | 3/9 | 7/9 | 9/9 | Finished | Finished | |
| Low rise 2 | 2/8 | 2/8 | 2/8 | 3/8 | 3/8 | 3/8 | 7/8 | 8/8 | |
| Low rise 3 | 2/5 | 2/5 | 2/5 | 2/5 | 5/5 | Finished | Finished | Finished | |
| Low rise 4 | 2/2 | Finished | Finished | Finished | Finished | Finished | Finished | Finished | |

*Table E.7: Phasing of loads during construction and operational phase - case study*

## E.1.7 Load transfer foundation plate

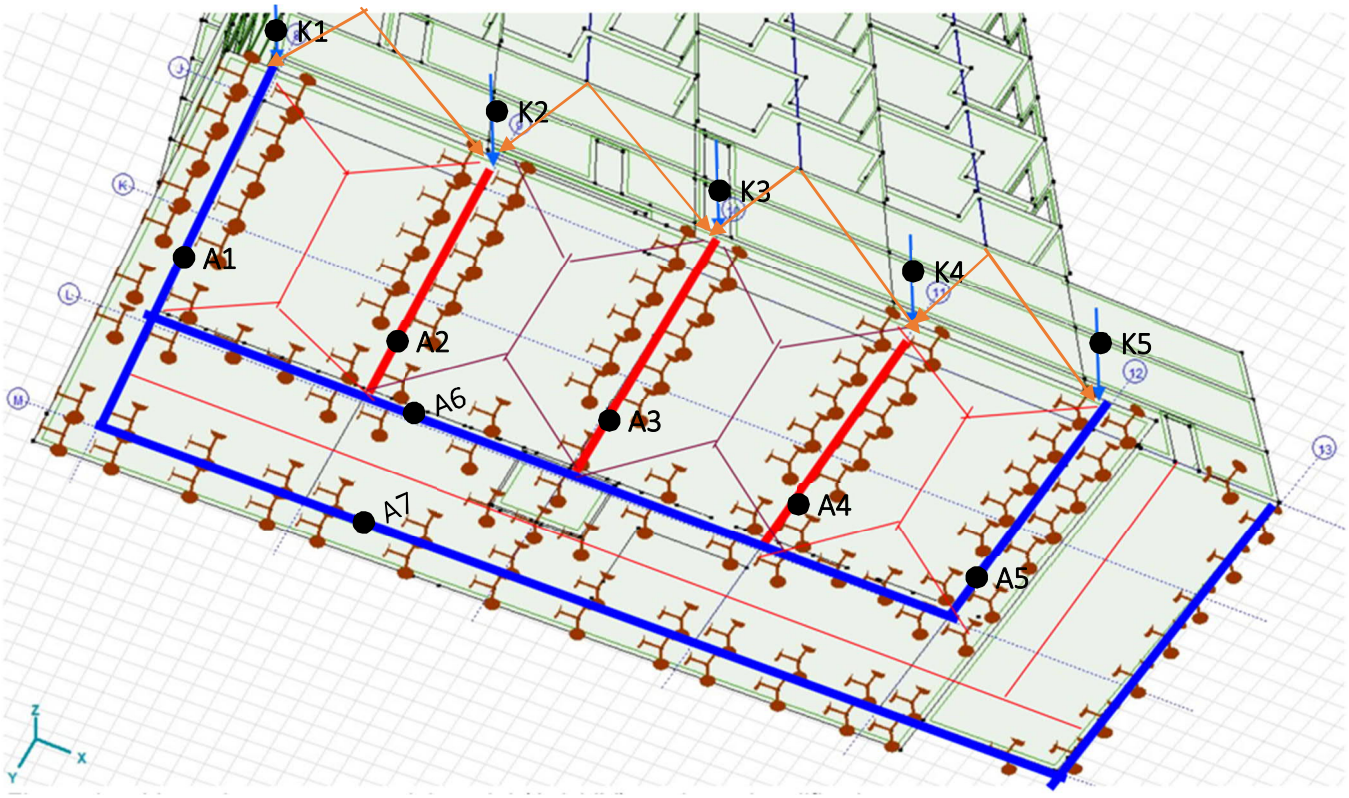


*Figure E.5: Load transfer tower 1*

Load foundation plate tower 1

| | *Load* | *Unit* | | *Wall length* | *Unit* |
|---|---|---|---|---|---|
| A1 | 695 | kN/m | Line load | 10,8 | m |
| A2 | 1340 | kN/m | Line load | 10,8 | m |
| A3 | 1413 | kN/m | Line load | 10,8 | m |
| A4 | 1490 | kN/m | Line load | 10,8 | m |
| A5 | 750 | kN/m | Line load | 10,8 | m |
| A6 | 1308 | kN/m | Line load | 32,4 | m |
| A7 | 784 | kN/m | Line load | 32,4 | m |
| K1 | 1982,2 | kN | Point load | | |
| K2 | 4086,9 | kN | Point load | | |
| K3 | 4073,5 | kN | Point load | | |
| K4 | 4001,5 | kN | Point load | | |
| K5 | 2032,7 | kN | Point load | | |

*Table E.8: Load on foundation plate tower 1*

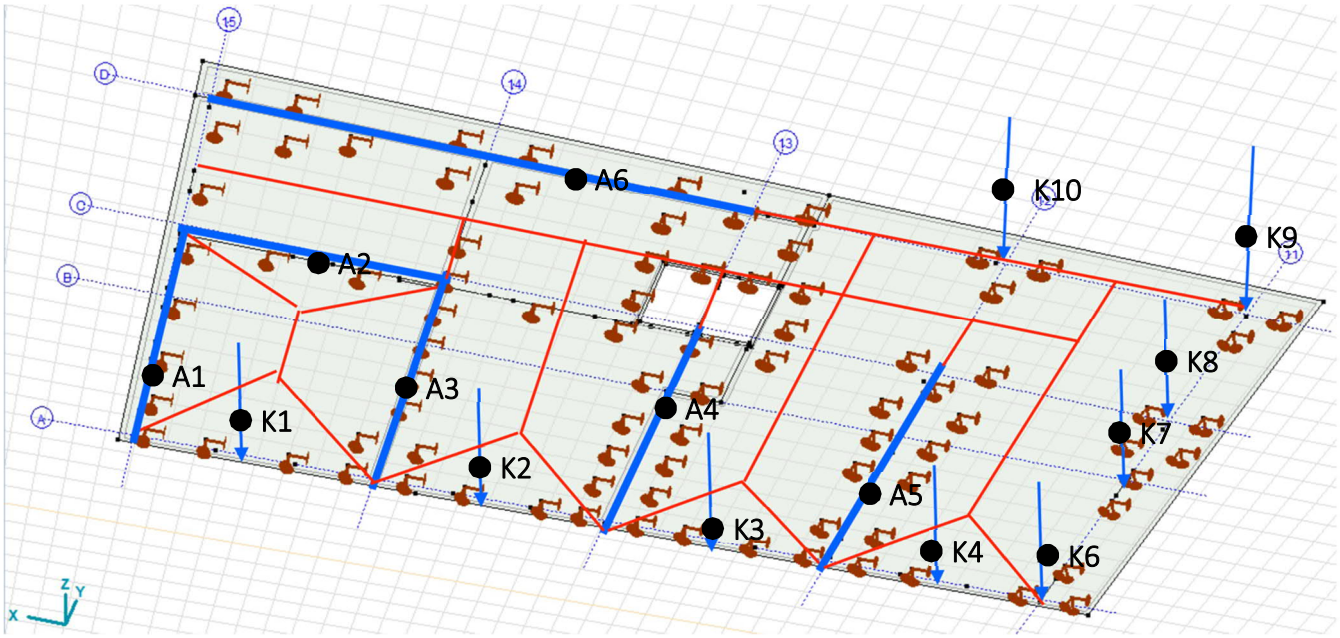


*Figure E.6: Load transfer tower 2*

Load foundation plate tower 2

| | *Load* | *Unit* | | *Wall length* | *Unit* |
|---|---|---|---|---|---|
| A1 | 577 | kN/m | Line load | 10,65 | m |
| A2 | 997 | kN/m | Line load | 8,1 | m |
| A3 | 1479 | kN/m | Line load | 10,65 | m |
| A4 | 1758 | kN/m | Line load | 10,65 | m |
| A5 | 1779 | kN/m | Line load | 10,65 | m |
| A6 | 733 | kN/m | Line load | 16,2 | m |
| K1 | 1305 | kN | Point load | | |
| K2 | 1305 | kN | Point load | | |
| K3 | 1305 | kN | Point load | | |
| K4 | 1305 | kN | Point load | | |
| K6 | 10887 | kN | Point load | | |
| K7 | 10887 | kN | Point load | | |
| K8 | 10887 | kN | Point load | | |
| K9 | 10887 | kN | Point load | | |
| K10 | 4841 | kN | Point load | | |

*Table E.9: Load on foundation plate tower 2*

## E.2 Results

### E.2.1 Current embedded beam – case study

Finally, a comparison is made between the current and new embedded pile. Chapter 6 already discussed the difference between both formulations for a single pile case. Here, the response is tested in exactly the same model as Graph 9.1. Moreover, also in this calculation it turned out that the new formulation is less mesh sensitive and behaves stiffer compared to the current one, which has already been proven in chapter 6. However, the difference in stiffness between both formulations is smaller compared to the single pile model. That approves the claim that the response and the fit of the embedded beam is problem dependent.

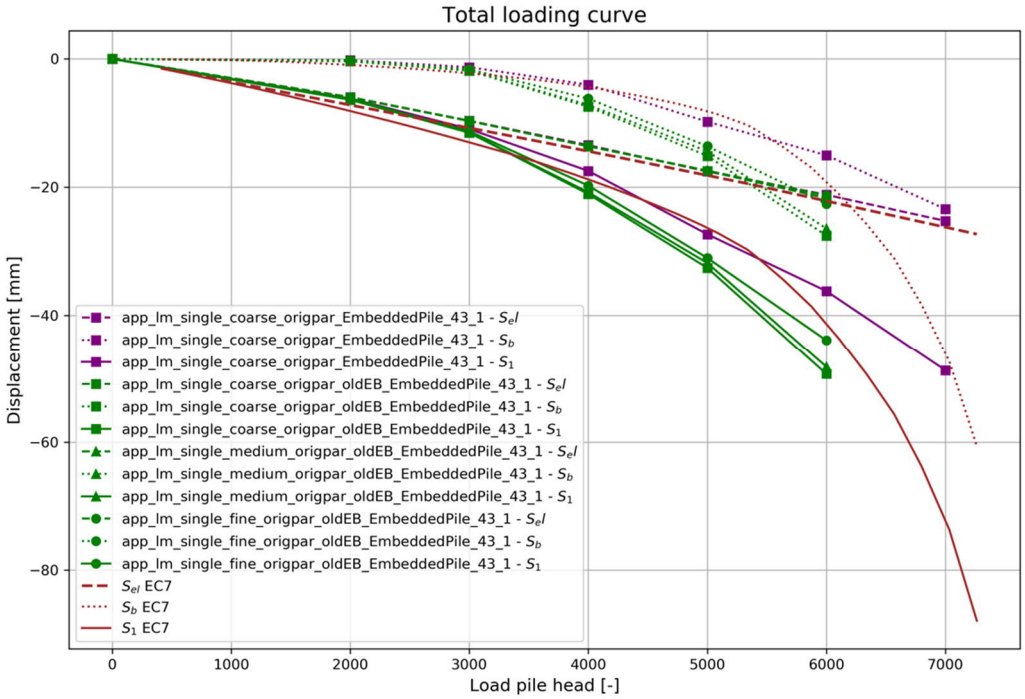


*Graph E.2: Current and new embedded beam formulation case study*

### E.2.2 Embedded beam formulation comparison

Improvements regarding load-displacement stiffness behaviour between the current and new embedded beam are visible in Graph E.3. The individual pile behaviour is stiffer in the new formulation, where the group settlement ($s_2$) is equal. The equal group settlement can be clarified by the equal load on top of the pile in both models. For this reason, the (elastic) compression of the deeper layers (4D below pile tip level) remains the same regardless of the EB formulation because of the equal load.

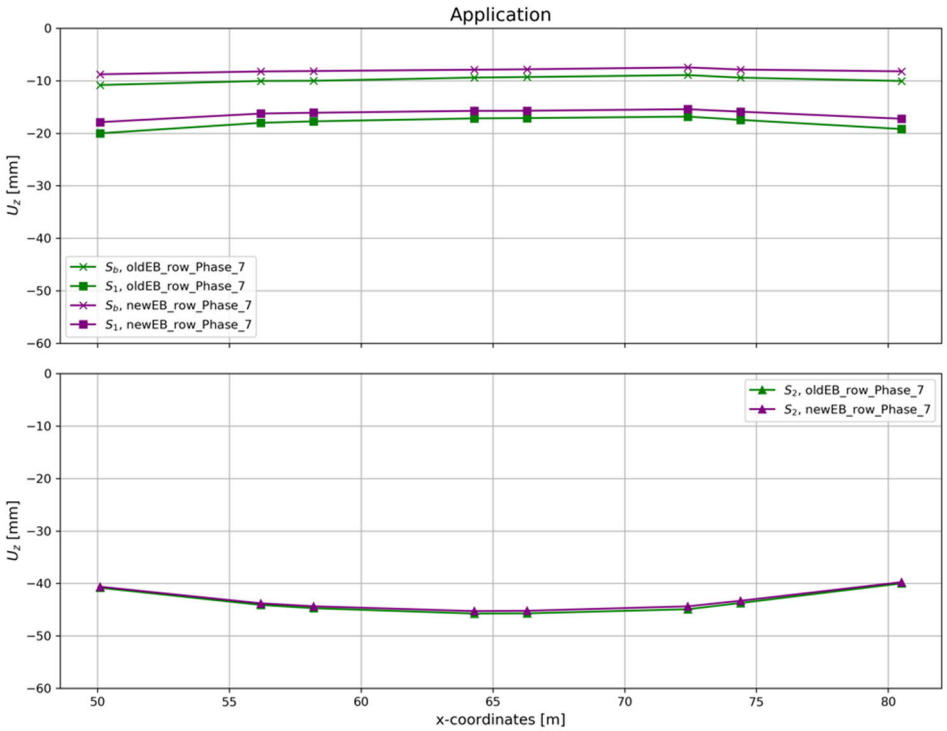


*Graph E.3: Comparison current and new embedded beam formulations phase 7*

| x [m] | 50.1 | 56.1 | 58.1 | 64.3 | 66.3 | 72.4 | 74.4 | 80.5 |
|---|---|---|---|---|---|---|---|---|
| F [kN] | -1750 | -2750 | -2750 | -2750 | -2750 | -2750 | -2750 | -1750 |

## E.2.3 Influence plate stiffness y-direction

Influence of the bending stiffness in y direction tower 1. The observed tilt of the foundation is due to the influence of tower 2 and the low-rise building situated directly besides tower 1.

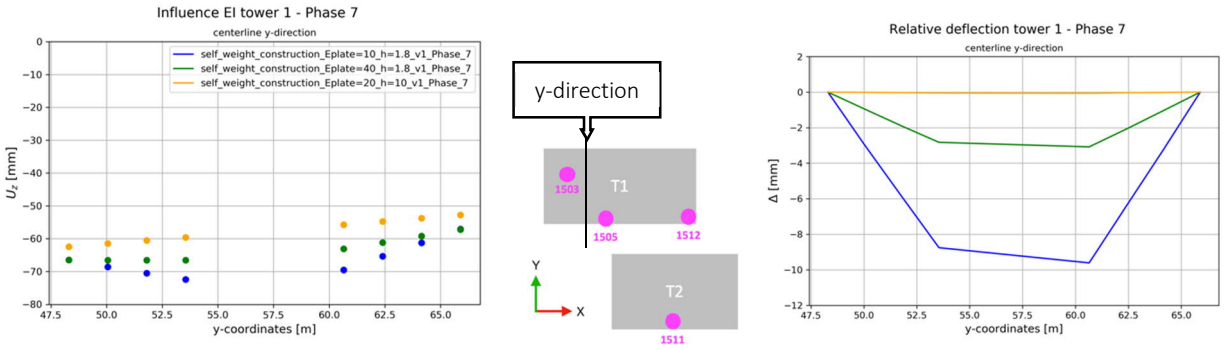


*Graph E.4: Influence plate stiffness phase 7 (almost all load applied) tower 1, $s_1$ + $s_2$, y-direction*